# Albitisation et oxydation des roches granitoïdes en relation avec la paléosurface triasique des Sudètes (SW Pologne)

Kouakou Fulgence Eric Yao

ParisTech
INSTITUT DES SCIENCES ET TECHNOLOGIES
PARIS INSTITUTE OF TECHNOLOGY

PAŃSTWOWY INSTYTUT GEOLOGICZNY
MENTE ET MALLEO
1919
PAŃSTWOWY INSTYTUT BADAWCZY

MINES ParisTech

École doctorale n° 398 : Géosciences et Ressources Naturelles

# Doctorat ParisTech

# T H È S E

**pour obtenir le grade de docteur**

**préparée dans le cadre d'une cotutelle entre**

## l'École nationale supérieure des mines de Paris et Państwowy Instytut Geologiczny - Państwowy Instytut Badawczy à Varsovie, Pologne

**Spécialité "Dynamique et Ressources des Bassins Sédimentaires"**

soutenue publiquement le 16 décembre 2013 par

**Kouakou Fulgence Eric YAO**

# Albitization and oxidation of the granitoïd rocks related to the Triassic paleosurface in the Sudetes (SW Poland)

***Albitisation et oxydation des roches granitoïdes en relation avec la paléosurface triasique des Sudètes (SW Pologne)***

***Zjawiska albityzacji i oksydacji skał granitoidowych związane z triasową powierzchnią zrównania w Sudetach (południowo-zachodnia Polska)***

| | | |
|---|---|---|
| Directeurs de thèse : | **Médard THIRY** | (MINES ParisTech) |
| | **Pawel ALEKSANDROWSKI** | (Polish Geological Institute-National Research Institute) |
| Co-encadrante : | **Christine FRANKE** | (MINES ParisTech) |

**Jury**

| | |
|---|---|
| **Mme Isabelle COJAN**, Doct., HDR, Geosciences, MINES ParisTech, Fontainebleau, France | Présidente |
| **Mme Katarzyna JARMOLOWICZ-SZULC**, PhD, DHabil, Polish Geol. Inst.- NRI, Warsaw, Poland | Co-Présidente |
| **M. Pawel ALEKSANDROWSKI**, PhD, DHabil , Polish Geol. Inst.-Nat. Res. Inst., Warsaw, Poland | Examinateur |
| **M. Anicet BEAUVAIS**, Doct., HDR, CEREGE, Univ. of Aix-Marseille, Aix en Provence, France | Rapporteur |
| **Mme Christine FRANKE**, PhD, Geosciences, MINES ParisTech, Fontainebleau, France | Examinatrice |
| **M. David PARCERISA**, PhD, Polytechnical University of Catalonia, Manresa, Spain | Examinateur |
| **M. Jean-Michel SCHMITT**, Doct. és Sc., AREVA, Geosciences Dpt., Paris la Défense, France | Rapporteur |
| **M. Adam SZUSZKIEWICZ**, PhD, Inst. of Geological Sciences, University of Wroclaw, Poland | Examinateur |

T H È S E

**MINES ParisTech**
**Centre de Géosciences**
35 rue Saint-Honoré, 77305 Fontainebleau cedex

## AVANT-PROPOS

*Cette thèse a été réalisée dans le cadre d'une cotutelle entre l'École Nationale Supérieure des Mines de Paris (MINES ParisTech) et l'Institut Géologique Polonaise-Państwowy Instytut Geologicny (IGP-PIG).*

*Je voudrais d'abord remercier mon directeur de thèse, Médard Thiry, d'avoir cru en moi et de m'avoir proposé ce sujet de thèse. Merci pour son aide, sa rigueur ainsi que ses critiques constructives qui ont permis de faire progresser ce travail.*

*Je remercie Pawel Aleksandrowski d'avoir accepté de co-diriger cette thèse. Je voudrais le remercier spécialement pour l'hébergement, et tout ce qu'il a fait pour moi durant mes différents séjours à Wrocław.*

*Je tiens aussi à exprimer ma reconnaissance à Christine Franke qui a co-encadré cette thèse. Merci pour son aide, son investissement, sa capacité de communication. Je voudrais lui dire merci pour les datations paléomagnétiques.*

*Je voudrais exprimer ma gratitude à Anicet Beauvais d'avoir accepté d'être rapporteur de cette thèse. Je garde un bon souvenir de notre entretien à l'EGU 2010 à Vienne.*

*Je tiens aussi à remercier Jean-Michel Schmitt d'avoir accepté de rapporter cette thèse et d'apporter ainsi sa grande connaissance des albitisations triasiques. Ses travaux ont été pour moi une source d'inspiration en particulier le volet modélisation géochimique des albitisations.*

*Merci à Isabelle Cojan de m'avoir accueilli au sein de l'équipe géologie. C'est une joie personnelle et un honneur de la retrouver dans mon jury.*

*Merci à David Parcerisa pour son aide fort appréciable en pétrographie et sur le traitement des images de cathodoluminescence. Je suis heureux qu'il soit dans mon jury.*

*Je voudrais exprimer ma reconnaissance à Adam Szuszkiewicz pour son aide appréciable en pétrographie et son soutien au cours de mes différents séjours à Wrocław. Heureux de le retrouver dans mon jury.*

*Je suis reconnaissant à Krzystof Turniak de l'Université de Wrocław pour son aide sur le terrain à Szklarska Poręba.*

*Je remercie sincèrement Pawel Raczynski de l'Université de Wrocław pour les séances de cathodoluminescence, pour sa gentillesse.*

*Je n'oublie pas toute l'équipe géologie Caroline, Pierre, Sylvie et les thésards Maxime, Benjamin, Thomas, Frédéric, Benoît. Je vous souhaite le meilleur pour vos thèses respectives. Merci à Philippe Le Caer pour les photos et les dessins. Merci à Nelly Martineau pour les lames minces et les discussions philosophiques dans notre bureau. Je n'oublie pas Noëlia Carrillo pour les analyses de Rayons X et les causeries appréciables dans la navette.*

*Merci à ma famille. Je veux remercier ma mère pour tous les sacrifices qu'elle a consentis pour moi, et je souhaite qu'elle puisse obtenir sa greffe de reins. Je suis néanmoins heureux de la voir en meilleure santé après ces mois d'hospitalisation. Je suis reconnaissant à ma femme pour son soutien, et pour être resté à mes côtés dans les bons comme dans les moins bons moments.*

*Je voudrais dire un grand merci à tous ceux que je n'ai pas pu citer ici. Enfin, je veux remercier DIEU tout-puissant et JÉSUS en qui je crois, pour la force et la vie sans laquelle rien ne serait possible.*

## FOREWORD

This thesis has been achieved in the framework of a joint supervision between the Ecole Nationale Supérieure des Mines de Paris (MINES ParisTech) and the Polish Geological Institute-Państwowy Instytut Geologicny (PGI-PIG).

Foremost, I would like to thank my supervisor, Médard Thiry, for trusting in me and offered me this thesis opportunity. I'm grateful for his help, his rigor, and the constructive criticism and advices that allowed accomplishing this work.

In addition, I would like to thank Pawel Aleksandrowski for agreeing to co-supervise this thesis. Thank to him especially for the accommodation and all that he has done for me during my several stays in Wroclaw.

Besides, I would like to express my deep gratitude to Christine Franke who co-supervised this thesis, for her support, her investment, and her communicative skill. Thank also for the paleomagnetic datings conducted in parallel to this work.

I would like to express my gratitude to Anicet Beauvais for agreeing to be reviewer of this thesis. I have good memories of our brief discussion in 2010 at the EGU Congress in Vienna about the red facies in general and especially those of West Africa.

I would like to thank Jean Michel Schmitt for accepting to review this thesis and thus to bring his great knowledge of the Triassic albitisations. His works inspired me a lot especially those concerning the geochemical modelling of the albitization.

I would like to acknowledge Isabelle Cojan for welcoming me in the geology team. It is my personal satisfaction and a great honour to have her as examiner in my committee.

Thanks to Parcerisa David for his valuable assistance in petrography and in CL image processing. I'm glad he is member of my committee.

I would like to thank Adam Szuszkiewicz for his valuable assistance and his support during my stays in Wrocław. I do not forget those petrographic discussions we had, and his assistance in the CL images interpretation. It is gratifying to find him in my committee.

I'm thankful to Krzysztof Turniak from the University of Wrocław. I'm grateful for his support and his assistance during our field trip in Szklarska Poręba.

My sincere thanks to Pawel Raczyński from the University of Wrocław for the cathodoluminescence devices, his kindness and the office is made available to me.

I do not forget the team of geology, Caroline, Pierre, Sylvie and all the Phd students Maxime, Benjamin, Thomas, Frédéric, Benoît. I wish you the best for your theses. Thank to Philippe Le Caer for the photos and the drawings. My special appreciations go to Nelly Martineau for the thin sections and for our philosophical conversation. I do not forget Noëlia Carrillo for X-ray analysis and our very appreciable talks in the shuttle.

Thanks to my family, especially to my mother for all the sacrifices she made for me. My most ardent wish is for her to get a kidney transplant in order to appease her suffering. Nevertheless, I am happy to see her in better health after these months of hospitalization. My sincere appreciation goes to my sweetheart wife for her support and for standing at my side in the good and the difficult moments.

I would like to express my gratitude to all those I forgot to mentione here. Thanks to all mighty God and JESUS in whom I believe, for the strength and for the life without which nothing would have been possible.

## *RESUME*

*Les granitoïdes des Sudètes Polonaises montrent des faciès albitisés/oxydés, généralement considérés comme des altérations tardi-magmatiques en référence aux paragenèses de saussuritisation et de séricitisation qui leur sont parfois associées. Or l'éventualité d'une origine superficielle triasique a été récemment établie pour certains de ces faciès. Cette étude visait à préciser les caractéristiques de ces altérations dans les Sudètes.*

*Les granitoïdes des Sudètes polonaises montrent 3 types d'altération : (1) l'albitisation, (2) la saussuritisation et (3) la séricitisation. Ces altérations et les paragenèses qu'elles induisent sont liées aux fractures. L'albitisation apparaît dans les faciès rouges à proximité des fractures tandis que la saussuritisation et la séricitisation sont dominantes dans les faciès clairs loin des fractures et au cœur des blocs. Une zonalité prévaut donc dans ces faciès granitoïdes depuis les fractures vers l'intérieur des blocs.*

*Dans les faciès clairs au cœur des blocs, les plagioclases primaires altérés montrent des assemblages caractéristiques de la saussuritisation, constitués de prehnite-albite-séricite, ou le développement invasif de séricite associée à des cristallites d'albite. Dans les faciès rouges en bordure des fractures, les plagioclases et les feldspaths potassiques sont partiellement ou entièrement remplacés par de l'albite secondaire systématiquement pigmentée par de l'hématite. En plus d'être albitisés, les feldspaths potassiques sont également microclinisés.*

*L'altération des feldspaths primaires dans ces faciès (clairs ou rouges) s'accompagne de la chloritisation des minéraux ferromagnésiens. La chloritisation des biotites apparaît déjà dans les faciès clairs mais celle-ci est plus complète dans les faciès rouges, la chloritisation des amphiboles est exclusivement visible dans les faciès rouges, et totalement absente des faciès clairs. La chloritisation des biotites s'accompagne du développement de minéraux secondaires tels que le quartz, les feldspaths potassiques, la prehnite, de titanite et d'apatite.*

*Les minéraux typiques de la saussuritisation et la séricitisation des faciès clairs demeurent parfois visibles dans les faciès rouges albitisés/oxydés. Les paragenèses associées aux différentes altérations se superposent apparemment dans ces roches granitoïdes. Cette étude ne nous a pas permis de séparer ces paragenèses en phases d'altération distinctes n'ayant aucune relation entre elles comme cela a été mentionné par d'autres auteurs (par exemple Drake et al., 2009). Au contraire, il apparaît qu'il n'y a qu'une seule phase d'altération avec des réactions qui s'enchaînent spatialement. Les successions paragénétiques résultent donc du déplacement du front réactionnel de chaque paragenèse depuis les fractures vers le cœur des blocs.*

*Par ailleurs, l'albite secondaire est toujours associée à de l'hématite dans les faciès rouges . La datation par paléomagnétisme de cette hématite indique qu'elle est d'âge triasique, et par conséquent sa formation est nécessairement liée à la paléosurface triasique. Comme l'albite secondaire apparait contemporaine de l'hématite, sa formation doit aussi être d'âge triasique. L'albitisation/oxydation observée dans les granitoïdes des Sudètes polonaises apparaît liée à la paléosurface triasique et par conséquent être d'origine superficielle.*

*Les faciès albitisés/hématisés apparaissent comme des empreintes de la paléosurface triasique dans les Sudètes. La caractérisation de la paléosurface dans les socles constituerait un outil spatio-temporel précieux pour appréhendere l'évolution post-triasique des socles Européens et ainsi de contraindre les modèles géodynamiques de ces massifs.*

## ABSTRACT

The Sudetes show albitized/oxidized facies systematically considered as late-magmatic alterations due to the occurrence of saussuritization and sericitization parageneses. Yet, the possible Triassic superficial origin has recently been proposed for some of these facies. This study aimed to precise the features of these alterations in the Sudetes.

The granitoïd rocks in the polish Sudetes show three types of alterations: (1) the albitization, (2) the saussuritization and, (3) the sericitization. These alterations and the associated parageneses appear as related to the fractures. The albitization emerges as typical of the reddened facies close to the fracture wall whereas the saussuritization and the sericitization are dominant in the light/unstained facies further away from the fracture walls in the center of the blocks. Therefore, a paragenetic zonation depending on the alteration type is obvious from the fractures towards the inner part of the blocks of the granitoïd rocks.

In the light/unstained facies in the center of the blocks, primary plagioclases are sometimes altered showing either a typical saussuritization assemblage of prehnite-sericite-albite or an invasive development of sericite associated to tiny albite crystals.

In the reddened facies at the fracture walls, plagioclases and K-feldspars are entirely or partially replaced by secondary albite stained by hematite. Besides being albitized, the K-feldspars are also microclinized. Some accessory minerals occur, such as calcite associated to the secondary albite.

The alteration of the primary feldspars is associated to the chloritization of the ferromagnesian minerals within both, reddened and light facies. The chloritization of biotite is partial in the light facies and complete in the reddened facies. Biotite chloritization is also associated to the development of secondary minerals such as quartz, K-feldspar, prehnite, titanite, and apatite. Chloritization of the amphiboles is only visible in the reddened facies, and absent in the light/unstained facies.

Minerals typical of the saussuritization and the sericitization in the light facies are sometimes still visible in the reddened/oxidized facies. The parageneses associated to the different alteration type are likely to overlap within these granitoïd rocks. This study did not allow the separation of these parageneses into different alteration phases or independent events as it has been mentioned elsewhere by some authors (e.g. Drake et al., 2009). But it seems rather that there was only one alteration phase with reactions following spatially on from each other. Thus, the paragenetic successions result from the displacement of the reactional front of each paragenesis from the fractures wall towards the center of the blocks.

On the other hand, the secondary albite is systematically associated to hematite in the reddened facies. Paleomagnetic datings of this hematite indicates a Triassic remagnetization and therefore its formation must be necessarily related to the Triassic paleosurface. Since the albitization emerges as contemporaneous to the hematitization, consequently the albitization might also be of Triassic age. The albitization/oxidation observed in the granitoïds rocks of the Polish Sudetes appears likely as related to the Triassic paleosurface, hence of superficial origin.

The albitized/oxidized facies appear as an overprint of the Triassic paleosurface in the Sudetic basement. The characterization of the albitized/oxidized facies will constitute a good spatio-temporel tool to unravel the evolution of the European basement and thus permits to constrain the post-Triassic geodynamical model of these massifs.

# STRESZCZENIE

W krystalicznych kompleksach skalnych Sudetów powszechnie występuje facja skał zalbityzowanych i/lub utlenionych, tradycyjnie i konsekwentnie uważana za asocjację paragenetyczną, powstałą wskutek procesów saussurytyzacji i serycytyzacji tych kompleksów. W innych masywach waryscyjskich Europy zaproponowano jednak niedawno wyjaśnienie genezy niektórych przynajmniej wystąpień tej facji oddziaływaniem czynników przypowierzchniowych podczas triasu. Niniejsze studium ma za cel szczegółowy opis i wyjaśnienie genezy wspomnianej facji skalnej w wybranych dwóch jednostkach strukturalnych Sudetów – w karbońskich masywach granitoidowych kłodzko-złotostockim i karkonoskim.

Skały granitoidowe polskich Sudetów, reprezentowane przez duże plutony – kłodzko-złotostocki i karkonoski, dotknięte są generalnie trzema typami wtórnych zmian mineralnych: (1) albityzacją, (2) saussurytyzacją i (3) serycytyzacją. Zmiany te i związane z nimi paragenezy mineralne wykazują wyraźne związki przestrzenne z powierzchniami nieciągłości strukturalnych (spękań i uskoków). Efekty albityzacji typowo przejawiają się w postaci wtórnego, czerwonawego zabarwienia skał w pobliżu stref nieciągłości strukturalnych, podczas gdy efekty saussurytyzacji i serycytyzacji dominują w jaśniejszych partiach skał, położonych dalej od powierzchni nieciągłości, w centrach bloków skalnych wyznaczonych przez te powierzchnie. Tym samym zaznacza się strefowość paragenez związanych z wtórnymi przemianami mineralnymi w skali bloków skalnych w niektórych partiach przebadanych masywów granitoidowych.

W jasnych, wewnętrznych partiach bloków skalnych, generalnie niewykazujących plamistych przebarwień skały, pierwotne plagioklazy są niekiedy zmienione, wykazując już to typowe efekty saussurytyzacji, już to asocjację prehnit-serycyt-albit, względnie też inwazyjny rozwój serycytu stowarzyszony z utworzeniem drobnych kryształów albitu.

W facji zabarwionej na czerwono przy ścianach nieciągłości strukturalnych, plagioklazy i skalenie potasowe są całkowicie lub częściowo zastąpione przez wtórny albit z plamkami hematytu. Obserwuje się też występowanie takich minerałów akcesorycznych, jak kalcyt związany z utworzeniem wtórnego albitu.

Przemiany pierwotnych skaleni konsekwentnie stowarzyszone są z chlorytyzacją minerałów ferromagnezowych zarówno w facji zabarwionej na czerwono, jak i w facji niezmienionej kolorystycznie jasnej skały. Chlorytyzacja biotytu jest częściowa w skałach facji jasnej i całkowita w skałach facji zabarwionej na czerwono. Chlorytyzacja biotytu jest związana z rozwojem takich minerałów wtórnych, jak kwarc, skaleń potasowy, prehnit, tytanit i apatyt. Chlorytyzacja amfiboli zaznacza się jedynie w obrębie facji skał zabarwionych na czerwono i jest nieobecna w skałach facji jasnej bez plam o odmiennym zabarwieniu. Minerały typowe dla saussurytyzacji i serycytyzacji są czasem jeszcze widoczne w skałach facji utlenionej/o czerwonawym zabarwieniu. Paragenezy związane z różnymi typami przemian skał granitoidowych prawdopodobnie przenikają się tam nawzajem. Niniejsze studium nie pozwoliło na wydzielenie szeregu kolejno po sobie następujących paragenez mineralnych, ani na przypisanie tak wydzielonych etapów procesów wtórnych poszczególnym wydarzeniom geologicznym, w odróżnieniu od niektórych opracowań z innych obszarów (np. Drake et al., 2009). Na podstawie przeprowadzonych badań wydaje się jednak, że w badanych obszarach doszło do tylko jednego etapu przemian wtórnych, które w różnych miejscach ośrodka skalnego doprowadziły reakcje przemian mineralnych do różnych stadiów zaawansowania. Sukcesje paragenetyczne zaobserwowane w skałach granitoidowych Sudetów miałyby być zatem skutkiem przemieszczania w czasie frontu reakcyjnego

związanego z każdą paragenezą w kierunku od nieciągłości strukturalnych (spękań i uskoków) do wnętrza bloków skalnych wyznaczanych przez te nieciągłości.

Występowanie facji dotkniętych procesami albityzacji/oksydacji przywiązane jest w obu zbadanych masywach Sudetów do stref o geometrii generalnie płaskiej, zalegających połogo lub poziomo i nie przekraczających miąższości ok. 200 m.

Wtórny albit w obrębie facji o czerwonawym zabarwieniu skały jest konsekwentnie przestrzennie związany z występowaniem drobnokrystalicznego hematytu. Datowanie paleomagnetyczne tego hematytu wskazuje na jego triasowe namagnesowanie, co świadczy o utworzeniu się tego minerału w tym okresie. Ponieważ albityzacja zachodziła równocześnie z hematytyzacją, więc również jej można przypisać wiek triasowy, podobnie, jak w niektórych innych masywach waryscyjskich Europy. Zjawiska albityzacji/oksydacji obserwowane w granitoidach polskich Sudetów wydają się pozostawać w związku przestrzennym i przyczynowo-skutkowym z triasową powierzchnią zrównania, o której ówczesnym występowaniu można dodatkowo wnosić na podstawie generalnej geometrii stref występowania tych zjawisk. Wnioskuje się tym samym o przypowierzchniowej, hipergenicznej genezie wspomnianych zmian wtórnych granitoidów sudeckich.

Facja granitoidowych skał zmienionych w procesach albityzacji/oksydacji wydaje się zatem skutkiem oddziaływania przypowierzchniowych zjawisk związanych z triasową powierzchnią zrównania w Sudetach, występującą ówcześnie nieco powyżej dzisiejszego poziomu ścięcia erozyjnego badanych fragmentów masywów granitoidowych. Przedstawiona charakterystyka facji zalbityzowanych/zoksydowanych skał granitoidowych ma szansę zostać w przyszłości wykorzystana jako przydatne narzędzie badawcze, pozwalające na wyjaśnienie niektórych aspektów przestrzenno-czasowych ewolucji podłoża krystalicznego Europy i, tym samym, na uściślenie modeli geodynamicznych i geomorfologicznych dotyczących potriasowej tektoniki i rozwoju rzeźby w masywach górskich i wyżynnych odsłaniających to podłoże.

# CONTENT

## *INTRODUCTION*

*L'étude des régolithes et des paléoaltérations est importante pour la compréhension des relations géodynamiques entre les régions en subsidence et les régions en surrection. Peu d'informations sont disponibles sur les marges des bassins et sur les socles où dominent l'érosion et les altérations. Un grand contraste existe entre la connaissance des bassins sédimentaires et des régions de socle :alors que les dépôts sédimentaires sont subdivisés en séquence temporelle d'environ 100 ka, la résolution temporelle au niveau des socles cristallins n'est que de l'ordre de 100 Ma. Les paléoaltérations ayant affecté les socles cristallins peuvent fournir des jalons de leur longue période d'exposition après dénudation.*

*Le challenge de ce projet de thèse est de démontrer que les albitisations des socles cristallins, observées dans les chaînes Hercyniennes de l'Afrique du nord à la Scandinavie, ne sont pas dues à des circulations tardi-magmatiques profondes ou hydrothermales, mais qu'elles résultent plutôt d'une altération superficielle liée au domaine continental triasique. Ce sujet est susceptible d'amener à reconsidérer les idées sur l'évolution mesozoïque des socles paléozoïques. En effet, si les faciès rouges albitisés des socles hercyniens ne sont pas liés à des phénomènes tardi-magmatiques mais plutôt à une période d'altération continentale, alors ces faciès constitueraient un jalon précieux dans l'évolution géodynamique de ces socles.*

*Pour cela, il est essentiel de démontrer que les faciès rouges albitisés des socles hercyniens ne sont pas liés à des phénomènes tardi-magmatiques mais plutôt à une période d'altération continentale. Un fossé culturel sépare les deux conceptions. L'étude de l'albitisation a été le domaine des pétrographes qui considèrent naturellement les aspects pétrographiques et reconnaissent le caractère tardif de la paragenèse. Cependant, ils n'ont jamais vraiment pris en compte les aspects géométriques du phénomène d'albitisation. Nous devons désormais franchir les "barrières culturelles" pour faire progresser les connaissances dans ce domaine de recherche et échanger les compétences scientifiques en vue de faire évoluer l'argumentation. Pour toutes ces raisons, le projet a été mené par le biais d'un partenariat multidisciplinaire entre l'Institut Géologique Polonaise (PGI-Pologne) et le Centre de Géosciences de Mines-ParisTech (France).*

*Dans ce projet de thèse, l'accent a été mis sur les faciès albitisés du socle des Sudètes Polonaises, car il avait été reconnu précédemment des remagnétisations triasiques dans des roches cristallines de ce secteur. Le but de la présente étude est de vérifier que ces remagnétisations sont associées à de l'albitisation et que celle-ci pouvait être d'origine superficielle. Pour ce faire, nous décrirons d'abord les caractéristiques pétrographiques et minéralogiques des faciès rouges comparativement aux faciès clairs. Une attention particulière sera portée sur les relations entre minéraux primaires et secondaires, en vue d'établir la paragenèse et la géochimie de ces albitisations tout en précisant leur aspect contemporain par rapport à l'hématisation. Ensuite, nous nous attèlerons à présenter les résultats des datations paléomagnétiques réalisées sur ces faciès rouges albitisés en vue de mettre en évidence leur lien avec la paléosurface triasique. Enfin, nous essaierons de suivre la géométrie de la paléosurface triasique en corrélant les différents sites albitisés étudiés et en soulignant les différentes implications géodynamiques dans la région de Kłodzko Złoty-Stok.*

# INTRODUCTION

The study of regoliths and paleoweathering, is vital for understanding the geodynamic relationships between areas of subsidence and areas of uplift. Little information is available concerning basin margins and basement areas where weathering and erosion dominate. One of the requirements for modelling geodynamic evolution is a description and analysis of the paleoweathering profiles affecting the crystalline basements during long periods of continental exposure. Such profiles are the only records available at the edge of the sedimentary basins. A remarkable contrast exists between the knowledge on basin and crystalline basement areas: for example, the sedimentary deposits are often subdivided into temporal sequences of about 100 ka whereas the temporal resolution for the crystalline basement is rather in the order of 100 Ma.

The challenge of this thesis project is to demonstrate that the albitized crystalline basements observed in the Hercynian belt from North Africa to Scandinavia are not due to deep late-magmatic or hydrothermal circulation, but result from superficial weathering that is associated with the Triassic continental domain. This subject is likely to cause serious reconsideration of the ideas on the Mesozoic evolution of the Hercynian basements. Additionally, it is also linked to a paleoenvironmental and climatic question. The albitized facies are characterized by a sodium enrichment of the continental areas, and thus should be considered in association with the accumulation of sodium in the salt deposits of the Triassic basins. The question then arises if this is the imprint of a major global event?

In crystalline domains, albitization is commonly interpreted as related to deep and high temperature metasomatic alteration related to granite cooling during exhumation. At the beginning, it is necessary to present the demonstration that the albitized and reddened facies of the Hercynian basements are not associated with late-magmatic phenomena but correspond to a period of Triassic continental paleoweathering. A major cultural gap separates the two models. Work on albitization has principally been the domain of basement petrographers, who naturally consider the petrographic aspects and recognise the latish character of the parageneses. However, they have never really considered the geometric aspects of the albitization phenomenon. We must now cut across these “cultural barriers” to advance the knowledge in this research domain and to exchange scientific skills to improve the argumentation. For these reasons, the project has been carried out by a multidisciplinary partnership with the Polish Geological Institute (PGI-Poland) and the Geosciences Center of Mines ParisTech (France).

The focus on the albitized facies in the Polish Sudetes have been set for this thesis project, because for this area, first indications for Triassic paleomagnetic datings on remagnetization overprints of the crystalline basement had already been described in literature. Thus, the aim of the presented study is to check whether the albitization observed in the Sudetes could have also been of the above described superficial origin. For this purpose, the distinctive mineralogical and petrographical features of the reddened facies have been described in comparison to the light facies. Emphasize has been laid on the relationship between the primary and the secondary mineral phases, with a view on the establishment of the specific paragenesis and geochemistry for these albitization and with respect to their contemporary nature with hematite. Subsequently, results of the paleomagnetic datings performed on these reddened facies are presented, in order to establish the link with the Triassic paleosurface. Finally, the geometry of the Triassic paleosurface in the Sudetes has been followed by matching the different albitized sites studied in the Kłodzko Złoty-Stok area and by highlighting the respective geodynamical implications.

## *RESUME CHAPITRE 1*

## *ALBITISATION ET PROCESSUS METASOMATIQUES ASSOCIES*

*Ce chapitre traite des phénomènes d'albitisation, de saussuritisation et d'hématisation. L'accent y est principalement mis sur les réactions et les conditions d'occurrence des phénomènes susmentionnés.*

*L'**ALBITISATION** est une altération qui consiste au remplacement des feldspaths primaires, plagioclases et feldspaths potassiques par de l'albite secondaire. L'albitisation des plagioclases peut se faire selon trois réactions et les conditions chimiques ci-après :*

*à silice constante et mobilité de l'aluminium **(equ 1.1),***
*avec apport de silice et mobilité de l'aluminium **(equ 1.2),***
*avec apport de silice et à aluminium constant **(equ 1.3).***

*L'albitisation des feldspaths potassiques se fait par simple remplacement entre K et Na. **(equ 1.4).** En tout état de cause, l'apport de sodium paraît essentiel que ce soit pour l'albitisation des plagioclases ou des feldspaths potassiques.*

*Deux mécanismes fondamentaux d'albitisdation sont envisagés dans la littérature : (1) la diffusion et (2) la dissolution-recristallisation.*

*La **diffusion** consisterait en un simple échange ionique sans réorganisation du réseau cristallin. Celle-ci conviendrait à l'albitisation des feldspaths potassiques à haute température **(equ 1.4),** mais est difficilement concevable pour l'albitisation des plagioclases qui ne se résume pas seulement à un échange ionique mais implique aussi une réorganisation de la structure cristalline du plagioclase primaire (substitutions Si-Al).*

*La **dissolution-recristallisation** se caractérise par la dissolution du feldspath primaire et la recristallisation simultanée de l'albite secondaire à partir d'un fluide sursaturé (Boles, 1982 ; Aagaard et al., 1990 ; Ramseyer et al., 1992 ; Engvik et al., 2008 ; Hövelmann et al, 2010). Elle paraît donc possible pour l'albitisation des feldspaths potassiques et celle des plagioclases. Si la vitesse de dissolution est supérieure à la celle de recristallisation, l'albite secondaire formée est alors poreuse. L'albitisation peut également préserver l'orientation des macles du plagioclase primaire impliquant alors une croissance dite « épitatique » de l'albite liée à la dissolution-recristallisation (Engvik et al., 2008).*

*Les **CONTEXTES GEOLOGIQUES** de l'albitisation sont divers, elle est notamment reconnue dans les socles cristallins et dans les bassins sédimentaires, et plusieurs hypothèses sont envisagées pour l'origine du sodium.*

*En **domaine cristallin**, on distingue deux types d'albitisation : (1) une albitisation pervasive et homogène liée au métamorphisme (Coombs, 1954 ; Boles and Coombs, 1977 ; Moody et al., 1985) et (2) une albitisation limitée aux fractures liée à de l'hydrothermalisme et à des conditions tardi-magmatiques (Val'ter et al., 1993 ; De Jong and Williams, 1995 ; Lee and Parsons, 1997 ; Petersson and Eliasson, 1997 ; Putnis et al., 2007 ; Engvik et al., 2008 ; Plümper and Putnis, 2009 ; Sandström et al., 2010 ; Morad et al., 2010). Le sodium nécessaire à l'albitisation pervasive provient de la destruction de l'analcime (equ. 1.5, Coombs, 1954 ; Boles and Coombs, 1977), tandis qu'il est apporté par des fluides dans le cas de l'albitisation liée à des fractures. Ces fluides sont parfois considérés comme d'origine magmatiques (Aslund et al., 1995). Néanmoins, du point de vue du bilan de masse par rapport aux volumes affectés, les volumes de fluide smagmatiques ne semblent pas suffisants pour fournir de sodium nécessaire (Battles and Barton, 1995; Oliver, 1995) et qu'une source accessoire de Na doivent être envisagée. Les auteurs considèrent généralement que ces fluides sont nourris par des dépôts évaporitiques (Barton and Johnson, 1996;*

*McLelland et al., 2002). Les fluides superficiels et ceux des bassins jouent vraisemblablement un grand rôle dans ce type d'albitisation.*

*En **domaine sédimentaire**, les albitisations sont interprétées comme étant liées à des processus diagénétiques dans les réservoirs pétroliers arkosiques (Merino, 1975; Ogunyomi et al, 1981 ; Boles, 1982 ; Walker, 1984 ; Gold, 1987 ; Saigal et al., 1988 ; Aagaard et al., 1990 ; Morad et al., 1990; Ben Baccar et al., 1993 ; Yu et al., 1997 ; Perez and Boles, 2005 ; González-Acebrón et al., 2012). Ici, le sodium nécessaire à l'albitisation proviendrait du lessivage des dépôts évaporitiques par des eaux météoriques ou du bassin, car les fluides interstitiels même s'ils interviennent dans le processus global ne suffisent pas générer les volumes d'albite formée.*

*Les **albitisations liées aux paléosurfaces** affectent à la fois les roches sédimentaires et cristallines. Ce type d'albitisation a été reconnu dans le Massif Central où il a été démontré qu'il est liée à la paléosurface triasique (Yerle and Thiry, 1979 ; Schmitt, 1986 ; Schmitt and Clément, 1989 ; Parcerisa et al., 2009). Ces albitisations se caractérisent par des profils d'altération de 50-200 m d'épaisseur, d'intensité décroissante depuis la surface vers la profondeur. Trois faciès qui se distinguent par leur pétrographie et l'intensité de l'albitisation ont été proposés (Parcerisa et al., 2009) :*

- *un faciès rouge pervasivement albitisé, qui correspond au sommet des profils, est caractérisé par l'albitisation des plagioclases, la chloritisation des biotites et la formation d'hématite,*
- *un faciès rose/rouge le long des fractures : l'albitisation est intense au niveau des fractures et la minéralogie est identique à la zone précédente,*
- *un faciès tacheté, caractérisé par de petites taches roses et qui correspond à la partie profonde du profil. La minéralogie primaire est globalement préservée et la chloritisation est perceptible même en l'absence d'albitisation.*

*Le caractère superficiel de ce type d'albitisation est renforcé par des datations radiochronologiques K-Ar (Bonhomme et al., 1980 ; Schmitt, 1984 ; Schmitt et al., 1984) et paléomagnétiques (Ricordel et al., 2007), qui montrent toutes des âges triasiques. Les âges paléomagnétiques sont spécifiquement donnés par l'hématite interprétée comme étant cogénétique de l'albite secondaire.*

*Le sodium de ces albitisations proviendrait des grands dépôts de sel du Trias, introduit sur les continents par les vents sous forme de poussières salines (Parcerisa et al., 2009), puis entrainé vers les nappes profondes et les réseaux de fractures (Schmitt, 1986, Schmitt and Simon-Coiçon, 1985).*

*La **SAUSSURITISATION** est une altération qui consiste au remplacement des plagioclases calciques par un assemblage composé d'albite secondaire, de silicates calciques (prehnite, épidote, pumpellyite et laumontite), de séricite et parfois de calcite. (Allaby and Allaby, 1999). La saussuritisation des plagioclases est provoquée par l'instabilité de leur composante anorthitique. Cette réaction libère donc du calcium en excès et elle est généralement associé à plusieurs autres réactions notamment la chloritisation des biotites, qui fournit le potassium pour le développement de séricite et de feldspath potassique, le calcium libéré contribue à la formation de silicates calciques, de titanite et de calcite. Le détail des réactions couplées à la saussuritisation est résumé dans le **tableau 1**.*

*Lorsque l'albite secondaire est associée à la formation de prehnite et d'épidote, le phénomène est considéré comme de la saussuritisation (Eliasson, 1993) tandis qu'il est défini comme de l'albitisation au sens strict quand le plagioclase albitisé ne montre aucune épidote ou prehnite associée (Morad et al., 2010). Il peut cependant être difficile voire impossible de distinguer les deux phénomènes surtout quand la saussuritisation est suivie de l'albitisation*

*car il y a dans ce cas superposition des paragenèses et préservation des minéraux issus de la saussuritisation dans les faciès albitisés. Néanmoins, d'un point de vue pétrographique, certaines différences sont évidentes entre la saussuritisation et l'albitisation. Les paramètres cristallographiques (macles et zonation) sont préservés durant la saussuritisation tandis que les macles sont effacées durant l'albitisation. De plus, les albites issues de l'albitisation sont pures (Słaby, 1992 ; Lee et Parsons, 1997 ; Parcerisa et al., 2009) tandis que celles issues de la saussuritisation contiennent encore une fraction anorthitique (Sandström et al., 2010).*

*L'**HEMATISATION** des roches cristallines est associée quasi systématiquement à l'albitisation. L'aspect rose/rouge de ces faciès a été longtemps négligé dans le passé, car considéré comme étant lié à des processus tardifs (Bastin, 1935 ; Marmo et Hyrvarinen, 1958). Ce n'st que récemment que des études ont été consacrée spécifiquement à l'hématisation des roches granitiques en particulier dans les formations protérozoïques de Forsmark en Suède (Drake et al., 2008 ; Sandström et al., 2010).*

*L'hématisation apparaît parfois pervasive, envahissant toute la roche, mais plus souvent elle est limitée au bordures des fractures, décroisssant en intensité en s'éloignant des fractures. C'est le cas dans les granitoïdes Sudètes Polonaises. Cette relation avec les fractures indique que l'hématisation est liée à la circulation de fluides et résulte donc des interactions fluides-roches. Cela a également été observé en Suède ou le rougiement est interprété comme lié à des circulations hydrothermales induites par l'intrusion proximale des granites d'Uthammar et de Gotemmar (Drake et al., 2008). Cependant, aucune donnée n'est disponible sur la distribution en profondeur de ce rougiement qui semble atteindre 600 m de profondeur (Ehrenborg and Stejskal, 2004a,b ; Ehrenborg and Dahlin, 2005). Dans les albitisations liées à la paléosurface triasique du Massif Centra françaisl,l'hématisation diminue en intensité depuis la surface actuelle vers la profondeur (Schmitt, 1992, Parcerisa et al., 2009).*

*Il a été proposé que les pigments d'hématite colorant les granites étaient d'origines magmatiques (exsolution, cristallisation concomitante avec les feldspaths). Mais cette origine magmatique de l'hématite ne semble guère défendable car les environnements magmatiques sont dominés par des ions $Fe^{2+}$ et non de $Fe^{3+}$ (uniquement dans les magnétites). L'origine de l'hématite en tant que produit des interactions fluides-roches est très largement documentée. Le developpement de l'hématite en liaison directe avec les minéraux ferromagnésiens altérés montre que le fer provient, au moins en partie, de l'altération des ces minéraux. La composition chimique des roches oxydées montrent généralement très peu de changement par rapport aux roches primaires (<5% de changement) (Drake et al., 2008).*

*La formation de l'hématite nécessite une forte fugacité d'oxygène qui ne ne peut provenir que de la surface (atmosphère). Par ailleur, la composition isotopique du fer des hématites montre la contribution de solutions issues de l'altération météorique dans le système hydrothermal à forte fugacité d'oxygène (Markl et al., 2006; Dideriksen et al., 2007, Dideriksen et al., 2010). Dans les cas des hématisations associées aux paléosurfaces, les fluides oxydants de surface contribuent directement à la formation de l'hématite. La datation paléomagnétique de l'hématite constituerait ainsi un argument fort pour établir le lien entre l'hématite et la paléosurface (Ricordel et al., 2007 ; Franke et al., 2010).*

*La **CHLORITISATION** est généralement associée aux faciès albitisés et saussuritisés. Les chlorites apparaissent soit en remplacement des ferromagnésiens primaires à la suite d'interaction fluide-minéral ou formées directement à partir des fluides dans les vides et microfractures. Nonobstant leurs occurrences, les chlorites montrent des compositions chimiques variées au sein des roches altérées. Enfin, il faut souligner que la structure cristallographique des chlorites, avec deux couches de type octaédrique et la*

*possibilité de substitutions tétraédriques, rend le calcul de formule structurale très compliqué, entaché d'hypothèses. Il est illusoire de s'appuyer sur la neutralité électrique pour assurer la répartition du fer en $Fe^{2+}$ et $Fe^{3+}$ et différencier les chlorites par ce critère.*

***Chlorite héritées des minéraux primaires :*** *De façon intuitive, les chlorites héritées des biotites ont une composition différente de celles issues des amphiboles. En effet, les chlorites dérivées des biotites contiennent moins de Si que celles héritées des amphiboles. Cependant des différences apparaissent parfois entre la composition des ferromagnésiens primaires et celle des chlorites héritées. Aussi, la transformation biotite-chlorite peut conduire à une augmentation ou à une diminution de volume en fonction de la composition des fluides et du comportement des ions Mg, Fe, Si et Al.*

***Chlorite héritées de fluides hydrothermaux :*** *Les chlorites peuvent aussi se développer dans des microfractures et des pores des roches chloritisés. La composition chimique de ces chlorites très variée, a souvent été utilisée pour distinguer différentes variétés cristallochimiques au sein d'une même roche. La variabilité de la composition de ces chlorites a été utilisée pour argumenter l'existence d'altérations successives au sein de ces faciès. Cependant, il faut souligner que la composition du fluide varie au cours d'un unique évènement hydrothermal au fur et à mesure que celui-ci traverse la roche et interagit avec les différents minéraux. De ce fait, les chlorites héritées des premières interactions fluide-roche auront des compositions différentes de celles issues des dernières interactions. Par conséquent, des chlorites de compositions variées ne n'impliquent pas nécessairement plusieurs épisodes de chloritisation.*

*Les* ***CONDITIONS THERMIQUES*** *dans lesquelles se font la saussuritisation et l'albitisation peuvent être cernées au moyen d'expériences de laboratoire, de mesures d'inclusions fluides, de modélisations géochimiques, de calculs thermodynamiques et les contextes géologiques dans lesquels on rencontre ces paragénèses minérales.*

***Les températures de la saussuritisation*** *ont d'abord été estimées à partir des équilibres entre épidote, prehnite, laumontite et chlorite lors de l'évolution métamorphique (Spear, 1995). Ainsi il est estimé que la saussuritisation se développe entre 250°C- 400°C (Deer et al., 1992 ; Drake et al., 2008. Les expériences hydrothermales sur les paragenèses de l'épidote indiquent des températures de formation entre 300°C à 400°C (Liou et al., 1983; Frey et al., 1991) tandis que des paragénèses à épidote ont été décrites dans des champs géothermiques actifs entre 125 et 150°C (Bird and Spieler, 2004). Par ailleurs des inclusions fluides on conduit à estimer des conditions P-T plus élevées, entre 400-600°C sous des pressions de 150-250 Mpa (Que et Allen, 1996). Cependant, des températures plus basses ont été trouvées par les calculs thermodynamique, jusqu'à 100°C pour l'épidote ferrifère (Bird and Hegelson, 1981). L'occurrence d'épidote, de laumontite et de prehnite daqns les granitoïdes ne peut donc pas être systématiquement indicatrice de haute température.*

***Les températures de l'albitisation*** *suggérées par les expériences hydrothermales sont de l'ordre de 300°C à 600°C sous des pressions de 200 à 400 Mpa (Moody et al., 1985). Ces températures correspondent à des conditions métamorphiques et hydrothermales. Mais, de l'albitisation a aussi lieu à des témpératures comprises entre 60°C et 100°C dans les bassins sédimentaires (Merino, 1975 ; Saigal et al., 1988 ; Aagaard et al.,1990 ; Morad et al., 1990 ; Hirt et al., 1993 ; Ben Baccar et al., 1993). De plus, l'étude des inclusions fluides des albitisations de roches cristallines dans le Massif Central suggère des températures de l'ordre de 100°C (Georges, 1985).*

*L'albitisation peut donc se faire dans divers environnements géologiques (métamorphiques ou même en surface), d'autant plus que la température de 100°C peut être atteinte à moins de 1 000 m avec un gradient géothermique élevé.*

# CHAPTER 1

# 1 ALBITIZATION AND ASSOCIATED METASOMATIC PROCESSES

## 1.1 ALBITIZATION

Albitization is an alteration phenomenon that consists in the replacement of the igneous primary feldspars (K-feldspars or plagioclases) by secondary albite. Plagioclases and K-feldspars albitization involves chemical exchanges in connection with their respective compositions.

### *1.1.1 Albitization reactions*

#### *1.1.1.1 Plagioclases albitization reactions.*

Plagioclases albitization can proceed through three different reactions depending on the chemical elements supply or loss, and under consideration of subsequent volume changes. Albitization develops only if enough Na is provided and it may be described in the following three reactions:

- ***Constant silica and aluminium release,***

$$3(\underset{Anorthite}{CaAl_2Si_2O_8}) + 2Na^+ + 16H^+ \rightarrow 2(\underset{Albite}{NaAlSi_3O_8}) + 3Ca^{2+} + 4Al^{3+} + 8H_2O \qquad \textbf{(equ. 1.1)}$$

This reaction considers constant silica and subsequently leads to aluminium release. The number of mole of the formed albite represents two thirds the number of mole of the initial anorthite and leads to 30% volume loss.

- ***Silica supply and aluminium release***

$$\underset{Anorthite}{CaAl_2Si_2O_8} + Na^+ + SiO_2(aq) + 4H^+ \rightarrow \underset{Albite}{NaAlSi_3O_8} + Ca^{2+} + Al^{3+} + 2H_2O \qquad \textbf{(equ. 1.2)}$$

The volume is approximately conserved during this reaction. Under conservation of the original crystalline frame, one mole of anorthite is replaced by one mole of albite requiring addition of sodium and silica.

- ***Silica supply and constant aluminium***

$$\underset{Anorthite}{CaAl_2Si_2O_8} + 2Na^+ + 4SiO_2(aq) \rightarrow 2(\underset{Albite}{NaAlSi_3O_8}) + Ca^{2+} \qquad \textbf{(equ. 1.3)}$$

This third reaction shows the conservation of the molar balance of aluminium and reveals that the mole's number of the neogenic albite is the double with respect to the initial anorthite.

The calcium released during the albitization could either be leached by present fluids or be involved in the crystallization of Ca-bearing minerals. Those neogenic minerals may be silicates such as prehnite, laumontite, epidote, or non-silicates minerals such as calcite, gypsum and apatite.

#### *1.1.1.2 K-feldspars albitization*

K-feldspars albitization proceeds through the following reaction:

$$\underset{Orthose}{KAlSi_3O_8} + Na^+ \rightarrow \underset{Albite}{NaAlSi_3O_8} + K^+ \qquad \textbf{(equ. 1.4)}$$

The albitization of K-feldspars also requires $Na^+$ supply and releases $K^+$. A possible sink for the released potassium may be the precipitation of K-bearing minerals such as sericite.

### *1.1.2 Albitization mechanisms*

The mechanisms of albitization have been studied through petrographic observations, and/or by isotopic analyses (i.e. $^{18}O$). Two types of mechanisms can be distinguished (1) diffusion and (2) dissolution-recrystallization.

Albitization by simple diffusion process implies a simple Na exchange. This may be possible for K-feldspars albitization during which K and Na may exchange without any major disruption of the original silicate framework and is possible at high temperature, but rather difficult at lower temperature. Diffusion is difficult to be assumed for plagioclase albitization that requires also $Al^{3+}$ replacement by $Si^{4+}$, and thus a disruption of the silicate framework. Recent studies suggest rather dissolution-recrystallization mechanisms for albitization reactions.

Dissolution-recrystallization processes are characterized by feldspar dissolution (K-feldspars or plagioclases) and a simultaneous precipitation of albite from an oversaturated fluid (Boles, 1982; Aagaard et al., 1990; Ramseyer et al., 1992; Engvik et al., 2008; Hövelmann et al, 2010). If the primary crystalline structures are preserved, this would mean that the dissolution and the recrystallization occur in the same time related to an interface-coupled dissolution-recrystallization mechanism (Putnis et al., 2005; Engvik et al, 2008). The “thin fluid” confined to the mineral-fluid interface may be very different from that of the bulk fluid (Putnis and Putnis, 2007; Putnis and Ruiz-Agudo, 2013). Indeed, oxygen isotope studies show that the oxygen isotope composition changes between the primary and secondary feldspar phases pointing to a recrystallization of the silica and aluminium tetrahedron and re-equilibration with solution (Fiebig and Hoefs, 2002; Cole et al., 2004).

Albitized feldspars often show some micro-voids and are often associated with fractures and fluid infiltration (ref Clark et al., 2005). The development of micro-voids allows aqueous fluids to penetrate the rock (Hövelmann et al., 2010). These voids are interpreted as the results of faster dissolution and recrystallization kinetics (dissolution faster than the recrystallization; Engvik et al., 2008). They may also be seen as the results of a volume loss during the albitization reaction (aluminium loss, cf equation 1.4).

Secondary albite most often exhibits the crystallographic orientation of the primary plagioclases or one of the original twinnings orientations. This indicates that the crystallographic orientation of primary plagioclases acts as “nucleus” for the development of the secondary albite and that albitization proceeds through the primary twinnings. Preservation of the crystallographic orientation of the primary plagioclase demonstrates the epitatic growth of the albite and the related dissolution-recrystallization mechanisms (Engvik et al., 2008).

## 1.2 GEOLOGICAL OCCURRENCE OF ALBITIZATION

Albitization is a frequent alteration phenomenon known in various geological and tectonic settings. It affects in particular the crystalline and metamorphic rocks of the ancient massifs, but it is also described in sedimentary deposits.

### *1.2.1 Albitization in crystalline rocks*

Two types of albitization have been described in crystalline rocks such as tonalite, gabbro, granite, gneiss:

(1) Pervasive albitization affecting rocks homogeneously related to low grade metamorphism (Coombs, 1954; Boles and Coombs, 1977; Moody et al., 1985);

(2) Albitization bound to fractures related to hydrothermal and late magmatic processes (Val'ter et al., 1993; De Jong and Williams, 1995; Lee and Parsons, 1997; Petersson and Eliasson, 1997; Putnis et al., 2007; Engvik et al., 2008; Plümper and Putnis, 2009; Sandström et al., 2010; Morad et al., 2010).

#### *1.2.1.1 Origin of the sodium.*

Albitization during low-grade metamorphism may result from a dehydration of the zeolite facies by the reaction:

$$\text{“}NaAlSi_2O_6.H_2O_{\boldsymbol{analcime}} + SiO_2 = NaAlSi3O8_{\boldsymbol{albite}} + H_2O\text{”} \quad \textbf{\textit{(equ. 1.5)}}$$

described by Coombs (1954) and Boles and Coombs (1977). Here, albite forms directly from the analcime breakdown without any additional sodium supply. Nevertheless, the analcime breakdown may also happen without any systematic precipitation of albite (partially substituted by quartz), and the release of Na and Al feeding the albitization of the inherited plagioclases (Coombs, 1954).

The fracture-controlled albitization must be obviously related to fluids flow through the fractures. It is generally admit that the sodium must be added to the system. Sodium may originate directly from late-magmatic fluids (Aslund et al., 1995). Nevertheless, mass balance considerations with regard to the rock volume affected by the albitization versus the hypothesized volume of magmatic fluids and their sodium content seem in disaccord (Battles and Barton, 1995; Oliver, 1995). As Na-bearing fluids are ubiquitous near to the surface of the Earth, an alternative origin of the sodium may be hydrothermal fluid feed by superficial brines related to evaporitic deposits or directly by brines of evaporatic basins (Barton and Johnson, 1996; McLelland et al., 2002). Moreover, the fracture-controlled albitization is supposed also to be triggered by the superficial fluids penetrating the rock during its exhumation (Holness et al., 2003).

Anyway, the fracture controlled albitization appears related to fluids of suitable relative high sodium contents. It appears undoubtedly that superficial and/or basin fluids must play a major role in these albitization processes.

### *1.2.2 Albitization in sedimentary deposits*

Albitization in sedimentary environments are interpreted as related to diagenetic processes of arkosic formations in particular with respect to petroleum reservoirs (Merino, 1975; Ogunyomi et al, 1981; Boles, 1982; Walker, 1984; Gold, 1987; Saigal et al., 1988; Aagaard et al., 1990; Morad et al., 1990; Ben Baccar et al., 1993; Yu et al., 1997; Perez and Boles, 2005; González-Acebrón et al., 2012).

#### *1.2.2.1 Origin of the sodium*

Given the fact that, a sufficient $Na^+$ concentration is necessary for the albitization of the feldspars, several hypotheses on the origin of sodium have been proposed in the framework of the sedimentary context.

Basin fluids may contribute to the albitization process, nevertheless their sodium content is usually considered as being insufficient to justify the mass balance of the observed albitizations, and thus an additional sodium supply seems to be required (Aagaard et al., 1990).

In order to unravel this issue, leaching of halite deposits by meteoric water or basin fluids have been suggested (Saigal et al., 1988; Aagaard et al., 1990). The latter hypothesis may be possible for basins bearing salts levels, nevertheless it does not match with all basins. For basins without halite deposits, it is assumed that the sodium could originate from expulsion of the marine pore waters during burial (Walker, 1984), or from the alteration of the detrital sodium-rich plagioclases (when only the K-feldspar are albitized) (Walker, 1984; Morad, 1986).

### *1.2.3 Albitization related to the paleosurface*

In general, albitization has been interpreted as related to hydrothermal or diagenetic processes, nevertheless studies in the French Massif Central (Yerle and Thiry, 1979; Schmitt, 1986; Schmitt and Clement, 1989; Parcerisa et al., 2009) highlighted albitization events related to the Triassic paleosurface. This paleosurface-related albitization has been described in crystalline environments as well as in the Permo-Carboniferous sediments. According to these studies, the superficial albitization develops according to 50 to 200 m thick alteration profile with a decreasing intensity from the Triassic paleosurface toward the depth (Schmitt, 1992; Parcerisa et al., 2009).

Parcerisa et al., (2009) defined three albitization facies according to their petrographic characteristics, colour and albitization intensity.

- **Reddish facies**: A reddish, intensively and pervasively albitized facies that corresponds to the top of profile (closed to the surface), with albite, chlorite and hematite as the dominating secondary mineralogical phases

- **Pink facies or pink-fracture facies**. A pinkish facies in which albitization is controlled by the fractures, and which matches to the middle part of the profile, Typically the intense albitization is limited here to fracture walls; albite, chlorite and hematite appears as the main mineralogical phases.

- **Spotted facies**: A spotted facies corresponding to the deeper part of the profile which is characterized by small pink alteration spots within the unaltered rocks. The primary mineralogy is globally preserved nevertheless the chloritization of mafic minerals is well expressed since the rocks are entirely chloritized even when no albitization is

expressed directly. It seems like the chloritization is linked to the albitization but appears in a slightly earlier stage.

From a mineralogical point of view, plagioclases albitization is associated with biotites chloritization (Yerle and Thiry, 1979), including the development of tiny mineralogical inclusions such as calcite, titanite, and apatite (Parcerisa et al., 2009). Muscovite may also be albitized (Schmitt, 1986; Clément, 1986).

#### *1.2.3.1 Dating of the albitization related to the paleosurface*

Several age estimations were carried out on these albitized facies. First datings were performed by using the K-Ar method (Bonhomme et al., 1980; Schmitt, 1984; Schmitt et al., 1984). These datings indicate that the albitization in the French Massif Central correspond to the upper limit of the Trias (200-210 Ma). More recently paleomagnetic dating of the hematite associated with the albitized granite facies in the Morvan (French Massif Central) also resulted in Triassic age (Ricordel et al., 2007).

Triassic remagnetizations have been also found in reddened facies of the crystalline unit of the Kłodzko Złoty-Stok Massif (Sudetes, Poland, Edel et al., 1997; Franke et al., 2013). Hematite of these pinkish/reddish facies crystalline facies appears as tiny inclusions in the neogenic albite, within the albitized plagioclases as well as in the albitized K-feldspars. This hematite is interpreted as cogenetic of the albitization/alteration.

Moreover, as the altered Palaeozoic granites are part of the Triassic paleosurface, hematite is clearly related to the paleosurface, and consequently albitization has to be related to the Triassic paleosurface.

#### *1.2.3.2 Origin of the sodium*

Several paleo-environmental assumptions have been made to argue on the sodium origin during the albitization process related to the Triassic paleosurface. The albitization in the Massif Central is linked to the surface evolution in connection with confined sodic-rich environments, emplace during hot and dry climate conditions (Yerle and Thiry, 1979). The sodium present in the albitization process may originate from the widespread Triassic salt deposits. It could have been brought to the landsurfaces by eolian transport as salt particles from the Triassic evaporitic basin (Parcerisa et al., 2009) and the Na-enriched groundwater brines subsequently migrated to depth through the fracture networks (Schmitt, 1986, Schmitt and Simon-Coiçon, 1985).

The albitization could have also been favoured by the long period of post tectonic stability and subsequent exposure of the massifs relative to the Triassic inconformity (Parcerisa et al., 2009).

## 1.3 SAUSSURITIZATION

Ca-rich plagioclases in granitoïds are often altered with a characteristic mineral assemblage composed of secondary albite, Ca-silicates (epidote, prehnite, and frequently also laumontite and pumpellyite) next to sericite, and in some cases calcite (Allaby and Allaby, 1999). The crystallographic orientation of the primary plagioclase is preserved, including the layout of the polysynthetic twins and often the distribution of the secondary Ca-silicates tallies with the zoning of the primary plagioclase that implies an alteration conservative of the volumes (Goldschmidt, 1916; de la Roche, 1957).

### *1.3.1 Saussuritization reactions*

There are several coupled reactions that occur during saussuritization (Table 1). Saussuritization is firstly inducted (provoked) by the thermodynamic instability of anorthite and intermediary Ca-plagioclases at low-temperature and in presence of water or hydroxyls. Anorthitic plagioclase instability triggers saussuritization.

Whatever will be the secondary Ca-silicate that form, there is always Ca released in excess. It implies the coupling of anorthite alteration to other reactions that consume Al, mostly the formation of sericite, or even of K-feldspar, if K is available. K may be provided from the biotite chloritization that is frequently associated with the saussuritization. In most cases the biotite transformation is pseudomorphic, with a rather small net volume change, Al-conservation, and the release of iron that forms magnetite and even pyrite sprinkled between the altered flakes (Nakamura et al., 2010). There is release of considerable amount of potassium (Chayes, 1955; Parry and Downey, 1982). Biotite chloritization corresponds to a true breakdown of the biotite crystal, accompanied by a redistribution of elements including oxygen isotopes in both tetrahedral and octahedral sheets of the biotite (Fiebig and Hoefs, 2002). Moreover, in the granitic rocks from the Proterozoic basement of SE Sweden, that have been extensively studied recently, it appears that the saussuritization intensity is directly linked with the chloritization intensity (Morad et al., 2010). Accessory minerals containing Fe, F, and Ti, such as magnetite, hematite, titanite, rutile, apatite, and fluorite are often associated with these chloritized biotites.

Indeed, biotite chloritization appears as a potential source of potash for sericite formation associated with the saussuritized plagioclases. Biotite alteration may be triggered by Fe oxidation. At all, no alteration of the Ca-plagioclase will happens if the system remains blocked, without introduction of $H_2O$ or $O_2$ (de la Roche, 1957).

**Table 1 – Saussuritization reactions including plagioclase albitization, biotite chloritization and the development of epidote, prehnite, laumontite, sericite, K-feldspars, and accessory minerals such as titanite and pumpellyite.**

***Tableau 1 – Les réactions de la saussuritisation montrant l'albitisation des plagioclases, la chloritisation des biotites et le développement d'épidote, de prehnite, de laumontite, de séricite, de feldspath potassique, ainsi que de minéraux accessoires tels que la titanite et la pumpellyite.***

| | | | | |
|---|---|---|---|---|
| **plagioclase alteration** | | | | |
| ***epidote / prehnite*** | | | | |
| $3(Na_{0.33}Ca_{0.66}Si_{2.33})$ | ➔ | $NaAlSi_3$ + | $Ca_2Al_3Si_3$ | + Al + Si |
| *labradorite* | | *albite* | *epidote (anhydre)* | |
| | | | *prehnite (hydrated)* | |
| ***laumontite*** | | | | |
| $3(Na_{0.33}Ca_{0.66}Si_{2.33})$ | ➔ | $NaAlSi_3$ + | $CaAl_2Si_4$ | + 2Al |
| *labradorite* | | *albite* | *laumontite* | |
| ***calcite*** | | | | |
| $3(Na_{0.33}Ca_{0.66}Si_{2.33}) + CO_2$ | ➔ | $NaAlSi_3$ + | $2(CaCO_3)$ | + 4Al + 5Si |
| *labradorite* | | *albite* | *calcite* | |
| **biotite chloritization** | | | | |
| $3(Si_3Al)(Mg_{1.5}Fe^{2+}_{1.5})K + O_2$ | ➔ | $2(Si_{3.25}Al_{0.75})(Fe^{3+}_2)(Mg_{2.25}Al_{0.75})$ | | + 0.5 Fe + 2.5 Si + K |
| *biotite* | | *chlorite* | | |
| $3(Si_3Al)(Mg_1Fe^{2+}_2)K + O_2$ | ➔ | $2(Si_{3.25}Al_{0.75})(Fe^{3+}_2)(Mg_{1.5}Fe^{2+}Al_{0.75})$ | | + 2.5 Si + K |
| *biotite* | | *chlorite* | | |
| **sericite and K-feldspar development** | | | | |
| 3.3Si + 2,7Al + 0.7K | ➔ | $(Si_{3.3}Al_{0.7})Al_2K_{0.7}$ | | |
| | | *séricite* | | |
| 3Si + Al + K | ➔ | $KAlSi_3$ | | |
| | | *K-feldspar* | | |
| **accessory minerals** | | | | |
| Ca + Ti + Si | ➔ | $CaTi(SiO_5)$ | | |
| | | *titanite* | | |
| Ca + Mg + Fe + Al + Si | ➔ | $Ca_2(Mg,Fe^{2+})Al_2Si_3$ | | |
| | | *pumpellyite* | | |

### *1.3.2 Saussuritization versus albitization*

Most of the times, saussuritization is coupled with plagioclase albitization. Nevertheless, authors frequently make distinction between albitization and saussuritization. When plagioclase alteration in albite is associated with epidote and sericite formation, the process is considered as saussuritization (Eliasson, 1993). On the other hand, the process is interpreted as a strict albitization when the altered plagioclase does not show any epidote or sericite (Morad et al., 2010). However, saussuritization comes always along with development of albite and thus it is difficult to distinguish both alterations, especially if plagioclase saussuritization is followed by an albitization. In this case, earlier formed minerals that are characteristic for saussuritization, such as epidote, prehnite and sericite, may remain unchanged or may be altered during the albitization. It has been specified that crystallographic characteristics of the primary plagioclase, including twining and zoning, are preserved during saussuritization (de la Roche, 1957; Sandström et al., 2010), while twins are erased during the plagioclase albitization (Parcerisa et al., 2009). Furthermore, secondary albites resulting from albitization are pure (Słaby, 1992; Lee and Parsons, 1997; Parcerisa et al., 2009) whereas those developed during saussuritization remain Ca-bearing (An<10%) (Sandström et al., 2010).

## 1.4 HEMATITIZATION

Crystalline rocks (granite, diorite, tonalite, etc) often show characteristic red to pink colouration due to (i) hematite pigments included in the feldspars, (ii) development of hematite granules in the vicinity of the ferromagnesian minerals, or even (iii) hematite deposits along micro-fractures in the rock. Only few attentions were drawn to these facies in the past. Crystalline rock petrography studies are rather focused on primary facies and their relation with magmatic processes and often neglect the red and pink facies, which are obviously related to secondary, post magmatic processes.

In older studies these facies were only mentioned and mainly considered as resulting from post-magmatic hydrothermal process (Bastin, 1935; Marmo and Hyvarinen, 1958). The question was reviewed by Boone (1969) who demonstrated that the iron oxides cannot be issued by exsolution processes of iron from the feldspars during magmatic cooling. Recently, more studies have been focused on hematitization, e.g. in granitic rocks in the Paleoproterozoic bedrocks of the Forsmark of central Sweden. This study is promoted by the investigation for a potential geological depository of highly radioactive nuclear waste (e.g. Drake et al., 2008; Sandström et al., 2010).

### *1.4.1 Spatial distribution*

Pervasive red-staining of granitic rocks was sometimes indicated. This is the case of the alkaline ring structures of the Oslo Graben (Norway) where reddish granite (Drammen batholith) and larvikite (monzonite) have been mapped separately and considered as primary facies or hydrothermally altered facies (Trønnes and Brandon, 1991). Nevertheless, most abandon red-staining in granitic rocks appears as related to fractures which is also the case of the facies studied in the Sudetes massif, where the reddening is bound to fracture walls and fluid circulation. Here, the reddening appears intense at the fracture walls and decreases in intensity further away from the fracture walls. This relationship between fractures and reddening suggests that it is related to fluid-rock interactions.

This is also the case of the Laxemar-Simpevarp area (SE Sweden) where the red-staining is adjacent to fractures and thought to be related to fluid-rock circulation associated to the intrusion of the Gotemmar and Uthammar granite nearby (Drake et al., 2008). Plümper and Putnis (2009) associated the red-staining with feldspars alteration in the vicinity of fractures.

Besides, in the Laxemar-Simpevarp area (SE Sweden) red-stained samples were observed up to a depth of 600 m below the present-day surface. About 25 to 40% of the drill cores have been mapped as red-stained (Ehrenborg and Stejskal, 2004a, 2004b; Ehrenborg and Dahlin, 2005), but nothing is known about the distribution of this reddening with depth: is it uniform or decreasing as apparently it disappears at depth?

Nevertheless, an intensity profile of the reddening with depth has been established to between 50 to 200 m for the French Massif Central (Schmitt, 1992; Parcerisa et al., 2009). Facies close to the actual surface are pervasively red, and they become less and less red with depth until in the end the coloration is scarce and finally disappears. This distribution of the reddening towards the depth clearly implies a closed link between the reddening and the oxidizing superficial conditions. Moreover, Schmitt (1992) and Parcerisa et al., (2009) suggested that the reddening in the oxidized facies of the French Massif Central are directly related to the Triassic paleosurface.

### *1.4.2 Iron origin*

It has been suggested that hematite pigment staining the granitic rocks may either be crystallized in parallel with the feldspar from the granitic melt, or they have been exsolved by solid state exsolution from the $Fe^{3+}$-bearing orthoclase solid solution [(K,Na)(Al $Fe^{3+}$)Si3O8]; Ernst, 1960; Neuman and Christie, 1962). This hypothesis of "primary magmatic" origin of the oxidized iron is difficult to defend in magmatic environments that are characterized by the dominance of $Fe^{2+}$, that is in particular present the ferromagnesian minerals. Primary $Fe^{3+}$ is mostly restricted to magnetite in mafic Fe-rich granitoïds. Moreover, Putnis et al. (2007) have shown that hematite in granitic rocks results from fluid-rock interactions and can not be considered as a solid state exsolution product from the feldspars.

Fluid-rock interaction has been forwarded by all recent studies devoted to red-staining of the granitic rocks (Boone, 1969; Putnis et al., 2007; Drake et al., 2008; Engvik et al., 2008, Sandström et al., 2010). The development of hematite pigments and granules in the vicinity of the ferromagnesian minerals of the red-stained rocks points out that the iron origins, at least partly, from the alteration of these minerals. In a similar way, the oxidation of magnetite also participates in the scattering of hematite pigments. Hematite deposits along micro-fractures in the red-stained rocks may result from the iron released during ferromagnesian mineral alteration, or either be introduced by Fe-bearing fluids subsequent to the crystallization of the granite. The changes in chemistry generally show very small changes (<5% change) between the red-stained rocks and the reference (primary) rock (Drake et al., 2008).

This fact raises the problem of the origin of the alteration and especially of the origin of the oxygen necessary to oxidize the primary $Fe^{2+}$of the ferromagnesian minerals.

### *1.4.3 Oxygen origin*

A high oxygen fugacity is necessary to form hematite. The oxygen can not originate from deep environments (nor magmatic or basin diagenetic fluids), it can only be found in superficial environments in exposure to the atmosphere. Therefore, the oxygen for hematite formation has clearly been brought into the hydrothermal system by fluids from the surface. The Fe-isotope composition of hematite emphasizes the contribution of superficial weathering solutions into the hydrothermal system as responsible of high oxygen fugacity (Markl et al., 2006; Dideriksen et al., 2007, Dideriksen et al., 2010). In that case, the oxidizing solutions would reach the depth through gigantic convective circulation systems, in relation with the cooling down of the granite massif (Taylor, 1977; Hoefs and Emmermann, 1983; Putnis et al., 2007; Drake et al., 2008). In the case of a spatial relation of the red-staining with a paleosurface, oxidizing fluids may relate to the infiltration of weathering solutions and groundwater flow at continental scale. Thus, paleomagnetic dating of the present hematite appears as the major argument to tightly link hematite crystallization with a geologically constrained paleosurface (Ricordel et al., 2007; Franke et al., 2010).

## 1.5 CHLORITIZATION

Chloritization is a process generally evoked for saussuritized and albitized granitoïd rocks. Chlorites occur in these facies either as isomorphic replacement of primary biotite and amphibole (Parry and Downey, 1982; Veblen and Ferry, 1983; Eggleton and Banfield, 1985) and/or as fillings in voids and microfractures (Parneix et al., 1985; Drake and Tullborg, 2006; Drake et al., 2009, Morad et al., 2011). Chlorite replacing amphibole and biotite may result from fluid-mineral interaction (Putnis, 2002), whereas those filling the microfractures precipitated directly in the fluids (Wilamowski, 2002). Regardless to the occurrence of chlorite, they show a wide range of chemical compositions within the altered rocks.

Finally, the crystallographic structure of chlorite with two types of octahedral layers and the possibility of tetrahedral substitutions makes the calculation of the structural formulae of chlorite very complicated and blemish with many hypotheses. In particular, it is not realistic to rely only on the electrical neutrality for the distribution of the iron $Fe^{2+}$ and $Fe^{3+}$ to differentiate the chlorite by this criterion. Hence, great caution must be taken as considering these interpretations.

### *1.5.1 Chlorite related to parental minerals*

Intuitively, chlorite substituting biotite may have a different composition compared to that replacing amphibole. Indeed, it appears that chlorite derived from biotite shows lower Si-content than chlorite formed from amphibole (Meunier et al., 1988). This appears in agreement with the chemistry of the parental ferromagnesian minerals, since biotites classically show lower Si-content in comparison to amphiboles. Moreover, Morad et al., (2011) indicate that chlorite replacing biotite in the Äspö crystalline rocks (SE-Sweden) are Fe-rich compared to the chlorite replacing amphiboles, which are Fe-poor. Besides, Parneix et al., (1985) established the influence of the parental biotite chemistry on the composition of the chlorite growths, because Mg-rich parental biotite allows the formation of Mg-rich chlorite.

Nevertheless, some differences may occur between the composition of the parental ferromagnesian minerals and that of the filial chlorite. Depending on the fluid composition and the behaviour of Mg and Fe, as well as Al and Si, the biotite-chlorite transformation may lead to volume expansion (Parneix et al., 1985) or shrinkage (Ferry, 1979, Parry and Downey, 1982; Veblen and Ferry, 1983).

### *1.5.2 Chlorite related to hydrothermal fluids*

Chlorite may also develop in micro-fractures and within the pores ofchloritized rocks. The chemical composition of these chlorites is relatively variable. The mentioned chlorites were clearly precipitated from fluids circulating within the micro-fractures. The chemical composition of these chlorites has often been used to distinguish different crystallo-chemical varieties within an altered facies or even within the same sample. The variability of the chemical composition of these chlorites was used to argue on the existence of successive alteration events within these facies (Drake and Tullborg, 2006; Sandström et al., 2008; Drake et al., 2009; Morad et al., 2011).

Nevertheless, caution must be paid when interpretating the different varieties of chlorite. Besides, during a single hydrothermal event, the fluid composition may change with time as it circulates through the rock and interacts with the minerals: (1) the fluid releases chemical elements and takes in others elements, hence its chemical composition progressively changes during its circulation through the rock; (2) the chemical composition of the rock also changes with time caused by the alteration and therefore fluid-rock exchanges will not be the same at the beginning and during the ongoing alteration process; (3) finally, towards the

center of the blocks, further away from the fractures of the hydrothermal circulation, diffusion exchanges will prevail and these processes are controlled by others kinetic laws.

Hence, chlorite resulting from the first fluid-rock interactions may not have the same composition as those inherited from later interactions. Therefore, chlorites of various compositions do not necessarily imply several chloritization events.

## 1.6 THERMAL CONDITIONS OF THE ALBITIZATION AND SAUSSURITIZATION DEVELOPMENT

Thermal conditions of the mineral parageneses equilibriums may be approached by various manners: laboratory experiments, study of present day natural conditions, measurement of fluid inclusions, general geological framework of the occurrences, and even geochemical modelling.

### *1.6.1 Thermal conditions for saussuritization*

Stability fields of the symptomatic epidote, laumontite and prehnite minerals of the saussuritization have been estimated in a first step in connection with metamorphic pathways and facies (Spear, 1995). In principle, the metamorphic limits are defined by the disappearance of a mineral belonging to the presumed lower metamorphic grade paragenesis in favour of another mineral belonging to a higher metamorphic grade paragenesis. Thus, the limit between the zeolite facies (laumontite, analcime, heulandite) is characterized by the disappearance of the laumontite in favour of prehnite.

Saussuritization has therefore been presented as occurring between 250 and 400°C by considering that 250°C correspond to the lowest limit of prehnite stability, while 400°C is the upper limit of chlorite stability (Deer et al., 1992; Drake et al., 2008).

Nevertheless, laumontite disappearance at 250°C may not correspond to the first prehnite appearance during the saussuritization/metamorphism and therefore prehnite may have a lower stability limit. Prehnite may appear as soon as laumontite is destabilized, and laumontite destabilization may begin long before 250°C, where it disappears completely. This shows that prehnite may form at temperatures lower that 250°C, coexisting with laumontite in the studied rocks.

Fluid inclusions have also been used to estimate the stability domains of saussuritization paragenesis. In this way, alteration related to saussuritization of the Rosses Granite Complex (Ireland) was estimated to occur under P-T conditions of 150-250 Mpa and 400-600°C (Que and Allen, 1996). Such an approach was conducted in the granites of the potential geological depository for nuclear waste in the Forsmark in central Sweden. Fluid inclusions of quartz in successive veins are associated with laumontite and epidote paragenesis (Drake and Tullborg, 2009). The 195°C temperature corresponds to the homogenization temperature of fluids inclusions in quartz veins presumed as contemporaneous to the laumontite, while the 370°C temperature corresponds to the inclusion in quartz associated to epidote.

Epidote paragenesis has been approached by hydrothermal experiments between 300 and 400°C (Liou et al., 1983; Frey et al., 1991), but has never been successfully synthesized at low pressures and temperatures (Coombs et al., 1959; Merrin, 1960; Fyfe, 1960). Nevertheless, epidote was discovered in drill hole samples from active geothermal logs that provided samples of epidote altered rocks and coexisting hydrothermal fluids. In these occurrences, epidote has been found in equilibrium with laumontite at 125°C and with prehnite-laumontite at 150°C (Bird and Spieler, 2004).

Thermodynamic equilibrium calculations have also been used to estimate the formation temperature of epidote. Epidote equilibrium with laumontite has been calculated at 125°C and with prehnite-laumontite at 150°C (Bird and Spieler, 2004). Besides, clinozoisite (Al-epidote) appears in equilibrium with quartz below 225°C, while Fe-epidote is stable around 100°C (Bird and Hegelson, 1981). This suggests that epidote may possibly form at low temperature (~100°C); thus it appears that epidote, laumontite, and prehnite occurrences in altered granitic facies are not exclusively indicative of high temperature conditions.

### *1.6.2 Thermal conditions of albitization*

Hydrothermal experiments were undertaken to estimate the albitization temperature of plagioclase. Experiments were carried out at temperatures ranging between 300 and 600°C, with pressures between 200 and 400 MPa, using a mixture of labradorite, albite, clinozoïsite, and in the presence of Na2SiO3 solution (Moody et al. 1985). The obtained temperatures suggest that the albitization occurs between 300 and 550°C and at pressure around 200 MPa. These conditions fit with metamorphic and hydrothermal conditions at about 10 km depth. The experiments show that albitization may potentially happen under these conditions, but it doesn't mean that albitization exclusively takes place under these conditions.

Plagioclase albitization as well as K-feldspar albitization have been described relative to sandstone diagenesis in several oil-fields (Merino, 1975; Saigal et al., 1988; Aagaard et al.,1990; Morad et al., 1990; Hirt et al., 1993). These albitizations occur at much lower temperatures as those described before. Temperature measurements in the bore holes indicate that the thermal conditions range between 65 and 120°C. Such albitization conditions have been tested by geochemical modelling and it was shown that albitization decreases with increasing temperature. For low $pCO_2$ conditions, it probably occurs between 60 and 100°C, while for higher volumes of $CO_2$ albitization continues at temperatures > 100°C (Ben Baccar et al., 1993). Moreover the models show that the fluid composition, especially the Na/K ratio, is a limiting factor and that the kinetic of the reactions are essential (Ben Baccar et al., 1993; Perez and Boles, 2005).

Fluid inclusion studies on the albitization that affects the basement rocks in the French Massif Central (Georges, 1985) reveal that: (1) fluid inclusions in albite are monophasic, which suggests relative low temperatures (~100°C), (2) and that fluid inclusions in contemporaneous quartz are NaCl-rich and have homogenization temperatures that lie between 135 and 140°C.

Therefore albitization appears possible in a wide range of geological environments, from metamorphic domains until near surface environments, since 100°C may be reached at less that 1000 m depth under high geothermic gradient.

.

## *RESUME CHAPITRE 2*

## *CONTEXTE GEOLOGIQUE*

*Ce chapitre résume le contexte géologique des Sudètes en général ainsi que les caractéristiques géologiques spécifiques aux massifs de Kłodzko Złoty-Stok (Fig. 2) et de Karkonosze (Fig. 3) au sein desquels des albitisations rouges caractéristiques apparaissent.*

***Les Sudètes** correspondent à la marge Nord-Est du massif des bohèmes, et montrent plusieurs ensembles de roches métamorphiques, ignées, et volcano-sédimentaires d'âges paléozoïques. Les accidents majeurs dominant dans les Sudètes sont la SBF (Faille bordière des Sudètes) et la ISF (Faille intra-Sudétique) (Fig. 1). Le carbonifère y est marqué par de nombreuses intrusions granitiques dans les roches préexistantes. On distingue deux générations d'intrusions : celles du carbonifère inférieur dont fait partie le massif de Kłodzko Złoty-Stok ainsi que celles du Carbonifère supérieur à laquelle appartient le massif de Karkonosze.*

***Le massif de Kłodzko Złoty-Stok (KZS)** situé dans les Sudètes centrales est composé pour l'essentiel de granite, de granodiorite, et de monzodiorite. (Fig. 2, Wierzchołowski, 1976 ; Bachliński and Bagiński, 2007). Les granitoïdes de KZS sont composés de quartz, de plagioclases, de hornblende, de feldspath potassique, de biotite et de minéraux mineurs tels que la titanite, l'apatite, l'allanite et d'oxydes de fer.*

***Le massif de Karkonosze** se localise dans la partie ouest des Sudètes et est surtout dominé par des unités granitiques variées, en l'occurrence porphyritiques, à grains moyens et à grains fins (Fig. 3). La composition minéralogique de ces granites est sensiblement identique à ceux de KZS, sauf que la hornblende ici n'apparaît que dans la variété porphyritique.*

# CHAPTER 2

# 2 GEOLOGICAL SETTING

## 2.1 THE POLISH SUDETES

The Polish Sudetes correspond to the north-east margin of the Bohemian massif (Fig. 1). They are made of mosaic of various Palaeozoic metamorphic, igneous, and volcano-sedimentary units, deformed mostly during the Variscan-late Devonian and Carboniferous tectonic events (Aleksandrowski & Mazur 2002; Mazur et al. 2006). These crystalline units are unconformably overlain by upper-Devonian to Carboniferous and Permian clastic and volcanic formations of local syn- and post-orogenic intramontane basins and troughs (eg. Nemec et al. 1982; Porebski 1990, Awdankiewicz 1999).

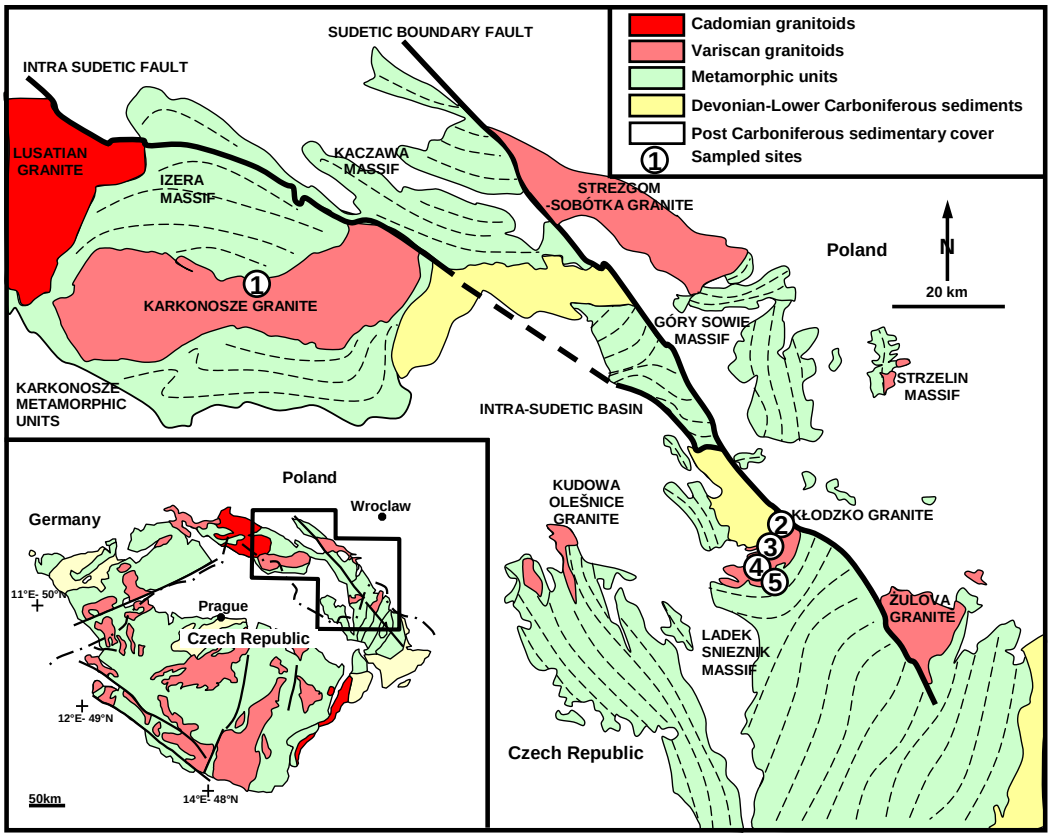


**Figure 1 - Geological map of the Sudetes (modified after Aleksandrowski et al., 1997). (1) Szklarska Poręba quarry ; (2) Laski quarry ; (3) Laskivillage ; (4) Chwalisław valley; (5) Chwalisław mountain.**

***Figure 1 – Carte géologique des Sudètes (modifié d'après Aleksandrowski et al., 1997). (1) Carrière de Szklarska Poręba ; (2) carrière de Laski ; (3) village de Laski ; (4) vallée de Chwalisław; (5) Montagne de Chwalisław.***

The major tectonic accidents that dominate the Sudetes are the Sudetic Boundary Fault (SBF) with a NW-SE trend, and the Intra Sudetic Fault (ISF) with a WNW-ESE trend (Fig. 1), both of Variscan descent, with prominent Cenozoic reactivation in the former case. These major brittle events are accompanied in the east by the Variscan, ductile Niemcza, Złoty-Stok i Stare Mesto shear zones of NNE-SSW to NE-SW trend (Mazur et al. 2006) that extend the south into the SE edge of the Bohemian massif.

During the Carboniferous several late- to post-orogenic granitic bodies intruded the previous units (Mazur et al., 2007). The Variscan orogeny (upper-Devonian to lower Carboniferous) that resulted in the emplacement of these granitic bodies was related to the

collision between the Gondwana and the Laurentia continental plates (eg Winchester & Pace, 2002).

Two Variscan granitoïds generation can be identified (cf Mazur et al., 2007): (1) the lower-Carboniferous granitoïds located in the central part of the Sudetes, and close to the Sudetic Boundary Fault (Žulowa massif, Kudowa massif, Olesnice massif, Kłodzko Złoty-Stok massif), and (2) the voluminous Upper-Carboniferous granitoïds mainly situated in the central and the western parts of the Sudetes (Karkonosze massif, Strzegom-Sobótka massif).

With a focus on the main albitizations features observed in the Sudetes granitoïds, this study is concentrated on the Kłodzko Złoty-Stok (Fig. 2) massif and the Karkonosze pluton (Fig. 3).

## 2.2 KŁODZKO ZŁOTY-STOK MASSIF

### *2.2.1 General characteristics*

The Kłodzko Złoty-Stok massif situated in the central-Sudetes is a Lower-Carboniferous granitic intrusion dated to around 331 Ma according by Rb-Sr method (Bachłinski and Halas, 2000).

It is limited in the South-East by the Cambrian metamorphic units of Ladek Śnieżnik (Gunia, 1984; Turniak et al., 1998), to the north-west by the Paleozoic metamorphic units of Kłodzko and in the North-East by the Sudetic Boundary Fault (SBF, Fig. 1). The Kłodzko Złoty-Stok intrusion consists in granite, granodiorite, monzodiorite, monzonite and hornfelses (Fig. 2).

Granite, granodiorite, tonalite, monzonite and monzodiorite are the main rocks that form the Kłodzko Złoty-Stok massif whereas diorite and syenite are less common (Wierzchołowski, 1976; Bachliński and Bagiński, 2007).

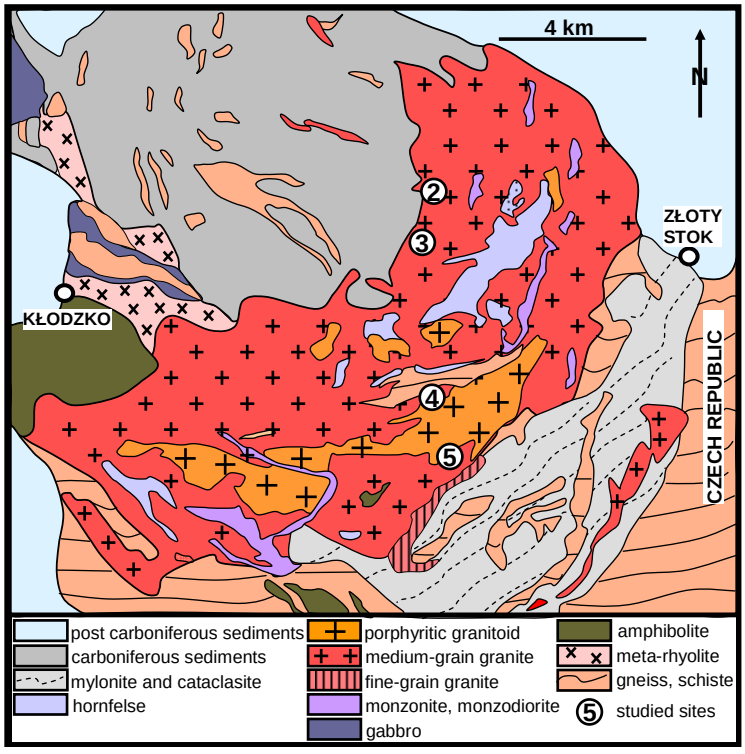


**Figure 2 - Simplified geological map of the Kłodzko Złoty-Stok massif (modified after Sawicki., 1980).**

***Figure 2 – Carte géologique simplifiée du massif du Kłodzko Złoty-Stok (modifiée d'après Sawicki, 1980)***

### *2.2.2 Petrographical and mineralogical characteristics*

Granitoïd rocks that composed the Kłodzko Złoty-Stok massif are made of quartz, hornblende, plagioclases, K-feldspars, biotite, clino-pyroxenes, and some minor minerals such as apatite, zircon, allanite, titanite, and iron oxides (Bachliński and Bagiński, 2007). The plagioclases are of andesine, labradorite and rarely of oligoclase composition. Albite occurs only as secondary mineral resulting from a metasomatic alteration of the anorthitic plagioclases. Anti-perthitic microclines, often with double albite-pericline twins, are the major K-feldspars, biotites are chloritized and the hornblendes show different colorations (Bachliński and Bagiński, 2007).

## 2.3 KARKONOSZE MASSIF

### *2.3.1 General characteristics*

In the Western part of the Sudetes, the Karkonosze massif is undoubtedly the most voluminous granitic intrusion in the Polish Sudetes. The intrusion emplacement happened between 311-330 Ma ago according to the Rb-Sr datings (Borkowska et al., 1980; Duthou et al., 1991). Similar age values of 315 and 318 Ma were also obtained by the SHRIMP method (Machowiak and Armstrong, 2007). It intruded the Izera metamorphic units and is limited in the North-East by the Intra Sudetic Fault (ISF). Three specific granitic facies are known in the Karkonosze massif: (1) porphyritic biotite granite, (2) medium biotite granite, and (3) two micas granite (Borkowska et al., 1980).

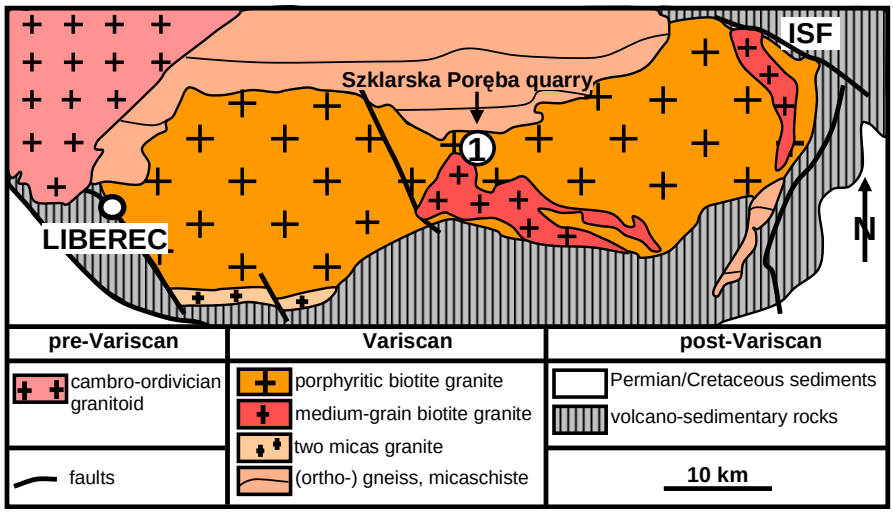


**Figure 3 - Simplified geological map of the Karkonosze massif (modified after Zak et al., 2009). The quarry intersects the contact between the porphyritic granite and the medium-grained granite. ISF=Intra Sudetic Fault.**

***Figure 3 - Carte géologique simplifiée du massif de Karkonosze (modifiée d'après Zak et al., 2009). La carrière de Szklarska Poręba se trouve au contact du granite porphyrique et du granite moyen. ISF: Faille intra sudétique.***

### *2.3.2 Petrographical and mineralogical characteristics*

The Karkonosze granite varieties are composed of K-feldspars, plagioclases, quartz, biotite, and minors mineralogical phases such as allanite, zircon, and apatite (Mazur et al., 2007). The amphiboles (hornblende) occur only in the prophyritic variety in which K-feldspars are often present as orthoclase phenocrysts. The Karkonosze massif granitoïd rocks are systemically chloritized. Two chlorites types have been recognized: (1) flake morphology and resulting from the biotite alteration along the cleavages planes; (2) rosette morphology, formed directly from fluids precipitation in pores (Wilamowski, 2002).

## *RESUME CHAPITRE 3*

## *METHODES*

*Ce chapitre présente les méthodes employées pour l'étude des faciès rougis identifiés dans les Sudètes, notamment la procédure d'échantillonnage, la minéralogie aux rayons X, la démagnétisation thermique pour l'étude des oxydes de fer, la pétrographie en cathodoluminescence, et la spectroscopie à dispersion d'énergie (EDS) .Les échantillons ont été sélectionnés en fonction de leur aspect rouge, de leurs relations texturales par rapport aux fractures, dans les régions de Laski, de Chwalisław (KZS) et de Szklarska Poręba (Karkonosze massif). Les faciès clairs et rouges ont été systématiquement prélevés en vue de mettre en évidence d'éventuelles différences entre ces faciès. Des lames minces pour l'étude pétrographique ont été préparées à partir de ces échantillons, les échantillons ont été broyés pour l'étude minéralogique aux rayons X, et des carottes orientées ont été prélevées pour le paléomagnétisme.*

***La cathodo-luminescence** est la lumière émise par une surface bombardée par un faisceau d'électrons. La pétrographie en cathodoluminescence permet de distinguer les minéraux primaires luminescents de haute température des minéraux secondaires non luminescents formés à basse température ou en surface (Kastner, 1971 ; González-Acebrón et al., 2012). Ces analyses de cathodoluminescence ont été réalisées à l'Université de Wrocław, en utilisant un dispositif constitué d'un canon à cathode froide montée sur un microscope optique. Les images prises par un appareil CANON Coolpix ont été ensuite traitées à l'aide du logiciel PHOTOSHOP en vue d'améliorer leurs qualités. Les feldspaths primaires apparaissent ainsi luminescents tandis que les feldspaths secondaires ne le sont pas (Kastner and Siever., 1979; Ramseyer et al., 1992; Finch and Klein, 1998), la calcite apparait en orange (Machel, 1985), la fluoroapatite en jaune (Blanc et al., 1994), le zircon en blanc brillant, et la titanite en vert terne (Parcerisa et al., 2009).*

***Les analyses aux rayons X** ont été utilisées pour reconnaître les phases présentes ainsi que leur estimation semi-quantitative. Ces analyses ont été réalisées à MINES ParisTech, au moyen du système PANanalytical X'Pert (méthode des poudres) associé à une cathode de cuivre, et un détecteur X'Celerator. Les diagrammes ont été traités par le logiciel EVA © software (Giencke, 2007). L'stimation semiquantitave a été effectuée à partir des rapports d'intensité de référence ($I/I_{cor}$: I = Intensité du pic principal du minéral; $I_{cor}$ = intensité du pic principal du corundon). La caractérisation fine des feldspaths (albite, microcline, orthose) a été faite sur fractions séparées avec déconvolution des diagrammes à l'aide du logiciel Fityk (Wojdyr, 2010).*

***La démagnétisation thermique** permet en plus de l'estimation des âges des oxydes de fer, l'identification et la caractérisation des oxydes de fer qui représentent parfois moins de 5 % de la roche totale (Rayons X). Cette démagnétisation a été réalisée, sur les carottes dont les azimuts et inclinaisons ont été mesurés sur le terrain, au moyen d'un magnétomètre cryogénique à l'Institut de Physique du Globe de Paris (IPGP). Les données ont été ensuite traitées à l'aide du logiciel PaleoMac 5 (Cogné, 2003), qui permet de choisir les directions paléomagnétiques moyennes par site ainsi que le calcul statistique du pôle paléomagnétique (Fischer, 1953 ; Mc Fadden et McElhinny, 1988).*

***SEM/EDS** est basée sur l'utilisation des rayons X émis lorsqu'une surface solide est bombardée par un faisceau d'électrons. Ces analyses ont été effectuées sur des lames minces au laboratoire du LSCE et à Mines ParisTech. D'abord, des analyses élémentaires point par point ont été réalisées sur chaque zone d'intérêt, ensuite des images numériques obtenues. Enfin, ces images ont été traitées et ont permis de caractériser les minéraux présents.*

# CHAPTER 3

# 3 MATERIALS AND METHODS

The samples for this study were collected in the Laski and Chawlisław valley (Kłodzko Złoty-Stok massif) and in the Szklarska Poręba quarry (Karkonosze massif) in southern Poland. The sampling sites were selected according to their reddish or pinkish aspect of the outcropping facies with respect to their textural relationship with the present fractures. The focus was drawn on large sections where the textural relationships with fracturing were the most noticeable. A particular attention has been paid on the additional sampling of the primary (unaltered) facies for highlighting the differences with the red facies due to the changes during the alteration. In addition to the hand samples taken for the petrographic investigations, oriented drill cores were collected for further paleomagnetics studies.

The handsamples were cut in cubes from which thin sections were prepared for petrographical studies; a small fraction of the cubes was crushed for X-Ray diffraction (XRD) mineralogical analyses.

## 3.1 CATHODOLUMINESCENCE PETROGRAPHY

### *3.1.1 Principles*

Luminescence is the light emitted by a surface bombarded by an electron beam (cathode tube). In minerals, the luminescence is caused by the amount of trace element, impurities in the structures or by lattice defects. Trace elements can be activators (enhancing the luminescence) or quenchers (decaying the luminescence); the luminescence observed is the results of the ratio between activators and quenchers (Pagel et al., 2000; Götze and Kempe, 2009). Thus, cathodoluminescence CL images may inform about the igneous formation conditions as well as the post magmatic history of a rock or a mineral (Ramseyer and Mullis, 1990; Kempe et al., 1991, 1999; Götze et al., 2000, 2001). CL is a useful tool to understand mineralogical changes during the main geological processes such as magmatism, metamorphism, diagenesis, hydrothermal alteration or even surface related alteration and weathering.

### *3.1.2 Cathodoluminescence for primary and secondary minerals characterization*

CL has often been used to distinguish primary minerals, formed under high-temperature conditions, from secondary minerals, formed at lower temperature or even under superficial conditions (Kastner, 1971; González-Acebrón et al., 2012). In general, primary minerals crystallized under magmatic conditions show a bright luminescence whereas the same minerals formed under superficial conditions are rather non-luminescent. Thus CL petrography often helps to distinguish primary from secondary minerals.

Moreover, CL often shows mineral growth sequences which are not visible in common petrographic microscopy, and this provides supplementary information on the geometrical relationship between the minerals and their crystallization conditions.

Furthermore, alteration processes often involve primary and secondary minerals that have similar optical characteristics and thus are not easily recognizable by classic optical microscopy. In that case, CL petrography allows to highlight geometrical/genetical relations between minerals and to unravel some issues in alteration phenomenon such as feldspars albitization (Ramseyer et al., 1992; Pagel et al., 1996; Leichman et al., 2003). Therefore, CL is a useful tool for a better understanding of low-temperature feldspar albitization (Leichman et al., 2003; Parcerisa et al., 2009; González-Acebrón et al., 2012).

### *3.1.3 Methodology*

Selected thin sections from the albitized rock samples were studied using the cathodoluminescence technique. The analyses were performed at the Wrocław Geological Institute using a *CL MK3* cold cathode gun mounted on a polarizing optical microscope. Pictures were captured with a *NIKON COOLPIX* camera associated to the microscope device. Raw images were treated using the *ADOBE PHOTOSHOP* software. The treatment technique for each image consists in correcting the tone range and colour balance by adjusting shadow mid-tones and clear intensity levels.

For a complete interpretation of the petrographical observations a set of three images (plane polarized, cross polarized, and CL) have systematically been taken for each investigated thin section zone or mineral. Final interpretations result from the analyses of these three image types.

The analyzed rocks (thin sections) have been chosen taking into account their degree of albitization, their reddening (oxidation state), their connection/relationship with the fractures in the rock, as well as their position towards the regional geological structure. .

### *3.1.4 CL properties of minerals*

Basic CL characteristics for several minerals have been considered in the following study: (1) secondary minerals are usually non-luminescent while primary igneous feldspars are luminescent (Kastner and Siever., 1979; Ramseyer et al., 1992; Finch and Klein, 1998); (2) calcite appears orange (Machel., 1985); (3) zircon is rather white and brilliant; (4) fluoro-apatite is yellow (Blanc et al., 1994); (5) titanite is green and dull (Parcerisa et al., 2009).

## 3.2 XRD

The mineralogy was studied by performing X-Ray diffraction analyses on homogenized powder bulk samples. When it was possible within an uncrushed sample (regarding the size of the crystals, in particular with respect of the K-feldspars), sub-samples of single crystals were extracted and subsequently homogenized and analyzed. The XRD provided the global mineralogy and a semi-quantitative estimation of the present mineral phases.

### *3.2.1 Equipment and references*

XRD analyses have been performed using a PANalytical X'Pert Powder X-Ray diffraction system fitted with a Cu-Anode and X'Celerator detector. XRD scans were run from 2 to 60° (2Θ). The XRD diagrams have been interpreted with the EVA© software developed by BRUKER (Giencke, 2007). The software provides all basic methods of diagram analysis, such as background substraction, Kα2-stripping, data smoothing, calculation of profile parameters (e.g. line position, integrated area, Wide at Half Maximum (WHM)), crystallite size determination by the Scherrer method, mineral phase identification, search for solid solutions and quantitative phase analysis based on RIRs (Reference Intensity Ratios). Reference files from the International Centre for Diffraction Data (ICDD PDF2 data file) have been used for the mineral phase identification.

### *3.2.2 ICDD reference files*

About 100 reference files of all the minerals expected in the studied series have been selected from the ICDD PDF2 data file to build a restrained data base in order to assure homogeny and steady phase determination and comparable quantitative estimation. A special attention has been drawn to the feldspar identification files. All selected feldspar files refer to the calculated XRD patterns by Borg and Smith (1969). Nevertheless, special attention has to

be made on the fact that no adapted orthoclase file exists that would be needed for pure K-orthoclase in the ICDD PDF2 data file base. Thus, the selected reference file of orthoclase matches with an orthoclase corresponding to the structural formula ($K_{0,91}Na_{0,08}Ca_{0,01}AlSi_3O_8$), which means that it is a solid solution between ~90% orthoclase and ~10% of albite-rich plagioclase.

### *3.2.3 Quantitative appraisal*

Reference Intensity Ratios ($I/I_{cor}$: I = Intensity of most peaks of the mineral; $I_{cor}$ = intensity of most of the intense peaks of corundum) have been applied for quantitative appraisal of the determined minerals. Since $I/I_{cor}$ ratios are not available for all the published ICDD files, we used our own restrained data file as average value of the ratios available in the ICDD PDF2 data file. For alkali feldspar species, we applied an $I/I_{cor}$= 0.8 for the orthoclase and the albite and an $I/I_{cor}$= 0.6 for the microcline. We are aware that the calculated values are not the true values, and that those would possibly provide even better quantitative assessment, but the applied method will at least garantie a consistent estimation within our sample series.

### *3.2.4 Peak deconvolution*

In order to determine precisely the alkali feldspars peak positions and the accurate value of their peak intensities, a XRD diagram profile fitting and peak decomposition (deconvolution) has been conducted on selected sub-samples of orthoclase phenocrysts. Peak deconvolution has been performed using the *Fityk* software (Wojdyr, 2010). The simulated Pearson VII function that fits best the XRD peak shapes (Hall et *al*., 1977) has been chosen to deconvolute the signal. Peak positions have been calibrated by the known position of quartz that is always present in the studied phenocrysts

### *3.2.5 Alkali feldspar identification*

The alkali feldspar group (K, Na)$AlSi_3O_8$ comprises sanidine (K) and orthoclase (K) that are monoclinic, and microcline (K), anorthoclase (Na, K) (sometimes called soda-microcline) and albite (Na) that are triclinic. There are two main changes that occur within the alkali feldspar group: the change of the crystal system between monoclinic and triclinic structure and the chemical composition with a more or less miscible series between Na and K end members.

The crystallographic system relates to the distribution of the $AlO_4$ tetrahedrons in the silicate framework: disordered arrangement of the Al tetrahedrons is relative to the monoclinic structure, whereas ordered arrangement of the Al tetrahedrons is due to the triclinic structure. The disappearance of the mirror plane in the triclinic crystallographic system causes the split of each crystallographic plane of the monoclinic system into two distinct planes in the triclinic system. This change from the monoclinic to the triclinic structure is well marked on the alkali feldspars diffraction signal, in particular by the splitting of one single orthoclase peak into two distinctive microcline peaks (Fig. 4). In order to have the best identification, the most significant peaks (easily detectable and relatively isolated from other peaks) have to be chosen. The XRD peaks relative to the (130) and ($1\bar{3}0$) crystallographic planes are well appropriated to discriminate the orthoclase and microcline abundance (Goldsmith & Laves, 1954).

The chemical composition of the alkali feldspars, in particular the range of the solid solution between Na and K can also be estimated by XRD analyses. Most diffraction peak positions are more or less affected by the Na-K substitution. This is particularly the case for the peak relative to the ($2\bar{0}1$) crystallographic plane of the albite, which is not affected by the Ca-content, and the ($2\bar{0}1$) plane of the orthoclase which is common to orthoclase and microcline (Fig. 4).

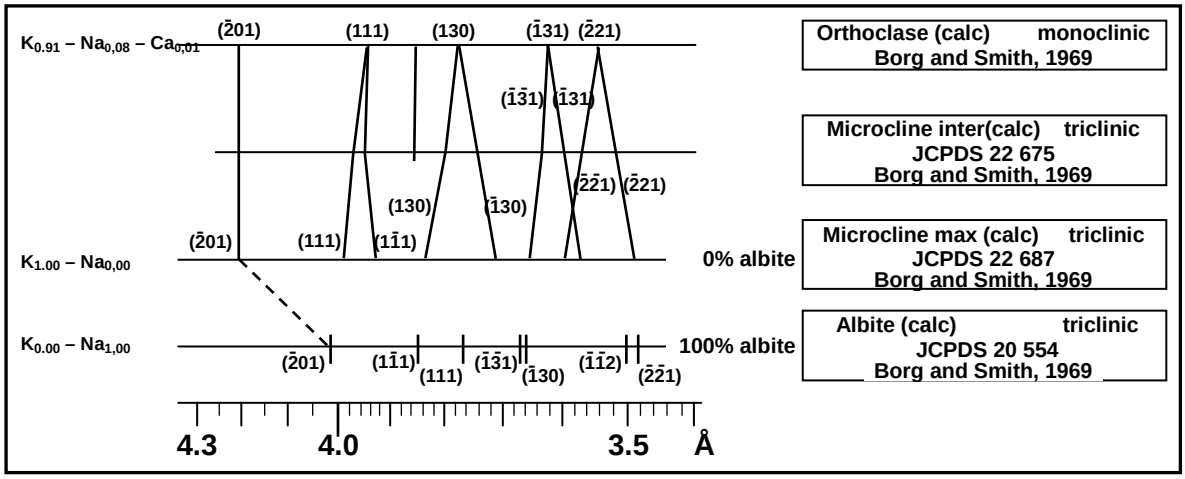


**Figure 4 - Chart showing the position and the shift of the indicative XRD peaks of the alkali feldspar mineral group relative to their crystallographic structure and their chemical composition. The chart illustrates the splitting of the XRD peaks of the orthoclase into two microcline peaks as well as the shift of the peaks due to Na-K substitution.**

***Figure 4 – Diagramme schématique montrant la position et le déplacement des raies de diffraction caractéristiques des feldspaths alcalins aux rayons X en fonction de leurs structures cristallographiques et de leur composition chimique. Le diagramme illustre bien la séparation du pic de l'orthoclase en deux pics de microcline ainsi que le décalage de la raie (2¯01) dû à la substitution Na-K.***

## 3.3 THERMAL DEMAGNETIZATION

Standard bulk sample X-ray diffraction is usually not very sensitive enough to detect iron oxide minerals in proportions < 5% in total, which is very common for natural rock samples. Therefore, we take advantage of the sensitivity of the thermal demagnetization technique that has been performed to achieve paleomagnetic age estimations on the iron oxides present in the albitized facies.

In total five sites were paleomagnetically sampled in the Kłodzko Złoty-Stok massif, using a gasoline powered hand drill machine equipped with a water-cooled diamond drill bit. Paleomagnetic drill cores were oriented in the field using a standard orientation tool (magnetic compass) that permits to recover the inclination and azimuth angle of the sample relative to the outcropping crystalline rock. In the laboratory, the drill cores are cut into standard 2.5 x 2.5 cm cylinders for thermal demagnetization experiments that were subsequently performed on the cylinders in the paleomagnetic laboratory of the Institute du Physique du Globe de Paris (IPGP) using a vertical three-axial 2G cryogenic magnetometer. Stepwise demagnetization of the NRM was applied on the samples, starting at room-temperature and embracing the complete temperature range up to the hematite temperature interval around 700°C. The resulting data is systematically corrected for the geographic site position and orientation of each individual sample.

Further data processing was performed using the PaleoMac 5 software (Cogné, 2003). Characteristic paleomagnetic directions were determined by a least-square straight line analysis (Kirschvink, 1980) in orthogonal Zijderveld diagrams (Zijderveld, 1967), either on equal areas or in great circle fits. The PaleoMac 5 software offers the opportunity to choose the respective site-mean directions and paleomagnetic pole statistics calculation (Fischer, 1953; Mc Fadden and McElhinny, 1988).

## 3.4 SEM/EDS AND ACC SYSTEM

### *3.4.1 Principles*

EDS (Energy Dispersive Spectrometry) in scanning electron microscopy consists in the use of the X-ray spectrum produced when a focussed electron beam bombards a solid surface, in order to obtain a restricted chemical composition. This technique allows an elemental analysis and to some extent chemical characterization of a sample. Chemical characterization by using EDS is common in Earth sciences, and specifically in mineralogic and petrologic studies (Reed, 2005). EDS can be useful for answering questions on topics such as mineral identification, mineral compositional evolution, conditions of minerals crystallization, and fluid-rock interaction.

### *3.4.2 Methodology*

SEM/EDS analyses were performed on selected thin sections from the altered facies in order to unravel compositional issues highlighted by the optical and cathodoluminescence microscopy. These questions are related to the albitized aspect of the partially altered plagioclases and K-feldspars, the nature of the observed lenses within the cleavages of the ferromagnesian minerals, and the characterization of some mineralogical inclusions.

The selected thin sections were coated with carbon to create a conductive surface needed for SEM analyses. The SEM/EDS analyses were performed: (1) In collaboration with Eric Robin at the LSCE/Gif-sur-Yvette using a JEOL 840 scanning electron microscope (SEM) coupled to an X-ray microanalysis system from Princeton Gamma Tech (PGT); (2) At Mines-ParisTech JEOL 840 scanning electron microscope (SEM) coupled to the Xflash 4010 X-ray microanalysis system from Bruker AXS.

### *3.4.3 5.1.3 ACC data treatment*

EDS point per point elemental analyses were conducted on each zones of interest of the selected thin sections. The obtained elemental data have been treated using an algorithm routine called ACC (Automated Counting and Classification) which allows to characterize points within crystals according to their chemical composition (Bernard et al., 1989, Robin et al., 2003). The routine consists then in applying a threshold to the obtained elemental analyses data based on the predefined theoretical mineral composition allowing the definition of minerals classes. A numerical image is obtained, then binarized and filtered according to the defined classes allowing the automatic sorting of the analyzed crystals. Image resolution is $525 \times 490$ pixels while their magnification is about $300\times$.

The ACC classification was carried out to highlight points of K-feldspar, albite, plagioclase and prehnite composition, as well as amphibole, chlorite and sericite composition in order to show spatial distribution and mutual relationships of these minerals.

## RESUME CHAPITRE 4

## *OXYDATION/ROSIMENT DES GRANITOÏDES DES SUDETES*

*Les faciès oxydés/rouges se localisent pour l'essentiel dans la région de Laski et de Chwalisław au sein dans le massif de Kłodzko Złoty-Stok et dans la carrière de Szklarska Poręba à l'intérieur du massif de Karkonosze.*

***La coupe monzonitique de la vallée de Laski*** *est très fracturée, et présente une altération rouge soutenue, pervasive et homogène, si bien qu'on y distingue plus aucun faciès clair (Fig. 5 et Fig. 6). Un système de fractures conjuguées de direction N65°-N70° et N10°-N15° découpe la roche en blocs polyèdres décimétriques et ces fractures sont systématiquement enduites d'hématite. La pigmentation rouge est surtout visible au niveau des feldspaths, et des minéraux verdâtres (probablement des chlorites) sont aussi perceptibles dans ces faciès (Fig. 7).*

***La coupe de la carrière de Laski*** *correspond à une granodiorite marquée par des fractures découpant la roche en blocs métriques (Fig. 8, Fig. 9). Les épontes des fractures majeures et mineures présentent systématiquement une altération rouge/rose. Cette altération se caractérise par une coloration rouge intense aux épontes des fractures et décroît graduellement en intensité en s'éloignant des fractures (fig. 8). Les fractures rouges montrent des minéraux ressemblant à de la chlorite et les feldspaths y sont rouges, tandis qu'à l'écart des fracture les feldpath restent clairs (Fig. 10). L'hématite est moins évidente que dans le cas de la vallée de Laski, mais la pigmentation rouge est vraisemblablement due à la présence d'hématites.*

***La carrière de Szklarska Poręba*** *montre deux variétés de granites : un granite fin à moyen et un granite porphyritique. Le granite fin est particulièrement compact montrant une coloration rose le long des fractures et une coloration plutôt verdâtre à l'intérieur des blocs (Fig. 11, Fig. 12). L'épaisseur de la zone rose le long des fractures varie entre 5 et 15 cm. Lorsque les fractures sont éloignées les unes des autres, le granite fin reste de couleur verdàatre, non oxydé, à l'intérieur des blocs délimités par les fractures. Quant au contraire les fractures sont rapprochées ou fréquentes, les blocs de granite apparaissent entièrement rougis ou rosis. Deux systèmes de fractures prédominent dans cette coupe : un système majeur de direction N40° avec un espacement de l'ordre de 0.1 à 1 m, et un système mineur de direction N135°. Les minéraux ne sont pas aisément distinguables dans le faciès fin, néanmoins la pigmentation rose est probablement due à la présence d'hématites dans les feldspaths (Fig. 13).*

*En fait la grande partie de la carrière est formée de granite porphyritique gris, présentant des phénocristaux de feldspaths potassiques (FK), et une abondance de minéraux sombres. La coloration rose et/ou la pigmentation rouge n'apparaissent pas dans cette variété prophyritique qui est arénisé en sommet de coupe.*

***La vallée de la Chwalisław*** *(en aval du village) se caractérise par une altération de coloration rose le long des plans de fractures et des spots roses d'altération loin des fractures (Fig. 14, Fig. 15, Fig. 16). Cette carrière est formée d'une granodiorite intrudée par des veines de lamprophyres. Elle montre deux directions de fractures : N-S et N60°. L'altération rouge y est peu intense et suit les plans de fractures de direction parallèles à celle des lamprophyres (Fig. 14). Il n'existe pas de relation directe entre les lamprophyres et l'altération rouge d'autant plus que ces dernières présentent des petits plagioclases rosis et albitisés (Awdankiecwicz et al., 2010). Les granodiorites et les lamprophyres sont affectés par le même type d'altération rouge incluant probablement l'albitisation des plagioclases. L'oxydation se développe le long des fractures et affecte des points millimétriques au sein de*

*la roche. Par endroits, la granodiorite de la vallée de Chwalisław montre des phénocristaux de FK roses, vraisemblablement colorés par des pigments d'hématite.*

***La montagne de Chwalisław-Kopciowa** située au sud-est du village, montre des similitudes avec la granodiorite de la vallée. Il s'agit d'une granodiorite présentant une altération rouge à rose limitée aux plans de fractures (front de 2-5 mm d'épaisseur), et des points roses loin des fractures. Cette granodiorite est intrudée par des veines de lamprophyres, et en contact avec les gneiss protérozoïques de Haniak. Les phénocristaux de FK sont roses au contact des fractures, mais restent blancs au-delà de 1 cm des fractures (Fig. 19). Les lamprophyres aussi bien que les gneiss de Haniak au contact de la granodiorite montrent également une altération rose/rouge des feldspaths (Fig. 20). Les feldspaths rouges des lamprophyres ont été interprétés comme étant albitisés durant la phase tardi-magmatique (Nemec, 1966).*

***Hématisation et albitisation** : La coloration rouge/rose des faciès oxydés étudiés dans les Sudètes est due à la présence de granules ou de pigments d'hématite dans les feldspaths. Ces feldspaths roses/rouges apparaissant aussi dans les lamprophyres sont systématiquement interprétés comme étant de l'albite secondaire issue de l'altération tardi-magmatique des plagioclases primaires (Awdankiewicz and Awdankiewicz, 2010). Puisque les feldspaths dans les autres faciès (granodiorite, monzonite) montrent des similarités avec ceux des lamprophyres, ceux-ci pourraient également être albitisés. Cependant, les conditions de ces albitisations semblent ne pas être tardi-magmatiques compte tenu de la présence d'hématites associée à l'albite secondaire qui requiert des conditions plus oxydantes.*

*Cette altération rouge/rose pourrait probablement correspondre à l'albitisation des feldspaths primaires. Ainsi, On pourrait distinguer trois facies d'albitisation/oxydation à travers les sites étudiés : (1) une albitisation rouge, intense et pervasive (vallée de Laski), (2) une albitisation rouge/rose limitée aux plans de fractures (carrière de Laski, montagne de Chwalisław et Szklarska Poręba), (3) une albitisation faible le long des fractures et des points roses dispersés au sein de la roche (vallée de Chwalisław).*

# CHAPTER 4

# 4 REDDENING/OXIDATION PATTERN IN THE POLISH SUDETES FACIES

Oxidized/albitized facies are localized in Laski and Chwalisław area within the Kłodzko Złoty-Stok massif, and in the Szklarska Poręba area within the Karkonosze massif. They are characterized by typical reddish to pinkish alteration in the studied sections. This reddish alteration occurs either as pervasive or as bound along the fracture planes and may also appear as some small pink spots within the rocks.

## 4.1 LASKI VALLEY

Laski valley comprises oxidized facies, showing pervasive and homogeneous reddish alteration (Fig. 5). This section situated in the center of the Laski village, is composed of fine-grained granitoïd rock with a composition close to quartz-monzonite, and it does not show any non-altered or primary facies.

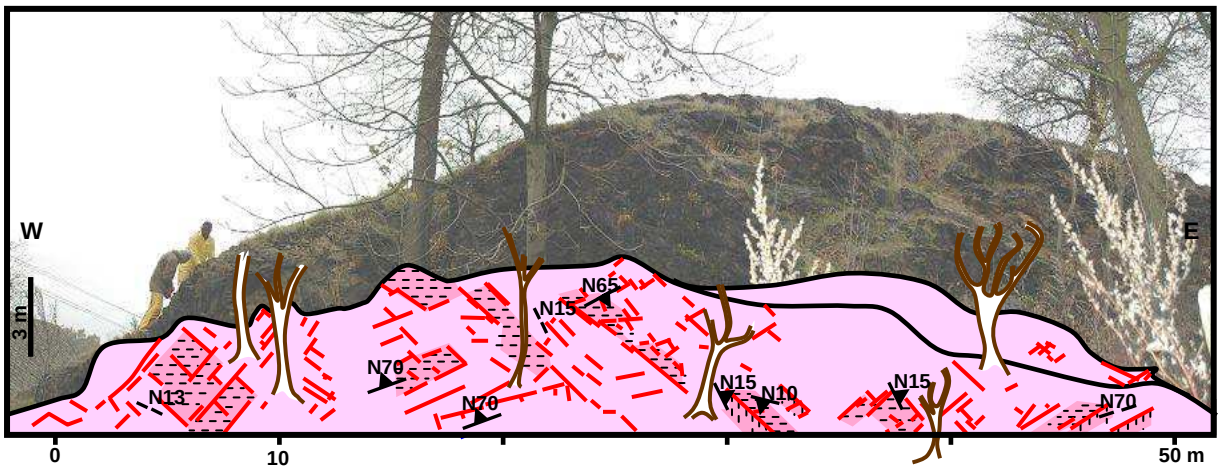


**Figure 5 – Sketch of reddish pervasive alteration of the Laski village outcrop. The rocks are highly fractured by a system in which the prevailing fractures are dipping towards 45°. Therefore, the rock is cut into decimetre polyhedron blocks. The reddish alteration entirely impregnates the rocks so that there is no evidence of grey facies.**

***Figure 5 – Schéma de l'albitisation rouge pervasive de la coupe du village de Laski. La roche est très fracturée par un système de fractures à pendage proche de 45°et qui découpent la roche en polyèdres de taille décimétriques. L'altération rouge imprègne entièrement la roche si bien qu'il n'y existe plus de facies clair***

The rock is highly fractured with two prevailing directions: N65°- N70° (dipping 45° to the East or West) and N10°- N15° (dipping mainly 50°-70° towards the SE).

The fractures are relatively close and cut the rock into decimetre polyhedral blocks (Fig. 6). The fracture planes are systematically coated with dark red iron oxides. The reddish oxidized facies show coarse hematite granules as well as some chlorite minerals of dark greenish colour and dull aspect. The reddish pigmentation is only recorded in the euhedral feldspar crystals, which appears as abundant in this facies (Fig. 7).

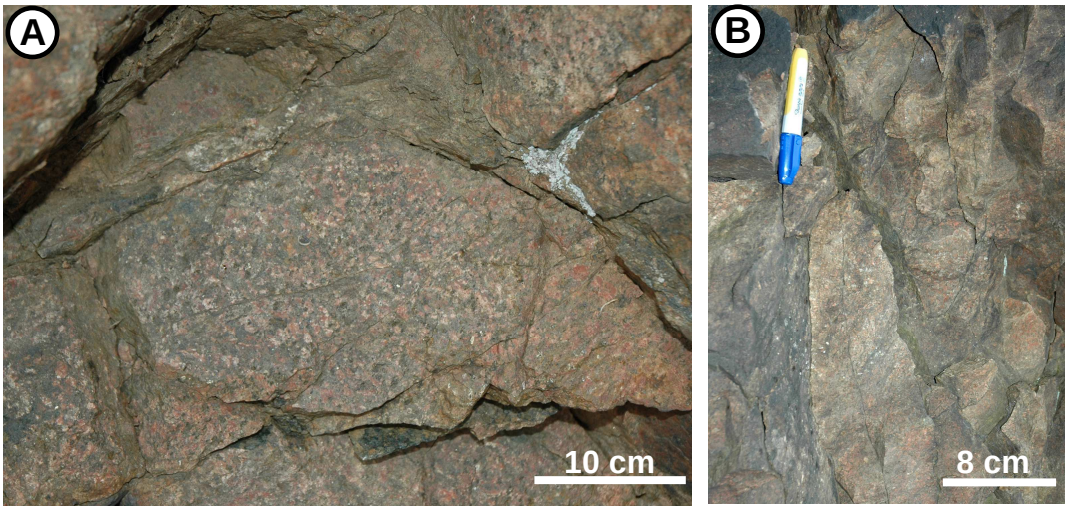


**Figure 6 – Pervasive and intense albitization of the Laski village outcrop. Secant fractures are delimiting the blocks which are massively albitized (red coloration).**

***Figure 6 - : Albitisation pervasive et intense du village de Laski avec fractures sécantes délimitant des blocs albitisés de façon massive (couleur rouge).***

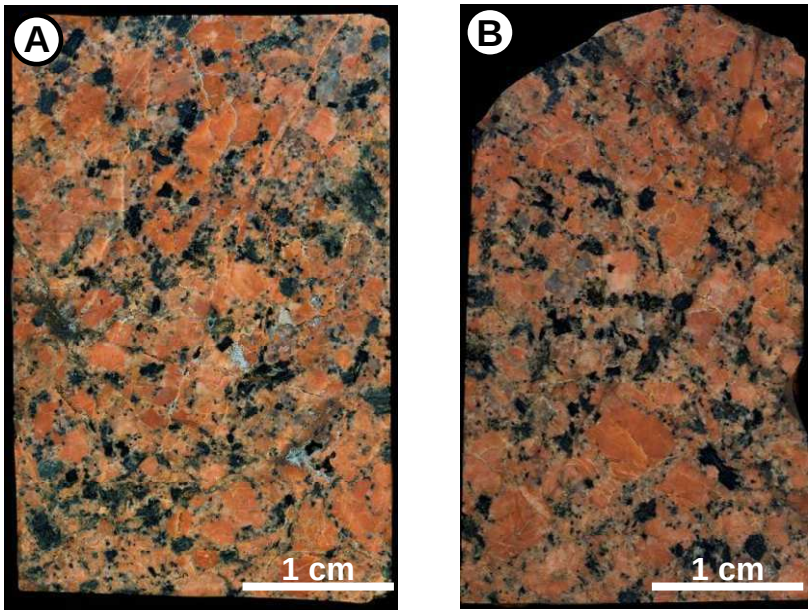


**Figure 7 - Pervasive and intense albitization of the Laski village outcrop (polished sections WL86 & WL87). (A) Homogeneous grain-size of red feldspars. (B) Larger red feldspars towards the bottom of the picture and more red fractures near the top of the picture.**

***Figure 7 - Albitisation rouge soutenue et pervasive du village de Laski (sections polies WL86 & WL87). (A) Feldspaths rouges de granulométrie homogène. (B) Feldspaths rouges plus grands vers le bas de la photo et fracture plus rouge en haut de la photo***

## 4.2 LASKI QUARRY

Laski quarry is a granodiorite outcrop, typical in the Kłodzko Złoty-Stok massif (Wierzchołowski, 1976). This facies shows a mainly reddish/pinkish alteration along the fracture walls. The fractures are metric-spaced, cutting the outcrop into 0.5 to 1 $m^3$ well defined blocks (Fig. 8). They systematically show more or less intense alterations of the primary granodiorite towards a pinkish coloration.


**Figure 8 – Picture and sketch of the red alteration that follows the fractures in the Laski quarry. The highly fractured zones, in the SE of the quarry are the most reddened. A direct relation exists between fractures frequency and the intensity of the alteration.**

***Figure 8 – Photo et schéma de l'altération rouge suivant les fractures dans la carrière de Laski. La zone la plus intensément fracturée dans la partie SE de la carrière correspond à la zone la plus rouge. Une relation directe existe entre la fréquence de la fracturation et l'intensité de l'altération***

The alteration emerges only weak along the minor fractures, or rather intensive along the major fractures. Nevertheless, the alteration may be pervasive, affecting the whole rock in zones where close stacked fractures cut the rock into decimetre blocks. The alteration along the fractures varies in thickness (1-10 cm) with a relatively regular gradient. The alteration gradient along the fractures is characterized by an intense red/pink coloration at the fracture walls and is less intense further away from the fractures (Fig. 8). There is a direct relation between the frequency of the fractures and the intensity of the reddish coloration. In the SE part of the quarry, the most intensive altered facies occur along a metric thick zone, weakly defined corresponding to the tightly fractured shear-zone. Silica deposits and silica impregnated facies are associated with these strongly reddened zones. A granular disintegration facies due to recent weathering developed at the NW edge of the quarry.

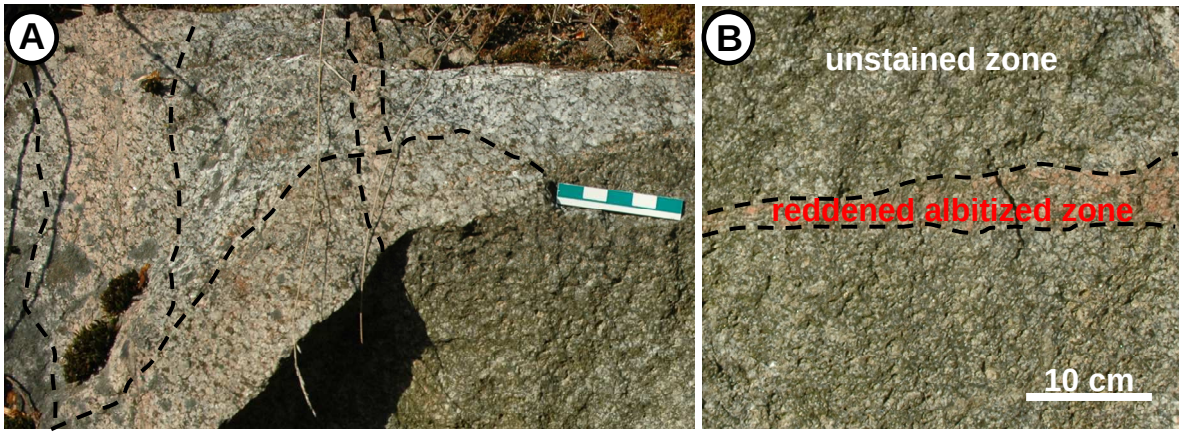


**Figure 9 - Red to pinkish alteration along the fractures in the Laski quarry section. (A) Angular block with pinkish alteration corridors and non-altered light or greenish zones; (B) horizontal pink altered fracture in a rock of greenish appearance.**

***Figure 9 - Albitisation rouge à rose le long des fractures dans la carrière de Laski. (A) Bloc anguleux présentant des couloirs roses d'albitisation et des zones claires et verdâtres non altérées ; (B) Fracture horizontale rose altérée dans une roche globalement verdâtre***

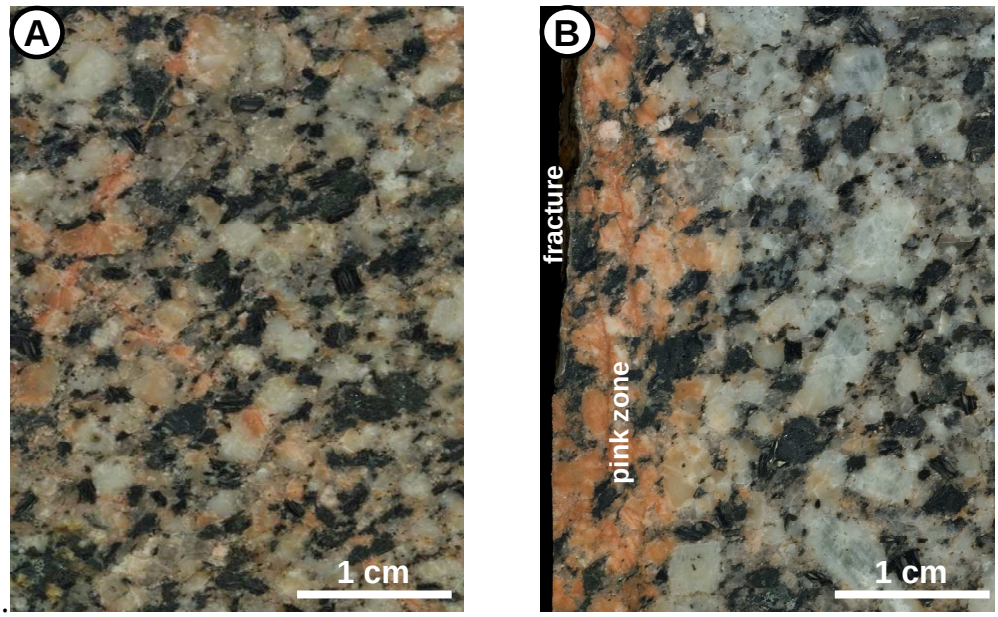


**Figure 10 – Reddish alteration pattern along fractures at the Laski quarry outcrop (polished sections WL71, WL64 & WL75). (A) Reddened alteration around two secants micro-fractures; (B) intense red alteration on the left edge of the sample (fracture) that is decreasing further away from the fracture.**

***Figure 10 - Altération rouge le long des fractures dans la carrière de Laski (sections polies WL71, WL64 & WL75). (A) Altération rouge autour de deux microfractures sécantes. (B) Altération rouge intense sur le bord gauche de l'échantillon (fracture) et décroissante en s'éloignant de la fracture***

The reddened/altered fractures show greenish chlorite-like minerals while the light and non-altered zones exhibit dark ferromagnesian minerals, biotite or amphiboles. Feldspars appear as large euhedral crystals, which are white in the non-altered part but red or pink along the reddened fracture (Fig. 10). Hematite grains are not obvious macroscopically but the reddened/pinkish aspect of the alteration seems to be due to the presence of hematite grains (as in the Laski village section), but which are probably smaller here.

## 4.3 SZKLARSKA PORĘBA (SP)

Szklarszka Poręba is characterized by a specific pinkish alteration bounded to the fractures on the hanging walls (Fig. 11, Fig. 12). This section is composed of two different granites, characterized by their textures: (1) a fine to medium-grained granite and (2) a porphyritic granite. The fine to medium-grained granite is particularly solid and compact and shows two different colorations: (1) a light pink coloration, possibly a bleached aspect, along the fractures walls, and (2) a relatively dark and greenish coloration inside the blocks (Fig. 12).

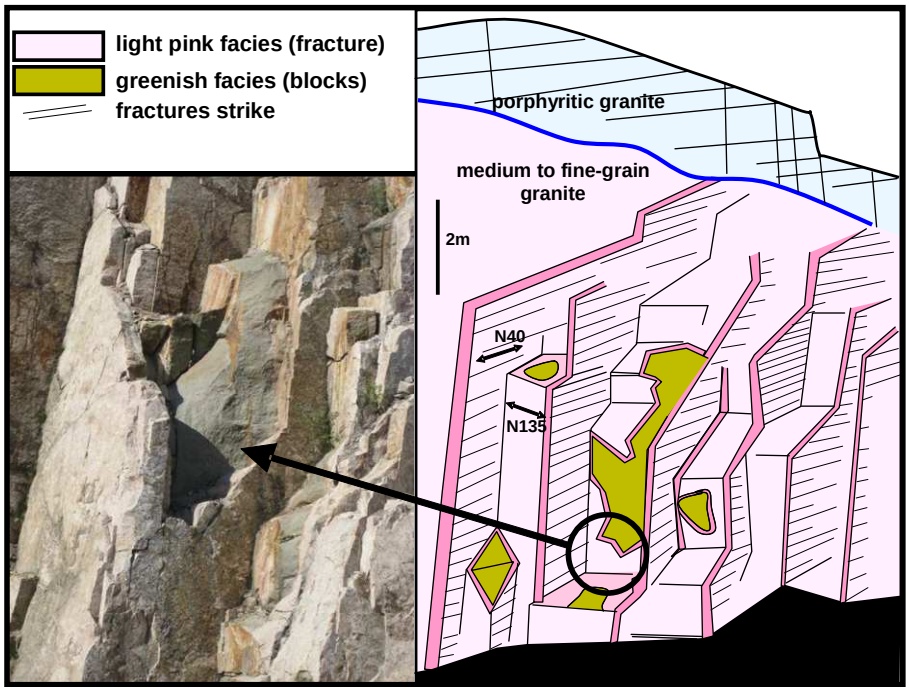


**Figure 11 – Szklarska Poręba quarry facies. The fine-grained granite is cut by N40° major fractures and N135° factures. The alterations (bleaching or reddening) proceed along the fractures, creating zones 5 to 15 cm thick.**

***Figure 11 - Faciès de la carrière de Szklarska Poręba. Le granite fin est recoupé par des fractures majeures d'orientation N40° et des fractures à N135°. L'altération du granite (blanchiment et coloration rose claire) se fait le long de ces fractures et affecte la roche sur 5 à 15 cm d'épaisseur.***

The thickness of the pinkish fracture walls varies from 5-15 cm up to 30-40 cm in the fractures zones (Fig. 11). When the fractures are wide spaced, greenish fine-grain granite remains in the center of the blocks delimited by fractures. In zones where the fractures are closer (chopping fractures), the medium-grained granite is entirely pink.

Two fractures systems prevail in this section: a major system dipping towards N40° with a spacing between 0.1 and 1m and a minor system dipping towards N135° with a metric spacing (Fig. 11). Minerals size within the fine-grained granite does not allow any naked eye mineral recognition. Nevertheless pale yellow pyrite flakes are sometimes distinguishable and the pinkish coloration of the facies could be related to the presence of microscopic hematite grains associated to feldspars (Fig. 13).

The porphyritic granite constitutes the major part of the quarry. This granite is grey with relatively abundant black minerals and K-feldspars phenocrysts. In the upper part of the quarry, a beige grussy facies exists: K-feldspars phenocrysts and quartz appears almost as individual minerals, since the plagioclases are weathered. The porphyritic granite does not show any red alteration features its contact with the fine-grained granite seems to be of late-tectonic origin.

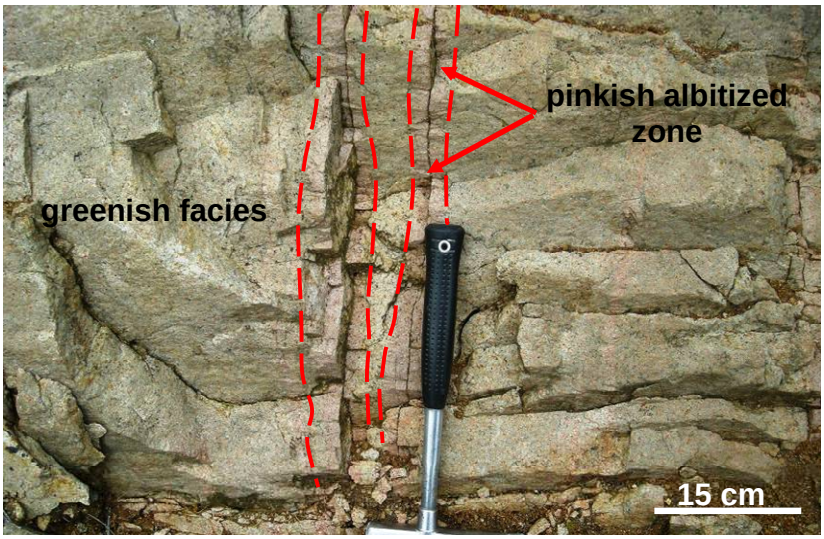


**Figure 12 – Greenish and pinkish facies in the fine to medium-grained granite in the Szklarska Poręba quarry. The granite is globally greenish and the pinkish alteration is bounded to the fractures.**

***Figure 12 - Faciès verdâtres et roses au sein du granite fin à moyen de la carrière de Szklarska Poręba. Le granite est globalement verdâtre et l'altération rose est limitée aux fractures***

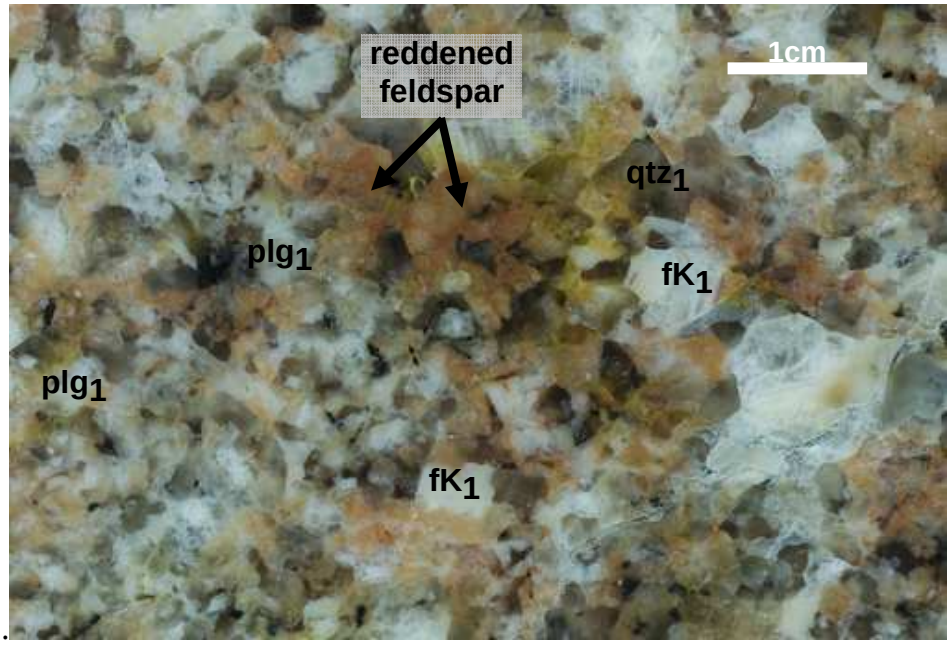


**Figure 13 – Medium-grained granite from the Szklarska Poręba quarry. The facies shows pinkish/reddened subhedral altered feldspars while the others remain milk-white or translucent. Quartz appears as anhedral translucent or smoky crystals. plg1: primary plagioclase; fk1: primary K-feldspar; qtz: quartz.**

***Figure 13 - Granite moyen de la carrière de Szklarska Poręba (échantillon WL7). Ce faciès présente certains feldspaths subautomorphes rouges/roses tandis que les autres restent blancs-laiteux ou translucides. Les quartz apparaissent comme des cristaux xénomorphes et fumés. Plg1 : plagioclase primaire ; fk1 : K-feldspath primaire ; qtz : quartz***

## 4.4 CHWALISŁAW VALLEY

This section is characterized by a slightly pinkish staining along the fractures planes, and the development of millimetre pink alteration spots away from the fractures wall. The Chwalisław valley quarry (~500 m downstream of Chwalisław village) is a granodiorite unit intruded by lamprophyres veins and shows two sets of fractures (Fig. 14). One of them strikes

to the N-S and the second one is sub-vertical and strikes in direction of N60°. The pinkish alteration is weak and follows fracture corridors parallel to the strike of the lamprophyres (Fig. 14). There is no direct relationship between the lamprophyres intrusions and the reddish alteration that affects this facies, but lamprophyres veins also show some tiny pinkish feldspar minerals, that have been interpreted as plagioclases replaced by albite (Awdankiewicz and Awdankiewicz, 2010). The granodiorite as well as the lamprophyres are affected by the same reddish alteration that could involve plagioclases albitization.

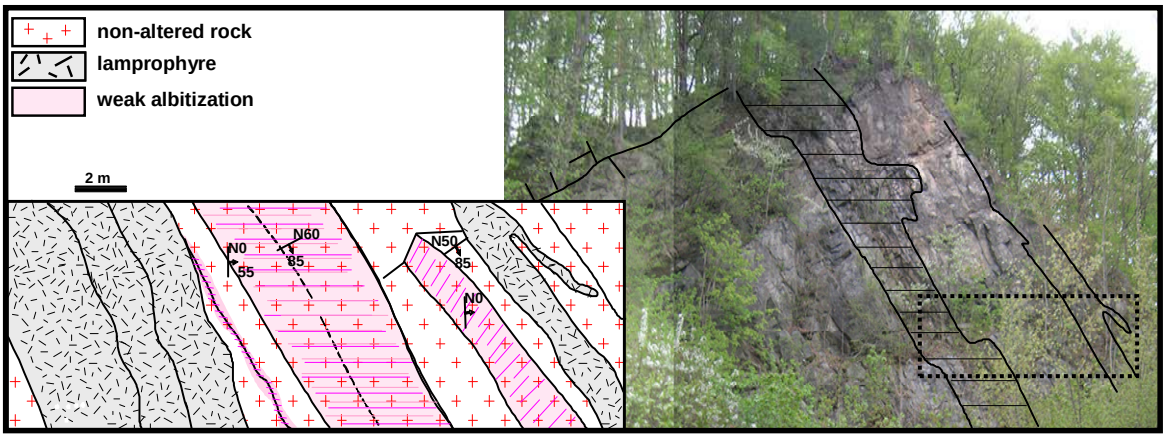


**Figure 14 – Sketch of the reddish alteration facies in the Chwalisław valley outcrop. The alteration is parallel to the lamprophyres veins that intruded the granodiorite.**

***Figure14 - Schéma des altérations rouges dans la carrière de la vallée de Chwalisław. L'altération rouge est parallèle aux veines de lamprophyres intrusives dans la granodiorite.***

Further away from the slightly pink fractures, the granodiorite exhibits an alteration represented by some small pink spots (Fig. 15, Fig. 16). Greenish chlorite-like minerals and pink feldspars are visible along the fractures. The slightly pink coloration along the fracture walls as well as in the spotted zone is caused by microscopic hematite. In further distance from the quarry, the Chwalisław valley granodiorite exhibits pinkish K-feldspar phenocrysts, probably stained by microscopic hematite.

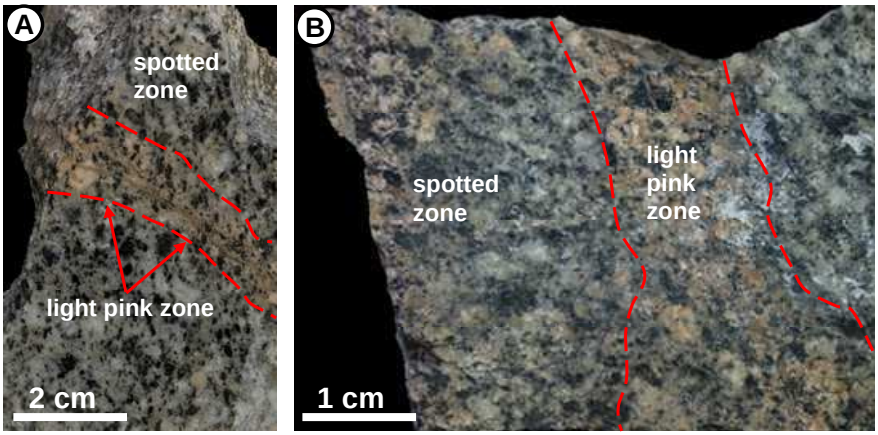


**Figure 15 – Light pink alteration along fractures and spotted zone away from the fracture. (A) Light pink zone restricted to a fracture and pink spot within the grey granodiorite, (B) the light pink zone is wider but still surrounded by spotted zone.**

***Figure 15 - Altération rose le long des fractures et zone tachetée rose loin des fractures.(A) Zone rose claire limitée aux fractures et taches roses au sein de la granodiorite grise, (B) la zone rose claire est plus large cependant environnée par une zone à taches rose.***


**Figure 16 – Pink spotted alteration facies from Chwalisław valley. Feldspar appears as euhedral and light pink probably due to the presence of minute hematite grains.**

***Figure 16 - Faciès présentant des altérations tachetées roses de la vallée de Chwalisław. Les feldspaths sont automorphes et présentent une couleur rose claire probablement due à la présence de petites inclusions d'hématite.***

## 4.5 CHWALISŁAW KOPCIOWA MOUNTAIN

The Kopciowa mountain section is located in the South-East of the Chwalisław valley and is characterized by a red to pinkish alteration along the fracture walls (Fig. 17). The rock is a relatively heterogeneous granodiorite with predominant equigranular facies (Fig. 18), and a coarse grained facies that exhibits some pink orthoclase phenocrysts (Fig. 19). Lamprophyre veins are injected through the granodiorite. The Kopciowa mountain is in contact with the Haniak gneiss that is interpreted as a Neoproterozoic to middle Devonian orthogneiss (Cwojdziński and Kozdrój, 2007). The Kopciowa mountain granodiorite and lamprophyre veins as well as the Haniak gneiss exhibit pinkish alteration features (Fig. 20).

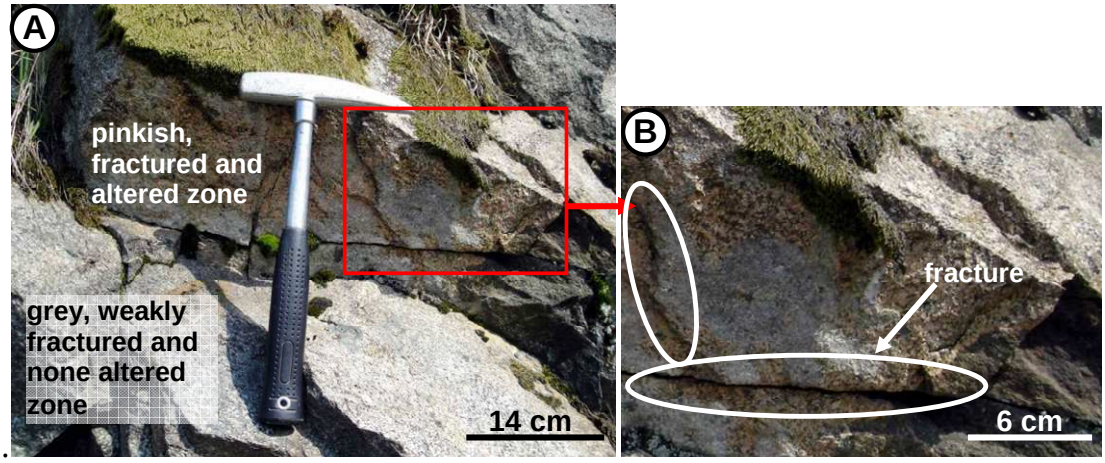


**Figure 17 – Weak and pinkish alteration along a fracture walls in Kopciowa mountain. (A) Pink and altered fracture walls close to a grey, non–altered zone. (B) Zoom on the pinkish fracture wall. The red altered zone appears as more fractured than the grey one.**

***Figure 17 - Albitisation limitée et rose le long des fractures dans la Montagne de Kopciowa. (A) Fractures roses altérés proches d'une zone grise et non altérée. (B) Zoom sur la fracture rose. La zone altérée rouge est plus fracturée que la zone grise non altérée.***

In the granodiorite, the alteration is weak (light color) and develops mainly along the fracture walls, restricted to a 2-5 mm wide reaction front. Away from the fracture walls, the alteration is restricted to some millimetre pink spots within the rocks. Orthoclase phenocrysts appear often partially or entirely pinkish. The pink orthoclase phenocrysts are mainly distinguishable along the reddened fracture planes and show Carlsbad twinnings. The coloration of the phenocrysts appears as also connected to the presence of microscopic hematite (Fig. 19).


**Figure 18 - Granodiorite from Chwalisław Kopciowa mountain showing bands and additional pink feldspars. Dark band seems to be constituted of mafic minerals such as amphiboles and biotites.**

***Figure 18 - Faciès granodioritique de la montagne de Chwalisław-Kopciowa montrant des bandes sombres et des feldspaths roses. Les bandes sombres sont constituées de minéraux mafiques tels que des amphiboles et des biotites.***

In the lamprophyres intersecting the granodiorite, feldspars appear with pink coloration. These pinkish feldspars have been interpreted as plagioclases hydrothermally albitized during the late magmatic consolidation stage (Němec, 1966). The albitized plagioclases in the lamprophyres show characteristics and paragenesis similar with that of the saussuritization with sericite, zoïsite-epidote minerals, prehnite and calcite within the neogenic albite (Němec, 1966).

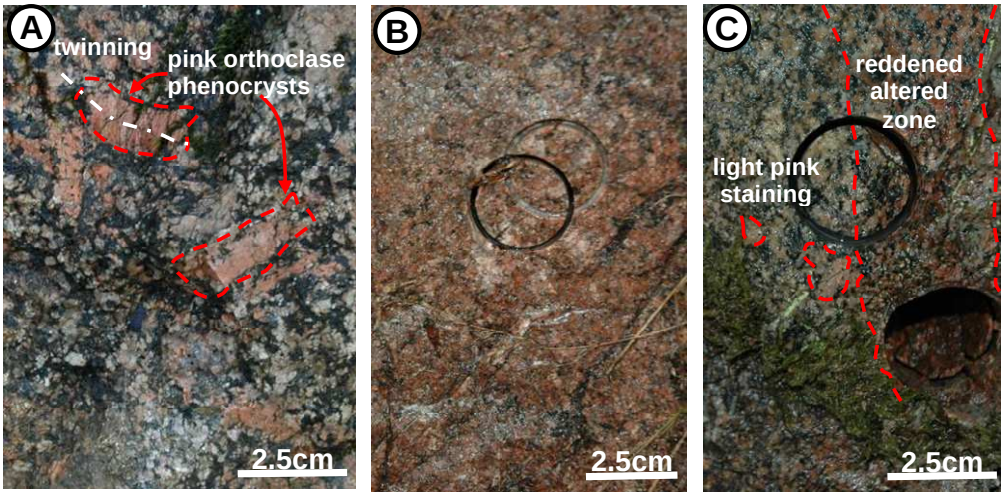


**Figure 19 – Red alteration features within the Chwalisław Kopciowa Mountain. (A) reddened orthoclase phenocrysts; (B) homogeneous pinkish reddening on a fracture wall; (C) reddening in a fracture corridor and light pink spots in the less-altered part of the rock.**

***Figure 19 - Caractéristiques de l'altération rouge dans la Montagne de Chwalisław (Kopciowa). (A) phénocristaux roses d'orthose. (B) Altération rouge homogène sur un plan de fracture. (C) Altération rouge dans un couloir de fracture et taches roses dans la partie la moins altérée de la roche***

The Haniak gneiss close to the Kopciowa Mountain is also reddened. The alteration is characterized by dark-greenish bands of ferromagnesian minerals alternating with pinkish quartzo-feldspathic bands (Fig. 20).


**Figure 20 – Reddening within the Haniak gneiss from the Kopciowa Mountain. The pinkish bands are quartzo-feldspathic while dark bands contain biotites.**

***Figure 20 - Rougiement dans la formation gneissique de "Haniak" près de la montagne de Kopciowa. Les bandes roses sont quartzo-feldspathiques tandis que les bandes sombres sont à biotites.***

## 4.6 HEMATITIZATION VERSUS ALBITIZATION PATTERNS

Oxidized sections exhibit red/pinkish alteration in the Polish Sudetes related to the presence of hematite granules or microscopic hematite pigments. This hematite pigmentation is obvious in the feldspars that compose the studied sections. The pinkish feldspars occurring in Chwalisław area lamprophyres are systemically interpreted as secondary albite originating from the late-magmatic alteration of the primary plagioclase (Awdankiewicz and Awdankiewicz, 2010). Besides, feldspars in the other rocks (granodiorite, monzonite) show similar aspects as those in the lamprophyres, suggesting that they could have also been albitized. Nevertheless, the conditions of this albitization seem not necessarily of late-magmatic origin, especially as hematite associated with this neogenic albite implies rather oxidizing conditions.

It appears likely that this alteration could at least correspond to the primary feldspar albitization. The particularities of this albitization/oxidation seem to result in three main patterns: (1) a reddish intense and pervasive albitization (Laski valley); (2) a red to pinkish albitization bound to fracture walls (Laski quarry and Szklarska Poręba quarry); (3) a weak albitization controlled by fractures and associated with some pinkish spots (Chwalisław valley).

# RESUME CHAPITRE 5

## *MINERALOGIE*

*La connaissance de la minéralogie primaire des granitoïdes est essentielle pour une comparaison avec les faciès rouges altérés en vue de faire des hypothèses qualitatives et quantitatives.*

***CARACTERISTIQUES MACROSCOPIQUES.*** *Les roches échantillonnées sont pour l'essentiel des granitoïdes, néanmoins des lamprophyres et des gneiss ont été échantillonnés dans le massif de Kłodzko Złoty-Stok. Dans les faciès clairs, les granitoïdes apparaissent gris, de grains moyens à grossiers, et montrent souvent des grands cristaux clairs et translucides de feldspaths potassiques et des minéraux ferromagnésiens sombres (Fig. 21A, Fig. 21B). Les lamprophyres microlithiques sont des spessartites et des micromonzodiorites avec un aspect parfois brunâtre (Fig. 21C), tandis que les gneiss montrent une alternance de bandes quartzo-feldspathiques claires et de bandes sombres de ferromagnésiens. Dans les faciès rouges, les roches apparaissent soit avec une coloration entièrement rouge ou limitée aux bordures des fractures et à des points dispersés (Fig. 22). Les grands feldspaths translucides dans les faciès clairs apparaissent rouges/roses dans les faciès rouges tandis que les minéraux ferromagnésiens préalablement noirset brillants y sont verdâtres et ternes.*

***COMPOSITION MINERALOGIQUE.*** *Les analyses aux rayons X montrent que les roches étudiées sont majoritairement composées quartz, feldspaths, minéraux ferromagnésiens et prehnite Fig. 23), accompagnés de minéraux accesoires comme la calcite, la laumontite et la sericite. Des différences notables apparaissent entre les faciès clairs et rouges. Les plagioclases-Ca présents dans tous les faciès clairs sont pratiquement absents des faciès rouges alors que l'albite et le microcline qui sont presqu'inexistants dans les faciès clairs sontabondants dans les faciès rouge . On retrouve mons d'albite dans les faciès rouges qu'il n'y a de plagioclases dans les faciès clairs. En revanche, les feldspaths-K sont plus abondants dans les faciès rouges que dans les faciès clairs.Néanmoins, l'interprétation de ces changements minéralogiques est d'autant plus difficile que les minéraux ferromagnésiens sont plus abondants dans les faciès rouges que dans les faciès clairs. Il n'est pas exclu que les granitoïdes avec une faible teneur en ferromagnésiens aient été échantillonnés préférentiellment comme représentatifs des faciès clairs.*

*Le* ***quartz****z constitue environ 20 % de la roche totale, que ce soit dans les faciès gris ou dans les faciès rouges. Ceci suggèreen première approximation que le quartz est uniquement d'origine magmatique et que celui-ci n'est pas affecté par l'altération rouge.*

*Les* ***feldspaths*** *sont la phase minéralogique la plus importante. Ils représentent environ 50 %-70 % de la roche totale dans le massif de Kłodzko Złoty-Stok. Les plagioclases sont toujours plus abondants que les feldspaths-K.*

***L****es plagioclases de composition labradorite (Ab55-An45) sont abondants dans les faciès clairs et absents des faciès rouges où ils sont remplacés par l'albite. L'albite constitue généralement 30 à 40 % de la roche totale des faciès rouges, et atteint même 50 % dans le faciès le plus albitisé du village de Laski. L'absence de plagioclases-Ca et l'apparition d'albite dans les faciès rouge indique clairement une altération des plagioclases en albite. Par ailleurs, la teneur en albite est généralement diminuée diminuée de façon concomittante de 25 % par rapport aux plagioclases dans les faciès clairs.*

*Les feldspaths potassiques (FK) montrent égalemnt des variations significatives. L'orthose est l'unique FK dans les granitoïdes clairs, tandis que le microcline apparaît en plus dans les faciès rouges. L'orthose représente environ 10 à 15 % de la roche totale dans*

*les différents faciès. La distribution du microcline est plus variable d'un site à l'autre. Dans le massif de Kłodzko Złoty-Stok (KZS), le microcline représente 5 % de la roche totale, et apparaît dans tous les faciès rouges sauf à Laski village. Le microcline est vraisemblablement lié à l'altération rouge puisque celui-ci n'apparaît que dans les faciès rouges. Dans le granite fin de la carrière de Szklarska Poręba (SP) l'albite (40 %) et le microcline (10 %) apparaissent à côté de l'orthose (10 %) dans le faciès vert présupposés non altérés. L'absence de plagioclase-ca et la présence de microcline dans ce faciès verdâtre laisse supposer qu'il est probablementdéjà altéré, mais éventuellement pas encore oxydé.*

*Les **minéraux ferromagnésiens** sont constitués de biotite, d'amphiboles et de chlorite. L'importance des minéraux ferromagnésiens apparaît liée à la nature des granitoïdes, l'amphibole est dominante dans les granodiorites alors que la biotite prédomine dans les granites. Mais, les teneurs totales en ferromagnésiens sont toujours supérieures dans les faciès rouges que dans les faciès clairs et les teneurs en chlorite et en amphibole semblent être anti-corrélées.*

*La chlorite (10 %-20 %) est le ferromagnésien le plus abondant dans tous les faciès rouges et est toujours plus abondante dans les faciès rouges qu'elle ne l'est dans les faciès clairs, suggérant que la formation de chlorite est plus intense dans les faciès rouges. L'absence de biotite et les faibles teneurs en amphiboles dans les faciès rouges montrent que ces minéraux sont partiellement transformées en chlorite. Corrolairement, la présence de chlorites dans les faciès clairs montre que ceux-ci sont déjà altérés. La chlorite semble se former essentiellement à partir des ferromagnésiens primaires. Mais dans les faciès rouges elle est plus abondante quela somme des teneurs en amphibole et biotite des faciès clairs, suggérant la formation de chlorite par précipitation à partir des fluides dans les pores et microfractures (Wilamoswki, 2002).*

*La **prehnite** (4 % de la roche totale) apparaît uniquement dans les faciès granodioritiques que ceux-ci soient clairs ou rouges. Ceci indique que l'occurrence est indépendante du type d'altération mais plutôt de la nature des roches. Quand la prehnite est absente des faciès clairs, elle n'apparaît pas non plus dans les unités rouges, montrant que son occurrence est également indépendante de la pigmentation rouge.*

*Les **minéraux accessoires**, en faible teneurs, sont essentiellement constitués de calcite, laumontite, sericite et hématite. L'hématite a uniquement été détectée dans le faciès le plus rouge du village de Laski, ailleurs la non-détection de l'hématite est liée au fait que leur rougiement n'est pas aussi intense que dans cette coupe. La calcite apparaît uniquement dans la carrière de Laski ou elle représente 3 % de la roche totale, la séricite moins de 1 % de la roche totale dans la granodiorite de la carrière de la vallée de Laski et de la montagne de Chwalisław. La laumontite est présente (moins de 0.4 %) dans la vallée de Chwalisław. La séricite apparaît à la fois dans les faciès clairs et rouges, tandis que hématite, calcite et laumontite n'apparaissent que dans les faciès rouges.*

# CHAPTER 5

# 5 BULK MINERALOGY

The knowledge of the primary mineralogy of the granitoïd facies is necessary to allow a comparison with the red altered facies and to be able to draw qualitative and quantitative interpretations. The samples that were chosen as references for this comparison are the light/grey facies (in particular the outcroping granitoïd rocks), with respect to the preservation of these facies in our sections. Therefore the light/unstained facies samples origin exclusively from the outcrop sections where the albitization is limited to fracture zones; the facies that show pervasive alterations, such as in the Laski village do not contain any light/unstained facies and thus no unaltered samples could be studied here.

## 5.1 MACROSCOPIC FEATURES

Most of rocks sampled in the framework of this study are granitoïd facies. Nevertheless, lamprophyres and gneisses from the Kłodzko Złoty-Stok massif have been additionally investigated for their specific alteration features. Granitoïd rocks are equigranular, medium to coarse grained, gray, and more or less mesocratic depending on the ratio of felsic and ferromagnesian minerals that they contained (Fig. 21A, Fig. 21B). They are sometimes porphyritic with large euhedral alkali feldspar crystals. Lamprophyres are mainly spessartites or micromonzodiorite (Awdankiewicz and Andankiewicz, 2010); they are microlithic with a dark to brownish aspect (Fig. 21C) and occur as veins or dikes that crosscut the granitoïd bodies of the Kłodzko Złoty-Stok massif. The Gneisses show orientated fabrics with alternation of light quartzo-feldspathic bands and dark ferromagnesian bands.

The reddened facies are characterized by several coloration features: some of them are homogenous and entirely red, while others are partially red showing at the same time unstained and reddened zones (Fig. 22). In the latter facies, the reddening appears either limited to the vicinities of fractures (Fig. 22A), to on the edges of the samples as related to open fractures (Fig. 22B), or to heterogeneous scattered red patches or spots within a sample that shows also unaltered zones (Fig. 22D).

The reddening is globally recorded within the feldspar crystals. Thus, K-feldspar phenocrysts, smaller K-feldspars, and plagioclases which are light and transluscent in the unstained facies appear here with a red/pink coloration. The ferromagnesian minerals (biotite, amphiboles) are dark in the unstained facies and emerge almost as dark-green minerals within the reddened zones of the samples. This probably indicates that the ferromagnesian minerals are also transformed in the reddened facies.

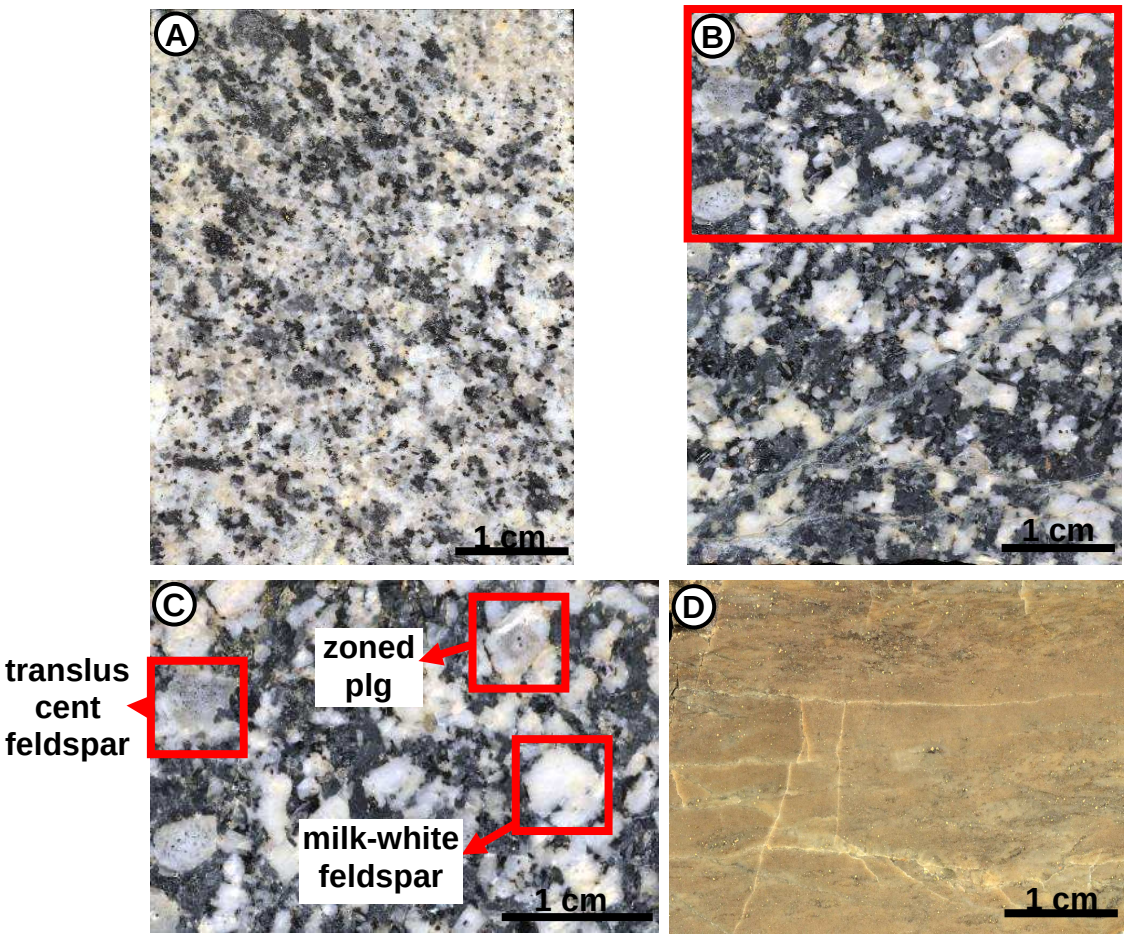


**Figure 21 – Representative light/unstained facies sampled from the Kłodzko Złoty-Stok Massif. (A) Medium-grained granodiorite from Chwalisław valley (CHR 24). The rock is grey and the primary ferromagnesian minerals remain dark and apparently non-chloritized. (B) Coarse grained granodiorite from Makolno close to Chwalisław (MKR 1b). There is obviously no or very light red staining. (C) Zoom of (B), feldspars appear as euhedral white or translucent crystals. Some of them show zoned plagioclase. (D) Lamprophyre from Chwalisław area (WL123), the rock has a brownish aspect; this lamprophyre is spessartite to micromonzodiorite composition (Awdankiewicz and Awdankiewicz, 2010).**

***Figure 21 – Faciès clair non pigmenté du massif de Kłodzko Złoty-Stok. (A) Granodiorite à grains moyens de la vallée de Chwalisław (CHR 24). La roche est grise et les minéraux ferromagnésiens apparaissent noirs, vraisemblablement non chloritisés. (B) Granodiorite grossière de Makolno près de Chwalisław (MKR 1b). Apparemment il n'y a pas ou très peu de pigmentation rouge. (C) Zoom de la photo (B). Les feldspaths sont automorphes, blancs et transparents. Certains d'entre eux sont des plagioclases zonés. (D) Lamprophyres de la région de Chwalisław (WL123), la roche montre un aspect brunâtre. Ces lamprophyres sont des spessartites et des micromozonites (Awdankiewicz and Awdankiewicz, 2010).***

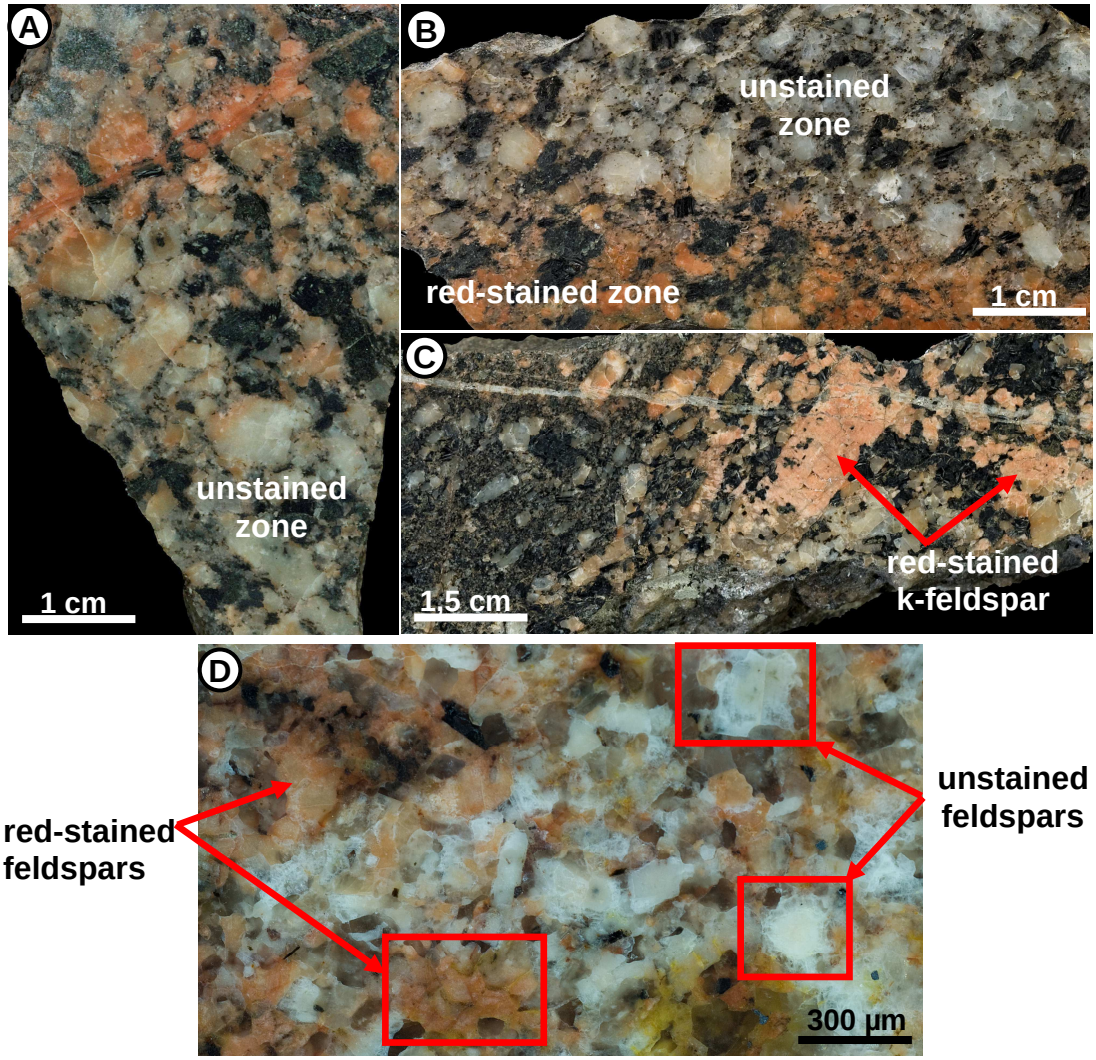


**Figure 22 – Reddened facies sampled in the Kłodzko Złoty-Stok massif and in Szklarska Poręba quarry. (A) Reddening along the vicinity of fractures within granodiorite from Laski quarry (WL 75). Feldspars in the vicinity of the fractures are entirely reddened whereas those further away from the fractures are light/unstained or show only weak partial reddening. (B) Reddening zone along one of the edges of a granodiorite sample from Laski valley (WL 52). The reddening is limited to the border of the sample meaning that the reddening is connected to a fracture. (C) Reddened heterogeneous granodiorite from Kopciowa mountain, showing two zones with different texture: a porphyritic zone and an almost microclithic zone dominated by mafic minerals (WL 55). K-feldspar phenocrysts and the smaller feldspar crystals are affected by the reddening only limited to the porphyritic zone. The feldspars in the"microlithic" zone in the center of the sample remain light/unstained. (D) Spotted and heterogeneous reddening in the fine-grained granite from Szklarska Poręba quarry (WL 7). Reddened and light/unstained zones coexist as scattering patches within the same sample.**

***Figure 22 – Faciès rougis provenant du massif de Kłodzko Złoty-Stok et de la carrière de Szklarska Poręba. (A) Coloration rouge apparaissant voisinage des fractures dans une granodiorite de la carrière de Laski (WL 75). Les feldspaths au voisinage de la fracture sont entièrement rouges tandis que ceux loin de la fracture sont soit clairs ou montrent une coloration rouge faible et partielle. (B) Zone rouge visible sur l'une des bordures d'un échantillon issu de la vallée de Laski (WL 52). La coloration rouge est limitée à une bordure montrant qu'elle est liée à une fracture. (C) Granodiorite rouge hétérogène de la Montagne de Kopciowa montrant deux zones avec des textures différentes : une zone porphyritique et une zone presque microlithique dominée par des minéraux sombres (WL 55). Les phénocristaux ainsi que les feldspaths de plus petite taille sont rougis uniquement dans la partie porphyritique. Les feldspaths dans la zone microlithique plus à l'intérieur de l'échantillon restent clairs et non colorés. (D) Coloration rouge non homogène, en spots dans le granite fin de la carrière de Szklarska Poręba (WL 7). Des zones rouges et claires ne montrent pas d'organisation précise au sein de l'échantillon.***

## 5.2 BULK ROCKS COMPOSITION

Analyses of the bulk rock composition allow to study the distribution of the mineralogical constituents of the light/unstained facies throughout the sampled sites. Their mineralogical composition appears basically as homogeneous even if some differences have been noticed from one facies to another (or one site to another). X-ray analyses of the bulk rock show that these facies are mainly composed of three mineral groups, such as quartz, feldspars, and ferromagnesian minerals in addition to prehnite. The results of the bulk rock composition of the reddened and the light facies are summarized in figure 23.

The comparison of the bulk rock composition between the unstained and the reddened facies allows to highlight the main mineralogical changes that interfere during the reddening such as the transformation of the main secondary mineralogical phases and their distribution within the sample sites. Basically, the reddened and the light/unstained light facies show some composition similarities; nevertheless noticeable differences exist between both mineralogical compositions. Besides the main minerals, quartz, feldspars, ferromagnesian minerals, and prehnite other minor components occur, such as calcite, laumontite, and sericite. Furthermore, the relative abundance of the main minerals shows systematic changes between the two facies types. Ca-bearing plagioclase that is present in all unstained samples is no longer detected in the reddened facies, whereas albite and microcline that are almost absent in the light/unstained facies appear as abundant in the reddened facies (Fig. 23). The general trend between unstained and reddened facies shows a lower albite and higher K-feldspar content in the unstained facies Nevertheless, the interpretation of these compositional changes are difficult because the Fe-Mg minerals are more abundant in the reddened facies than in the unstained ones.

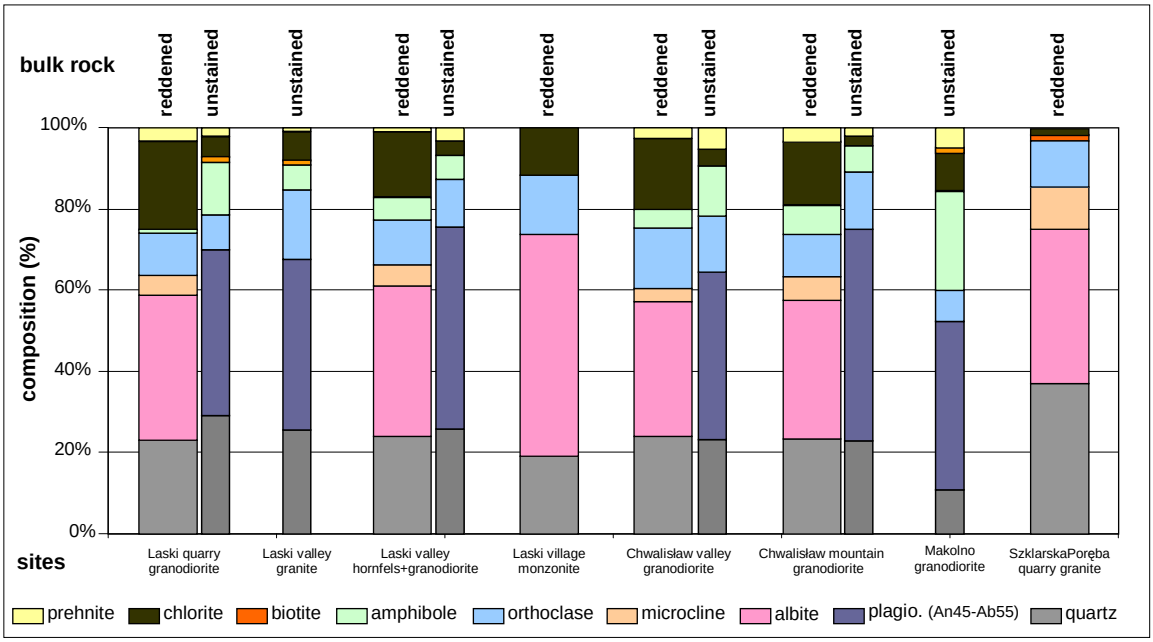


**Figure 23 – Comparison of the bulk rock compositions of the reddened facies with the light/unstained facies. Plagioclases are absent in the reddened bulk rocks, albite and microcline which are almost absent in the light/unstained rock appear as abundant in the reddened facies. Ferromagnesian minerals appear always comparatively more abundant in the reddened facies than in the light ones. Prehnite shows no significant variation.**

***Figure 23 – Comparaison de la composition minéralogique des faciès clairs et des faciès rouges. Les plagioclases sont absents des faciès rouges, l'albite et le microcline qui n'apparaissent presque pas dans les faciès clairs sont abondants dans les faciès rouges. Les minéraux ferromagnésiens sont toujours relativement plus abondants dans les faciès rouges que dans les faciès clairs. La prehnite ne montre pas de variation significative.***

### *5.2.1 Quartz*

The quartz content within the light/unstained and reddened facies forms about 20% of the bulk rock in all facies from Kłodzko Złoty-Stok and Szklarska Poręba massifs. The lower quartz content in Mąkolno is in accordance with its more basic nature (importance of the ferromagnesian minerals). In the reddened facies, the quartz content is similar to that of the unstained facies, meaning that it is, at first approximation, is not affected by the alteration processes that give rise to the reddening.

### *5.2.2 Feldspars*

Feldspars are the most abundant mineralogical group of the light/unstained facies. In the Kłodzko Złoty-Stok massif for instance, they represent at least 50% of the bulk rock in the Laski area and Chwalisław valley. They reach 70% of the bulk rock composition at the Chwalisław Kopciowa mountain facies and in the Laski village monzonite. Plagioclases are always more abundant than K-feldspars.

- **Plagioclases**

Plagioclase (labradorite Ab55-An45) which is the most abundant feldspar within the light/unstained facies is almost absent in the reddened facies and is entirely replaced by albite. The albite content within the reddened facies is about 30-40% in all studied sites and reaches 50% of the bulk composition in the Laski village section, where the red-staining is the most pronounced. This lack of plagioclase and the appearance of albite points to the alteration of plagioclase into albite. Moreover, the albite content is overall diminished of about 25% in comparison to the initial plagioclase content.

- **K-Feldspars**

Orthoclase is the solely K-feldspar that is present in the light/unstained granitoïd facies whereas K-Feldspars occurring in the reddened facies can be distinguished in two types: (i) orthose and (ii) microcline. Orthose occurs at all sites, where it provides about 10-15% of the bulk rock, its distribution appears as homogeneous throughout of the studied sites.

The microcline distribution and content seems more variable from one massif to another. In the Kłodzko Złoty-Stok massif, microcline represents about 5% of the bulk rock and occurs in all reddened facies, except in the Laski village quartz-monzonite. Besides, microcline occurring only in the reddened facies suggests that it is neogenic and non-magmatic. It may be associated with the reddening/alteration process.

The fine-grained granite in the Szklarska Poręba quarry appears quite particular. In the Szklarska Poręba quarry, albite and microcline appear in addition to orthoclase as the main feldspars in the bulk from the green and presumably unstained/unaltered facies. Albite represents at least 40% of the bulk rock whereas microcline constitutes about 10% and orthoclase less than 10%. This facies appears as the microcline-richest facies throughout the studied sites. Plagioclases do not occur in the bulk rock of the green facies of Szklarska Poręba. These greenish facies lack plagioclase similarly as the red-stained facies. They appear as clearly different to the Kłodzko Złoty-Stok massif light/unstained rocks that may mean that those greenish facies are probably already altered facies too.

### *5.2.3 Ferromagnesian minerals*

Fe-Mg minerals are mainly biotite, amphibole, and chlorite, and they appear systematically more abundant in the reddened facies than in the light/unstained facies ones. They are of course more abundant in the granodioritic than in the granitic facies. Amphibole

and chlorite occurs systematically in all facies whereas biotite is scarcer appearing only in the unstained granitic facies (Laski valley and Szklarska Poręba quarry) and in some granodiorite (Laski quarry and Mąkolno).

Amphibole is the most abundant Fe-Mg mineral in all light/unstained granodioritic facies of the Kłodzko Złoty-Stok massif. The Laski valley granite shows chlorite as the dominant Fe-Mg mineral and biotite appears as the main Fe-Mg mineral in Szklarska Poręba granite. The importance of the Fe-Mg minerals seems to be related to the nature of the granitoïd rocks, as amphibole is dominant in the granodiorite while biotite and chlorite are dominate in the granite.

Biotite has never been detected within the reddened facies in the Kłodzko Złoty-Stok massif, they have probably been altered into chlorite. Biotite remains in the reddened facies of the Szklarska Poręba fine-grained granite which has also a particular feldspar composition with regard to the other reddened facies.

Chlorite is always the most abundant ferromagnesian mineral in all reddened facies. It forms about 10-20% of the rock, amphibole makes up about 5% in Laski valley and in Chwalisław granodiorite, 1% in Laski quarry and it is absent in the Laski village quartz-monzonite. Chlorite is systemically most abundant than amphibole. Chlorite and amphibole content seem to be negatively correlated. In Laski quarry for instance chlorite reaches 20% of the bulk composition while the amphibole content is weak and about 1%. Chlorite content in the reddened facies is always more abundant than that in the light/unstained facies, pointing out that chlorite formation is more intense within the reddened facies. The weak content of amphibole in comparison to chlorite probably implies that amphiboles have been altered into chlorite within the reddened facies. Moreover, the absence of biotite argues in favour of the complete biotite alteration into chlorite within the reddened facies.

The presence of chlorite in the light/unstained rocks stresses the fact that they are already more or less altered. If the relationship between chlorite formation and biotite or amphibole alteration is not obvious within the bulk rock analyses, the amphibole abundance coupled with the low biotite content or its complete absence could suggest that chlorite mainly seems to be related to the biotite destabilization.

In Szklarska Poręba quarry, biotite and chlorite appear as the main ferromagnesian minerals whereas amphibole is completely absent from the granites. Chlorite and biotite appear in almost equal amounts in comparison with the green facies, they form about 2% of the bulk rock samples from Szklarska Poręba quarry. Here, it appears likely that chlorite may form exclusively from biotite, even if a possibility of neogenic chlorite within microfractures and voids can not be excluded.

Chlorite is generally much more important within the reddened facies, suggesting that neogenic chlorite formed as associated to the reddening. Chlorite content in the reddened facies appears also higher than that of the ferromagnesian minerals (biotite+amphibole) in the light/unstained facies. This suggests that the neogenic chlorite within the reddened facies may have not been formed exclusively from biotite or amphiboles, but others chlorite sources must be considered. A most probable source may be the chlorite crystallizing from fluids that circulate free in the voids, cavities, interstices or microfractures (Wilamowski, 2002). Petrographic observations allow to precise this fact and underline the different chlorite occurrences within the thin sections.

### *5.2.4 Prehnite*

Prehnite is present in all granodioritic facies of the Laski and Chwalisław area (Kłodzko Złoty-Stok massif) where it represents less than 4% of the granodiorite bulk rock.

Nevertheless, it has neither been detected in the quartz-monzonite of Laski village nor in the Szklarska Poręba granite.

Prehnite appears within the light/unstained facies as well as in the reddened granodioritic facies of the Kłodzko Złoty-Stok massif. The prehnite occurrence in both facies suggests at least that it is not dependent on the alteration type but depends rather on the nature of the primary rocks.

Moreover, this is confirmed by the absence of prehnite within the light facies as well as in the reddened facies of Szklarska Poręba quarry. Indeed, when prehnite is absent from the primary mineralogy, it never appears in the reddened/secondary facies as well. This points out that prehnite does not develop during the reddening.

### *5.2.5 Accessory minerals*

Calcite, laumontite, sericite, and hematite are considered as accessory minerals in the studied samples, because they have not been systemically detected by X-ray diffraction. Their content in the reddened facies is always below a few percents and very variable from one site to another, and even from one sample to the adjacent samples within the same studied site.

Hematite has only been clearly detected by XRD in the Laski village monzonite where it represents ~1% of the bulk of the rock (which corresponds to about the XRD detection limit for hematite). This monzonitic facies represents the most reddened site, thus it contains the most hematite-rich facies. The reddening is clearly associated to hematite content. Hematite has not been detected by XRD in the other reddened sites (although it is still present there) because their staining is not as much important as in Laski village monzonite and therefore below the XRD detection limit.

Calcite has only been detected in Laski quarry granodiorite where it comprises about 3% of the bulk rock. Sericite represents less than 1% of the bulk composition of the granodiorite at Laski valley and Chwalisław mountain, while laumontite represents less than 0.4% of the bulk rock in the Chwalisław valley granodiorite. Sericite has been identified in the light/primary facies as well as in the reddened/secondary facies. In contrary, calcite, laumontite, and hematite are only present in the reddened facies are clearly associated with the alteration processes.

## *RESUME CHAPITRE 6*

## *PETROGRAPHIE*

*L'étude pétrographique permet de préciser les altératios minéralogiques et de souligner les relations géométriques entre les minéraux. Ces relations géométriques sont de prime importance pour établir les séquences d'altération.*

### *LES PLAGIOCLASES*

*Dans les **faciès clairs,** les plagioclases forment des cristaux individuels bancs de 0.5-1.5 cm et des inclusions automorphes dans les phénocristaux de feldspath-K. Les plagioclases sont maclés polysynthétiques et zonés (Fig. 24, Fig. 25). Certains plagioclases montrent à la fois des domaines maclés et des domaines zonés (Fig. 24C, Fig. 25B). La zonation se caractérisegénéralement par une propagation de l'extinction du cœur du plagioclase vers ses bordures et correspond à une décroissance de la teneur en Ca du cœur du cristal vers les bordures enrichies en Na. Néanmoins la zonation peut aussi être oscillatoire. Par ailleurs, certains plagioclases montrent plusieurs nucleus de croissance pouvant correspondre à une coalescence de plusieurs cristaux dans un même plagioclase (Vance, 1957). En cathodoluminescence (CL), les plagioclases primaires montrent une luminescence jaune verte à jaune pâle (Leichmann et al., 2003). La variation de la luminescence est en adéquation avec la composition chimique du plagioclase. Les plagioclases montrent par endroits les inclusions de biotite et séricite (Fig. 26B, 26C).*

*Dans les **facies rouges**, les plagioclases sont soit entièrement albitisés et pigmentés d'hématite ou partiellement albitisés montrant des structures en échiquier caractérisées par des reliques de plagioclases primaires clairs au sein de l'albite secondaire rouge (Fig. 27, Fig. 28). L'albite secondaire montre une pigmentation rouge plus intense au voisinage des fractures qu'à l'écart de celles-ci. Les analyses élémentaires par sonde EDS confirment que les zones hématisées au sein des plagioclases sont formées d'albite. La CL met en exergue les contrastes optiques entre plagioclases primaires et albite secondaire et permet ainsi de montrer le dévelopement de l'albitisation. Les modes de développement de l'albite sont variés. La composition du plagioclase primaire intervient : quelquefois l'auréole extérieure est préservée en raison de son caractère albitique primaire (Fig. 30D) et ne présente alors pas de pigmentation par l'hématite ; d'autre fois c'est le cœur des cristaux qui est albitisé préférentiellement (Fig. 29A, 30C) en raison de sa composition plus anorthitique. Dans tous les cas l'albitisation est favorisée par les discontinuités au sein des cristaux : le long de fractures, selon un chevelu de micro-fractures, le long de plans de mâcle, etc. (Fig. 29B, C , D, Fig. 30A, B) .*

*D'autre part, l'albite secondaire est dépourvue de macles polysynthétiques impliquant une recristallisation totale du plagioclase. Néanmoins l'orientation de l'albite secondaire coïncide généralement avec celle de la macle majeure du plagioclase primaire suggérant que la recristallisation se fait suivant l'orientation de cette macle. Lorsque les zones albitisées sont amiboïdes, le plagioclase albitisé montre une extinction par bloc caractérisée par le fait que l'angle d'extinction de la zone albitisée correspond à celui de l'éclairement du plagioclase primaire. Mais par ailleurs, quand les zones albitisés sont amiboïdeselles montrent différentes orinetation de l'albite secondaire au sein d'un même plagioclase primaire. Cette disposition montre que l'albitisation se développe aussi en dehors de toute relation cristallographique avec le plagioclase primaire.*

*Enfin, albitisation et pigmentation hématitique sont strictement liés, il n'a jamais été observé de discorcdance entre les deux phénomènes, montrant qu'ils se sont dévéloppés de façon concomittante.*

### *LES FELDSPATHS POTASSIQUES (FK)*

*Dans les **faciès clairs**, les feldspaths potassiques apparaissent sous forme de cristaux automorphes individuels (Fig. 31) généralement de petite taille ou sous forme de phénocristaux (>1 cm). Les feldspaths potassiques peuvent ne pas être maclés ou présenter la macle de Carlsbad typique des orthoses et les macles polysynthétiques typique du microcline (Fig. 31B, Fig. 31C). Les orthosesmontrent des perthites ou des microperthites correspondant à des figures d'exsolution de lamelles d'albite (Fig. 31D) au cours du refroidissement. En CL, les orthoses montrent une luminescence bleue vif tandis que le microcline affiche une luminescence bleu pâle.*

*Dans les **faciès rouges**, les petits feldspaths potassiques les phénocristaux et sont entièrement ou partiellement perclus de pigments d'hématite, avec pigmentation plus intense au voisinage des fractures et moins intense à l'écart (Fig. 32, Fig. 33A, Fig. 33E). En CL, les zones rouges/roses apparaissent non-luminescentes voire faiblement luminescentes comme dans l'albite secondaire vue plus haut. Les zones claires montrent une luminescence bleue typique des FK primaires (Fig. 33A, Fig. 33B). Cette perte de luminescence dans les feldspaths potassiques est connue comme étant caractéristique de l'albite secondaire formée dans les conditions diagénétiques ou d'altérations météoritiques (González-Acebrón et al., 2010 ; González-Acebrón et al., 2012). Les lamelles d'exsolution d'albite restent claires et luminescentes et ne sont donc pas altérées (Fig. 33E et F). La cathodoluminescence permet de mettre en révéler les relations géométriques entre albite secondaire et FK primaire. Tout comme pour les plagiooclases, l'albitisation procède selon des fronts irréguiers et interpénétrés, procédant depuis la périphérie des cristaux, le long de fractures et selon un chevelu de microfractures (Fig. 33B, C et D).*

*Les phénocristaux d'orthose permettent de préveler des échantillons purs sélectionés dans les zones claires et roses d'un monocristal et ainsi préciser les transformations minéralogiques qui accompagnent leur albitisation. La déconvolution des diagrammes montre que ces cristaux sont formés d'orthose, de microcline et d'albite (Fig. 34). Les raies de diffractions de l'orthose sont toujours déplacées vers les plus grands angles de diffraction, correspondant à des substitutions en Na qui peuvent être estimées à environ 15%. Les déterminations quantitatives monrent que (Fig. 35) : (1) les phénocristaux de FK blancs sont exclusivement formés d'orthose accompagnée d'environ 15% d'albite ; (2) les phenocristaux roses contiennent toujours environ 30% de microcline à côté de l'hortose et de l'albite ; et (3) la teneur en albite augmente (d'environ 15 à 50%) corrélativement avec la diminition de l'orthose dans les phénocristaux roses. La pigmentation rouge des phénocristaux s'accompagne d'une vraie albitisation et d'une microclinisation.*

*L'albite qui accompagne l'orthose dans les phénocristaux blancs correspond à l'albite d'exsolution lors du refroidissement. Apparemment le microcline se développe en premier dans les orthose les moins altérées ; l'albite ne se développe que quand l'altération augmente. De plus, les raies de diffractions de l'orthose sont toujours déplacé vers les plus grands angles de diffraction, correspondant à des substitutions en Na qui peuvent être estimées à environ 15%. L'orthose associée aux phénocristaux les plus altérés montre des taux de substitution en moyenne supérieurs à ceux des phénocristaux non altérés. Ces orthoses plus substituées apparaisent ainsi résiduelles plutot que résultant que de l'aggradation/recristallisation d'orthoses primaires et seraient plus stable dans les environnement enrichis en Na à l'origine de l'albitisation.*

***LES MINERAUX FERROMAGNESIENS***

*Les biotites et amphiboles forment les minéraux ferromagnésiens primaires des* ***faciès clairs****. Les biotites sont moins fréquentes dans les granodiorites de Kłodzko Złoty-Stok (KZS) que dans les granite de Szklarska Poręba (SP). Elles apparaissent sous forme de minéraux tabulaires, automorphes, avec des clivages fins et réguliers, soit de couleur brun-clair (Fig. 36A, Fig. 36B) ou brun-foncé (Fig. 36C, Fig. 36D). Les biotites montrent deux types d'inclusions. (1) Des inclusions sans relation avec les clivages de la biotite, essentielement formées de zircon, d'apatite et d'oxydes de fer. Le zircon forme des cristaux automorphes avec leur auréole de radioactivité typique (Fig. 36B), l'apatite se présente en baguettes ou en minéraux trapus (Fig. 36A, Fig. 36D), tandis que les oxydes de fer, probablement de la magnétite ou de la pyrite, sont automorphes et sombres. (2) Des inclusions formées de silicates non ferrifères, quartz et FK, se disposent entre les clivages de la biotite. Le quartz se présente sous forme de baguettes tandis que les FK sont en lentilles (Fig. 37 et 41). Le quartz semble provenir d'une altération de la biotite qui libère les cations et laisse sur place la silice, tandis que le FK semble avoir cristallisé entre les feuillets de la biotite à partir d'un fluide alcalin. On note aussi la présence de minéraux plus exotiques tels que l'euxinite-polycrase connus dans les séries REE du magmatisme (Fig. 41H).*

*Les amphiboles sont présentes dans les granitoïdes de Kłodzko Złoty-Stok (KZS) mais absentes à Szklarska Poręba (SP). Elles apparaissent comme des hornblendes verdâtres, automorphes, maclées ou non avec des macles de Carlsbad (Fig. 38A) ou des macles multiples (Fig. 38B). Ces amphiboles forment néanmoins des agrégats xénomorphes avec la biotite (Fig. 38C) et comportent parfois des inclusions de zircon, d'apatite et d'oxyde de fer.*

*Les chlorites apparaissent dans les faciès clairs, mais sont plus abondantes dans les faciès rouges, jusqu'à devenir l'unique minéral ferromagnésien dans les faciès les plus rouges. Dans les faciès clairs, la chlorite est exclusivement associée à la biotite et jamais aux amphiboles. La chlorite se développe le long des clivages de la biotite, dont certaines paraissent beaucoup moins sensibles que d'autres à la chloritisation qui se limite dans ce cas aux bordures de la biotite (Fig. 39). La teneur en chlorite augmente de l'intérieur des blocs clairs vers les plans de fracture rouge.*

*Dans les* ***faciès rouges****, la chlorite est le minéral ferromagnésiens prépondérant, elle se développe par chloritisation des biotites et des amphiboles, mais accessoirement aussi dans les microfractures et pores. Les biotites sont presque entièrement chloritisées dans les faciès rouges. La chlorite apparaît verte en lumière naturelle, et montre une réfringence violette en lumière polarisée. Le stade initial correspond au développement de la chlorite sur les bordures de la biotite, tandis que dans le stade le plus avancé, seules demeurent quelques reliques de biotite brune au sein de la chlorite. (Fig. 40A, Fig. 40B). De l'hématite et quelque fois da la pyrite sont disposés le long des clivages des biotites chloritisées. L'hématite formant soit des granules, soit des plaquettes, le long des feuillets de biotite. Les relations géométriques entre biotite, hématite et chlorite suggèrent que ces hématites se sont formées dans une stade précose d'altération, dès l'initiation de la chloritisation. Titanite et rutile sont également associés aux biotite chloritisées (Fig. 41) et paraissent absents des biotites non altérées(Fig. 41) et correspondraient à la libération du Ti contenu dans les biotites.*

*Les amphiboles apparaissent moins sensibles à la chloritisation, elles ne sont pas altérées dans les faciès clairs et sont souvent préservées en reliques au sein des biotites chloritisées (Fig. 40D et Fig. 40E). La chlorite issue de l'altération des amphiboles présente les mêmes caractéristiques pétrographiques que celle provenant des biotites.*

*Des chlorites automorphes vertes se développent localement dans des pores et des fractures. L'occurrence la plus spectaculaire est le remplacement d'un minéral primaire par*

*de larges cristaux hexagonaux de chlorite et d'agrégats vermiculaires et associé à de l'hématite (Fig. 40F). L'occurrence de chlorites automorphes montre qu'elle a précipité à partir de fluides.*

***LA SERICITE***

*La séricite se présente sous forme de cristaux en feuillets birefringents associés aux plagioclases et rarement aux FK. Elle apparaît en feuillets fins et très peu développés dans les faciès granitiques (SP) (Fig. 42A, Fig. 42B) et en grands feuillets au cœur des plagioclases primaires (dont la bordure albitique est préservée) dans les faciès granodioritiques de Laski et de Chwalisław (Fig. 43). Dans les deux cas, les macles du plagioclase primaire sont oblitérées, voire effacées traduisant une recristallisation du plagioclase. Aussi, la formation de séricite au cœur du plagioclase est clairement liée à la déstabilisation de l'anorthite. La séricite est plus abondante dans les faciès clairs que dans les rouges, cependant sa distribution au sein des faciès rouges est moins évidente.*

***LES MINERAUX CALCIQUES***

***La prehnite*** *apparaît soit sous forme d'agrégats de cristaux au sein de plagioclases, en cristaux en éventail dans des joints intergranulaires de plagioclases et dans les clivages des biotiteset enfin dans fes fractures, indifférents aux minéraux des épontes. La prehnite en agrégats apparaît sans orientation particulière dans le cœur des plagioclases dont les bordures sont dépourvues de prehnite (Fig. 44A, Fig. 44B). La prehnite y est associée à de la séricite et à de fin grains d'albite qui préservent les clivages originel du plagioclase altéré. Cet habitus est celui communément décrit dans les plagioclases saussuritisés (Plümper and Putnis, 2009, Sandström et al., 2010). Les cristaux individuels de prehnite à l'extérieur des cristaux de plagioclase (Fig. 44C) ou les long des clivages des biotites faiblement chloritisées (Fig. 45). Cette disposition montre de façon indubitables qu'ils ont cristalllisé à partir de solutions. Les veines de prehnite recoupent les feldspaths-K, les plagioclases et les amphiboles sansque ceux-ci soient altérés (Fig. 46A, Fig. 46B).*

*La prehnite en agrégats dans les plagioclases est plus fréquente à l'intérieur des blocs, tandis qu'elle est moins abondante et plutôt sous forme de veines au voisinage des fractures. La distribution spatiale de la séricite et de la prehnite traduitvraisemblablement un gradient géochimique des fractures vers l'intérieur des blocs. Elles semblent favorisées dans les zones confinées éloignées des fractures.*

***La calcite*** *apparaît uniquement dans les faciès rouges et jamais dans les facies clairs. La calcite est le plus souvent dispersée et de distribution hétérogène au sein des faciès rouges, néanmoins elle forme aussi des veines qui recoupent les minéraux. La calcite forme des cristaux automorphes dans les veines et les pores (Fig. 47A, Fig. 47B) ainsi qu'entre les clivages de la biotite chloritisé (Fig. 47F). Sa luminescence est brun foncé, typique de la dolomite et/ou des calcites ferrifères, près des épontes des veines et orange vif caractéristique de la calcite vers le centre des veines. La cristallisation de ces calcite automorphes apparaît liée à des fluides enrichis en Ca et en* $CO_2$.

*D'autre part, de petites calcites dispersées sont perceptibles au cœur des plagioclases rouges/albitisés dont les bordures ne montrent aucune calcite (Fig. 47D). Cette disposition indique que cette calcite est cogénétique de l'albitisation des plagioclases qui libère du calcium. Une partie du Ca peut aussi provenir de la chloritisation des amphiboles.*

***L'apatite*** *apparaît à la fois dans les faciès clairs et dans les faciès rouges, elle semble néanmoins plus abondante dans les faciès rouges intensément chloritisés. Elle forme des inclusions sans orientation particulière, soit petites et nombreuses (Fig. 48B) ou plus grandes et automorphes (Fig. 48C). Il semble que les apatites soient en partie formées et/ou nourries*

*lors de l'altération des biotites, éventuellment aussi des amphiboles. Le fait que ces apatites puissent être néogeniques ou nourries semble confirmé au MEB par les images en électron rétrodiffusés (BSE) qui montrent des auréoles de réaction concenriques autour des apatites dans les biotites chloritisées des faciès rouges (Fig. 49E).*

***LES MINERAUX FERRIFERES***

*L'hématite, la pyrite et la maghémite sont les principaux minéraux du fer apparaissant dans les faciès rouges. Ces minéraux ont été caractérisés au microscope optique, en lumière réfléchie et par démagnétisation thermique, cette dernière permettant de pallier à la difficulté de détecter les oxydes de fer en faible quantité par difraction des rayons X. L'hématite est le plus abondant dans les faciès les plus rouges et le long des fractures, la maghémite dans les faciès à l'écart des fractures. La pyrite quant à elle ne montre aucune distribution particulière.*

*Les **pyrites** apparaissent comme de grands cristaux automorphes (50-200 µm), de formes hexagonales en connexion avec des minéraux mafiques. Certaines pyrites sont partiellement altérées montrant de l'hématite sur leurs bordures et un cœur de pyrite (Fig. 50B), tandis que d'autres correspondant à des remplissages de microfractures dans des minéraux xénomorphes (Fig. 50E). La pyrite forme aussi des lentilles allongées le long des clivages des biotites chloritisées (Fig. 51). Les relations entre pyrite et hématite montrent que l'héatite s'est formée par oxydation (liée à de l'altération météorique).*

*L'**hématite** apparaît soit sous forme de (1) pigments ; ou de (2) granules et microcristaux individualisés, ou (3) de cristaux sub-automorphes. L'hématite en pigments colore toutes les occurrences d'albite secondaire (Fig. 52A).. L'hématite en pigment est directement liée à l'albitisation des plagioclases et des FK et ne montre aucun lien avec les microfractures, ni avec les vides. Elle apparaît cogénétique de l'albite secondaire.*

*Des granules et microcristaux d'hématite apparaissent dans des microfractures et des joints intragranulaires et souvent en association avec de la chlorite. Mais si hématite et chlorite sont souvent associés spatialement, leurs relations mutuelles ne sont pas toujours évidentes (Fig. 52A et B). Les fractures à remplissage d'hématite sont toujours en connexion avec des biotites ou des amphiboles chloritisées et dans aucun cas il n'apparaît de liaison entre les fractures délimitants les blocs et une fréquence plus grande de veines à hématite. Localement, les hématites en veine forment des cristaux prismatiques subautomorphes en lumière réfléchie (Fig. 52C) qui dans ce cas résultent probablement de précipitations ou recristallisations sous l'effet de fluides.*

*Enfin, de grands cristaux d'hématite sont disposés dans les clivages des biotites chloritisées (Fig. 52D et E) et souvent des lentilles de quartz y sont associées.*

*La **maghémite** est moins fréquente que l'hématite mais elle semble être liée aux facies les moins altérés/oxydés. Son occurrence n'a pas pu être caractérisée au microscope optique, ni en lumière réfléchie mais uniquement par la démagnétisation thermique.*

***Conclusion***

*La distribution de la pigmentation rouge montre une relation étroite entre les minéraux primaire et secondaire. Les faciès rouges sont caractérisés par de l'albite secondaire, l'hématite et la chlorite tandis que les faciès clairs sont caractérisés par des minéraux primaires tels que les plagioclases, les biotites et les amphiboles mais aussi des minéraux d'altération formant des agrégats de prehnite-albite-séricite. Les plagioclases, les amphiboles et les biotites montrent une évolution progressive des faciès clairs vers les plans*

*de fracture rouge qui recoupent la roche. Les plagioclases disparaissent en faveur de l'albite, tandis que les biotites et les amphiboles sont remplacées par la chlorite (Fig. 53).*

*L'altération la plus marquante dans les faciès rouges est l'albitisation entière ou totale des plagioclases, avec parfois la préservation d'auréoles ou de zones irrégulières faites de plagioclases clairs au sein de l'albite secondaire. L'albite secondaire est non-maclée, pigmentée par de l'hématite et associée parfois à de la séricite et à de la calcite. La disparition des macles primaires du plagioclase au cours de l'albitisation différencie clairement celle-ci de la saussuritisation au cours de laquelle ces macles sont préservées.*

*D'autre part, l'hématite apparaît indubitablement comme cogénétique de l'albite. En particulier il est exclu que l'hématite ai pu précipiter tardivement dans des micro-pores au sein de l'albite secondaire : dans ce cas on s'attendrait à voir des microfractures à hématitequi n'ont en fait pas été observées dans ces facies. Les seules fractures à hématites sont locales et toujours en relation avec des minéraux ferromagnésiens chloritisés. Dans cette perspective l'hématite apparaît cogénétique de l'albite secondaire, ce qui signifie que l'albitisation s'est faite dans des conditions oxydantes.*

*L'albitisation des plagioclases et des feldspaths potassiques est associée à la chloritisation des amphiboles et des biotites. Certaines biotites chloritisées montrent des lentilles de titanite, de feldspath-K et de pyrit einsérées entre les clivages, ellescorrespondent au lessivage de Ti, K, Si et Fe lors de la chloritisation. De même, les amphiboles chloritisées montrent des lentilles de calcites le long de leur clivage et qui résultent directement du relargage de Ca lors de la chloritisation des amphiboles.*

*La balance géochimique entre pigments hématite et chloritisation des biotites et des amphiboles mériterait d'être quantifiée.*

# CHAPTER 6

# 6 PETROGRAPHY

Petrographical investigations allow to precise the mineralogical changes and to underline the geometrical relationships between mineral phases which are of prime importance to reconstruct the alteration sequences and to define the mass balance of these alteration processes.

## 6.1 PLAGIOCLASES

### *6.1.1 Plagioclases within the light/unstained facies*

Plagioclases (Ab45 - An55) are the most abundant feldspars in all light/unstained facies. They generally appear as white, either large euhedral crystals reaching 0.5-1.5 cm (Fig. 24A) or as smaller euhedral inclusions within K-feldspars phenocrysts, in particular in the Chwalisław area and at Szklarska Poręba quarry.

Both larger and smaller plagioclases globally emerge either as zoned crystals or crystals with typical albite polysynthetic twinnings (Fig. 24, Fig. 25). Nevertheless, they often occur as crystals with both features, i.e. zoning and twinning. Thus, their habits and characteristics appear as related to the disposition and arrangement of the twinning versus zoning.

Some of the plagioclases are exclusively zoned and without twinnings. Even when some twinnings exist, these are limited to the external edge of the crystals (Fig. 25A). The zoning is characterized by the propagation of the extinction (dark tint) from the core of the crystal toward its rim. Some zonings are continuous with a regular propagation of the extinction from the core towards the rim. This extinction propagation from plagioclases core toward their rim corresponds to a lowering of their $Ca2^{+}$ content and an increase in their $Na^{+}$ content. Others zonings are discontinuous, showing oscillating extinction between the core of the crystal towards the rim. Thus, the crystal appears with recurrent concentric dark rings (Fig. 24D). The oscillating extinction corresponds to a recurrent inversion in the lowering direction of their $Ca2^{+}$ content (Roubault et al., 1963). Oscillatory zoned plagioclases have compositions varying between alternately more or less albitic zones (Turner and Verhoogen, 1980). The oscillatory zoning in plagioclase is generally attributed to magmatic pulses or magma mixing as it has been described in detail in the Szklarska Poręba Massif (Słaby and Martin, 2008).

Other plagioclases are entirely (Fig 24B) or partially twinned (Fig. 24C, Fig. 25B). Two kinds of partial twinning were observed: (1) non-twinned zones occur within the twinned plagioclases (Fig. 24B). Twinned and non-twinned zones have the same optical orientation, testifying that they are part of a single crystal. Moreover, non-twinned zones show a compositional zoning. (2) Twinnings develop throughout the plagioclase crystal except to the external aureole which remains non-twinned (Fig. 25C). Most of the twinning appears as continuous, either with a uniform width along the crystals or with a narrowing width along some crystals. However, some of them appear as discontinuous or even interrupted by inclusions.

Primary twinning in plagioclase depends on the crystal growth velocity during the magmatic cooling, rapid growth favours polysynthetic twinning formation while slow growth minimizes twinning formation (Brueger., 1945; Vance., 1961). Multiple cores (without twinning; Fig. 25B) in plagioclases may correspond to the result of coalescent growth where

these cores are visible in the same crystals (Vance, 1957) or due to resorption-regrowth textures during mixing of felsic and mafic magmas likely in the Szklarska Poręba Massif (Słaby et al., 2002; Słaby and Martin, 2008).

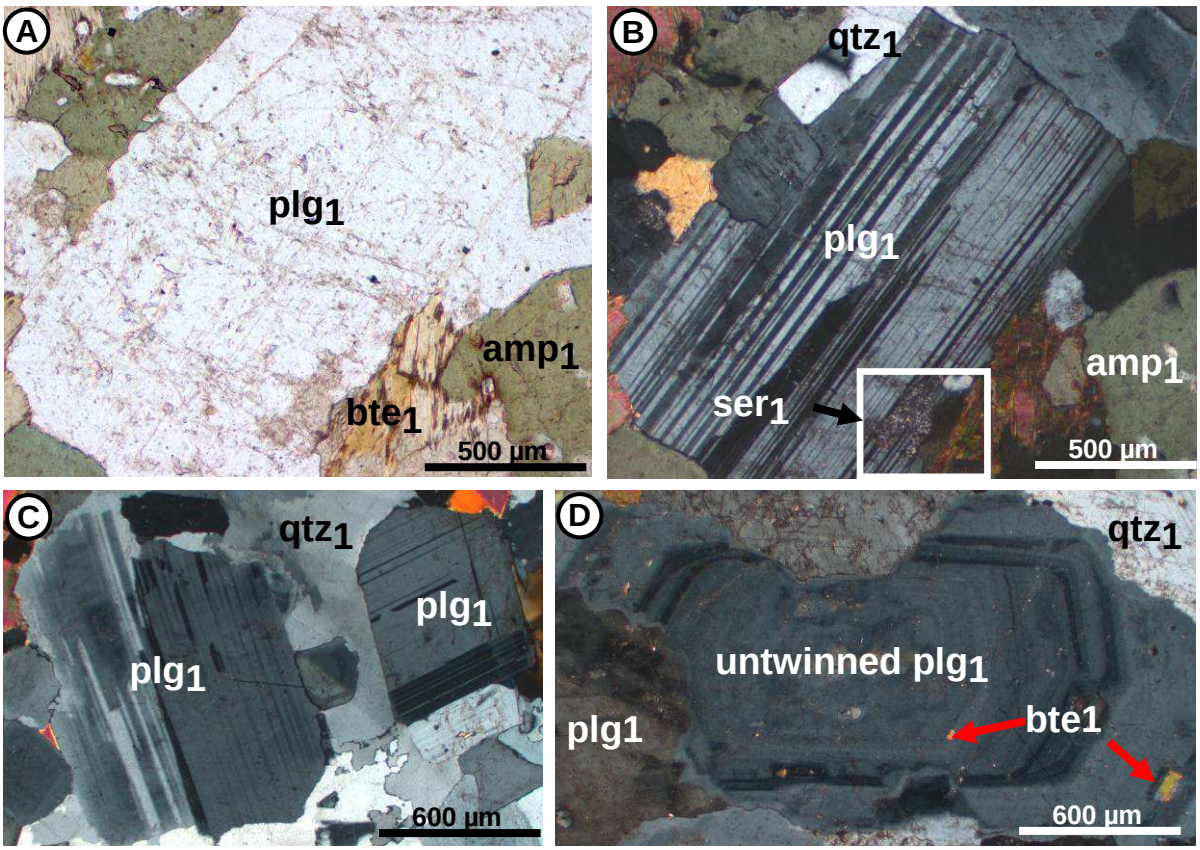


**Figure 24 – Plagioclase occurrence within the light/unstained granitoïd rocks from the Kłodzko Złoty-Stok massif. (A) and (B) Primary white and non-altered plagioclase crystal. The plagioclase is entirely twinned (polysynthetic parallel twinning), however sericite appears in an area at its edge. (A)_Plane polarized. (B) Cross polarized; (LAR77, Laski valley). (C) Two partially twinned plagioclase crystals. The biggest (on the left of the pictures) show a non-twinned and a twinned area. The twinnings appear as discontinuous. The smallest (upper right corner) show non-twinned and twinned zones and the twinning directions are perpendicular; cross polarized; (WL18, Chwalisław valley). (D) Plagioclase showing dark concentric extinction rings and biotite inclusions; cross polarized; (WL18, Chwalisław valley); plg1: plagioclase; bte1: biotite; amp1: amphibole; qtz1: quartz; ser1: sericite.**

***Figure 24 – Plagioclases dans les granitoïdes de faciès clairs du massif de Kłodzko Złoty-Stok. (A) et (B) plagioclase primaire non altéré. Le plagioclase est entièrement maclé (macles polysynthétiques parallèles), cependant quelques séricites sont visibles sur l'une des bordures du cristal. (A)_lumière naturelle. (B)_lumière polarisée. (LAR77_vallée de Laski). (C) Deux plagioclases partiellement maclés. Le plus grand (sur la gauche de l'image) montre à la fois des zones maclées et non maclées. Les macles sont discontinues. Le plus petit (coin droit de l'image) montre aussi des zones maclées et non maclées et les macles sont même perpendiculaires. Lumière polarisée. (WL18_vallée de Chwalisław). (D) Plagioclase montrant des auréoles d'extinction sombres et concentriques et des inclusions de biotite. Lumière polarisée. (WL18_vallée de Chwalisław). plg1: plagioclase; bte1: biotite; amp1: amphibole; qtz1: quartz; ser1: séricite***

Few chemical compositions of the primary plagioclases are available in the litterature, especially in the Szklarska Poręba Massif (Słaby et al., 2002; Słaby and Martin, 2008). They show that plagioclase composition of the Szklarska Poręba microgranite (equigranular) are variable (Table 2).

**Table 2 - Chemical composition and calculated structural formulae of plagioclases from the equigranular granite (µgranite) in the Szklarska Poręba Huta quarry (from Słaby and Martin, 2008).**

***Tableau 2 - Compositions chimiques et formules structurales calculées de plagioclases du microgranite de la carrière de Szklarska Poręba Huta (extrait de Słaby and Martin, 2008).***

| | $SiO_2$ | $Al_2O_3$ | CaO | BaO | $Na_2O$ | $K_2O$ | Σ | Ab | An | Or |
|---|---|---|---|---|---|---|---|---|---|---|
| EQUI-1 | 61.97 | 23.13 | 5.12 | 0.05 | 8.51 | 0.60 | 99.38 | 72.54 | 24.11 | 3.35 |
| EQUI-12 | 67.37 | 20.26 | 1.06 | 0.04 | 10.99 | 0.19 | 99.91 | 93.96 | 5.03 | 1.01 |

The CL characteristics of the primary plagioclases from the unstained facies generally exhibit a yellow-green to pale yellow luminescence, typical of igneous plagioclases (Leichman et al., 2003).

Furthermore, the CL images highlight the geometrical features of the plagioclases such as twinnings and zoning. The luminescence of the primary plagioclases varies in intensity from their core towards their rim (Fig. 26). This luminescence intensity variation is in agreement with the chemical composition changes from their $Ca^{2+}$-rich core towards their $Na^{+}$-rich rim. Mora and Ramseyer (1992) suggest that yellow luminescence intensity in plagioclase appears as related to the Na/Ca ratio from calcic-rich plagioclase to an intermediate plagioclase. Chemical changes in single plagioclases, such as zoning, may be underlined by alternation of pale yellow to yellow rings (Fig. 26B) or even large isochemical zones (Fig. 26D). Plagioclases also contain small biotite flakes (Fig. 24D) and sericite as inclusions (Fig. 26B, Fig. 25C).

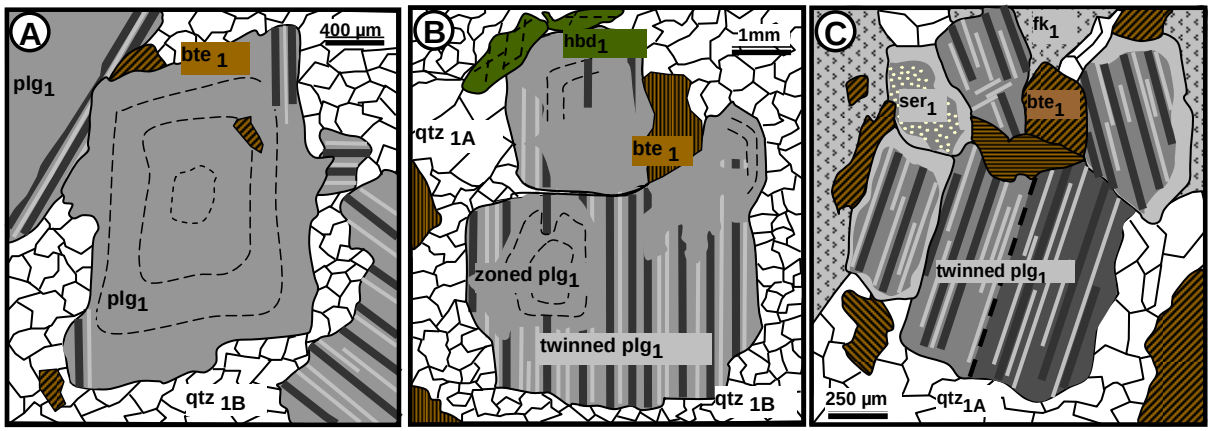


**Figure 25 - Sketch of primary plagioclases from the Kłodzko Złoty-Stok massif. (A) Zoned plagioclases with polysynthetic twinning on its edges (LSA30, Laski quarry). (B) Twinned plagioclase with zoned and non-twinned areas (LSA31, Laski quarry). (C) Plagioclase showing a non-twinned aureole/rim; sericite develops in the core of the plagioclase on the left. Plg1: primary plagioclase, bte1: primary biotite, qtz1A: large quartz crystals, qtz1B: small quartz crystals, hbd1: primary hornblende, ser1: primary sericite.**

***Figure 25 – Schéma de plagioclases primaires dans le massif de Kłodzko Złoty-Stok. (A) Plagioclases zonés montrant des macles polysynthétiques limitées à sa bordure (LSA 30_carrière de Laski). (B) Plagioclases maclés avec à la fois des domaines zonés et non maclés (LSA 31_carrière de Laski). (C) Plagioclase montrant une auréole non maclée. La séricite se développe au cœur du plagioclase sur la gauche (CHS 5_vallée de Chwalisław). Plg1: plagioclase primaire, bte1: biotite primaire, qtz1A: larges cristaux de quartz, qtz1B: petits cristaux de quartz, hbd1: hornblende primaire, ser1: séricite.***

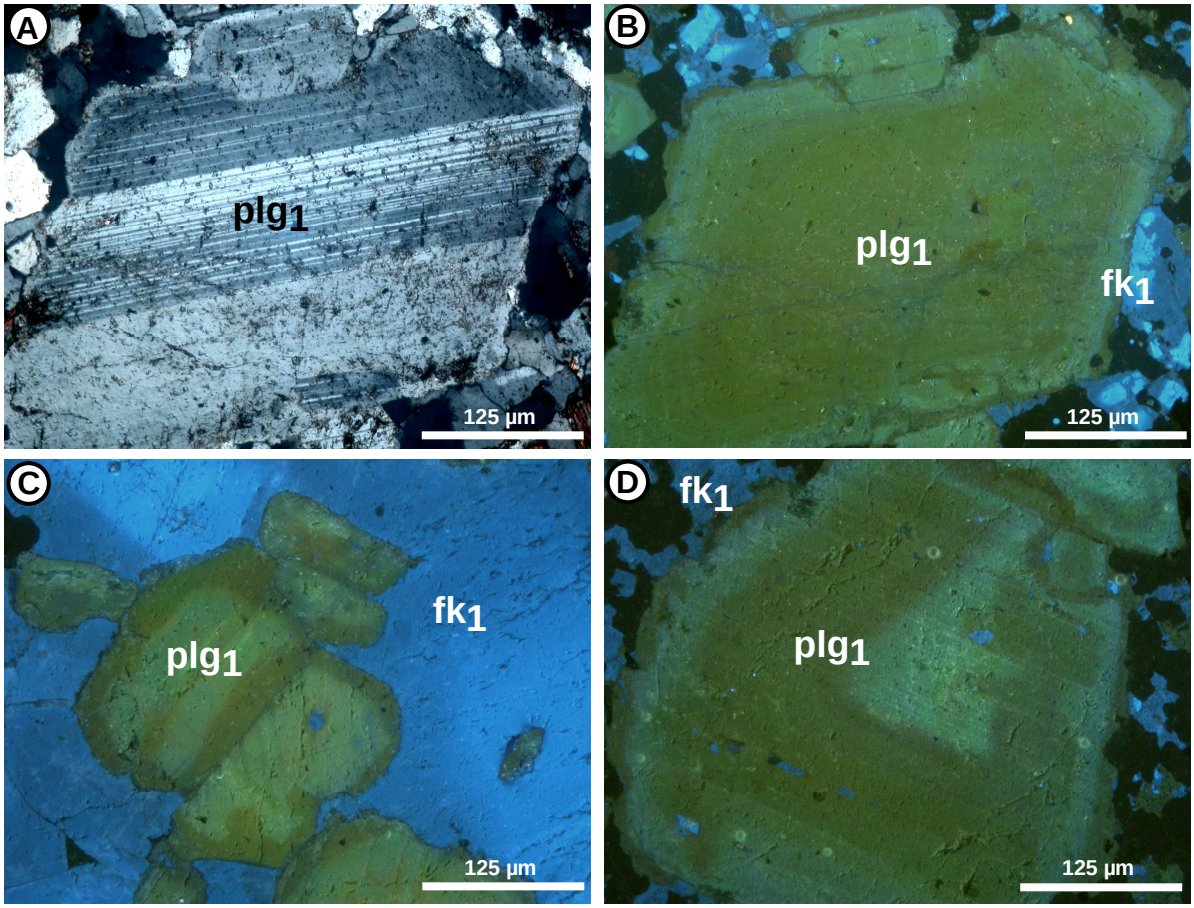


**Figure 26 - Cathodoluminescence (CL) images of the primary plagioclases (A) and (B) Primary plagioclase partially twinned. CL image of this plagioclases show a yellow core and a pale-yellow rim. Twinnings are not distinguishable here, but CL also reveals that the crystals are zoned; (A) cross polarized. (B) CL image (LAR65, Laski valley). (C) Plagioclase crystals within the K-feldspars showing regular zoning characterized by pale-yellow rims and yellow luminescence in their cores; CL image; (LAR77, Laski valley). (D) Plagioclase exhibiting yellow to pale-yellow domains from the core towards the rims suggesting also oscillating zoning; CL image; (LAR57, Laski valley). Plg1: primary plagioclase, fK1: primary K feldspar.**

***Figure 26 – Images en cathodoluminescence (CL) de plagioclases primaires. (A) et (B) Plagioclase primaire partiellement maclé. En CL, ce plagioclase montre un cœur jaune et une bordure jaune pâle. Les macles ne sont pas distinguables mais les images en CL révèlent que le plagioclase est zoné. (A)_lumière polarisée. (B)_images de CL. (LAR 65_vallée de Laski). (C) Cristaux de plagioclases au sein de feldspaths potassiques et montrant une zonation régulière caractérisée par des bordures jaune pâle et un cœur jaune. Image en CL. (LAR77_vallée de Laski). (D) Plagioclase montrant des domaines à luminescence jaune et jaune pale depuis le coeur vers la bordure et qui dénote d'une zonation oscillante. Image en CL. (LAR57_vallée de Laski). Plg1: plagioclase primaire, fK1: feldspath potassique primaire.***

### *6.1.2 Albite of the reddened facies*

Throughout the studied facies, altered plagioclase show specific microscopic features in relation with the type of reddening and with their textural relationship with the fractures.

Most of the plagioclases from the pervasive reddened facies (Laski village) and from fracture walls are entirely stained (Fig 27A), but some of them show chessboard like features characterized by reddened patches together with light plagioclase (Fig. 27B). Plagioclases from the pinkish and less intensively reddened zones (halfway from fracture walls or in the spotted zone) are partially reddened (Fig. 27C), in fact, they appear together within the same crystal light primary plagioclase and pinkish albitized zones.

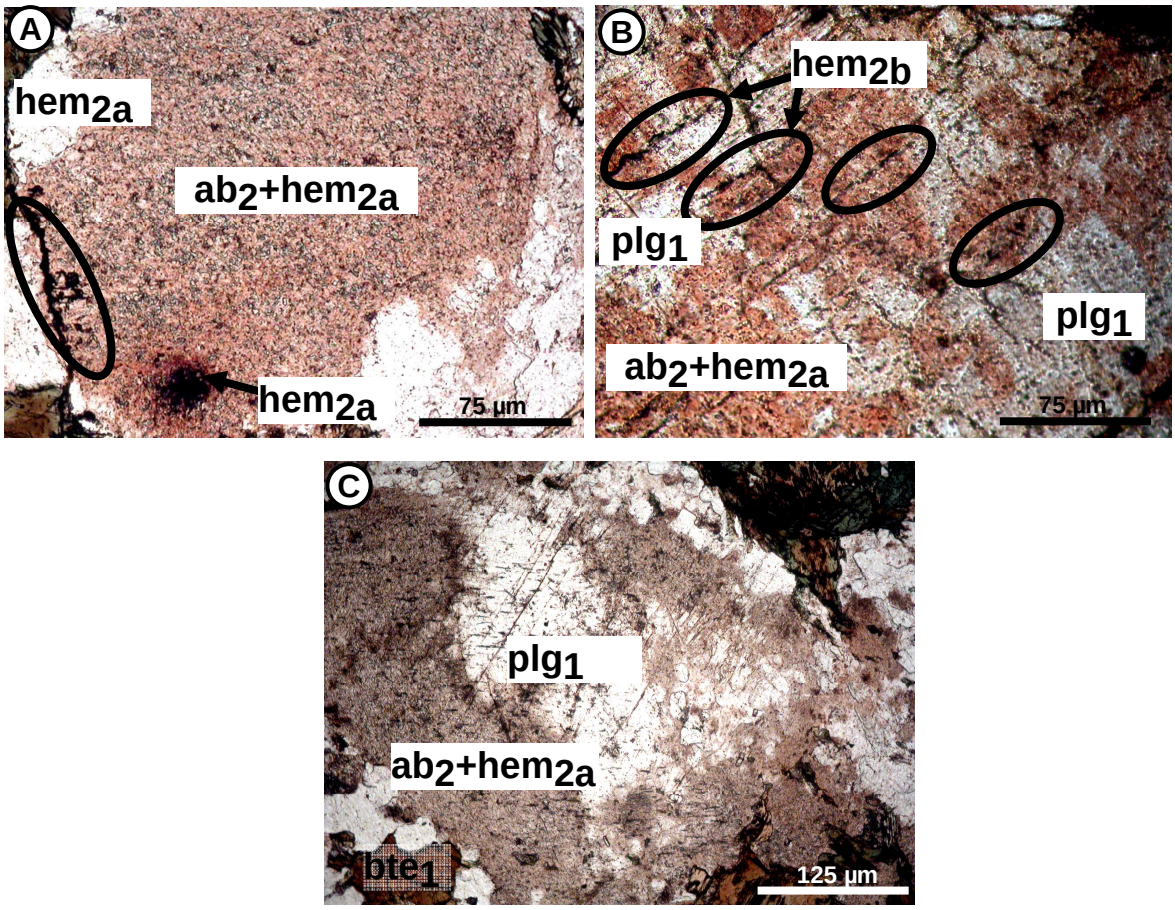


**Figure 27 - Albitized plagioclase in the reddened facies. (A) plagioclase entirely reddened and albitized from pervasive reddened facies. Hematite appears as pigment within the secondary albite and also as granules within the microfractures; plane polarized; (WL93, Laski village) . (B) Plagioclase from pervasive reddened facies showing scattered albitized/reddened areas and light areas. The reddened zones are composed of albite and hematite while the light areas are made of plagioclase. Microfractures are stained with hematite, contributing to the red coloration. Some of these microfractures even show hematite as dark granules and red vicinities; plane polarized; (WL97, Laski village). (C) Light pink albitized plagioclase away from the reddened fracture walls. Remnant primary plagioclase are light (plg1) surrounded by secondary pinkish albite that develops from the crystal rim and in favour of microfractures; plane polarized; (WL71b, Laski quarry).**

***Figure 27 – Plagioclases albitisés dans les faciès rouges. (A) Plagioclases entièrement rougies et albitisés issus des facies pervasivement rouges. L'hématite apparaît sous forme de pigments au sein de l'albite secondaire mais aussi sous forme de granules au sein des microfractures. Lumière naturelle. (WL 93_village de Laski). (B) Plagioclases issus des facies pervasifs rouges montrant à la fois des zones rouges/albitisées et des zones claires. Les faciès rouges sont constitués d'albite et d'hématite tandis les zones claires sont faites de plagioclase et dépourvues d'hématite. Les microfractures sont pigmentées d'hématite, contribuant à la coloration globale des roches. Certaines de ces microfractures montrent même de l'hématite sombre mais aussi des bordures rouges. Lumière polarisée. (WL97_village de Laski). (C) Plagioclase rose clair albitisé issu de zones éloignées des fractures rouges. Les reliques de plagioclase primaire (plg1) demeurant clairs sont environnées par l'albite secondaire rose développée sur la bordure du cristal et cela à la faveur des microfractures. Lumière naturelle. (WL71b_carrière de Laski).***

**EDS maps** obtained on the partially reddened/altered plagioclases in the SEM allow to precise the composition of reddened zones within plagioclase crystals and allow to establish if they are actually albitized or not. Petrochemical calculations on EDS maps help to highlight zones using a specific color code in relation with their chemical composition (Fig. 28). The emphasis has been put on determining zones composed of pure sodium, potassium, and calcium within the plagioclases.

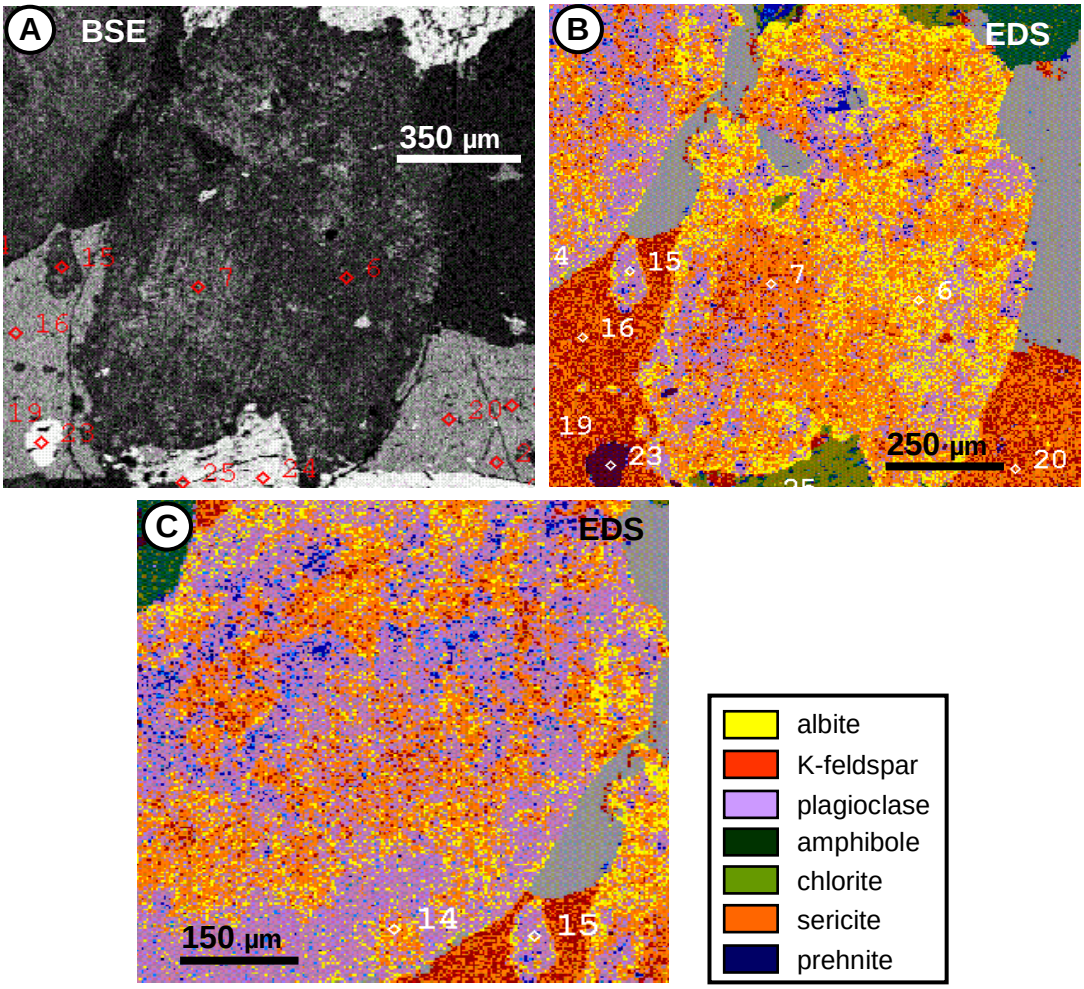


**Figure 28 – Combined BSE image and elemental distribution map of the reddened/altered zone within a plagioclase crystal. (A) Altered plagioclase in the center of the picture showing white unaltered zones and a dark reddened/altered zone; BSE image. (B) Plagioclase almost entirely reddened/altered. The reddened/altered zones show yellow colour composed of albite stained with tiny reddened dots corresponding to sericite. Relics of primary plagioclase appear as mauve; EDS mapping image. (C) Weakly reddened/altered plagioclase, showing more relics of plagioclases in mauve, while albite and sericite are composed of the reddened/altered zone; EDS image (WL145, Chwalisław mountain). Phases appearing as green are Fe-Mg minerals (chlorite, amphibole) while large red minerals showing tiny scattered yellow dots are K-feldspars with tiny albite inclusions.**

***Figure 28 – Image en BSE et cartes élémentaires d'une zone altérée/rougie au sein d'un plagioclase. (A) Plagioclases altérés dans le centre de l'image montrant des zones non altérées en blanc et des zones rouges/altérées sombres. Image en BSE. (B) Plagioclases presqu'entièrement rouges/altérés. Les zones rouges/altérées montrent une coloration jaune composées d'albite, et pigmentées de petits points rouges correspondent à des séricites. Les reliques de plagioclases sont mauves. Images en EDS. (C) Plagioclase faiblement rougi/altéré montrant plus de reliques de plagioclases en mauve, tandis que la zone altérée est composée d'albite et de séricite. Image en EDS. (WL145_Montagne de Chwalisław). Les minéraux apparaissant en vert sont des ferromagnésiens (chlorite, amphibole), tandis que les grands minéraux rouges montrant des petits points jaunes sont des feldspaths potassiques avec des inclusions d'albite.***

Reddened/altered zones within plagioclase appear as yellow and stuffed with several tiny red dots while the primary plagioclase is mauve (Fig. 28B & 28C). This shows that the reddened/altered zones within plagioclase are composed of 100% $Na^+$ corresponding to albite and tiny minerals composed of 100% $K^+$ matching with sericite. This clearly indicates that the reddened/altered zones of plagioclases are albitized.

In the meantime, it appears that large red minerals stuffed with yellow dots correspond to K-feldspars. This suggests that the K-feldspars are not pure but that they are composed of minute albite probably perthites. This may be considered from the study of the probable albitization of the reddened K-feldspars.

The reddened plagioclases are clearly albitized but the ways the albitization process and the microfabrics inherited from the primary plagioclase proceed should be precised. This will be underlined by CL images which provide useful contrasts between the albitized zones and the unaltered zones within plagioclases.

**Cathodoluminescence** (CL) allows to precise the microfabrics related to the plagioclase albitization. Such microfabrics are best visible in partly albitized plagioclase crystals that occur in intermediate pink and spotted facies. Dark or light luminescence in the feldspars is documented which is characteristic respectively for the neogenic low-temperature feldspars (Kastner and Siever, 1979; Ramseyer et al., 1992; Leichman et al., 2003) or for the primary igneous feldspars (Leichman et al., 2003). Therefore, CL images are a useful tool to highlight the contrast between the primary plagioclase and the secondary albite and to allow the determination of the geometrical relationship between reddened and unaltered zones.

When using CL microscopy, the reddened albitized zones show dark luminescence whereas the light unaltered plagioclases exhibit a bright yellow-green luminescence (Fig. 29). Often, plagioclase crystals show a dark luminescence core corresponding to neogenic low-temperature albite, surrounded by an aureole remaining bright, characteristic of primary igneous palagioclase (Fig. 29A). In detail, plagioclase albitization processes through a network of hair-thin micro-fractures (Fig. 29B, 29C & 29D).

Twinned plagioclases often match with the alternating dark non-luminescent and bright luminescent twinning lamellae (Fig. 29C & 29D). In this case, albitization develops preferentially along some of the twinning laths. Dark luminescent albitized microfractures are particularly well expressed and visible in the vicinity of the dark luminescent twinnings and patches.

CL contrasts show that micro-fractures as well as the twinnings are preferential pathways favouring the albitization process. The CL images also show that the albitization is related to all type of structural defects within the minerals. It seems that specific crystallographic orientations favour the ionic exchanges via solution that are needed to alter the Ca-bearing plagioclase into albite. This may be do to the spatial arrangement of the atoms in the crystal framework or to preferential fracturation along specific crystallographic orientations with regard to the tectonic stresses.

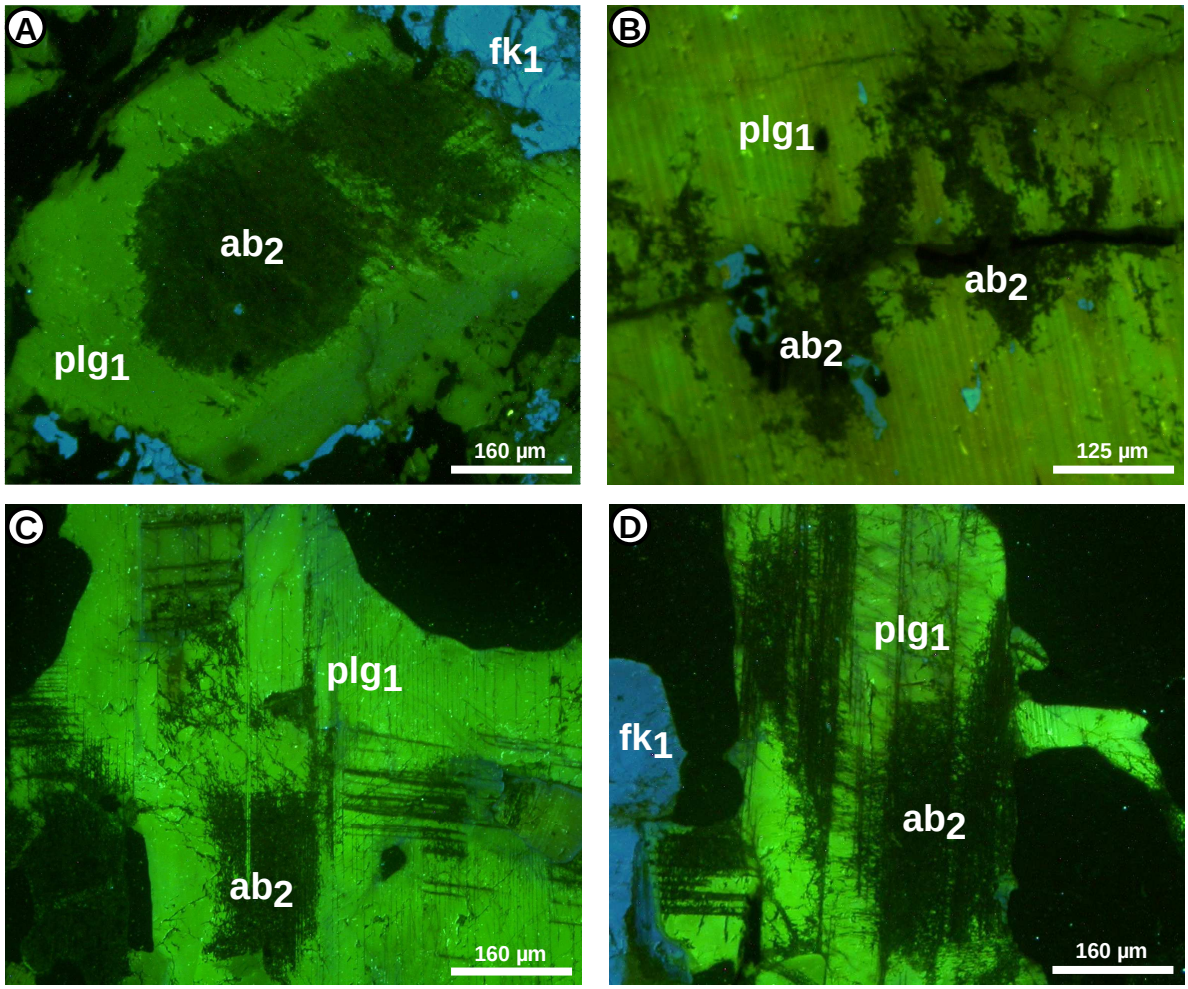


**Figure 29 - CL petrographic image of albitized plagioclases (A) plagioclase with a non-luminescent albitized core and yellow luminescent rim, (ZLR 2_ZłotyStok-Kopciowa Mountain). (B) Plagioclase albitization adjacent to a micro-fracture, (LAR 78_east of Laski valley). (C) Albitization along twinning and micro-fractures (SPR 1C, Szklarska Poręba quarry). (D) Albitization exclusively expressed along the major twinning features. The albitized-twinnings are interconnected by many micro-fractures (SPR1b, Szklarska Poręba quarry). fK1: primary K-feldspar; plg1: primary plagioclase; ab2: untwined secondary albite.**

***Figure 29 – Pétrographie en cathodoluminescence des plagioclases albitisés. (A) Plagioclase avec un cœur non luminescent albitisé et une bordure luminescence (ZLR 2_ZłotyStok-Montagne de Kopciowa). (B) Albitisation d'un plagioclase au voisinage d'une fracture (LAR 78_A l'est de la vallée de Laski). (C) Albitisation selon les macles et les microfractures (SPR 1C_carrière de Szklarska Poręba). (D) Albitisation exclusivement le long des macles majeures. Les macles avec albitisation sont reliées par des microfractures (SPR 1b_carrière de Szklarska Poręba). fK1 : feldspath potassique primaire ; plg1 : plagioclase primaire ; ab2 : albite secondaire non maclée.***

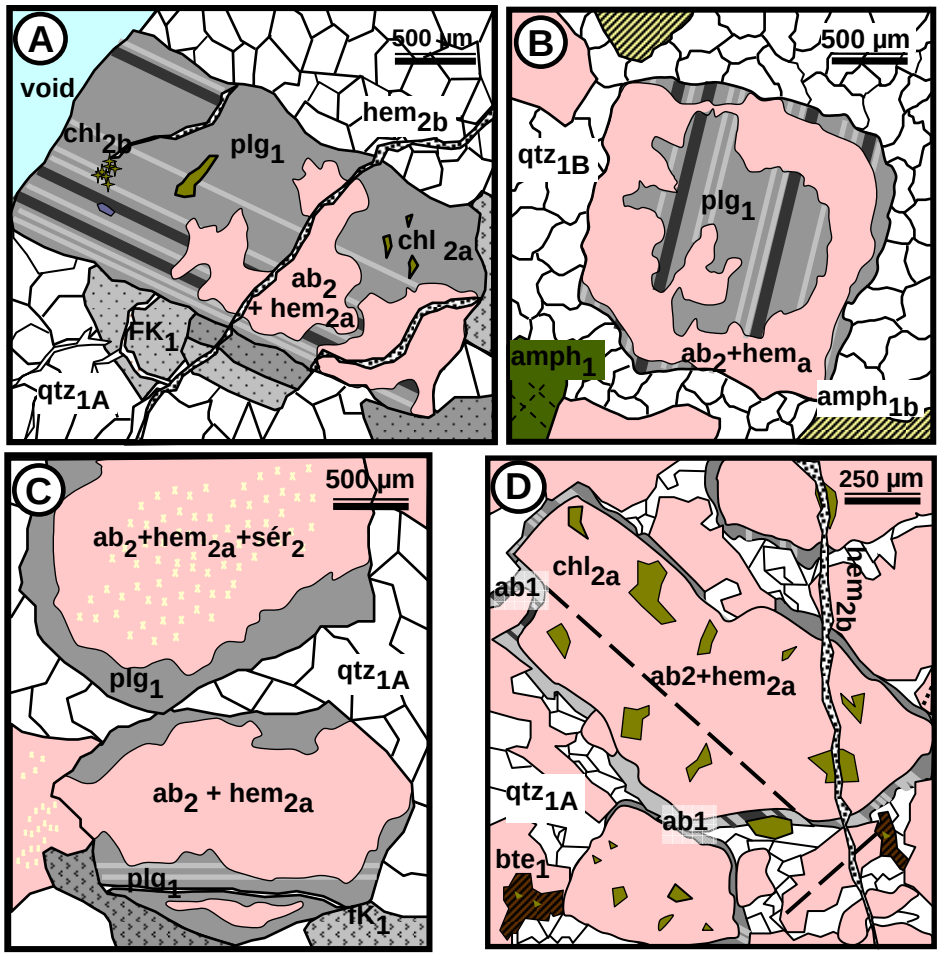


**Figure 30 – Sketches of albitized red/pinkish plagioclase patterns. (A) Albitized plagioclase in the vicinity of two microfractures. The reddened zones are composed of secondary albite and hematite while the rest of the crystal remains of clear and twinned labradorite. The primary twinnings disappear towards the reddened area (WL95, Laski village). (B) Albitized plagioclase showing irregular limits between the albitized area and the non-albitized zone. The plagioclase shows a preserved core area and rim; however an albitized ring developed between the primary aureole and the core (WL80, Laski valley). (C) Albitized plagioclase showing a non-twinned primary rim. The primary aureole is non-twinned but shows extinction pattern of zoned plagioclase while the non-twinned albitized core does not show any zoning. The reddened albitized contains sericite in addition to albite and hematite (WL71b, Laski quarry). (D) Albitized plagioclase showing a primary twinned albite rim. The core appears as non-twinned and composed of secondary albite and hematite. Some chlorites inherited from biotite are also visible within the albitized plagioclase (WL100, Laski village). plg1: primary plagioclase; ab1: primary albite; qtz1A: large euhedral quartz, qtz1B: small anhedral quartz; ab2: untwined secondary albite, hem2a: pigmentary hematite, hem2b: dark hematite granules. amph1b: partially chloritized amphibole.**

***Figure 30 – Schéma de plagioclases albitisés rouges/roses. (A) Plagioclase albitisé le long de deux microfractures. Les zones rougies en bordure des microfractures sont constituées d'albite secondaire, tandis que le reste du cristal demeure clair, non altéré et correspond à de la labradorite. Les macles du plagioclase disparaissent au niveau de la zone rougie. (WL 95_village de Laski). (B) Plagioclase albitisé montrant une limite irrégulière entre la zone albitisée et la zone non albitisée. Le plagioclase présente un cœur et une bordure préservé, avec une zone intermédiaire albitisée (WL 80_vallée de Laski). (C) Plagioclase albitisé avec auréole albitique non maclée. L'auréole primaire est non maclée et montre une extinction caractéristique de plagioclase zoné, tandis que le cœur non maclé et albitisé ne montre aucune zonation. La zone rougie albitisée contient de la séricite en plus de l'albite et de l'hématite (WL 71b_carrière de Laski). (D) Plagioclase albitisé montrant une bordure primaire maclée. Le cœur du plagioclase non maclé est composé d'albite secondaire et d'hématite. Des biotites chloritisées sont aussi visibles au sein du plagioclase albitisé (WL 100_village de Laski). Plg1: plagioclase primaire; ab1: albite primaire; qtz1A: larges cristaux automorphes de quartz, qtz1B: petits cristaux xénomorphes de quartz; ab2: albite secondaire non-maclée , hem2a: hématite en pigment , hem2b: hématite noir en granules. amph1b: amphibole partiellement chloritisée. chl2a : chlorite issu de biotite.***

### *6.1.3 Development of the albitization*

The spatial arrangements of the albitized/reddened zones within the primary plagioclases give information how the albitization develops. Most arrangements are either relative to the pathways of the solutions that cause the alterations or relatives to the composition of the primary plagioclases.

1) Development of the reddening/albitization along the microfractures is the most common pattern (Fig. 30A). Limits between the primary plagioclase zones and the secondary albite appear as irregular and interpenetrated. Albitized zones are patchy, amoeboid, and without any specific relationship to the crystallographic structure of the primary plagioclase. Nevertheless, sometimes albitization shows development of plagioclase along the cleavages, but in this case the cleavages act just like microfractures that favour albitization.
2) Often albitization develops from the outer rim of the plagioclase crystals towards the central part of the crystal, which may remain unaltered (Fig. 30B). In this case we can consider that the peripheral crystal junctions act likely microfractures.
3) Preferential albitization of the core of the primary plagioclase happens frequently. There are two different kinds of features: Either the albitized core is of irregular shape and often contains scattered tinny sericite crystals (Fig. 30C). Here albitization clearly affects the Ca-rich core of the primary plagioclase and was furthermore sericitized by an early alteration. The albitized core may be much more homogeneous and the non-albitized rim is of regular shape and thickness (Fig. 30D). This later arrangement relays on a zoned primary plagioclase which has been entirely albitized, except for the outer rim which already had a primary composition of albite.

Crystallographic relations between primary plagioclase and secondary albite can be specified by the respective crystallographic orientations in primary and secondary crystals and twins.

1) The secondary and hematite-stained albite does never show any polysynthetic twins. It appears that the primary twinnings are erased during the albitization. This points out that the secondary albite results from the recrystallization of the primary plagioclase and not only from a "simple" cation exchange. Nevertheless, optical extinction of the secondary albite fits always with the orientation of the widest twinning laths of the primary plagioclase. This means that the recrystallization follows the orientation of the widest twinning laths that appear as a preferential orientation. When twinned primary plagioclase crystals show two domains in which the first twinning orientation is dominant and a second where the second twinning orientation is dominant. The resulting secondary albite shows also two domains with distinct extinctions according to the dominant twinning orientation in the plagioclases (Fig. 30D).
2) Besides, when the albitized zones are amoeboid, the albitized plagioclase crystals show blocky extinction of the albitized zone whereas the primary plagioclase appears luminescent. Often, several different orientations of the secondary albite can be observed within the primary plagioclase. This arrangement points out that secondary albite develops without any relationship with respect to the crystallographic orientation of the primary plagioclase. Such blocky extinction has been reported as typical textures of diagenetic albitization in arkosic sandstones (Walker, 1984; Gold, 1985).

Lastly, there are several different kinds of mutual orientation of primary plagioclase and secondary albite. On the other hand, albitization and hematite staining are always strictly bound together, there has never been observed any discrepancy between the two phenomena, pointing out that both develop together. If this would not be the case, secondary albite would

have been observed without any hematite-staining and/or places where hematite would develop within non-albitized plagioclases.

## 6.2 K-FELDSPARS

### *6.2.1 K-feldspar in the unstained facies*

Orthoclase appears as a frequent mineral phase in all studied facies except for the lamprophyres where orthhoclases are totally absent. They occur as white individual euhedral crystals (Fig. 31) generally of smaller size than plagioclases in all the light/unstained facies except in Chwalisław area and the Szklarska Poręba quarry. In the latter sites, they often form phenocryst (>1cm) that contain many plagioclase and biotite inclusions.

K-feldspars may appear as non-twinned or twinned crystals (Fig. 31B, Fig. 31D). Two types of twinning are visible in the primary K-feldspars. Most of the K-feldspars exhibit Carlsbad twinning characteristic of orthoclase (Fig. 31D). This is in agreement with the XRD results that identified orthoclase as the unique K-feldspar phase in the light/unstained facies. Published chemical analyses of the K-feldspars from the Szklarska Poręba microgranite facies show that they correspond to a solid solution between Na and K (Słaby et al., 2002; Słaby and Martin, 2008). They have apparently a steady composition corresponding to about 8% of albite and 92% of K-feldspar, and additionally a minor amount of Ca, likely than most of the high (Table 3).

**Table 3 - Chemical composition and calculated structural formulae of K-feldspars from the equigranular granite (µgranite) of the Szklarska Poręba Huta quarry (from Słaby and Martin, 2008).**

***Tableau 3 - Compositions chimiques et formules structurales calculées de feldspaths-K du microgranite de la carrière de Szklarska Poręba Huta (extrait de Słaby and Martin, 2008).***

| | $SiO_2$ | $Al_2O_3$ | CaO | BaO | $Na_2O$ | $K_2O$ | Σ | Ab | An | Or |
|---|---|---|---|---|---|---|---|---|---|---|
| EQUI-1 | 63.30 | 19.48 | 0.02 | 0.23 | 0.89 | 14.58 | 98.5 | 8.33 | 0.10 | 91.57 |
| EQUI-12 | 64.75 | 18.22 | 0.03 | 0.03 | 0.92 | 15.42 | 99.37 | 8.33 | 0.10 | 91.57 |

Nevertheless, some few K-feldspars from the Szklarska Poręba quarry granite and the Laski valley granite that were analyzed under the optical microscope show tartan or crosshatched twinning typical for microcline (Fig. 31B & Fig. 31C). The tartan twinnings are localized within these K-feldspars and do not occupy the entire crystals (Fig. 31B &Fig. 31C). Tartan twinning development may be produced during the magmatic cooling when the prime monoclinic K-feldspars (sanidine, orthoclase) inverts into triclinic microcline (Winter, 2001).

Twinned orthoclases also show microperthites or perthites (Fig. 31D). These features correspond to exsolution during magmatic cooling of the orthoclase (mixed Na-K crystals) into two feldspars phases: Na-rich feldspar (albite) and K-rich feldspars (pure orthoclase). The more abundant of the two feldspars constitutes the crystal matrix while the less abundant appears as lamellae within the matrix. Here, the Carlsbad twinned matrix is composed of pure-orthoclase while the lamellae (perthites) are formed of albite. Those lamellae show identical extinction directions as typical for perthites.

Orthoclase shows a bright blue luminescence whereas microcline shows a pale blue luminescence. Blue luminescence of both orthoclase and microcline relate to a high formation temperature (Ramseyer et al., 1992; Finch and Klein, 1998).

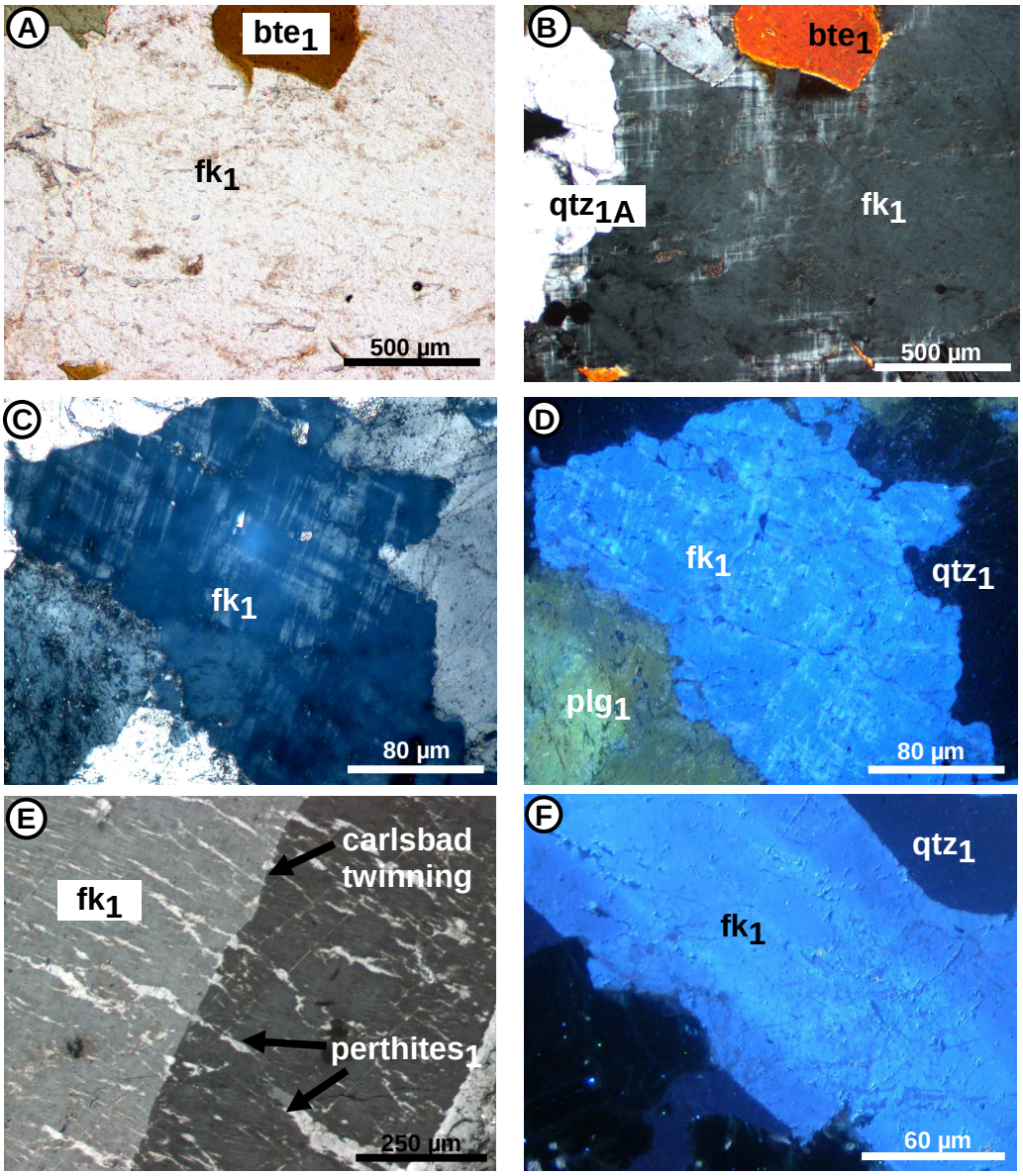


**Figure 31 – K-feldspar occurrence within the light/unstained granitoïd rocks from the Polish Sudetes. (A) and (B) light and non-altered K-feldspar showing in some places microcline cross hatched twins. The non-twinned part of this K-feldspar may correspond to orthoclase whereas the twinned one is microcline; (A) plane polarized; (B) cross polarized; (LAR77, Laski valley). (C) and (D) subhedral K-feldspar with microcline tartan twins; the microcline exhibits a pale blue luminescence. Cross hatched zones within the feldspars show a light blue luminescence; (C) cross polarized; (D) CL image; (LAR77, Laski valley). (E) K-feldspar phenocryst showing perthitic features and Carlsbad twinning (light zone and dark zone; cross polarized; WL6, Szklarska Poręba). (F) Orthoclase showing light blue luminescence; CL image. (CHR10, Chwalisław valley); fK1: primary K feldspar, bte1: biotite; qtz1A: large quartz crystals; plg1: primary plagioclases.**

***Figure 31 – Feldspaths des granitoïdes clairs des Sudètes. (A) et (B) Feldspath potassique clair non altéré montrant par endroits des macles en quadrillage du microcline. La partie non maclée de ce feldspath potassique correspond à de l'orthose tandis que la partie maclée est du microcline. (A)_lumière naturelle. (B)_lumière polarisée (LAR77_vallée de Laski). (C) et (D) Feldspath potassique subautomorphe montrant les macles quadrillées du microcline. Le microcline montre une luminescence bleue pâle. Les macles quadrillées apparaissent avec une luminescence bleu clair. (C)_Lumière polarisée. (D) Image en CL. (LAR77_vallée de Laski). (E) phénocristal de feldspath potassique montrant des perthites et une macle de Carlsbad. (Zone claire adjacente d'une zone sombre). Lumière polarisée. (WL6_carrière de Szklarska Poręba). (F) Orthose montrant une luminescence bleu clair. Image en CL. (CHR10_vallée de Chwalisław). fK1 : feldspath potassique primaire, bte1 : biotite primaire ; qtz1A : grands cristaux de quartz ; plg1 : plagioclase primaire.***

### *6.2.2 K-feldspars in the reddened/albitized facies*

K-feldspar phenocrysts (>1cm) and the smaller K-feldspars (<1cm) occurring within the reddened facies appear as entirely or partially pinkish, with some dirty aspect. Both feldspars show various habits and staining intensities in relation to the reddening distribution throughout the facies and with respect to the distance to the fractures. They are intense pink/red at the reddened fracture walls (Chwalisław area and Szklarska Poręba quarry) as well as in the pervasively reddened facies (Laski village) while they are less pink and even light away from the fracture walls.

Partially pinkish feldspars make it possible to underline the main geometrical relationships between the primary light zones and the secondary pinkish zones. These geometrical relationships as well as the main mineralogical characteristics differ slightly in the phenocrysts and in the smaller K-feldspars. Perthitic igneous albite lamellae for instance, which are frequent in the phenocrysts and scarcer in the smaller K-feldspars and may influence the alteration characterization.

#### *6.2.2.1 Phenocrysts*

Euhedral to sub-euhedral K-feldspar phenocrysts are common in the granitoïd facies of the Polish Sudetes. They are light in the unstained facies while they partly or entirely turned pink in the reddened facies (Fig. 32). The pinkish phenocrysts are particularly spectacular along the pinkish fracture walls. The significance of the pinkish colour in the K-feldspar phenocrysts has to be questioned: is the pinkish colour only related to the hematite pigments that invaded the primary K-feldspars or is it caused by further alteration that affects the K-feldspar itself,especially with the development of the neogenic albite?

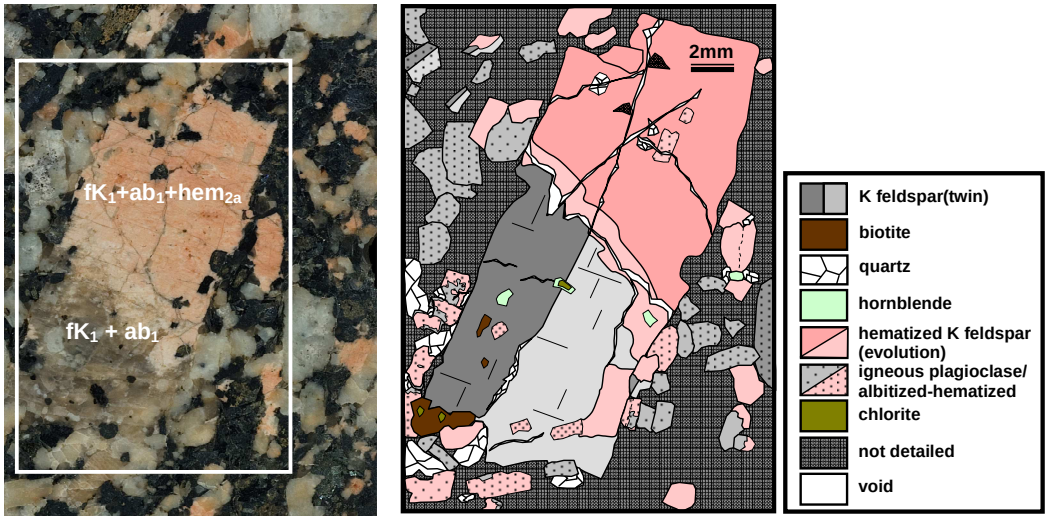


**Figure 32 – Orthoclase phenocryst partially reddened. (A) Macro-photograph of a polished section. The upper part of the phenocryst is pink and dull whereas the lower part seems translucent. (B) Sketch showing the phenocryst optical properties. The orthoclase phenocryst exhibits a classical Carlsbad twinning in the translucent part, and hornblende, chlorite, biotite and plagioclases as inclusions. In the pinkish part, plagioclases are albitized and hematitized as well as those in the vicinity of the phenocryst whereas biotite and amphibole are partially chloritized (WL146_Chwalisław Mountain).**

***Figure 32 – Phénocristal d'orthose partiellement rougi. (A) Image macroscopique en section polie. La partie supérieure du phénocristal est rose terne tandis que la partie inférieure est translucide. (B) Schéma montrant les propriétés optiques de ce phénocristal. Le phénocristal d'orthose montre la macle classique de Carlsbad dans la partie translucide, et des inclusions de hornblende, de chlorite, de biotite et de plagioclases. Dans la partie rose, les inclusions de plagioclase sont albitisées et hématisées comme ceux au voisinage du phénocristal, tandis que les biotites et les amphiboles sont partiellement chloritisées (WL146_Montagne de Chwalisław).***

The presence of primary albite (in form of crypto- to micro-perthitic exsolution lamellae) within the phenocrysts complicates highlighting the development of secondary albite in the pinkish K-feldspar phenocrysts. Stressing the development of albite in the pinkish phenocrysts consists in discerning the primary albite from the secondary one. Therefore, measuring the amount of albite in the light and pinkish phenocryst parts may allow to estimate to which amount they have been altered. A detailed XRD experiment has been conducted on hand picked areas within the single phenocrysts (by micro drilling) to determine their mineralogical composition.

#### *6.2.2.2 Smaller pinkish crystals*

Smaller pinkish K-feldspar occurrences are macroscopically less obvious and spectacular than those of the phenocrysts. They are characterized by a red/pink colour due to hematite pigments and sometimes show a turbid brownish aspect stained by pigmentary hematite. Partially pink K-feldspars exhibit many different geometrical features in relation with the distribution of the reddening within the single crystals that become obvious through cathodoluminescence images.

Some of the smaller K-feldspar crystals show blue luminescence patches that appear as light patches in plane polarized light, associated with non-luminescent or weak luminescent patches that are red/pink in plane polarized light (Fig. 33A & 33B). The non-luminescent zones are brownish in their centre, while their rims exclusively exhibit blue luminescence (Fig. 33B). The blue luminescence is typical of igneous K-feldspars whereas the non-luminescence/weak luminescence shows similarlies with the previously shown secondary albite. Indeed, this non- or weak luminescence in K-feldspars corresponds to secondary albite formed in a low-temperature context, more precisely under diagenetic or weathering conditions (González-Acebrón et *al*., 2010, González-Acebrón et *al*., 2012). The quenching of the luminescence and the fact that the luminescence becomes weak in albitized K-feldspars may be due to variable chemical compositions between the centre and the aureole of the primary orthoclase crystals. The centers of these crystals are composed of secondary albite in addition to secondary K-feldspar (González-Acebrón et *al*., 2010, González-Acebrón et *al*., 2012). Microfractures that cross sometimes the crystals may favour the alteration of these primary K-feldspars (Fig. 33B).

Indeed, some smaller K-feldspars clearly show non-luminescent secondary albite developed in the vicinity of microfractures (Fig. 33D) while the others exhibit non-luminescent secondary albite on the boundaries of the igneous K-feldspars. In both cases, the rest of the crystals show the classical blue luminescence of the igneous K-feldspars. Thus, albitization in the vicinity of microfractures develops from the microfractures and penetrates the rest of the crystals, whereas albitization along the crystal boundaries may be favoured by the intergranular joints and develops through the crystals

CL contrasts between the primary K-feldspars and the secondary albite underline that albitization started along the microfractures and/or the intergranular joints of the rocks and spreaded through the crystals.

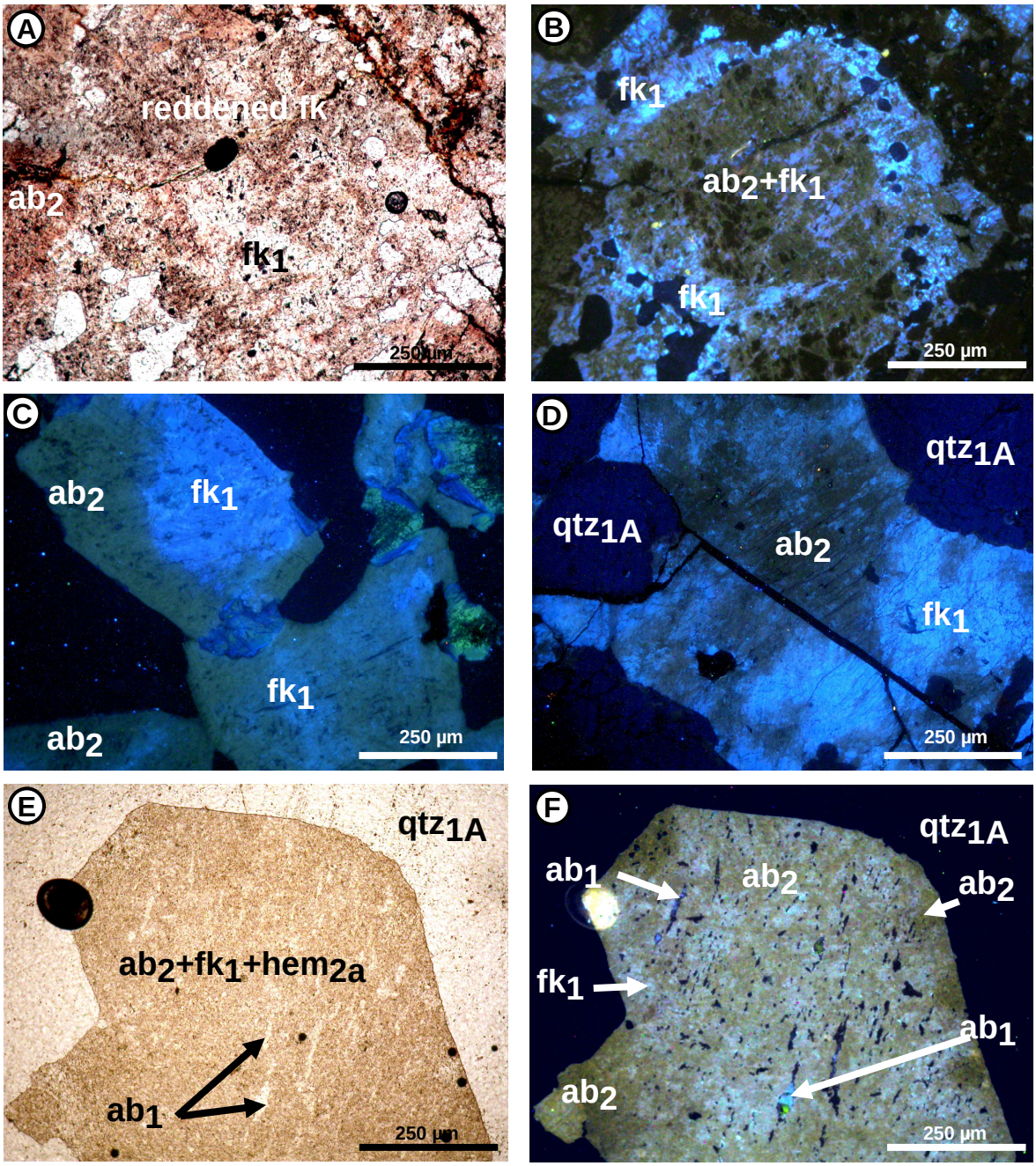


**Figure 33 – Pinkish altered K-feldspar features. (A) and (B) partially reddened/altered K-feldspars showing some unaltered light patches. The reddened zones are stuffed with pigmentary hematite and show non-luminescent zones corresponding to secondary albite and bluish luminescent zones made of igneous K-feldspar. The rims of the crystals also show igneous K-feldspars with a bluish luminescence. Round-shape crystals appearing as light in plane polarized light and anhedral quartz exhibits dark luminescence; (A) plane polarized; (B) CL image (WL98, Laski village). (C) Partially altered K-feldspar showing non-luminescent secondary albite on the rims; CL image; (SPR1a, Szklarska Poręba). (D) Partially altered K-feldspar showing non-luminescent secondary albite along the microfractures; CL image; (JGR 2, Jaskowka Gorna, close to the Chwalisław area). (E) and (F) K-feldspar with an entirely pink matrix and light perthitic albite lamellae. The matrix shows non-luminescent secondary albite, primary perthitic albite, and luminescent relics of igneous K-feldspars. The dark-round object in plane-polarized light that appears as highlightened in CL corresponds to an air bubble; (E) Plane polarized; (F) CL image; (WL5, Szklarska Poręba); fK1: primary K-feldspar; ab1: primary albite; qtz1A: euhedral large quartz crystals, ab2: untwined secondary albite, hem2a: pigmentary hematite.**

***Figure 33 – Feldspaths potassiques roses altérés. (A) et (B) Feldspath potassique partiellement rougi/altéré montrant des zones claires/non altérées. Les zones rougies sont pigmentées d'hématite, elles montrent aussi des zones non luminescentes correspondant à de l'albite secondaire et des zones à luminescence bleue correspondant au feldspath-K igné. Les bordures du cristal montrent aussi des feldspaths ignés à luminescence bleue. Les cristaux globuleux, clairs en lumière naturelle et sombre en cathodoluminescence, correspondent à des quartz xénomorphes. (A)_Lumière naturelle. (B)_Image en CL (WL98_village de Laski). (C) Feldspath potassique partiellement altéré et montrant des bordures non luminescentes à albite secondaire. Image en CL. (SPR1a_carrière de Szklarska Poręba). (D) Feldspath potassique partiellement altéré et montrant de l'albite secondaire non luminescente le long de microfractures. Image en CL (JGR 2_Jaskowka Gorna près de la région de Chwalisław). (E) et (F) Feldspath potassique avec une matrice entièrement rose et des lamelles perthitiques claires d'albite. L'objet rond en lumière polarisée et apparaissant vivement éclairée en cathodoluminescence correspond à une bulle d'air. (E)_lumière naturelle. (F)_Image en CL (WL5_carrière de Szklarska Poręba). fK1 : feldspath potassique primaire ; ab1 : albite primaire ; qtz1A : grands cristaux automorphes de quartz, ab2 : albite secondaire non maclée, hem2a : hématite en pigment.***

### *6.2.2.3 Alkali feldspar mineralogy*

Three main minerals have been determined by the XRD experiments on the hand picked phenocryst: orthoclase, microcline and albite (next to some minor amount of quartz). Albite appears in all diagrams in variable amount with respect of the nature of the sample/crystal. K-feldspars shows four types of diagrams after deconvolution fitting (Fig. 34): i) a single peak corresponding to orthoclase; ii) conjugate peaks of intermediate disordered microcline; iii) orthoclase next to subsidiary microcline; and iiii) microcline with minor amount of orthoclase. In the crystals with prevailing orthoclase this later peak shows always a relative narrow Wide at Half Maximum (WHM) whereas microcline appears with broader peaks revealing a lower crystallinity. Nevertheless, in crystals with minor orthoclase content, orthoclase shows much broader peak revealing a weaker crystallinity (more structural defects). Intermediate disordered microcline appears only in two samples (CHR32 from Chwalisław valley and MKR12 from Mąkolno), whereas all other microcline occurrences correspond to more ordered microcline, with an ordering state between intermediate and maximum microcline of the calculated pattern of Borg and Smith (1969).

.

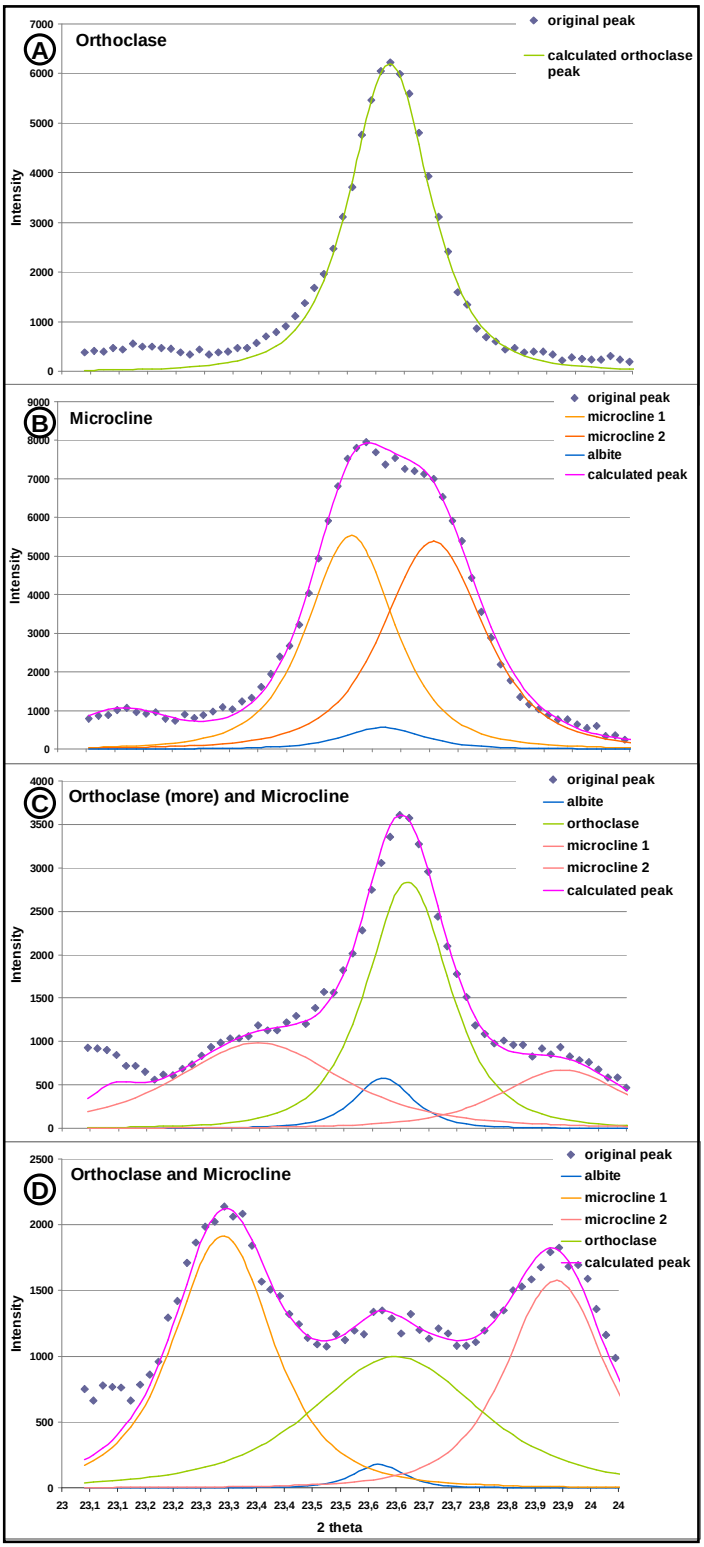


**Figure 34 - Deconvolution of the K-feldspar phenocrysts XRD peaks in between 23 and 24°(2θ) (Cukα). Orthoclase and microcline coexist in variable amounts. Orthoclase has usually a relative low WHM in comparison to microcline but its WHM becomes wider in the samples with minor orthoclase content. The deconvolution was performed with Fityk (Wojdyr, 2010).**

***Figure 34 – Déconvolution des raies de diffraction des rayons X de phénocristaux de feldspath potassique entre 23 et 24° (2θ) (Cukα). L'orthose et le microcline coexistent en quantité variable. La raie de l'orthose a habituellement une largeur à mi-hauteur (WHM) relativement plus faible que celle du microcline, mais la largeur (WHM) est plus large dans les échantillons où l'orthose n'est pas résiduelle. La déconvolution a été effectuée au moyen du programme Fityk (Wojdyr, 2010).***

Moreover, the peak position of the orthoclase is always shifted towards higher diffraction angles, which implies lower d-spacing than in the orthoclase reference calculated pattern of Borg and Smith (1969), which already contain some Na and traces of Ca ($K_{0,91}Na_{0,08}Ca_{0,01}AlSi_3O_8$). Comparing the position of the diffraction peak of the orthoclase recorded in the phenocrysts to the positions of the diffraction lines relative to the ($2^{-}01$) crystallographic planes of orthoclase and albite shows, that the recorded peaks are shifted toward the albite diffraction line. This means that the orthoclase phenocrysts show Na-substitution. A raw estimation suggests that the orthoclase of the phenocrysts contains about 15% of albite corresponding to a approximate composition of $K_{0,85}Na_{0,15}AlSi_3O_8$.

Quantitative appraisal allows to clarify the mineralogical composition of the light and pinkish coloured K-feldspar phenocrysts (Fig. 35): (1) the primary light coloured K-feldspar phenocrysts show only orthoclase in addition with minor amounts of albite; (2) the pinkish coloured K-feldspar phenocrysts of the altered granitoïds contain always microcline (average 30%), together with orthoclase and albite; and (3) the amount of albite increases (from about 15% to 50%) in correlation with decreasing amounts of orthoclase in the pinkish phenocrysts. It appears likely that orthoclase disappears within the pinkish phenocrysts in favour of albite and microcline. This clearly suggests that microcline and albite developed from the primary light phenocrysts which where turned into pink.

Additionally, the pinkish phenocrysts that show higher amounts of albite, and in which the orthoclase is the subsidiary compound, show a peak position that is slightly more shifted than that of the light phenocrysts of the primary facies (Fig. 35B). Orthoclase of the pinkish phenocrysts appears slightly more substituted in Na than the primary orthoclase.

#### *6.2.2.4 Discussion*

The pink colouration of the K-feldspars phenocrysts in the Polish Sudetes granitoïds results not only from a staining of the crystals by iron oxides, but comes along as a major alteration of the primary K-feldspars.

The primary light coloured phenocrysts are formed from a mixture of about 85% of orthoclase and 15% of albite. The composition of the primary phenocrysts is identical in the different studied localities. Albite observed next to orthoclase in these primary phenocrysts results from the unmixing of the original phenocrysts during cooling of the granite, forming micro- to nano-perthites (Turner and Verhoogen, 1960; Deer et al., 1963; Winter 2001). Pink colouration appears during the development of microcline and albite at the expense of orthoclase. Apparently, microcline develops first in the less affected phenocrysts and before the albite content rises; albite develops only when alteration progresses as shown by the decrease of the orthoclase content. Pink colouration of the phenocrysts goes along with the true albitization of the primary orthoclase, resulting in a final composition of about 50% albite and 50% K-feldspars (orthoclase + microcline). There is definitely a transformation or recrystallysation of the orthoclase into microcline and albite. Alteration occurrs probably through the mass redistribution by fluid-rock interaction even at micro- or nanoscale (Eggleton & Banfield, 1985; Fiebig and Hoefs, 2002; Boulvais et al., 2007). As the bulk composition of the primary phenocrysts has changed, K-Na interchange on a large scale provided a chemical driving force for replacement.

The orthoclases with somewhat higher Na-content are associated with the most altered phenocrysts and appear as residual rather than resulting from an aggradation/recrystallisation of the primary orthoclase. Indeed, orthoclase is unstable during the alteration belonging to the development of the pinkish colouration and thus recrystallyzes into microcline. If a Na-enriched K-feldspar would develop it would be microcline. The orthoclase with higher Na-substitution appears as residual. Consequently the primary orthoclase must have been

inhomogeneous, formed of crystallites or crystal domains with different Na-contents, the less substituted altering first, the more substituted appearing more stable in the Na-enriched environment that triggers albite development.

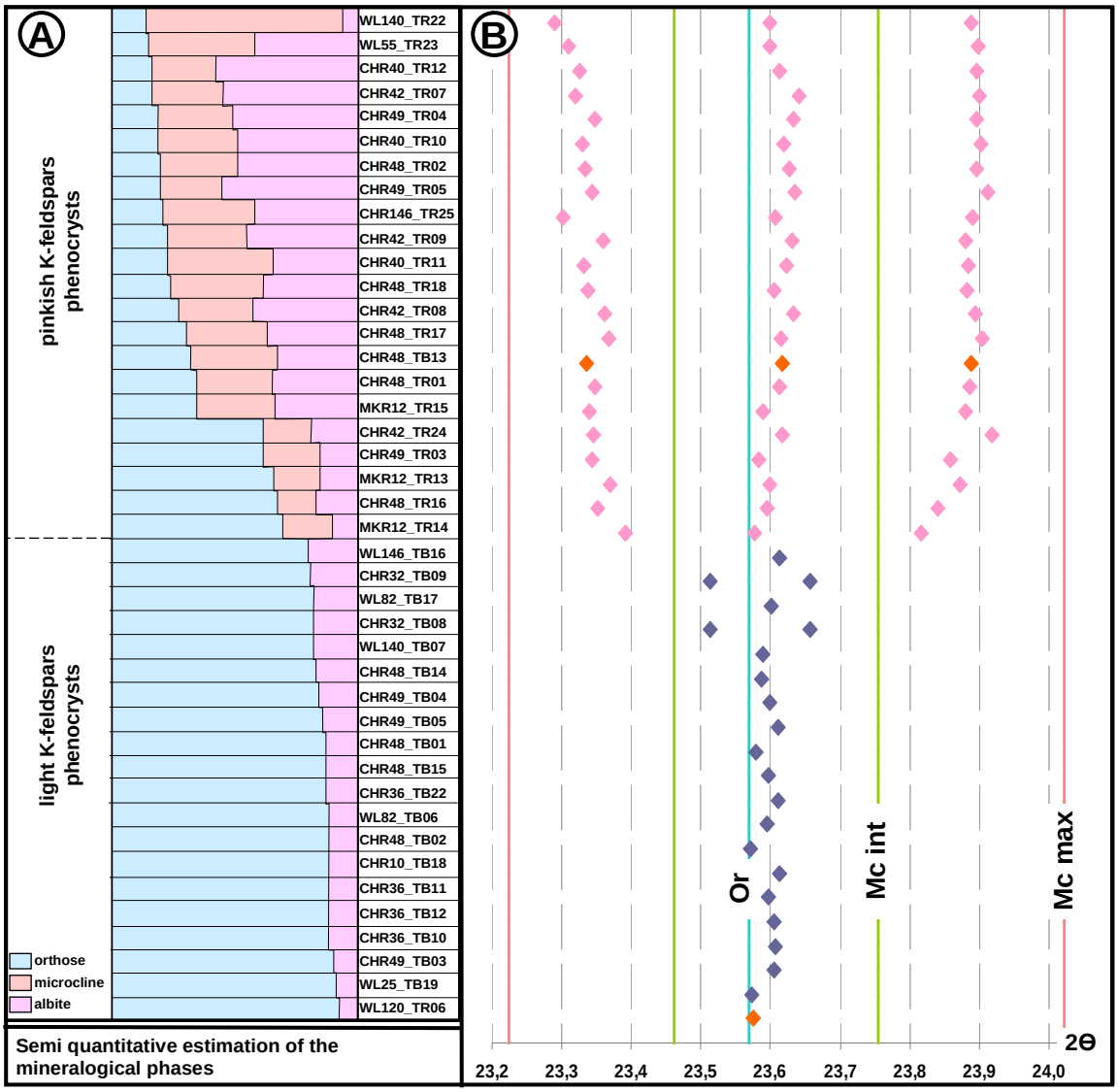


**Figure 35 – Crystallographic parameters after XRD peak deconvolution treatment. (A) Orthoclase, albite and microcline semi-quantitative contents within the light and the pinkish K-feldspar phenocryst; (B) Peak positions of orthoclase and microcline. Blue dots mark the light phenocrysts, pinkish dots mark the pinkish phenocrysts and orange dots stand for the uncertain staining aspects. The blue line is the exact position of the intermediate microcline, whereas the red line indicates the maximum microcline composition, which corresponds to the respective maximum deviation from the monoclinic symmetry while intermediate microcline corresponds to those with less deviation.**

***Figure35- Paramètres cristallographiques des phénocristaux après déconvolution des raies de diffraction. (A) Concentration relative de l'orthose, de l'albite et du microcline dans les phénocristaux roses et clairs. (B) Positions des raies de diffraction de l'orthose et du microcline. Les points bleus correspondent aux phénocristaux clairs, les points roses aux phénocristaux roses/rouges, et les points orange pour les cristaux dont l'aspect ou la coloration est incertain. La ligne verte correspond à la position exacte du microcline intermédiaire, tandis que la ligne rouge est pour le microcline maximum. Le microcline maximum correspond au type de microcline ayant le maximum de déviation par rapport à la symétrie monoclinique tandis que le microcline intermédiaire correspond à la déviation la plus faible.***

## 6.3 FERROMAGNESIAN MINERALS

Although the ferromagnesian minerals are relatively abundant in the granodioritic facies, they appear as less abundant in the granitic facies (Fig. 23, bulk rock composition). The biotite and amphibole behaviour is examined mainly in the light/unstained facies in which they are best preserved. Subsequently, their respective alteration behaviour into chlorite is studied in the reddened samples, because it is more developed in these facies.

### *6.3.1 Biotites*

Non-chloritized biotites are the less abundant ferromagnesian minerals in the Kłodzko Złoty-Stok (KZS) facies, whereas they are the most abundant in Szklarska Poręba. In fact, altered biotites are much more abundant than the non-altered biotites in the KZS. They occur in the granodiorite from Laski quarry and Mąkolno and in the granite of Laski valley.

Biotites appear as tabular and subhedral crystals generally showing fine, regular and parallel cleavages. Some biotites exhibit a light brown colour (Fig. 36A, Fig. 36B) while the others show rather dark-brown tones (Fig. 36C, Fig. 36D). The colour of the biotites is likely related to their chemical composition and depends mainly on their $TiO_2$ content and $Fe_2O_3/(Fe_2O_3+FeO)$ ratio (Hayama, 1959). High $TiO_2$ contents are responsible for a brown colour while high ferric iron cause a greenish aspect (Deer et al., 2003). Thus light brown biotites are richer in $TiO_2$ while the dark brown biotites may be rather iron-rich biotites. Light brown and dark brown biotites occurrences do not obey to any particular distribution throughout the sampled sites. The biotites of the microgranitic facies of Szklarska Poręba Huta quarry show high Fe content and low Fe/Mg ratio (Słaby and Martin, 2008) (Table 4).

**Table 4 - Chemical composition of biotites from the equigranular granite (µgranite) in the Szklarska Poręba Huta quarry (from Słaby and Martin, 2008).**

***Tableau 4 - Composition chimique des biotites du microgranite de la carrière de Szklarska Poręba Huta (extrait de Słaby and Martin, 2008).***

| | $SiO_2$ | $TiO_2$ | $Al_2O_3$ | FeO | MnO | MgO | $Na_2O$ | $K_2O$ | Σ | | Fe/(Mg+Fe) |
|---|---|---|---|---|---|---|---|---|---|---|---|
| EQUI-2 | 35.48 | 4.02 | 13.11 | 26.55 | 0.66 | 6.34 | 0.04 | 9.31 | 95.51 | | 0.70 |
| EQUI-6 | 31.54 | 2.31 | 14.59 | 31.07 | 0.53 | 7.27 | 0.01 | 5.20 | 92.52 | | 0.71 |

Somes biotites show zircon, apatite and iron oxide inclusions. They do not show any particular arrangement with respect to the biotite cleavages. Zircons appear as euhedral individual crystals, showing a typical dark radioactivity and pleochroic aureole (Fig. 36B). Apatites occur as euhedral crystals either as stubby (Fig. 36A, Fig. 36D) or as elongated needles within the biotites (Fig. 36A). Apatite and zircon appear as of primary origin because of their specific euhedral shape and the fresh aspect of the biotite; they are reported as frequent inclusions in biotite (Roubault et al., 1963). Iron oxides occur as opaque dark subhedral crystals within the biotites. The euhedral to subhedral shape of the iron oxides clearly suggests that they are probably of primary origin as early-formed minerals. These opaque iron oxides may be oxidized pyrite/magnetite or maghemite as typically reported within biotite and especially in granitoïds (e.g. Whalen and Chappel, 1988).

Some other inclusions are disposed exclusively along the cleavages of the primary biotite. They do not show any features in agreement with the pseudomorphic alteration minerals such as chlorite which may be typically found along biotite cleavages.

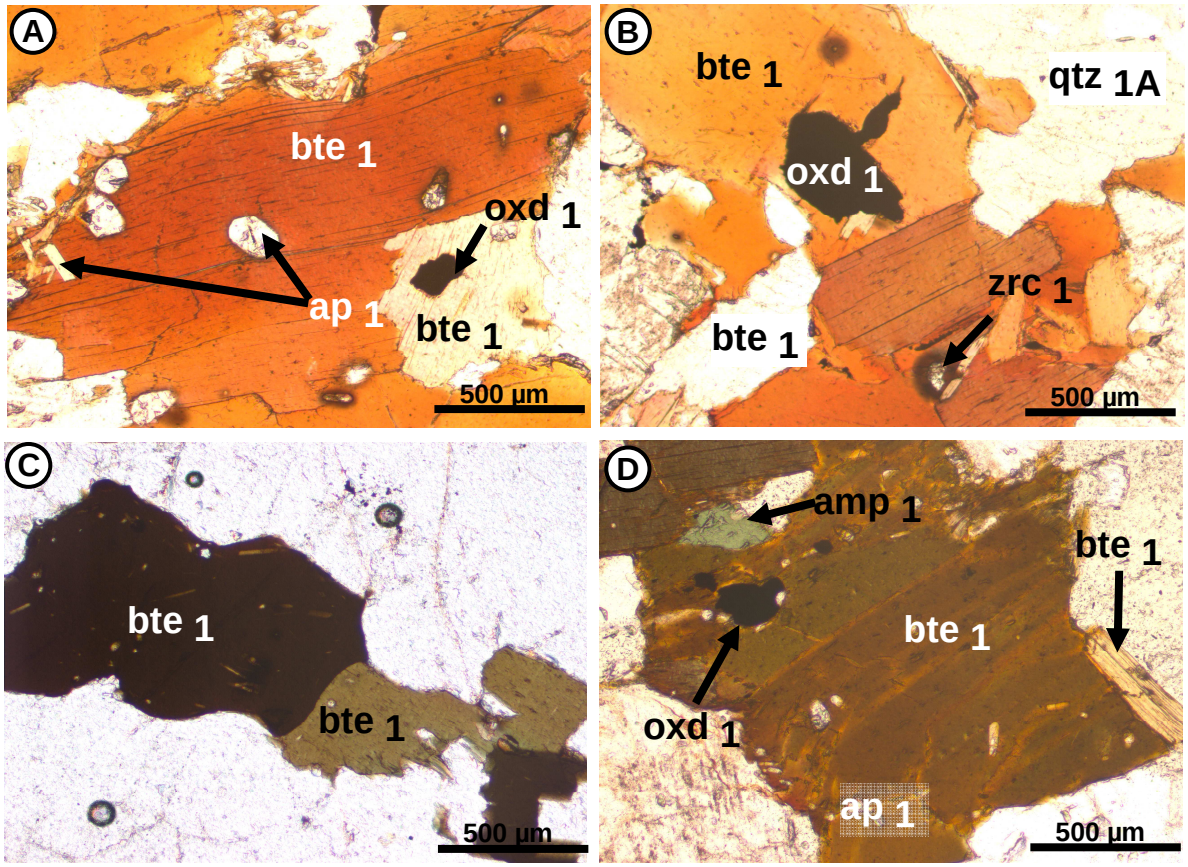


**Figure 36 - Biotite occurrence in the unstained facies from the Polish Sudetes. (A) Brownish biotite showing euhedral colourless apatite as inclusions. Apatite shows stubby and elongated needles; plane polarized; (CHR48, Chwalisław valley). (B) Biotite showing a light brown colour, some of the crystals are almost colourless. Biotite also shows zircon inclusions characterized by their radioactivity halo and additional inclusions of dark opaque iron oxide; plane polarized; (CHR48, Chwalisław valley). (C) Biotite showing a dark brown colour; plane polarized; (SP3, Szklarska Poręba quarry). (D) Brownish biotite showing apatite and opaque iron oxide inclusions; plane polarized; (CHR19, Chwalisław valley); bte1: primary biotite, ap1: primary apatite, oxd1: primary iron oxide, zrc1: zircon.**

***Figure 36 – Occurrence de biotite dans les facies clairs/non colorés des Sudètes. (A) Biotite brune montrant des inclusions d'apatite incolores. Les apatites se présentent sous forme de cristaux trapus ou d'aiguilles. Lumière naturelle. (CHR48_vallée de Chwalisław). (B) Biotites brun-clair et d'autres presqu'incolores. Les biotites présentent également des inclusions de zircons caractérisés par leurs auréoles de radioactivité ainsi que des oxydes de fer opaques. Lumière naturelle. (CHR48_vallée de Chwalisław). (C) Biotite brune sombre. Lumière naturelle. (SP3_carrière de Szklarska Poręba). (D) Biotite brune avec des inclusions d'apatite et d'oxydes de fer opaque. Lumière naturelle. (CHR19_vallée de Chwalisław). bte1 : biotite primaire, ap1 : apatite primaire, oxd1 : oxyde de fer primaire, zrc1 : zircon.***

These minerals along the biotite cleavages are quartz and K-feldspars. In addition of the presence of classical biotite inclusions (apatite, zircon), quartz occurs as elongated rods in parallel to the biotite cleavages, while K-feldspars show a lens-like shape along the cleavages of the biotite (Fig. 37). The quartz elongated rods show a uniform shape and regular rims, moreover they do not show any thickness variation. Quartz rods do not distort the biotite flakes but the flakes seem rather interrupted by the rods. Moreover, all rods show identical extinction orientations suggesting epitatic growth during biotite alteration. This alteration may result from biotite cation leaching, except for the silica which may remain in place and crystallize as in the rod-like habit. This biotite alteration is different to the below described biotite chloritization.

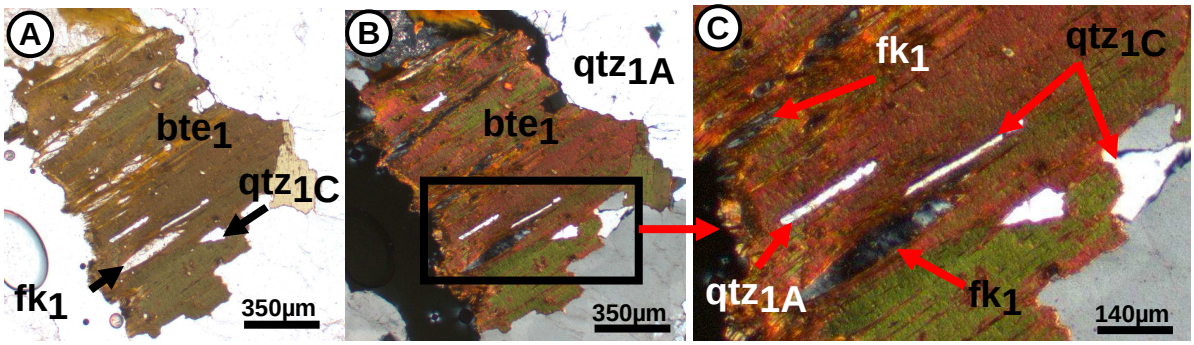


**Figure 37 – Non-euhedral mineral inclusions in biotite investigated in the Polish Sudetes; (A) and (B) Primary biotite showing colourless mineral inclusions with a common shape or as elongated lenses according to the biotite cleavage planes (c-axis section); (A) plane polarized; (B) cross polarized; (LKR11, west of Laski valley). (C) Zoom on the framed zone given in (B); inclusions with thin elongated shape are quartz, while those with lenses-like shape are K-feldspars. The K-feldspar features observed here suggest that they have grown along the biotite cleavages; cross polarized; (LKR11, west of Laski valley); bte1: primary biotite, fk1: primary K-feldspars, zrc1: zircon; qtz1A: large quartz crystals, qtz1C: quartz rods.**

***Figure 37 – Inclusions xénomorphes dans les biotites des granitoïdes des Sudètes. (A) et (B) Biotite primaire comportant des inclusions allongées et xénomorphes le long des clivages de la biotite. (Section axe-c). (A)_lumière naturelle. (B)_lumière polarisée. (LKR11_ouest de la vallée de Laski). (C) Agrandissement de la zone encadrée sur la figure (B). Les inclusions de forme quelconque correspondent à du quartz tandis que celles qui sont allongées sont des feldspaths potassiques. La forme des feldspaths potassiques suggère que ceux-ci ont cru le long des clivages de la biotite. Lumière polarisée. (LKR11_ouest du village de Laski). bte1: biotite primaire, fk1: feldspath potassique primaire, zrc1: zircon; qtz1A: grands cristaux de quartz, qtz1C: quartz en baguette.***

K-feldspars form lens-like aggregates that distort the biotite sheets, pointing to a displacement growth of the feldspars in between the biotite sheets. The biotite cleavages may provide a suitable substrate for the growth of K-feldspar lenses (Holness, 2003; Machev et al., 2004). K-feldspars are fresh, unaltered and may be related to the low-temperature biotite breakdown (Holness, 2003). Nevertheless, the lenses are obvious within the unaltered biotite (Fig. 37), therefore an alkali-rich fluid circulation may be considered for this process. These alkali-rich fluids may be connected to late-magmatic conditions.

### *6.3.2 Amphiboles*

Amphiboles occur in all light/unstained facies. Nevertheless, they are most abundant in the granodiorite of Mąkolno, Laski quarry, and Chwalisław valley. They show greenish colours, typically found in the calcic amphibole and hornblendes. They have the classical euhedral habit, either non-twinned or showing multiple twinnings (Fig. 38B) or even simple Carlsbad twinnings (Fig. 38A). They may also form anhedral aggregates with biotite (Fig. 38C). Besides, amphiboles show euhedral zircon inclusions, opaque iron oxides and elongated apatite needles

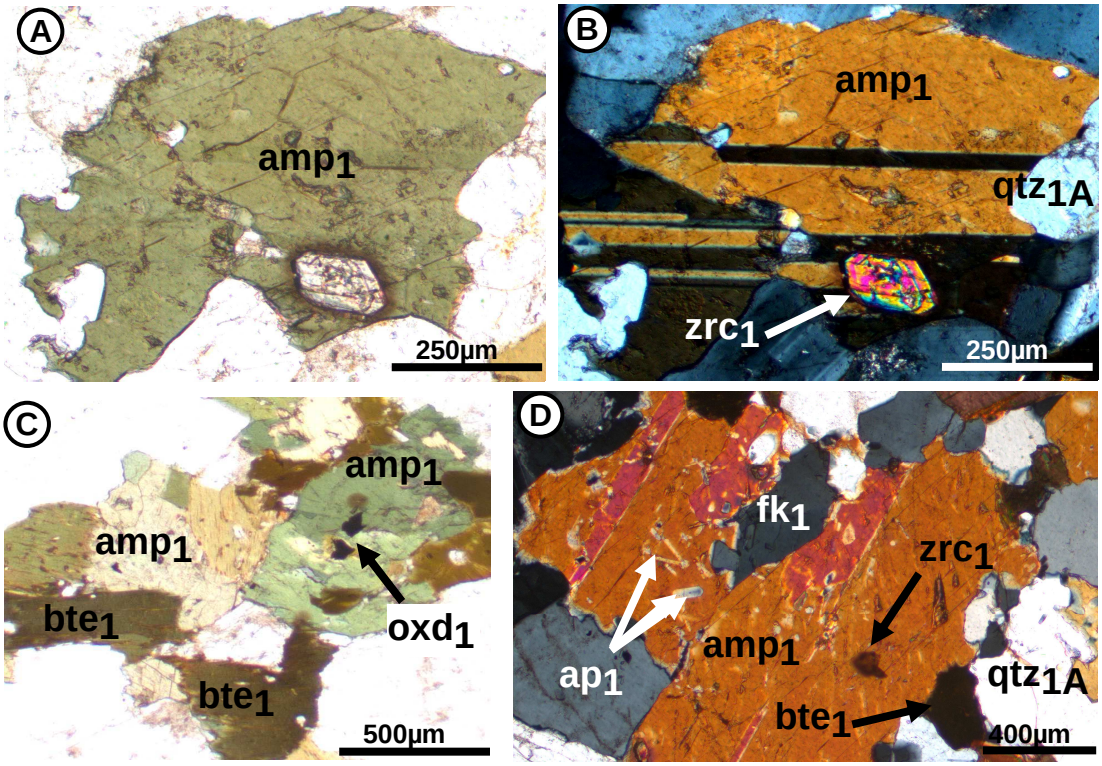


**Figure 38 – Amphibole occurrences within the light/unstained facies; (A) and (B) Subhedral greenish hornblende crystal with the typical 120° cleavage patterns and exhibiting euhedral zircon inclusions. The hornblende crystal appears as twinned: multiple twinnings and Carlsbad twinning are distinguishable; (A) plane polarized; (B) cross polarized; (LAR77, Laski valley). (C) Amphibole forming aggregates with biotite. Amphibole also shows opaque iron oxides; plane polarized (CHR18, Chwalisław valley). (D) Birefringent amphiboles, showing euhedral elongated apatite inclusions; cross polarized; (LKR77, Laski valley); amp1: primary hornblende bte1: primary biotite, ap1: primary apatite, zrc1: zircon, fk1: primary K-feldspar, qtz1A: large quartz crystals, oxd1: primary iron oxide.**

***Figure 38 – Amphiboles des facies clairs/non hématisés. (A) et (B) Cristal de hornblende verdâtre subautomorphe présentant des clivages classiques à 120°ainsi que des inclusions de zircons automorphes. Le cristal de hornblende est maclé par des macles multiples et des macles de Carlsbad. (A_lumière naturelle. (B)_lumière polarisée (LAR 77_vallée de Laski). (C) Agrégats d'amphibole et de biotite. Les amphiboles présentent des oxydes de fer opaques. Lumière naturelle (CHR18_vallée de Chwalisław). (D) Amphibole biréfringente présentant des inclusions d'apatites automorphes et allongées. Lumière polarisée. (LKR 77_vallée de Laski). amp1 : hornblende primaire, bte1 : biotite primaire, ap1 : apatite primaire, zrc1 : zircon, fk1 : feldspath potassique primaire, qtz1A : grands cristaux de quartz, oxd1 : oxyde de fer primaire.***

### *6.3.3 Chlorite*

Chlorites are generally considered as secondary minerals of in igneous rocks (Deer et al., 2003). In the present series it appears already in the light/unstained facies, but develops more frequent in the reddened facies, ultimately being the sole ferromagnesian mineral in the most altered/stained facies.

In the light/unstained facies, chlorite occurs exclusively associated with biotite whereas amphiboles never show any alteration into chlorite. Chlorite develops along the primary biotite cleavages (001). The invasion of the chlorite along the cleavages is very variable: some cleavages are particularly sensitive to chloritization, most probably because they were mechanically in extension; whereas others are much less invaded, or even chloritization was restricted to the edges of the biotite (Fig. 39). It results in typical interfingered contacts between biotite and chlorite.

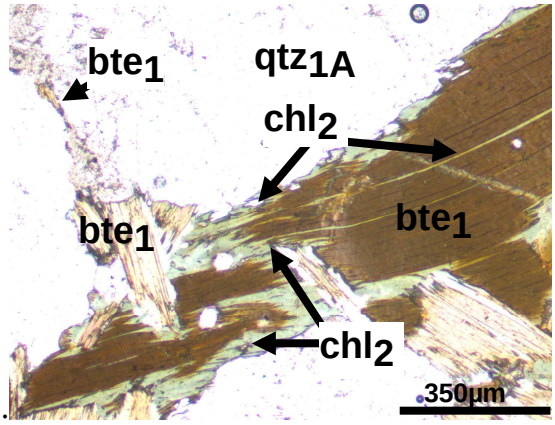


**Figure 39 – Chlorite occurrence within the light/unstained facies. Chlorite appears as greenish and along the cleavages of primary biotite and is localized at their edges (rims); plane polarized; (LAR78, Laski valley); bte1: primary biotite, chl2: secondary chlorite, qtz1A, large quartz crystals.**

***Figure 39 – Chlorite des faciès clairs. La chlorite est verdâtre et elle apparaît le long des clivages des biotites primaires et sur leurs bordures. Lumière polarisée. (LAR 78_vallée de Laski) bte1 : biotite primaire, chl2 : chlorite secondaire, qtz1A, grands cristaux de quartz.***

The chlorite content increases from the light/primary facies towards the reddened facies while in parallel the biotite and amphibole content decreases (Fig. 23, bulk rock composition). This is also obvious in the hand samples where the chlorite content increase in the reddened fracture walls is macroscopically observable.

In the reddened facies, chlorite is associated either with the primary ferromagnesian minerals (biotite and amphibole) or develops in microfractures and pores.

- **Biotite chloritization**

Unaltered biotites are scarce, even non-existent within the reddened facies. Most of the biotites are partially or entirely isomorphically replaced by chlorite. The replacement ranges from partial to complete. The partially chloritized biotites allow to underline the textural relationship between primary biotite and secondary chlorite. Chlorite is greenish with a violet interference colour. At the initial stages of the alteration, chlorite develops at the biotite edges and along specific cleavage planes. With ongoing alteration only sheet-like relics of the primary brownish biotite are preserved within the secondary chlorite (Fig. 40A & 40B). There is no clear evidence for a volume change during the chloritization. Hematite sheets also appear in between the biotite cleavages and continue in the chlorite crystals (Fig. 40C). The continuity of the hematite sheets from the biotite to the chlorite points out that hematite (or a ferruginous precursor of hematite) develops within the biotite crystals.

As such ferruginous accumulations are not known in the fresh biotite of the light facies, the ferruginous mineral must have formed in an early stage of the biotite alteration, preceding the chlorite development.

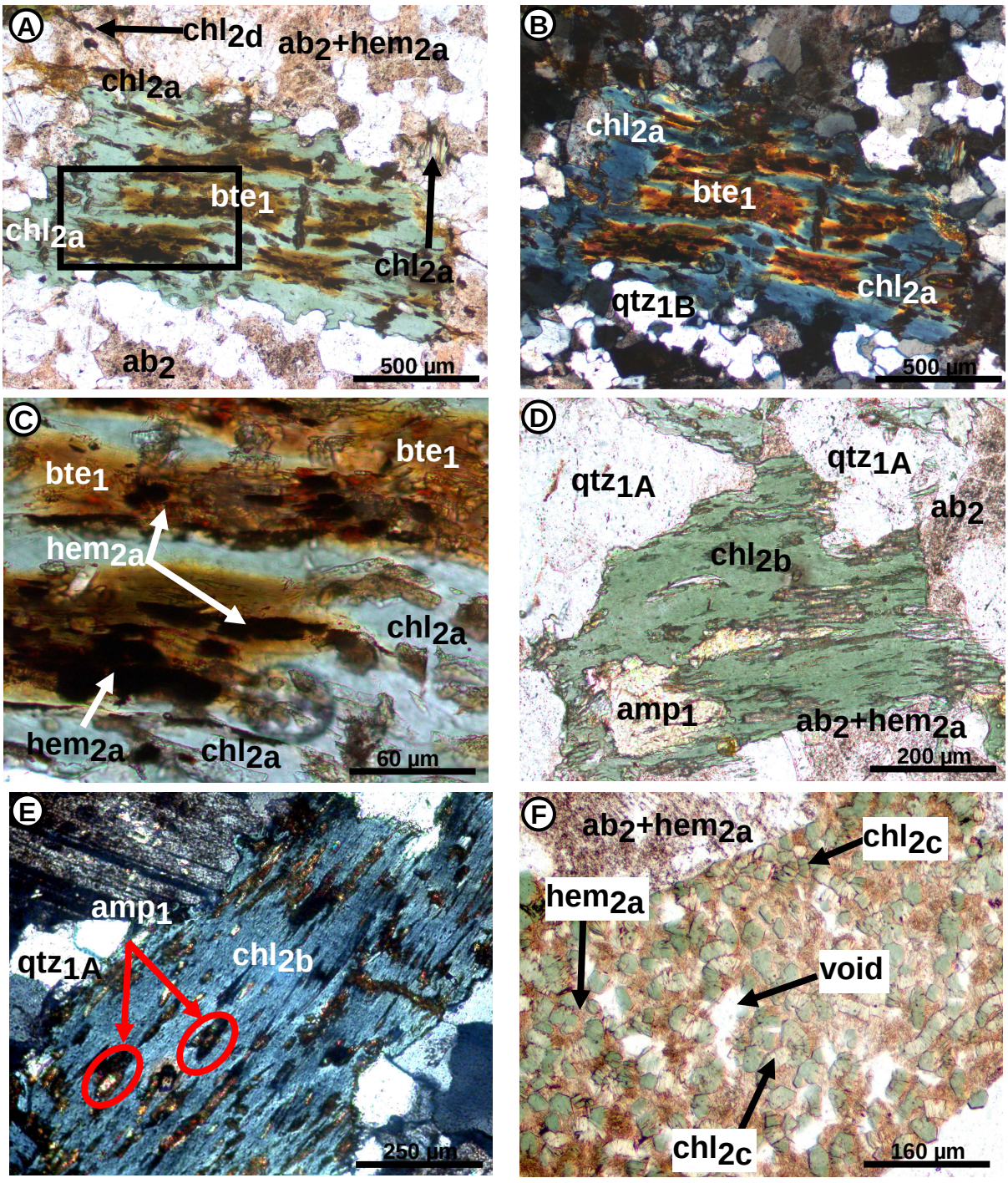


**Figure 40 – Chlorite occurrence in the albitized facies. (A) and (B) chloritized biotite showing patches of primary biotite. Chlorite preserved the frame of the primary biotite, showing a green colour and violet refringence; (A) plane polarized; (B) cross polarized; (WL94, Laski village). (C) Enlargement of the framed zone in (A) chloritized biotite showing dark elongated hematite along their cleavages planes; plane polarized; (WL94, Laski village). (D) Chloritized amphibole showing subhedral green-pale amphibole relics; plane polarized; (WL65, Laski quarry). (E) Amphibole almost entirely chloritized, showing small amphibole relics. The chlorite shows violet refringence such as in the case of chlorite after amphibole alteration; cross polarized; (WL71a, Laski quarry). (F) Euhedral chlorite crystal stacks and vermicules associated with hematite pigments in a wide geometrically shaped occurrence which resembles a mineral-ghost; plane polarized; (WL12, Szklarska Poręba); bte1: primary biotite, amp1: primary amphibole,**

**qtz1A: large euhedral quartz crystals; qtz1B: small quartz crystals; ab2: secondary albite; chl2a: secondary chlorite after biotite; chl2b: secondary chlorite after amphibole, chl2d: neogenic chlorite in microfracture; hem2a: pigmentary hematite; hem 2b: dark hematite: hem 2c: sub-euhedral hematite.**

***Figure 40 – Chlorite des faciès rouges albitisés. (A) et (B) Biotite chloritisée montrant des îlots de biotite primaire. La chlorite préserve la structure de la biotite primaire, elle présente une biréfringence verte à violette. A_Lumière naturelle. (B)_Lumière polarisée. (WL94_village de Laski). (C) Agrandissement de la zone encadrée dans la figure (B). Biotite chloritisée avec hématite allongée le long de ses clivages. Lumière naturelle. (WL94_village de Laski). (D) Amphibole chloritisée avec reliques d'amphibole vert pâle. Lumière naturelle. (WL 65_carrière de Laski). (E) Amphibole presqu'entièrement chloritisée présentant des reliques non chloritisées. La chlorite a également une réfringence violette comme celle issue de l'altération des biotites. Lumière polarisée. (WL71a_Laski carrière). (F) Agrégats de cristaux de chlorite automorphes, de vermicules de chlorite associées à des pigments d'hématite apparaissant dans une structure ayant la forme du fantôme d'un minéral. Lumière naturelle. (WL12_carrière de Szklarska Poręba). bte1: biotite primaire, amp1: amphibole primaire, qtz1A: grands cristaux automorphes de quartz; qtz1B: petits cristaux de quartz; ab2: albite secondaire; chl2a: chlorite secondaire issu de l'altération de biotite; chl2b: chlorite secondaire issue de l'altération d'amphibole, chl2d: chlorite néogénique dans les microfractures; hem2a: hématite en pigment; hem 2b: hématite sombre: hem 2c: hématite subautomorphe.***

- **Accessory minerals associated with chloritized biotite**

Chloritized biotite often shows accessory minerals interfingered with the cleavage planes of the former biotite (Fig. 41). There is a whole variety of minerals that cannot always be confidently identified by petrographic microscopy. SEM/EDS analysis provides help to determine narrow minerals plates between the biotite sheets. K-feldspar, titanite, quartz, rutile and pyrite show frequently micro-lenses between the biotite cleavage planes (Fig. 41). K-feldspar and quartz have already been identified as forming lenses within the primary biotite in the light facies, while pyrite has been suggested as one of the usual opaque crystals within the primary biotite and amphibole. K-feldspar and quartz show the same habits like in the light facies meaning that they may not be related to the reddening.

Ti-minerals have not been clearly identified through optical microscope study of the primary facies. Their identification as lenses embedded in the chloritized biotite allow considering that they could be of secondary origin and related to the chloritization of biotite which may release titanium. It may also be considered that they are related to a late-magmatic opaque mineral alteration such as ilemite alteration into rutile. The latter seems more unlikely as titanite and rutile appear as individual crystals and not as alteration aureole or zone within primary iron minerals.

More "exotic" minerals exist also in the between crystals, like rare-earth-rich minerals from the Euxenite-Polycrase series (Fig. 41H). This corresponds to REE series generally associated to the magmatism.

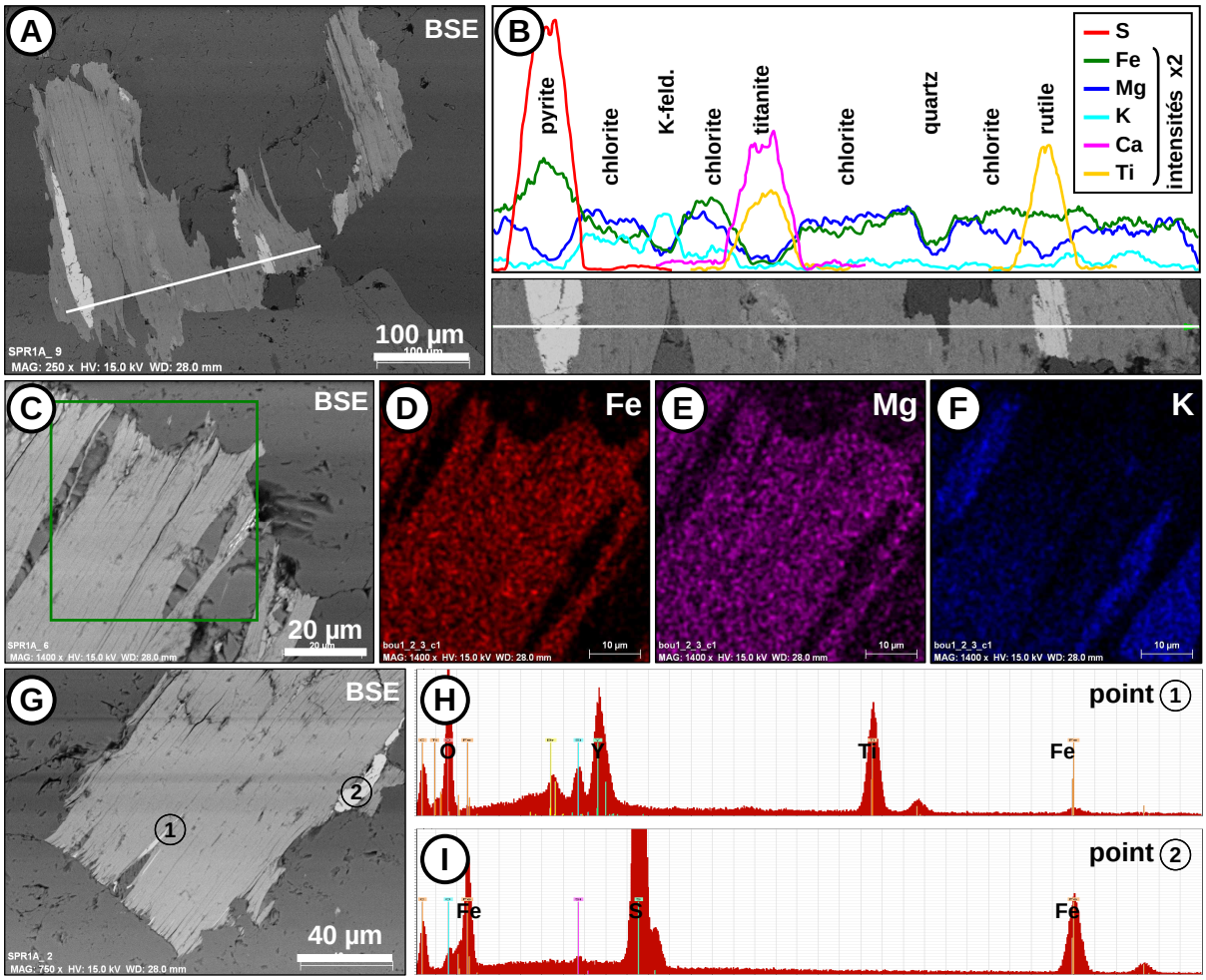


**Figure 41 - Accessory minerals in the biotite cleavage planes. (A) Biotite crystal with several interfingered mineral lenses. (B) EDS analyses in SEM along the transect marked in (A). Pyrite, titanite and rutile form lenses inserted between the biotite cleave planes. The K-feldspar also appears as inserted within biotite, nevertheless it is also connected/bound to the neighbouring K-feldspar crystals. (C) Biotite crystal with interfingered mineral lenses. (D–E–F) EDS spectra showing that the lenses are K-rich (K-feldspars). (G) Biotite crystal with interfingered minerals. (H–I) An EDS XR spectrum of point 1 corresponds to an Yttrium oxide (Euxenite) and point 2 is composed of pyrite; (SPR1A, Szklarska Poręba); BSE = back scattered electron image.**

***Figure 41 – Minéraux accessoires dans les plans de clivage des biotites. (A) Cristal de biotite avec plusieurs minéraux en lentilles et en interdigitation. (B) Spectre EDS le long de la ligne marquée sur la figure A. La pyrite, la titanite et le rutile forme des lentilles insérées entre les clivages de la biotite. Le feldspath potassique apparaît inséré au sein de la biotite, cependant il semble aussi connecté au feldspath potassique voisin. (C) Cristal de biotite avec des interdigitations de minéraux en lentilles. (D-E-F) Images EDS montrant que les lentilles sont riches en K (feldspath potassique). (G) cristal de biotite comportant des minéraux interdigités. (H-I) Spectre EDS-XR indiquant que le point 1 correspond à un oxyde d'Yttrium (Euxénite) et le point 2 est une pyrite. SPR1A_Szklarska Poręba. BSE = image en électrons rétrodiffusés.***

### ➢ Amphibole chloritization

Non-chloritized amphiboles are more frequent than non-chloritized biotite. Amphiboles appear less sensitive to alteration than biotite, indeed altered amphiboles always show relics preserved within the secondary chlorite (Fig. 40D & 40E). Chlorites developed within the amphibole show similar petrographic characteristics than chlorites associated with biotite: green colour in plane polarized light, violet colour in cross polarized light and they are elongated and oriented in accordance with the cleavages of the amphiboles (Fig 40D & 40E).

➢ **Chlorite in fractures and microcracks**

Microcrystalline thin and flaky chlorites occur also within fractures and micro-pores or intergranular joints, showing no direct relationship with biotite and amphibole. Some of these chlorites within microfractures appear as green-brownish, arranged perpendicularly to the pore walls or even forming rosettes. The most spectacular occurrences are related to the pseudomorphic replacement of primary minerals which appear only as ghosts. In this later occurrence, large euhedral hexagonal chlorite crystals form thick stacks and vermicular aggregates associated with hematite pigments and quartz (Fig. 40F). Euhedral chlorite crystals in fractures and voids suggest that they crystallized directly and freely in pores and intragranular joints.

## 6.4 SERICITE

Sericite appears as flaky, highly bi-refringent crystals associated to plagioclases and rarely shown within the K-feldspar. Sericite shows two flake sizes depending on the facies in which it occurs: tiny, weakly developed sericite flakes (about 5 µm), occur within the primary plagioclases (Fig. 42A, Fig. 42B) in the sections from the Szklarska Poręba granite and in the less fractured granodiorites. Here, plagioclases show limited sericite zones, which locally obliterates the primary polysynthetic twinning and even seems to have erased them anyway. Twinnings obliteration (erasure) has been reported as feature in saussuritized plagioclase where sericite development is associated with albite-prehnite or epidote (Morad et al., 2010). However in the studied facies, neither albite, nor prehnite, nor epidote has been identified as directly associated with the tiny sericite. This raises the question of the behaviour of the $Ca^{2+}$ released during plagioclase sericitization. It may probably supply the crystallization of the prehnite in microfractures or as lenses within the close granodioritic facies (see further prehnite occurrence). Or it may simply be evacuated from the system.

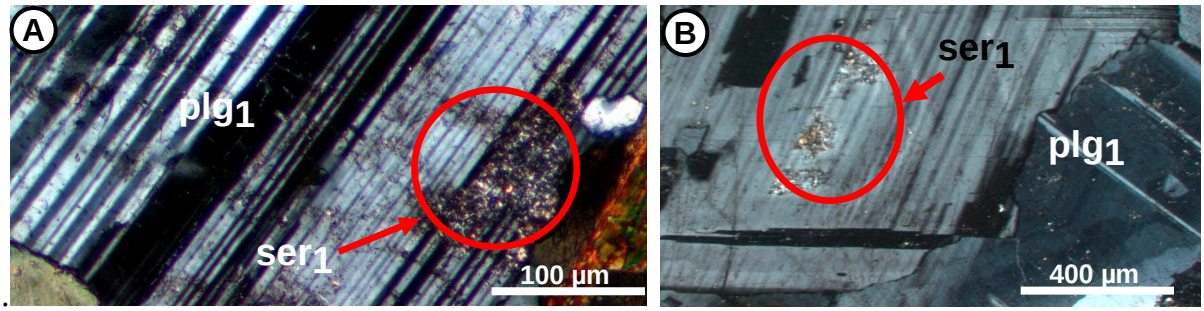


**Figure 42 - Sericite occurrence in the primary plagioclases from the Kłodzko Złoty-Stok massif, (A) Sericite occurrence on the rim of primary plagioclase. Sericite appears as fine inclusions with high bi-refringence, they obliterate the polysynthetic twinnings; cross polarized; (LAR77, Laski valley). (B) Sericite close to the core of a primary plagioclase. Some sericitic zones appear related to microfractures; cross polarized, (CHR18, Chwalisław valley); plg1: primary plagioclase, ser1: primary sericite.**

***Figure 42 – Séricite dans les plagioclases primaires du massif de Kłodzko Złoty-Stok. (A) Occurrence de séricite sur la bordure d'un plagioclase primaire. La séricite apparaît en inclusions fines et fortement biréfringentes qui oblitèrent pratiquement les macles polysynthétiques. Lumière polarisée. (LAR 77_vallée de Laski). (B) Séricite au cœur d'un plagioclase primaire. Le développement de certaines zones séricitisées apparaît associé aux microfractures. Lumière polarisée. (CHR 18_vallée de Chwalisław). Plg1: plagioclase primaire, ser1: séricite.***

Large and well developed sericite flakes are associated with prehnite in the core of the primary plagioclases in granodioritic facies from the Chwalisław and Laski area. Here, the plagioclase is entirely invaded by sericite. The features are especially spectacular when the primary plagioclase comprised an external aureole of albite, then the formed plagioclase is completely riddled by sericite whereas the albite rim remains unaltered (Fig. 43).

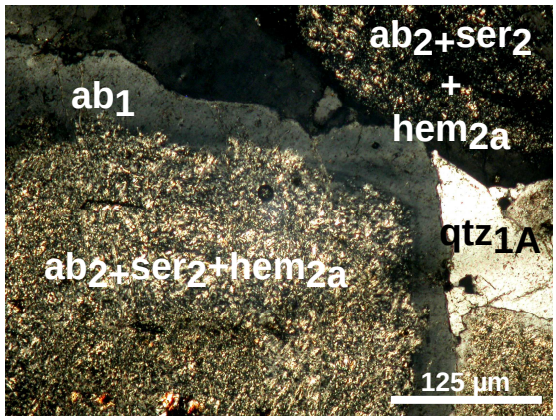


**Figure 43 – Sericite occurrence within the reddened/albitized facies. Sericite appears as large developed and highly bi-refringent flakes, associated with secondary albite and hematite pigments in the core of the primary plagioclases; cross polarized; (WL71b, Laski quarry).**

***Figure 43 – Occurrence de sericite dans les faciès rouges/albitisés. La séricite apparaît sous forme de feuillets biréfringents relativement larges associés à l'albite secondaire et aux pigments d'hématite au sein d'un plagioclase primaire dont le cœur est albitisé. Lumière polarisée. (WL71b_carrière de Laski).***

In both cases, sericite appears in close relation with plagioclase destabilization. Sericite comes always along with the erasing of the plagioclase twinning features which point out the recrystallization processes of the plagioclase. Sericite occurrence in the core of the plagioclases appears as related to the alteration of the anorthite component of the plagioclase that becomes unstable at low-temperature and in presence of OH. Destabilization of the anorthite-rich plagioclase cores releases Ca, Al, and Si that may combine to form prehnite, whereas Na is involved in the albite formation. Exceeding released Al may combine to form sericite, if K is available.

Sericite appears of relatively higher abundance in the light/unstained facies than in the reddened ones. The most reddened facies are in majority sericite-poorer than the less reddened facies. Nevertheless, the sericite distribution and its abundance within the reddened facies is not clearly obvious and cannot be exactly established. The less reddened facies or zones of the Chwalisław area and Laski quarry appear clearly as the most sericitized. Sericite develops further away from the reddened fractures, in the core of the blocks delimited by the fractures. Close to the fractures, plagioclases are albitized and show no or very few sericite flakes.

## 6.5 CA-BEARING MINERALS

### *6.5.1 Prehnite*

Prehnites occur either as crystal aggregates associated with some plagioclases or as individual crystals along intergranular joints, within microfractures, or as lenses along the cleavages of biotite.

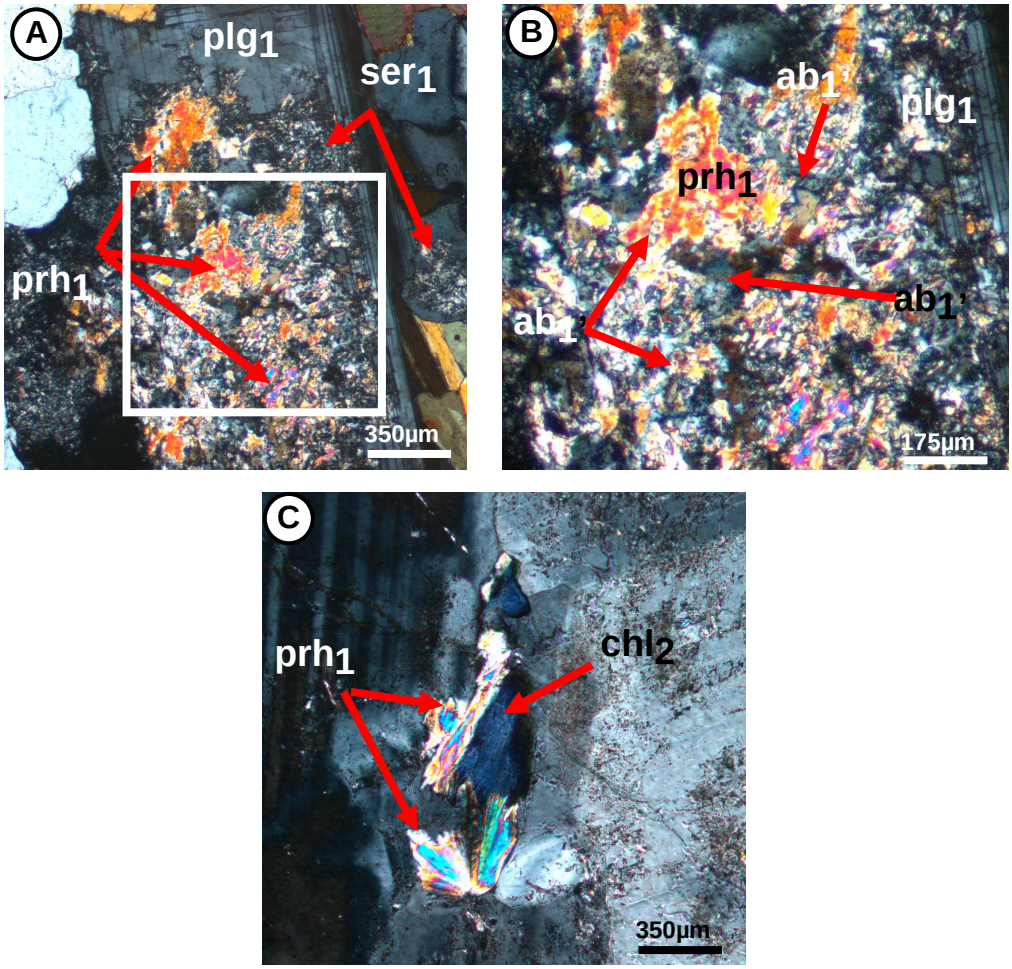


**Figure 44 – Prehnite aggregates within the samples from the Kłodzko Złoty-Stok massif. (A) Prehnite, albite and sericite occurrence in saussuritized plagioclase. Both prehnite and sericite occurs as bi-refringent alteration minerals within the plagioclase while albite exhibits low refringence; cross polarized; (LAR 77, Laski valley). (B) Enlargement of the framed zone in (A); albite occurs as weakly bi-refringent (grey) grains with various sizes scattered between prehnite and sericite. Albite is porous showing similar orientations with the surrounding igneous plagioclase, which does not show any pores (LAR77, Laski valley). (C) Individual prehnite and chlorite occurring closely. Prehnite appears as highly bi-refringent with bow-tie like structures, while chlorite shows a lower bi-refringence; cross polarized; (LKR11, Laski Laskowska); plg1: primary plagioclase, ab1': albite; prh1: primary prehnite; ser1: secondary sericite.**

***Figure 44 – Agrégats de prehnite dans le massif de Kłodzko Złoty-Stok. (A) Occurrences de prehnite, d'albite et de séricite dans un plagioclase saussuritisé. La prehnite et la séricite apparaissent comme des minéraux d'altération fortement biréfringents tandis que l'albite montre une biréfringence plus faible. Lumière polarisée. (LAR 77_vallée de Laski). (B) Agrandissement de la zone encadrée dans (A). L'albite se présente sous forme de grains faiblement réfringents (gris) dispersés entre la prehnite et la séricite. L'albite est poreuse et a une orientation identique au plagioclase primaire qui n'est pas poreux. Lumière polarisée (LAR77_vallée de Laski). (C) Prehnite individuelle apparaissant à proximité d'une chlorite. La prehnite apparaît comme fortement biréfringente avec une structure en papillon, tandis que la chlorite a une biréfringence plus faible. Lumière polarisée. LKR11_Laski-Laskowka). plg1 : plagioclase primaire, ab1' : albite ; prh1 : prehnite ; ser1 : sericite.***

**Prehnite aggregates** occur within the plagioclase cores while the rims of these plagioclases are devoid of prehnite as classically described in literature. Prehnite aggregates do not show any particular orientation or habit, they appear rather as substitution minerals after plagioclase alteration occupying most part of their core (Fig. 44A, Fig. 44B). It appears likely that the prehnite aggregate formation is closely related to the composition and the stability of the plagioclase core. Prehnite aggregates of the studied samples appear as associated with sericite and albite. Albite grains appear as weakly bi-refringent grains with various sizes scattered between sericite and prehnite (Fig. 44C). They show similar orientations with the surrounding igneous plagioclases and some of the (larger) albite grains exhibit twinnings that are usually visible in the igneous plagioclases. This shows that the albite grains crystallized under preservation of the crystal frame of the original igneous plagioclase. Moreover, at high magnification albite appears as porous whereas the igneous plagioclases around do not show any pores. This is typical of albite usually described in saussuritized plagioclase (Plümper and Putnis, 2009; Sandström et al., 2010). The pores indicate the removing of elements such as $Ca^{2+}$ and $Al^{3+}$ from the igneous plagioclase during their alteration and $Na^{+}$-enrichment of the remaining plagioclase and its transformation into albite. Indeed, chemical analyses suggest that sericite and Ca-Al silicates development within the primary plagioclase and result in more sodic plagioclases (Que and Allen, 1996).

**Prehnite individual crystals** crystals appear as distinct crystals forming fan-shaped or bow-tie like features within the intergranular joints (Fig. 44C). These crystals are not of epigenetic nature. They are clearly neogenicly feed from fluids.

Prehnite in biotite or weakly chloritized biotite forms elongated lenses that distort the sheet of the biotite and correspond to dislocation growth (Fig. 45). This suggests undoubtedly that the lenses are neogenic and directly formed from fluids. Moreover, biotite cleavages leave no doubts about the formation of pathways for fluids, allowing an easy alteration and therefore favour the prehnite growth along the biotite cleavages (Tulloch, 1979). Prehnite lenses often occur in biotite of the light/unstained facies. Furthermore, prehnite appears in some partially chloritized biotite cleavages and not along the cleavages of completely chloritized biotite that is usually present in the reddened facies.

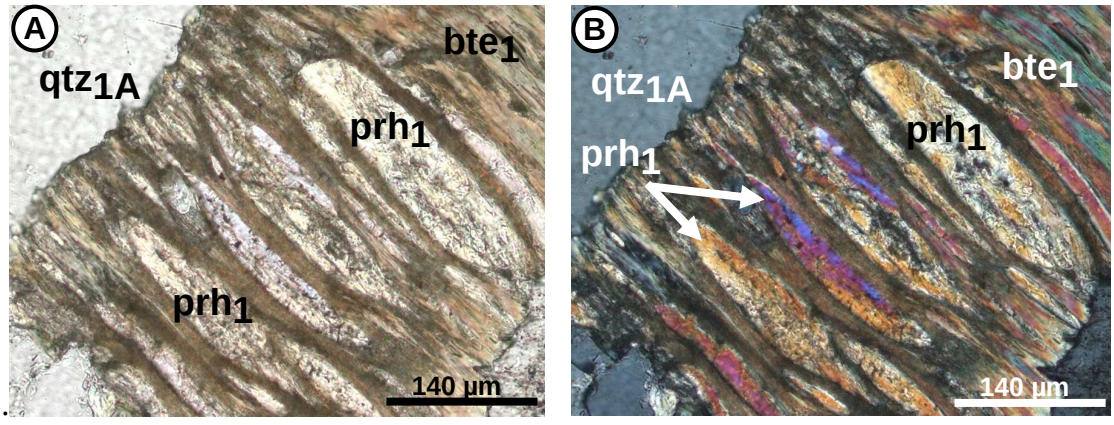


**Figure 45 – Prehnite veins within the primary biotite of the Kłodzko Złoty-Stok massif. (A) and (B) Prehnite appears as elongated lenses along the cleavages of the primary biotite. The lenses distort the sheets of the biotite, suggesting a displacement growth of the prehnite; (A) plane polarized; (B) cross polarized; (CHR21, Chwalisław valley); bte1: primary biotite, qtz1A: large quartz crystals, prh1: primary prehnite.**

***Figure 45 – Lentilles de prehnite au sein d'une biotite dans le massif de Kłodzko Złoty-Stok. (A) et (B) La prehnite forme des lentilles allongées qui déforment les feuillets de la biotite, indiquant une croissance en expansion de la prehnite. (A)_Lumière naturelle. (B)_Lumière polarisée. (CHR21_vallée de Chwalisław). bte1: biotite primaire, qtz1A: grands cristaux de quartz, prh1: prehnite.***

**Prehnite veins** crosscut the crystal frameworks, especially the K-feldspars, plagioclases and amphiboles (Fig. 46A, Fig. 46B), but without showing any reactions with the surrounded crystals.

Besides, the amphibole crystals close to prehnite microfractures do not show any chlorite developed in the vicinity of the microfractures. This also shows that prehnite is not connected to the amphibole chloritization visible in the reddened facies.

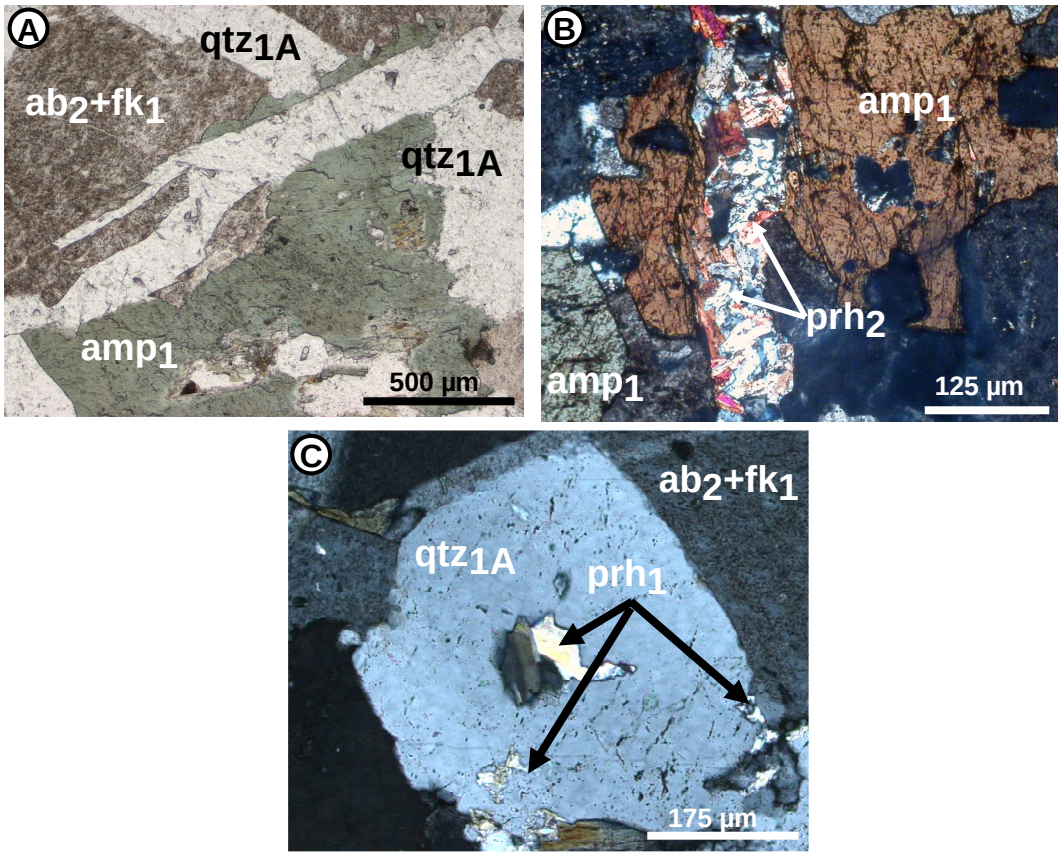


**Figure 46 – Prehnite veins within the secondary reddened facies. (A) Prehnite occurrence in microfractures crosscutting unaltered amphibole as well as an albitized K-feldspar. Prehnite appears as white, the microfracture boundaries are straight. Moreover, no amphibole chloritization is visible in the vicinity of the microfractures. The albitized K-feldspars do not show any alteration gradient from the microfractures towards the core of the crystals; plane polarized. (B) Prehnite in a microfracture. The boundary of the microfracture is irregular and the cross-cutted amphibole remains non-chloritized; cross polarized. (C) Prehnite occurring in pores, cracks within quartz; cross polarized; (MKR6, Makolno, close to the Chwalisław area); amp1: primary amphibole; fk1: primary K-feldspar, qtz1A euhedral quartz crystals, ab2: secondary albite; prh2: secondary prehnite.**

***Figure 46 – Veines de prehnite au sein des faciès rougis. (A) Prehnite dans une microfracture recoupant une amphibole primaire ainsi qu'un feldspath potassique albitisé. La prehnite est blanche et les bordures de la microfracture sont rectilignes ; l'amphibole en bordure de veine n'est pas chloritisée. Le feldspath potassique albitisé ne montre aucun gradient d'albitisation depuis la microfracture vers le cœur du cristal. Lumière naturelle. (B) Prehnite biréfringente dans une microfracture. Les bordures de la microfracture sont interpénétrées cependant l'amphibole demeure non chloritisée. Lumière polarisée. (C) Prehnite dans les pores au sein d'un cristal de quartz. Lumière polarisée. (MKR6_Makolno proche du secteur de Chwalisław). amp1 : amphibole primaire ; fk1 : feldspath potassique primaire, qtz1A grand cristaux de quartz automorphes ab2 : albite secondaire; prh1 prehnite.***

Prehnite, in particular in aggregates, is most abundant in the center of the blocks delimited by the fractures. On the other hand, in the vicinity of the fractures, prehnite appears less abundant and more frequently in form of veins. Sericite and prehnite show clearly a gradient with respect to the position of fractures, their development is apparently favoured in the more "confined" environments away from the fractures.

### *6.5.2 Calcite*

Calcite occurs only in the reddened albitized facies and never in the light/unstained facies. Calcite distribution is heterogeneous and calcite minerals occur in a scattered way throughout the reddened albitized facies. Nevertheless, in some places distinctive calcite veins appear bound to fractures, especially in the Laski quarry.

Calcite that fills fractures, that crosscut the mineral framework (Fig. 47A), show euhedral crystals with dark red-brownish cathodoluminescence adjacent to the fracture walls and bright orange to yellow luminescence towards the centre of the veins (Fig. 47B). The bright orange luminescence is typical of calcite (Machaël, 1985) while the dark red-brownish may be characteristic of dolomite (Šťastná et al., 2011) or even of $Fe^{2+}$-calcite luminescence, depending on the $Mn^{2+}/Fe^{2+}$ ratio (Machel, 1985, Savard et *al*, 1995), Therefore calcite with dark-brownish luminescence is characterized by a low $Mn^{2+}/Fe^{2+}$ ratio. Large calcite crystals also observed incidentally in pores within the mineral framework (Fig. 47C). These euhedral calcite occurrences appear as freely crystallized in fractures and voids. This may be the case of the calcite in pores and voids within albitized K-feldspars (Fig. 47C). They result from the circulation of Ca-rich fluids and may be related to late events feed from an eventual sedimentary cover.

On the other hand, dispersed tiny scattered calcite crystals occur frequently in the core of the reddened/albitized plagioclases whereas the outer unaltered rim of these crystals (formed of primary albite) does not show any calcite (Fig. 47D). This geometrical disposition suggests that this calcite is linked to the release of Ca from Ca-rich plagioclase due to albitization. It appears undoubtedly that here calcite is co-genetic to the secondary albite and to the associated hematite pigments.

Elongated calcite lenses occur in the chloritized biotite cleavage planes (Chl2a, Fig. 47F) and in the chloritized amphiboles (Chl2b, Fig. 47E). This calcite is absent in the primary biotite as well as in the primary amphibole, suggesting that calcite formation may be probably linked to the chloritization. Indeed, chloritization may generate the suitable substrate for calcite growth and moreover $Ca^{2+}$ may be released from the amphiboles during the chloritization. Calcite appears as co-genetic to the secondary chlorite formation which is itself related to the secondary albite, since plagioclase albitization may also provide $Ca^{2+}$ to feed calcite growth along the chloritized biotite and chloritized amphibole.

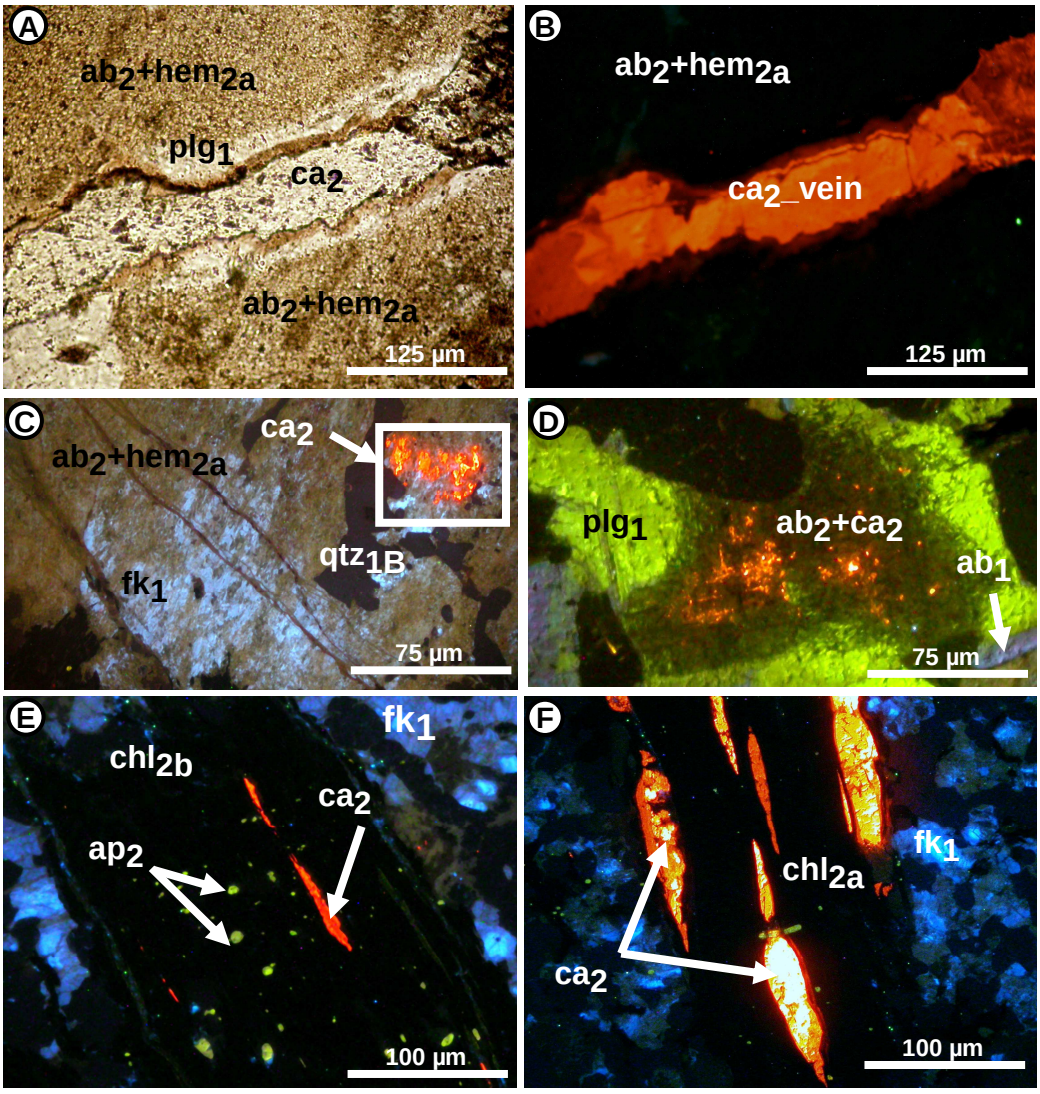


**Figure 47 – Calcite occurrences within the reddened/albitized facies. (A) and (B) calcite within a microfracture crosscutting an albitized plagioclase and showing darker brownish luminescence adjacent to the fracture walls (Fe-calcite or even dolomite) and bright orange luminescence toward the centre of the veins; (A)_plane polarized; (B)_CL image; (WL65, Laski quarry). (C) Calcite aggregates within the micropores of an albitized K-feldspar; (WL71a, Laski quarry). (D) Tiny scattered calcite occurring within the core of an albitized plagioclase while the aureole made of igneous plagioclase does not show any calcite; (WL9, Szklarska Poręba). (E) Calcite lenses along the cleavages of chloritized amphiboles. Calcite occurs next to yellow apatite; CL image; (WL87, Laski village). (F) Calcite lenses along a chloritized biotite. Calcite appears with bright orange luminescence in the center part of the lenses and darker-brownish at their edges; bte1: primary biotite; plg1: primary plagioclase; fk1: primary K-feldspar; ab1: primary albite; ca2: secondary calcite; hem2a: pigmentary hematite; chl2a: secondary chlorite after biotite; chl2b: secondary chlorite after amphibole; qtz1B: anhedral quartz.**

***Figure 47 – Calcite dans les facies rouges/albitisés. (A) et (B) Calcite avec luminescence brune foncé aux épontes de la microfracture (Calcite-Fe ou même dolomite) et une luminescence orange vif vers le centre. A_Lumière naturelle. B_Image en CL. (WL65_carrière de Laski). (C) Agrégat de cristaux de calcite au sein d'un feldspath potassique albitisé. Images en CL. (WL71a_Laski carrière). (D) Petits cristaux de calcite au cœur d'un plagioclase albitisé tandis que son l'auréole primaire ne montre pas de calcite (WL9_carrière de Szklarska Poręba). (E) Calcite sous forme de lentilles le long des clivages d'une amphibole chloritisée. La calcite apparaît aux côtés d'apatites jaunes. Image en CL. (WL87_village de Laski). (F) Calcite au sein d'une biotite chloritisée. La calcite forme des lentilles le long des clivages de la chlorite avec une luminescence orange vif dans la partie centrale de la lentille et une luminescence brun-foncée sur les bords. Image en CL. (WL63_ carrière de Laski). bte1: biotite; primaire; plg1: plagioclase primaire; fk1: feldspath potassique primaire; ab1: albite primaire; ca2: calcite secondaire; hem2a: hématite en pigment; chl2a: chlorite issue de l'altération de biotite; chl2b: chlorite issue de l'altération de l'amphibole; qtz1B: quartz xénomorphe.***

### *6.5.3 Apatites*

Apatites occur within the reddened/albitized facies as well as in the light/unstained facies. In the reddened facies, they are present within the neogenic chlorite inherited form biotite or amphibole (Fig. 48). They form numerous tiny inclusions within the secondary chlorite (Fig. 48B) or bigger euhedral but less numerous inclusions (Fig. 48C). In both cases, apatite crystals do not show any obvious orientation or features in relation with the secondary chlorite. Nevertheless, considering their size and amounts, some hypothesis may be considered.

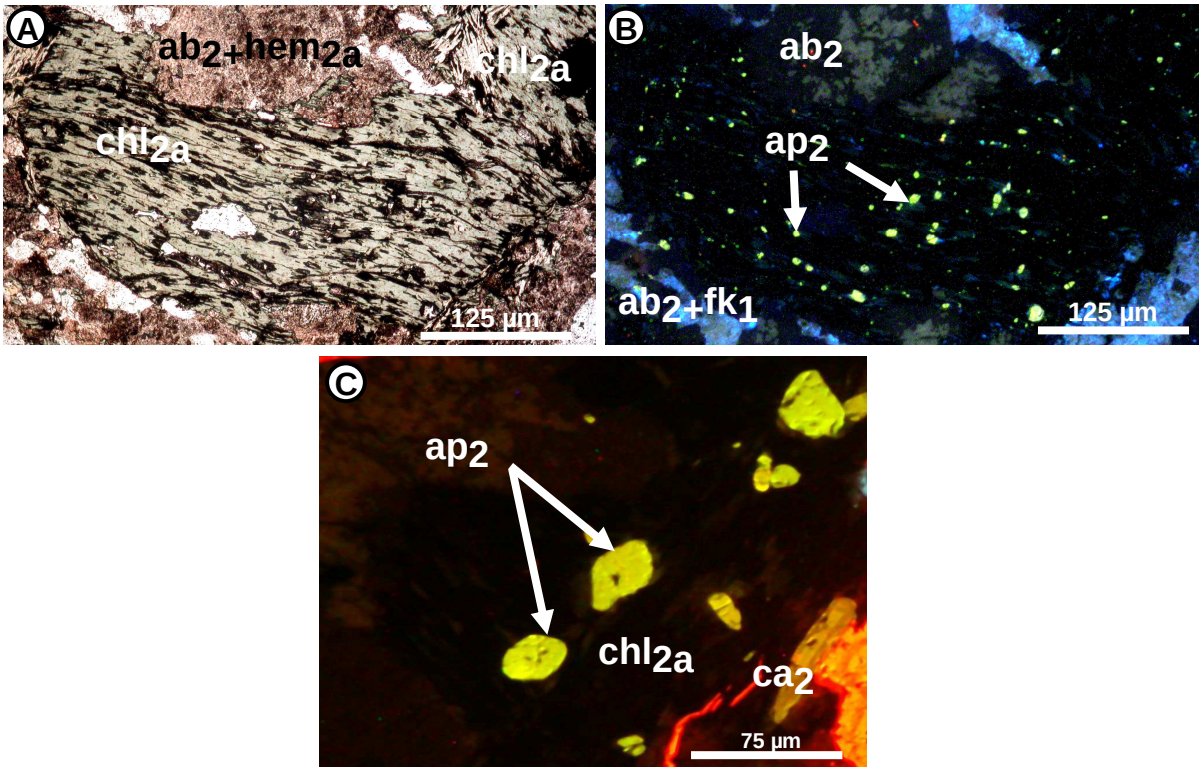


**Figure 48 - Apatite occurrence within the reddened/albitized facies. (A) and (B) apatite occurrence within secondary chlorite inherited from amphiboles. Apatite crystals show bright yellow luminescence, they are tiny and numerous within this secondary chlorite; (A) plane polarized; (B) CL image; (WL70, Laski quarry). (C) Euhedral apatite crystals within secondary chlorite. Here, apatite is bigger and less numerous than previously described. It does not show any obvious orientation in relation with the neogenic chlorite structure; CL image; (WL73, Laski quarry); ab2: secondary albite; hem2a: pigmentary hematite; chl2a: secondary chlorite after biotite, chl2b: secondary chlorite after amphibole; ap2: secondary apatite, ca2: secondary calcite.**

***Figure 48 – Occurrence d'apatite dans les faciès rouges albitisés. (A) et (B) Apatite au sein d'une chlorite correspondant à une amphibole altérée. Les cristaux d'apatite présentent une luminescence jaune vif, ils apparaissent petits et nombreux au sein de la chlorite secondaire. (A)_Lumière naturelle. (B) Image en CL. (WL70_carrière de Laski). (C) Cristal d'apatite automorphe au sein d'une chlorite d'altération d'une biotite. Ici, les apatites sont grandes et moins nombreuses que précédemment. Elles ne montrent aucune orientation en relation avec la structure de la chlorite néogénique. Image en CL. (WL 73_carrière de Laski). ab2 : albite secondaire ; hem2a : hématite en pigments ; chl2a : chlorite secondaire héritée des biotites, chl2b : chlorite secondaire héritée des amphiboles ; ap2 : apatite secondaire, ca2 : calcite secondaire.***

It may be considered that bigger apatite crystals in the secondary facies belong to the small phases present in the light/unstained facies which have grown during the chloritization process. Alternately, it may also be assumed that the tiny apatites are the primary crystals which have not grown during the alteration or that the bigger ones are neogenic apatite formed during the chloritization.

The fact that apatite may be neogenic appears as obvious on back scattered images of euhedral apatite within chloritized biotite. Indeed, SEM BSE images show that apatite euhedral crystals within chloritized biotite are surrounded by scalloped rings (Fig. 49E). These aureoles clearly evoke reaction effect haloes and suggest that the apatite crystals are not primary inclusions in the biotite but could have developed later, most probably during or even after chloritization. Such apatite recrystallization in relation with metasomtic albitization has been shown in a metagabbro from Norway (Engvik et al., 2009). Moreover, apatite within the chloritized amphiboles and biotites appears as more numerous than those within the primary minerals. This may be an argument in favour of neogenic crystallization of apatite during the chloritization.

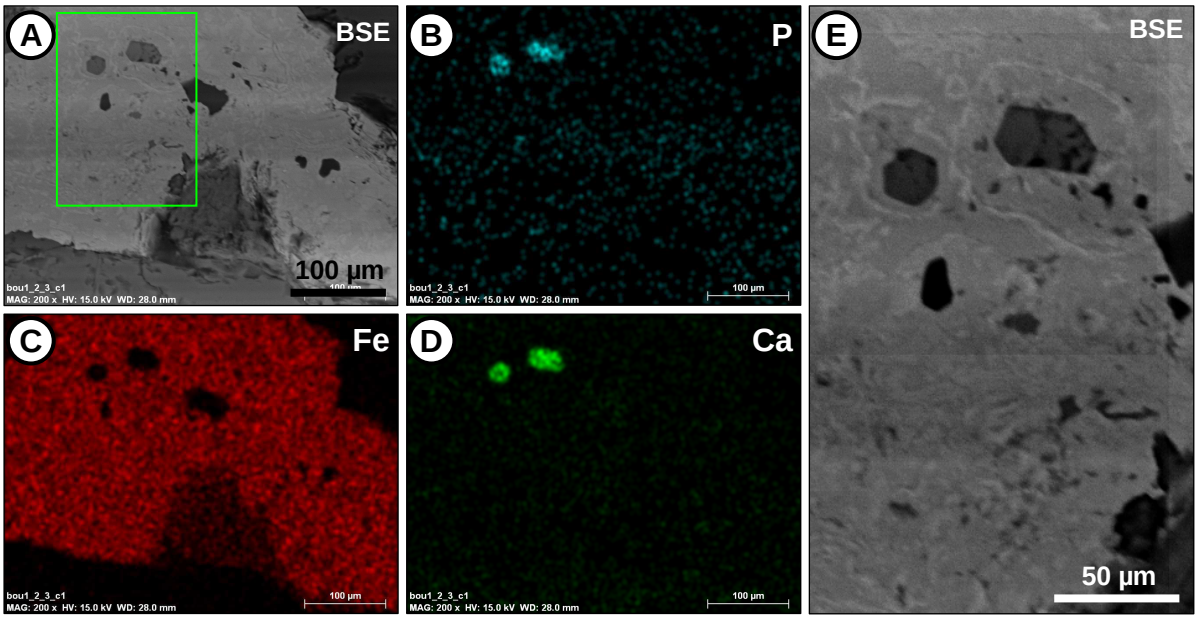


**Figure 49 - Euhedral apatite crystals in a chloritized biotite crystal. (A) SEM back scattered electron image; (B–C–D) EDS spectra. (E) Enlarged BSE image showing scalloped reactional rings around the apatite crystals. The apatite appears as dark euhedral crystals while the reactional rings are white around the apatite.**

***Figure 49 – Cristaux automorphes d'apatite dans une biotite chloritisée. (A) SEM_Image en électrons rétrodiffusée. (B-C-D) Spectre d'images en EDS. (E) Agrandissement de l'image en électrons rétrodiffusée montrant des auréoles de réaction concentriques autour des cristaux d'apatite. L'apatite se présente sous forme de cristaux automorphes sombres tandis que les auréoles de réaction sont claires.***

## 6.6 IRON MINERALS

Iron oxides have low XRD efficiency and are hardly to detect by XRD when occurring in low quantity. Therefore, hematite and maghemite have rather been analysed by thermal demagnetization that is particularly sensitive to detect maghemite which has strong specific magnetic properties. Reflected- and transmitted-light microscopy was performed to precise the paragenetic relation between the different iron oxide occurrences and determines the degree of alteration of the granitoïds.

Hematite, maghemite, and (partially oxidized) pyrite are the main iron oxides occurring in the reddened facies. Hematite is most abundant in the pervasively reddened facies, such as at Laski village, or along the fractures walls, while maghemite may be dominant away from the fractures walls and in the dark/spotted facies. Pyrite does not show any particular distribution in relation with the reddening intensity or distribution within the facies.

### *6.6.1 Pyrite*

Pyrite has been identified in all the studied facies. Pyrite appears as single large euhedral crystals typically bright yellow under reflected light.

Pyrite occurs in relative large (50 to 200 µm in diameter) and geometrically shaped grains in connexion with mafic minerals (amphibole and chlorite). The grains are often square or pseudo hexagonal shaped, agreeing to the cubic system. Euhedral shapes indicating that these crystals developed early, during the formation of the host mineral. Some of these crystals may be partially altered showing hematite formation on the outer rim, contouring a core of pyrite (Fig. 50B). Anhedral crystals appear as well and often show interconnected small cracks, filled with pyrite, pointing out their development after the formation of the host mineral (Fig. 50E).

Pyrite occurs also in chloritized biotite crystals where it forms elongated opaque lenses in between the cleavage planes (Fig. 51). Here, they show signs of alteration exhibiting an outer rim of hematite and the inner pyrite core of the lenses (Fig. 51). The pyrite/hematite contact shows clearly predominant crystallographic directions related to the primary pyrite.

The hematite and pyrite geometrical disposition (outer rim of hematite and inner part of pyrite) is usually reported as near-surface weathering alteration within granitoïds (Whalen and Chappell, 1988). This suggests that hematite is formed by the weathering (oxidation) of primary pyrite.

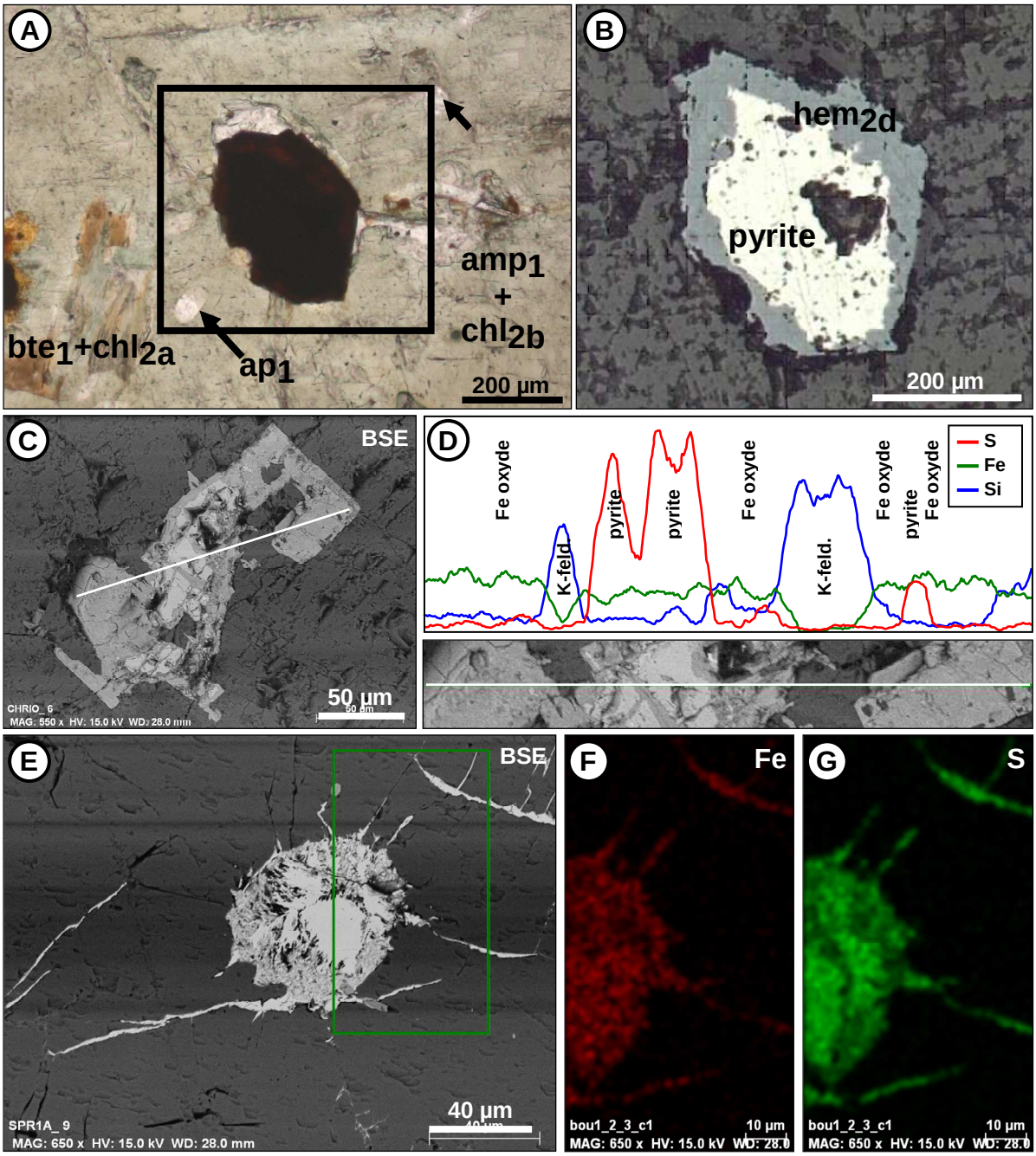


**Figure 50 – Pyrite and pyrite/hematite occurrences. (A) Pseudo-hexagonal shaped grain with a brownish rim and dark core in an amphibole crystal containing remnant biotite. Biotite and amphibole are partly chloritized; plane polarized; (MKR1b, Mąkolno). (B) Enlargement underreflected light microscope, the outer rim is made of hematite, the core shows pyrite; (MKR1b, Mąkolno). (C) SEM BSE image of a cubic shaped pyrite grain partly oxidized and hosted in feldspar. (D) EDS spectra along the transect marked in (C); (SPR1A, Szklarska Poręba). (E-F-G) pyrite inclusions in feldspar and in cracks; (SPR1A, Szklarska Poręba); BSE = back scattered electron image.**

***Figure 50 – Occurrence de pyrite et de pyrite/hématite. (A) Grain à forme pseudo-hexagonal avec une bordure brune et un cœur sombre au sein d'une amphibole présentant des reliques de biotite. La biotite et l'amphibole sont partiellement chloritisées. Lumière naturelle. (MKR1b_Mąkolno). (B) Agrandissement en lumière réfléchie, la bordure extérieure est constituée d'hématite et le cœur de pyrite. (MKR1b_Mąkolno). (C) Image SEM d'un grain de pyrite cubique et partiellement oxydé au sein d'un feldspath. (D) Spectre d'analyse EDS le long de la ligne indiqué dans C. (SPR1A_carrière de Szklarska Poręba). (E-F-G) Pyrite en inclusions dans un feldspath dont elle pénètre les microfractures (SPR1A_carrière de Szklarska Poręba). BSE = image en électrons rétrodiffusés.***

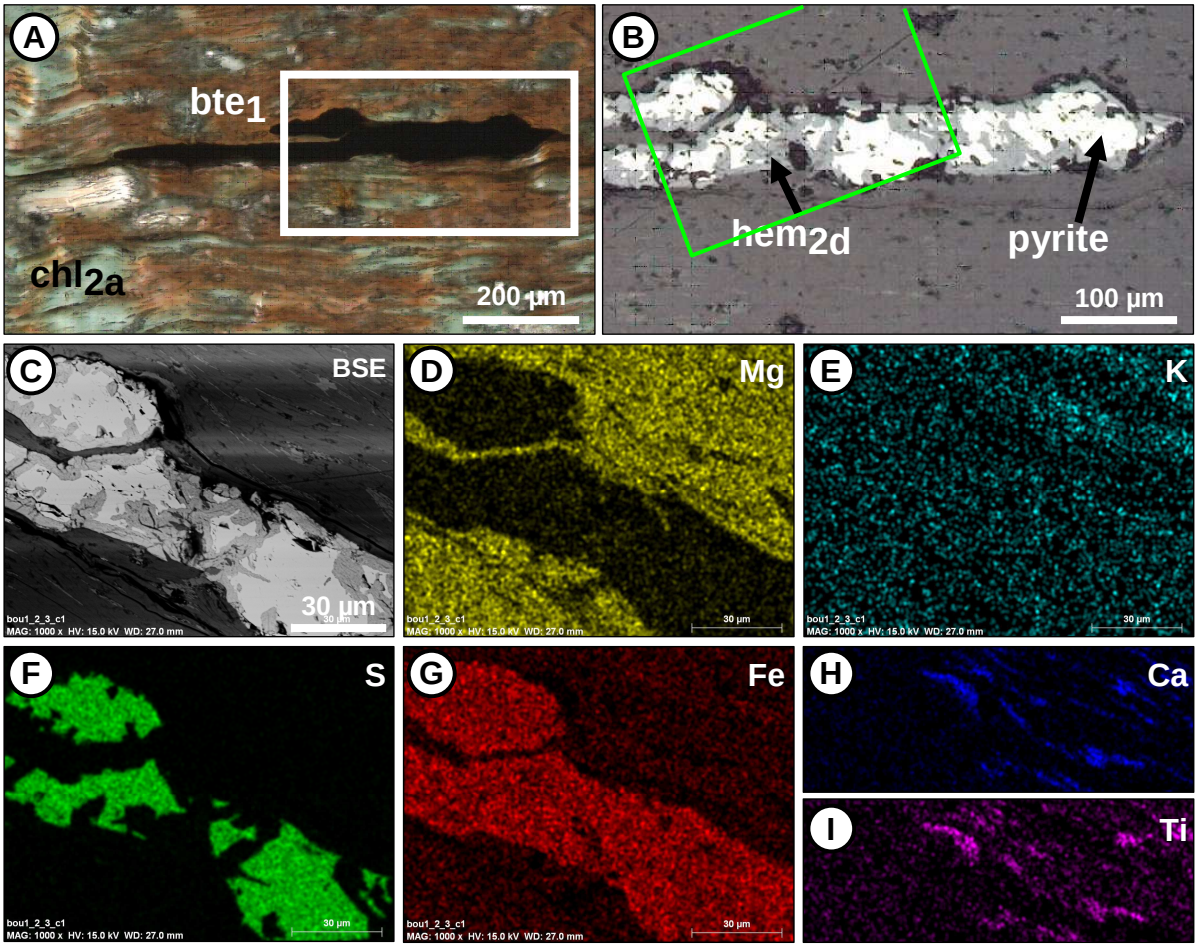


**Figure 51 – Sheet-like lenses of iron oxides in a biotite crystal; (A) plane polarized. (B) Enlargement under reflected light microscopy. Notice that the contact between pyrite and hematite shows crystalline directions. (C) SEM image of the area marked on (B). (D-E-F-G-H-I) EDS elemental mapping images. Pyrite (Fe + S) appears as residual, enclosed by iron oxide (Fe without S). The partially chloritized biotite that host the iron mineral shows no K-feldspar inclusions, but sheets of titanite (Ca + Ti) are embedded in between the biotite cleavage planes; (WL147, Chwalisław mountain); BSE = back scattered electron image.**

***Figure 51 – Oxyde de fer sous forme de lentilles au sein d'un cristal de biotite. (A) lumière naturelle. (B) Agrandissement en lumière réfléchie : remarquez que le contact entre la pyrite et l'hématite montre des directions cristallographiques. (C) Image en SEM de la zone marquée en B. (D-E-F-G-H-I) Images en EDS. Pyrite (Fe + S) apparaît comme étant résiduelle, replace par des oxydes de fer (Fe sans S). La biotite partiellement chloritisée dans laquelle se situe les minéraux ferriques ne montrant pas d'inclusion de feldspath potassique, mais des feuillets de titanite (Ca + Ti) sont intercalés entre les clivages de la biotite. WL147_montagne de Chwalisław). BSE= image en électrons rétrodiffusés.***

### *6.6.2 Hematite and maghemite*

Hematite is the most frequent iron oxide in the pinkish/reddish granitoïd rocks in the Polish Sudetes. Hematite occurs as (1) fine pigments, (2) distinctive granules and flakes, or (3) sub-euhedral crystals.

Hematite pigments cloud the albitized plagioclases (Fig. 52A) as well as the pinkish K-feldspar phenocrysts. Nevertheless, some scattered pigments are visible in the primary and unaltered feldspars. Hematite pigments are clearly related to the alteration (i.e. albitization) of the plagioclases and K-feldspars; they never show any particular link with secondary features, like microfractures, voids, cleavages, etc. and thus appear as syngenetic (cogenetic) inclusions formed during development of the secondary albite.

Hematite flakes occur in microfractures and along intergranular joints. They are made up of distinctive dark and uniform accumulations and often appear concomitant with chlorite flakes either (1) in secondary albite, forming flakes of similar size as the initial chlorite flakes (Fig. 52A) or (2) in microfractures crosscutting diverse crystals (Fig. 52B). Hematite and chlorite are often spatially related, but their mutual relationship is not always clear. In some places it can be seen that chlorite and hematite are coexisting in the same fracture: hematite occurring when the fracture crosscuts quartz or albite crystals, whereas chlorite elongated/oriented along the fracture occurs when the fracture crosscuts a chloritized biotite (Fig. 52B). In this later occurrence one can imagine that: (i) depending of the geochemistry of the microenvironment, hematite may form in contact with the feldspar and chlorite in contact with ferromagnesian silicates; (ii) or the fracture was already "smeared" with chlorite due to the shearing and that hematite developed later by alteration of the chlorite as seen similarly in the chloritized biotites. Besides, hematite often forms dark irregular granules within the hematite clouded albites and K-feldspars, without any clear relation to the remaining or former chlorite. But the relation with former chlorite inclusions cannot been completely excluded for these occurrences.

Fractures filled by dark hematite occur also without any connection with the chlorite. In this case, hematite forms as distinctive prismatic sub-euhedral crystals as shown through reflected light microscopy (Fig. 52C). Obviously, these hematite occurrences result from precipitations from fluid migrations in open fractures.

Large dark hematite patches occur within the cleavages of the chloritized biotite crystals. They appear as well defined lenses elongated in between the former biotite cleavage planes (Fig. 52D) and as more irregular and less defined patches in sections oblique or in accordance to the former cleavage planes (Fig. 52E), pointing out that hematite forms as disc-like aggregates in between thechlorite sheets. Quartz is often associated with hematite in these intra-chlorite hematite patches. In some samples, similar shaped lenses are filled only with quartz or even with calcite. These lenses probably result from the alteration/oxidation of a primary ferruginous mineral, which has been dissolved and replaced either by quartz or by calcite.

Maghemite seems less abundant than hematite and appears related to the less altered/oxidized granitoïd facies.Its occurrence in thin sections is not evident and therefore maghemite could not be characterized neither through optical nor by reflected light microscopy. The only unambigious characterization of maghemite and its distribution throughout the studied facies is established by the thermal demagnetization.

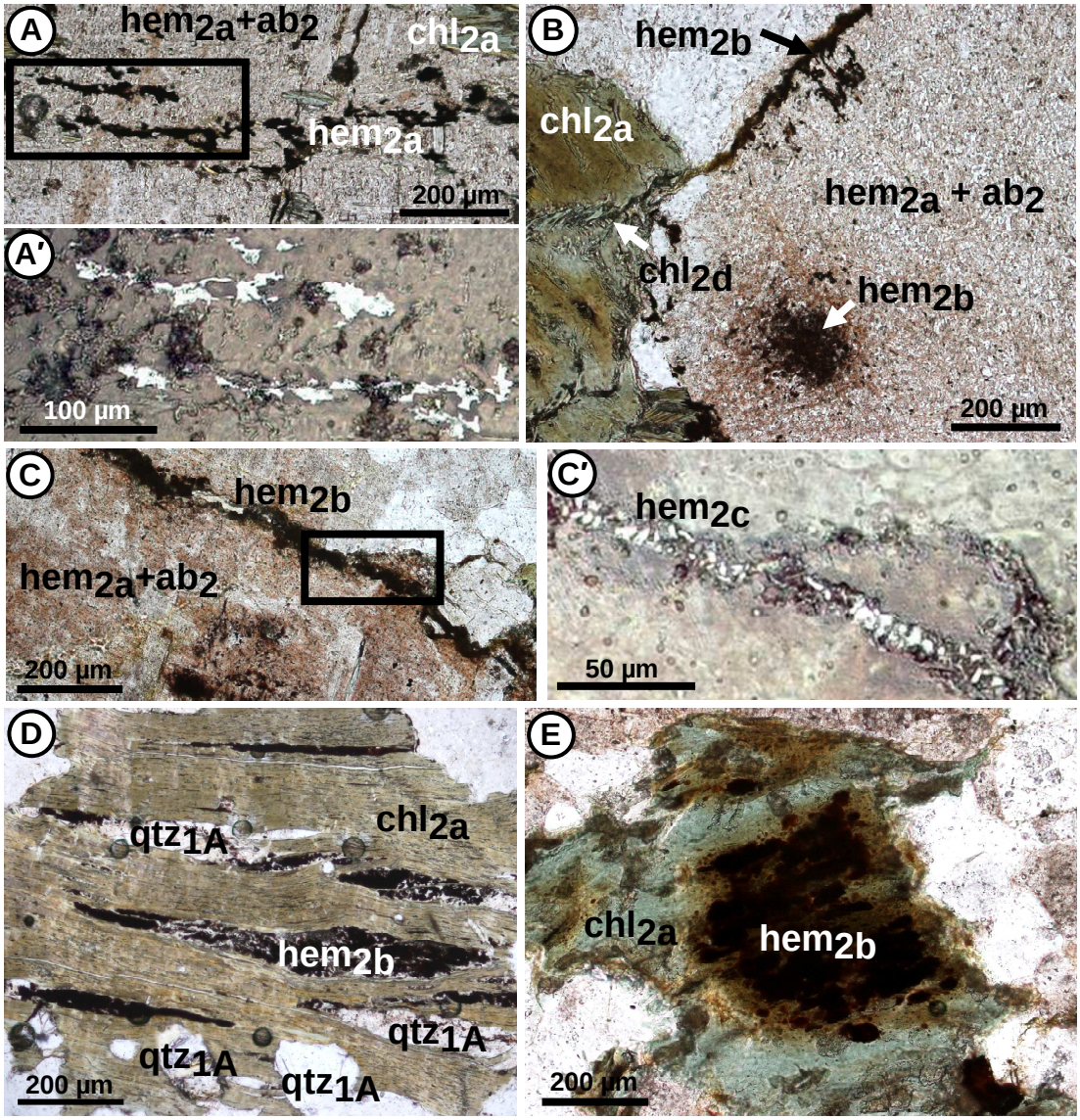


**Figure 52 - Hematite occurrence within the albitized granitoïd rocks. (A) Fine hematite red pigments within the secondary albite and dark and elongated hematite flakes related with remaining chlorite flakes; plane polarized; (WL97, Laski village); (A′) enlargement of A; reflected light; hematite appears in bright white contrast. (B) Red/brown pigmentary hematite within secondary albite and dark hematite in a microfracture, notice the small chlorite flakes that are oriented across the orientation of the large chlorite crystal, Additional presence of irregular shaped hematite granules; plane polarized; (WL93, Laski village). (C) Dark hematite in fractures cross cutting hematite stained secondary albite; plane polarized; (WL93, Laski village); (C′) enlargement showing bright white sub-euhedral hematite crystals; reflected light; (WL93, Laski village). (D) Hematite lenses flattened parallel to the cleavages of a large chloritized biotite crystal; plane polarized; (WL92, Laski village). (E) Hematite lens, similar to that of (D), view in a thin section in the vicinity of the cleavage planes. Notice that there are also smaller rod-like hematite aggregates. Aggregates, that appear more irregular within the cleavage planes; plane polarized; (WL94, Laski village); ab2: albite; chl2a: secondary chlorite after biotite; chl2b: secondary chlorite after amphibole, chl2d: neogenic chlorite in micro-fracture; hem2a: pigmentary hematite; hem 2b: dark hematite: hem 2c: sub-euhedarl hematite.**

***Figure 52 – Occurrence d'hématite dans les granitoïdes rouges/albitisés. (A) Fin pigment rouge d'hématite au sein de l'albite secondaire et d'hématite en plaquettes sombres associée à des feuillets résiduels de chlorite. Lumière polarisée. (WL97_village de Laski). (A') Agrandissement de A. Lumière réfléchie, l'hématite apparaît en blanc vif. (B) pigments rouge/brun d'hématite au sein de l'albite secondaire et hématite sombre associée à des feuillets de chlorite dans une microfracture en communication avec une biotite chloritisée.. Aussi, hématite en granule irrégulier au sein de l'albite. Lumière naturelle. (WL93_village de Laski). (C) Hématite sombre dans une fracture recoupant une albite secondaire pigmentée d'hématite. Lumière naturelle. (WL93_village de Laski). (D) Lentilles d'hématite allongée parallèlement aux clivages d'une grande biotite chloritisée. Lumière naturelle. (WL92_village de Laski). (E) Lentilles d'hématite identique à ceux de (D) mais vue dans le plan de clivage. Notez qu'il y a aussi des agrégats de baguettes d'hématite plus petites. Ces agrégats apparaissent plus irréguliers au sein des plans de clivage. Lumière naturelle. (WL94_village de Laski). ab2: albite secondaire; chl2a: chlorite secondaire héritée de biotite; chl2b: chlorite secondaire héritée d'amphibole, chl2d: chlorite néogénique dans les microfractures; hem2a: hématite en pigments; hem 2b: hématite sombre: hem 2c: hématite subautomorphe.***

## 6.7 CONCLUSION

The study of the reddened facies reveals that the distribution of the red coloration shows a close link with the distribution of the primary or secondary minerals. The reddened facies are mainly dominated by the presence of secondary albite, hematite, and chlorite, while the light/unstained facies are dominated by igneous minerals such as plagioclases, biotite, and amphibole and also alteration minerals, forming aggregates of prehnite-albite (ab2')-sericite. Plagioclase, amphibole, and biotite show a progressive evolution from the light facies towards the reddened fracture walls highlighting some specific mineralogical changes. Plagioclases disappear in favour of albite as approaching towards the reddened fracture walls, while the amphibole and biotite content decreases in favour of chlorite. Thus, albite replaces plagioclase in the reddened facies whereas chlorite replaces amphibole and biotite (Fig. 53).

The most outstanding phenomenon of the reddened facies is the albitization of the primary plagioclases. Plagioclases are entirely or partially albitized showing the preservation of aureoles or irregular zones of clear primary albite within the zones of secondary hematite clouded albite. The neogenic albite (ab2) is non-twinned and associated with pigmentary hematite, sericite, and calcite. The primary polysynthetic twinnings of the plagioclase tend to disappear during the albite formation. This is clearly different to "the classical" saussuritization in which secondary albite (ab1) is porous and forms aggregates with prehnite-sericite and where petrographic features of the primary plagioclases are preserved (de la Roche, 1957; Sandström et al., 2010). Even if twinning glooming, obliteration or obscuring have been reported in some saussuritized plagioclases (Jenkin et al., 1992; Morad et al., 2010) they have never been completely erased. Indeed, it assumes that the lack of twinnings in the saussuritization is just apparent (Martin and Parsons, 1997).

Besides, hematite appears as paragenetic with secondary albite. In particular, it is excluded that the hematite may have precipitated late in pores within the secondary albite: in this case one would expect that iron oxides form in the pore through microfractures yet the latter is not observed in the studied facies. Under the assumption that hematite and secondary albite are paragenetic, it means that the albitization took place under oxidizing conditions.

Albitization of both, plagioclases and K-feldspars, is associated with the chloritization of the primary amphiboles and biotites. Some chloritized biotites show lenses of titanite, calcite, K-feldspars and pyrite along the cleavages, resulting from of Ti, K, Si and Fe released by the chloritization of the biotites. Similarly, the chloritized amphiboles show calcite lenses along their cleavages, resulting directly from the Ca-release by the amphibole chloritization.

Thus, for conclusion, the reddening processes include the replacement of the primary K-feldspars by secondary albite (ab2) and microcline, and the inclusion of pigmentary hematite. Several minor minerals such as calcite, apatite, and even titanite appear as associated with the reddening/albitization alteration.

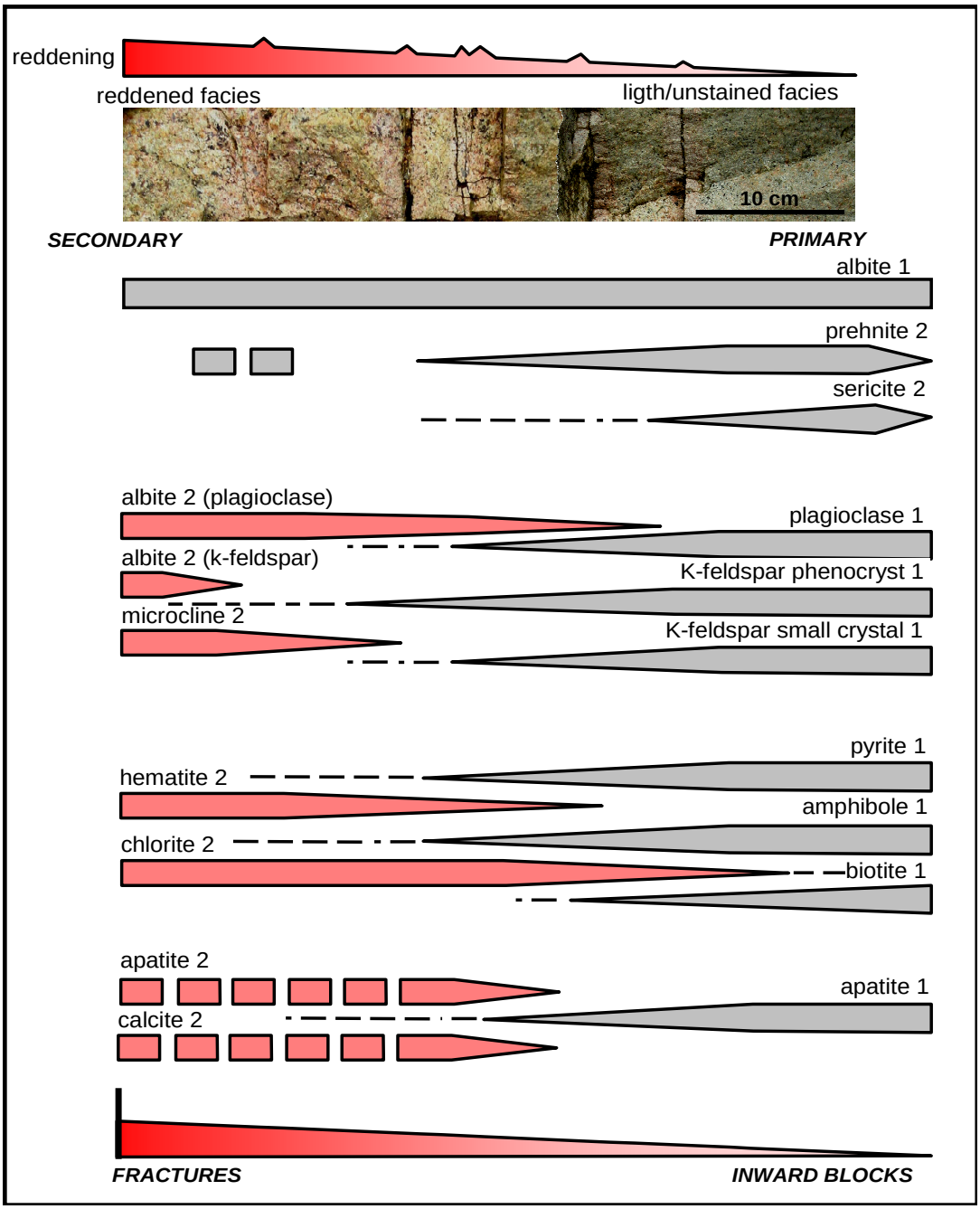


**Figure 53 – Minerals distribution from the reddish zone towards the light zone. (1) is for the primary minerals and even the saussuritization minerals and (2) for the secondary. Igneous minerals and the minerals related to saussuritization appear in grey, and those related to reddened facies are in red. The reddened zone is dominated by the occurrence of the secondary minerals such as albite, hematite and chlorite whereas plagioclase, amphibole and biotite are the significant minerals in the light zone. Secondary minerals towards the reddened zone progressively replace the primary minerals. Saussuritization minerals are represents by albite-sericite-prehnite aggregates; they are not affected by the reddening alteration.**

***Figure 53 – Distribution des minéraux depuis la zone rouge vers la zone claire. (1) désigne les minéraux primaires et le (2) les minéraux secondaires. Les minéraux ignés et les minéraux de la saussuritisation apparaissent en gris tandis que les minéraux liés aux faciès albitisés en rouge. La zone rouge est dominée par l'occurrence de minéraux secondaires tels que l'albite, 'l'hématite et la chlorite tandis que plagioclase, amphibole et biotite sont les minéraux importants dans la zone claire. Les minéraux secondaires remplacent progressivement les minéraux primaires en allant vers la zone rouge. Les minéraux de la saussuritisation sont représentés par les agrégats d'albite-prehnite-séricite qui ne sont pas affectés par l'altération rougissante.***

# *RESUME CHAPITRE 7*

# *INTERPRETATION DES PARAGENESES MINERALES*

## *CIRCULATIONS DE FLUIDES ET PROCESSUS METASOMATIQUES*

*Les altérations décrites dans l'étude pétrographique sont entièrement liées aux fractures de la roche. Le rougiement montre un gradient décroissant depuis les fractures vers l'intérieur des blocs où les faciès sont clairs. Aussi, les fractures majeures ayant eu des circulations importants de fluides montrent des altérations plus intenses (épontes colorées d'oxyde de fer) que les fractures mineures. Il apparaît que ces altérations sont dues à la* ***circulation de fluides*** *dans les fractures.*

*L'altération des plagioclases donne lieu à trois types d'altération ; (1) l'albitisation des plagioclases (avec préservation de volume) associée à de l'hématite en pigments à proximité des fractures ; et loin des fractures (2) la saussuritisation et (3) la séricitisation des plagioclases (Fig. 54). Ces altérations s'accompagnent aussi de la chloritisation des minéraux ferromagnésiens primaires (biotite et amphiboles). Cette chloritisation s'accompagne de la formation de minéraux secondaires (quartz, FK, prehnite, minéraux ferrugineux, de titanite, apatite) le long des feuillets de la chlorite. Ces altérations apparaissent géochimiquement différenciées entre le cœur et la bordure des blocs délimités par les fractures (Fig. 54). La bordure des blocs (faciès rouge) est ainsi enrichie en* $Na^+$ *et appauvrie en K, tandis que le cœur des blocs (faciès clairs) apparaît relativement enrichi en* $K^+$*, en* $Ca^{2+}$ *et en* $Al^{3+}$*. La composition chimique de l'ensemble évolue peu. Ces altérations correspondent à un* ***processus métasomatique*** *de ré-ajustement des équilibres thermodynamiques.*

*Les différentes altérations et paragenèses associées se présentent comme des continuums ou des gradients passant de l'un à l'autre puisqu'elles ne montrent jamais de front d'altération entre elles. Les différentes paragenèses observées sont donc la traduction de* ***gradients géochimiques*** *entre le fluide des fentes et les blocs de granitoïdes. Les successions paragénétiques résultent du déplacement progressif du front réactionnel de chaque paragenèse des fractures vers l'intérieur des blocs. L'albitisation et les pigments d'oxydes présentent le même type de gradient traduisant une diminution vers l'intérieur des blocs des teneurs en* $Na^+$ *et* $O_2$ *(et/ou Fe) (Fig. 54), tandis que la teneur en* $K^+$ *semble diminuer en sens inverse.*

## *REACTIONS COUPLEES DE DISSOLUTION-PRECIPITATION*

*L'anorthite des plagioclases étant très instable en présence d'eau (Mathews and Goldsmith, 1984), la déstabilisation des plagioclases semble être le processus d'altération qui déclenche et entretient des réactions en chaînes qui en découlent.*

*L'****albitisation des plagioclases*** *à volume constant en bordure des fentes se fait avec apport en* $Na^+$ *et relargage de* $Ca^{2+}$ *et éventuellment de* $Al^{3+}$*, et donne naissance à une albite très peu poreuse. La réaction d'albitisation se réduit au fur et à mesure que les fluides pénètrent la roche par convection et diffusion jusqu'à s'arrêter lorsque le* $Na^+$ *devient insuffisant pour nourrir l'albitisation.*

*Les* ***biotites*** *sont altérées en bordure des fractures par le double effet du lessivage du* $K^+$ *interfoliaire et de l'oxydation de* $Fe^{2+}$ *de leur couche octaédrique (Fig. 54). La chloritisation des biotites se fait avec recristallisation de la structure phylliteuse et a minima avec libération de* $Si(OH)_4$*, qui pourra d'ailleurs être consommé par les néoformations de FK ou de quartz, ou même nourrir l'albitisation des plagioclases. Il est à noter que la nature des chlorites va dépendre de la composition initiale des biotites et de la composition des fluides.*

*Or la composition des fluides varie vers l'intérieur des blocs, donc la nature des chlorites va évoluer dans le même sens. La reconnaissance de chlorite de différentes compositions ne traduit aucunement des phases successives mais plutôt une évolution des fluides au cours de la chloritisation.*

*Les **amphiboles** globalement calciques semblent moins sensibles à la chloritisation, probablement protégées par le $Ca^{2+}$ libéré par l'albitisation des plagioclases. Pour cette raisonla chloritisation des amphiboles n'apparaît que dans les faciès les plus albitisés. La déstabilisation des amphiboles intervient probablement aussi sous l'effet du lessivage de Mg et éventuellement de l'oxydation de $Fe^{2+}$*

*L'**hématite** est systématiquement associée à l'albitisation. En dehors de la pyrite et des magnétites primaires oxydées, l'hématite apparaît soit en pigment dans l'albite néogénique, ou en granules ou feuillets associés aux minéraux ferromagnésiens. Toutes les occurrences d'hématite en dehors de l'albite néogénique sont directement associées à la chloritisation des minéraux ferromagnésiens et jamais directement liées aux fluides des fractures. D'ailleurs cette relation (hématite-chlorite) est renforcée par l'études isotopique du Fe dans les faciès albitisés et saussuritisés de Suède qui indique l'apport de Fe des chlorites dans la formation de l'hématite (Dideriksen et al., 2007). Le fer n'apparaît jamais lié directement aux solutions des fractures, celles-ci ne sont visiblement pas ferrugineuses.*

*La formation de **séricite** dépend de la disponibilité de $Al^{3}$ et $Si^{4+}$ mais surtout de $K^{+}$. Le $K^{+}$ proviendrait exclusivement de la chloritisation des biotites, puisque l'albitisation des feldspaths-K est marginale et limitée à la bordure des fentes. Or en bordure des fractures le $K^{+}$ libéré par la chloritisation est en grande partie évacué. Ce n'est qu'en s'éloignant des fentes, vers l'intérieurs des blocs, que le flux convectif se réduit et que les phénomènes de diffusion prennent de l'importance dans le transport des éléments, expliquant ainsi pourquoi la séricite est plutôt plus développée au cœur des blocs, loin des fractures.*

*La **prehnite** présente plusieurs occurrences témoignant d'une certaine mobilité des éléments constitutifs. Cette mobilité est aisément envisageable pour le $Ca^{2+}$ et le $Si^{4+}$, mais plutôt singulière pour l' $Al^{3+}$ considéré globalement immobile. Il apparaît néanmoins dans le cas présent que l'aluminium est relativement mobile mais son évacuation du système par les fluides est difficilement appréciable.*

*La faible fréquence de **calcite** dans les faciès étudiés dénote des fluides relativement pauvres en $CO_2$.*

***INTERACTIONS FLUIDE-ROCHE***

*La distribution des altérations par rapport aux fractures montre qu'il n'y a qu'une phase d'altération avec des réactions liées les unes aux autres. Ces réactions induisent des échanges géochimiques conditionnés par le déplacement des ions en solution. Les circulations de fluides sont plus intenses dans les fractures principales ouvertes par convection, tendent à s'annuler dans les microfractures en « cul-de-sac », et se limitent même à de fins films aux limites des grains au cœur des blocs. À ce niveau, la diffusion l'emporte sur la convection.*

*Les vides, fractures et limites de grains sont donc essentiels dans les réactions d'altération car ceux-ci permettent le mouvement de fluide. Quand les mouvements de fluide sont réduits, la sursaturation d'un fluide par rapport à une phase minérale est limitée à l'interface minérale-fluide (Putnis et al., 2005) et le film de fluide à l'interface peut avoir une composition très différente de celle du fluide qui circule et qui peut rester sous-saturé par rapport au minéral qui précipite à l'interface. Dans ce cas, les réactions couplées présentées plus haut ne s'inscrivent plus dans un équilibre global mais plutôt dans des équilibres*

*géochimiques dynamiques s'enchaînant spatialement, et entretenue par la progression des altérations. Une zonalité géochimique se développe alors et progresse à la manière d'une chromatographie typique d'un système métasomatique (Korzhinskii et Oestreich, 1965 ; Brinhall et Dietrich, 1987 ; Guy, 1993).*

*Dans une roche limitée par une fracture, il s'établit une zonalité du transport des ions qui va conditionner la zonalité géochimique (Fig. 54). Près des fractures, les échanges se font par convection et les minéraux précipités sont en équilibre avec le fluide des fractures, tandis que loin des fractures, la diffusion prédomine et les paragenèses sont conditionnées par les équilibres locaux qui sont de plus en plus éloignés de l'équilibre avec les solutions des fractures à mesure qu'on s'éloigne de celles-ci. Ce sont les réactions couplées au voisinage des fractures qui sont les témoins de la nature des fluides qui circulent.*

*L'albitisation des plagioclases et la formation d'hématite témoignet de la géochimie des fluides. Ce sont des fluides enrichis en $Na^+$ et appauvris en $K^+$ qui permettent la formation d'albite. Ces fluides sont également enrichis en oxygène comme le montrent la présence et l'abondance d'hématite près des fractures, relativement pauvres en $CO_2$ car peu de calcite précipite, désaturés en $SiO_2$, $Al^{3+}$ et $Mg^{2+}$ puisque les biotites et sont partiellement altérés en hématite. En sortie du système, les fluides sont appauvris en $Na^+$ et $O_2$, consommés par l'albitisation et l'hématisation mais enrichis en $K^+$ car peu de séricite se forme en début d'altération. Le bilan est plus difficile à établir pour $SiO_2$, $Al^{3+}$ et $Ca^{2+}$. Au final, les fluides à l'origine des altérations étudiées ici sont riches en $Na^+$, relativement appauvris en $K^+$ par rapport à $Na^+$ et oxydés.*

***COMPORTEMENT DES OXYDES DE FER***

*Les oxydes de fer présents dans ces faciès peuvent constituer un excellent outil pour la datation paléomagnétique du phénomène d'altération, en supposant que albitisation et oxydes de fer sont paragénétiques. Deux interprétations de l'association albite-hématite sont possibles : soit elle est paragénétique et correspond donc à un seul évènement géodynamique, soit albite et hématite correspondent à des altérations successives. Ces deux points de vue sont largement discutés dans la littérature. Jenkins et al., (1992) qui considérent que la saussuritisation, la chloritisation et la séricitisation des granites de Connemara correspondent à un événement unique, tandis que les auteurs travaillant dans le Protérozoïque de Suède évoquent plusieurs évènements géodynamiques et séquences d'infiltrations pour expliquer l'association albite-hématite (Drake et al., 2009 ; Sandström et Tullborg, 2009).*

*L'**origine des fluides oxydants** est toujours rattaché à la surface. Dans les hypothèses post-magmatiques ils sont expliqués par des circuits convectifs apportant les fluides superficiels au contact des roches granitiques chaudes et profondes. La participation de fluides météoriques a été argumentée au travers d'études isotopiques des minéraux d'altération. Mais la faiblesse de ce modèle réside dans le fait que les fluides superficiels sont censés descendre à des profondeurs de l'ordre de 10 km et vont perdre progressivement leur pouvoir oxydant en interagissant avec les terrains sédimentaires et métamorphiques traversés. Récemment, une modélisation géochimiques des fluides circulants dans des fractures a montré une réduction rapide de la fugacité de l'oxygène des fluides (MacQuarrie et al., 2010).*

*La **distribution des oxydes de fer** à l'échelle microscopique montre que l'hématite n'est jamais associée aux fractures et joints comme on pourrait l'imaginer si le fer avait été introduit dans la roche par des solutions. En fait, l'hématite forme un pigment diffus dans l'albite secondaire qui comporte très peu de pores. En revanche, les albites poreuses sont celles associées à la précipitation de prehnite et de séricite et celles-ci ne montrent pas*

*d'oxyde de fer associé. L'hématite est donc cogénétique de l'albitisation et correspond vraisemblablement à une redistribution du fer lors de la chloritisation des biotites. A l'échelle macroscopique, la coloration rouge est directement associée aux fractures et les oxydes de fer sont associés à l'albitisation. De plus, les fractures rouges albitisées ne sont recoupées par aucune fracture postérieure, indiquant que l'albitisation rouge est récente par rapport à l'histoire géodynamique du granite et certainement portérieure à son exhumation.*

*La distribution des porteurs magnétiques résultants de la démagnétisation thermique indique un mode de distribution en fonction de la coloration rouge des faciès et de leurs caractéristiques structurales (Fig. 55). Les faciès intensément et pervasivement albitisés de Laski village montrent uniquement de l'hématite tandis que les faciès à pigmentation légèrement rose comme ceux de la carrière de Chwalisław présentent soit un mélange hématite-maghémite ou uniquement de la maghémite (carrière de Szklarska Poręba). La distribution dans les coupes avec albitisation rouge intense le long des fractures est plus contrastée. Les fractures les plus rouges contiennent de l'hématite ou un mélange hématite-maghémite tandis que les fractures les moins rouges montrent une prédominance de maghémite. De la magnétite résiduelle est présxente dans les faciès clairs, non altérés, et semble être un porteur primaire. L'hématite caractérise les faciès les plus altérés tandis que la maghémite semble se développer dans les premiers stades d'oxydation.*

*La maghémite semble typique des faciès les moins altérés et non affectés par l'hématisation dans lesquels subsistent des biotites non chloritisées. Il est généralement admis que, l'oxydation lente de la magnétite produit de la maghémite tandis qu'une oxydation rapide conduit directement à la formation d'hématite (Steinthorsson and Helgason, 1992 ; Bowles et al. 2011). La transition maghémite-hématite traduirait donc un changement des conditions environnementales pendant l'oxydation de la magnétite. L'altération commencerait par la formation de la maghémite dans des conditions oxydantes faibles, tamponnes par la présence de minéraux ferromagnésiens primaires, et continuerait avec la formation d'hématite dans les conditions oxydantes plus franches, quand les minéraux ferromagnésiens sont oxydés. La distribution spatiale de ces deux oxydes permettrait de retracer le gradient de ces conditions oxydantes lors de l'altération albitisante.*

*D'un point de vue géochimique, il n'y a aucune contradiction pour avoir une* ***différentiation spatiale entre la distribution des silicates et des oxydes de fer****. Cependant, l'altération et la cristallisation des silicates dépendent du pH tandis que l'Eh et la fugacité de l'oxygène gouvernent la formation des oxydes de fer. Ces deux paramètres peuvent varier indépendamment, mais la précipitation des oxydes de fer est facilitée par toute élévation du pH. Ainsi une chute locale de l'activité de* $H^+$ *favoriserait localement la précipitation d'inclusions d'hématite dans les feldspaths (Boone, 1969), expliquant la précipitation d'hématite au cours de l'albitisation des plagioclases et des feldspaths potassiques. D'autre part, l'intensité de la pigmentation rouge et l'abondance d'hématite sont liées à la fugacité de l'oxygène qui décroît également en s'éloignant des fractures. D'un point de vue géochimique, la distribution de l'hématite concorde avec la séquence d'altération des silicates suggérant de ce fait que l'hématite fait partie intégrante de la paragenèse.*

# CHAPTER 7

# 7 INTERPRETATION OF THE MINERALOGICAL PARAGENESES

## 7.1 FLUID CIRCULATION AND METASOMATIC PROCESSES

**Fluid circulation** in the fractures trigger the alterations. The mineralogical parageneses described in the petrographical study are entirely linked to the fractures within the rocks. The reddening develops with a decreasing gradient from the fractures towards the inner part of the blocks which are themselves delimited by these fractures. The light/unstained facies are always situated further away from the fractures, towards the core of the blocks (Fig. 54). This geometrical arrangement is systematic, but the intensity of the alteration phenomena varies significantly.

Some fractures emerge as major with respect to the alterations and the staining of their walls by iron oxides may reach several decimetres in thickness, whereas other fractures are thinner and appear as secondary and less extended with respect to the alterations and to the oxidation phenomena on the fracture walls, that are limited here and often penetrate the rocks only a few millimetres. This geometrical arrangement clearly shows that the alterations must be related to fluid circulation through the fractures.

Major fractures showing the most intense alterations are opened and interconnected, and therefore they presumably had significant fluid flow rates. Fractures with limited alterations therefore had less significant fluid flow rates, due to the fact that they are narrow (compressive tectonic) and/or to their lack of connectivity with other fractures.

**Chain reactions** occur within the fracture isolated blocks. The alterations described in the petrographical section affect primarly and intensively the plagioclases and only to a lesser extent the ferromagnesian minerals (biotite and amphiboles). The alteration of plagioclases generates three types of alteration (Fig. 54):

1) An albitization of the primary feldspars, apparently with conservation of the volume, directly linked to the proximity with the fracture, and accompanied by the staining of the neogenic albite by iron oxides. Some Ca-bearing silicates may be associated to this albitization facies. Nevertheless, they are rather connected to veins and not directly included in the albitized plagioclases, at least in the most albitized facies along the fractures.
2) The saussuritization of the primary plagioclases with the development of Ca-bearing silicates (in particular prehnite) is typical for the light/unstained facies situated further away from the fractures. Prehnite forms euhedral crystals within the altered primary plagioclases and in micro-fractures as well. The development of albite goes along with the saussuritization of the primary plagioclases. Here, albite forms a frame of crystals of common orientation, but with a substantial porosity that makes the crystal framework discontinuous.
3) The invasive development of sericite (sericitization) sometimes affects the primary plagioclases within the light/unstained facies, without development of Ca-bearing silicates. Here, the development of sericite is also associated with the formation of albite that develops as small and discontinuous crystals which nevertheless preserve the orientation of the primary plagioclases.

The alteration of the ferromagnesian minerals is connected to the plagioclase alteration. All facies show a gradual biotite chloritization in the light/unstained facies, and is

stained with pigmentary hematite in the albitized facies. Biotite chloritization seems to occur either with volume conservation or with slight decrease of the volume. The chloritization of biotite is sometimes associated with the formation of secondary minerals imbedded between the layers of the chlorite, which include quartz, K-feldspar, prehnite, iron-bearing minerals, and accessory minerals, such as titanite and apatite. The nature of the secondary minerals seems to depend on the geochemical context in which the chloritization in relation to the albitization, saussuritization, and sericitization occurred. The amphiboles are chloritized in the same context; nevertheless, they are practically non-altered in the light/unstained saussuritized facies whereas they are much more chloritized in the most albitized and hematitized facies.

These alterations cause a strong geochemical overprint to the fracture isolated blocks, which can be differentiated between the core and the boundaries of the blocks (Fig. 54). Thus, the edges of the block appear as strongly Na-enriched, considering the plagioclase albitization, and they are incidentally depleted in K, due to the biotite chloritization and partial albitization of the K-feldspars. On the other side, the light/unstained facies in the core of the block emerge as relatively enriched in K with regard to the plagioclase sericitization, but they are also characterized by a relative accumulation of Ca and Al in comparison to the albitized facies, considering the saussuritization of the plagioclases.

**Geochemical gradients** are revealed by the succession of the mineral parageneses. The different mineralogical parageneses related to the alterations described above do never exhibit a interruption or clear alteration front, but they appear rather as continuum or gradients from one to another.

There are overlapping parageneses, in particular with respect of the small sericite in the core of the albitized/hematitized plagioclases that clearly illustrate a first stage of alteration with partial sericitization, relieved and set by the alteration of the residual plagioclases, just like small prehnite crystals are observed within albitized plagioclases. However, no obvious temporal succession between these parageneses have ever been observed, i.e. the alteration of a secondary mineral by the another one. Thus, these parageneses might rather be seen as the expression of the geochemical gradients between the fluids within the fractures and the granitoïd blocks. The paragenetic successions observed here, are successions indeed, but they result from the progressive shifting of the reactional front of each paragenesis towards the inner part of the blocks, while their outer part is gradually altered, i.e. in equilibrium with the interstitial fluids.

The albitization as well as the iron oxides pigments exhibit a decreasing gradient in intensity from the walls of the fractures towards the inner part of the blocks. This gradient reflects a decrease in $Na^+$ and $O_2$ (and/or Fe) content of the interstitial fluids between the minerals and in the micro-fractures (Fig. 54). In contrast, the $K^+$ content of the interstitial fluids seems likely to decrease in the opposite way: K-bearing minerals (K-feldspar, biotites) are altered at the fractures walls whereas sericite develops within the light/unstained facies away from the fractures walls.

Therefore, it might be appropriate to talk here about sequence or metasomatic zonation rather than a typical paragenesis and in particular not about successive or different alterations processes.

## 7.2 COUPLED DISSOLUTION-PRECIPITATION REACTIONS

First of all, the high instability of the anorthite and plagioclase anorthitic component in presence of water (Matthews and Goldsmith, 1984) may be considered increasing dissolution rates of plagioclase with respect to their anorthite content (Stillings and Brandtley, 1995). Plagioclase destabilization appears most probably as the alteration process that triggers the resulting chain reactions.

**Plagioclase albitization** occurs at constant volume along the fractures walls, where fluids circulate unhampered, and results in the formation of albite with a very low porosity. This indicates, that the albitization reaction takes place with Na supply, probably additional silica, and Ca and Al release. In the vicinity of the fractures, the released cations may be leached and evacuated by the fluids. As the reaction goes on, fluid penetrating the rock by diffusion and convection depletes in Na, and the albitization of plagioclases becomes gradually reduced or even stops, when the Na-content of the fluids is no longer sufficient to feed the albitization process.

**The biotites** are also destabilized in the vicinity of the fractures, probably through a double effect of their K-interlayer leaching and of their $Fe^{2+}$ octahedral-layer oxidation (Fig. 54). This chloritization of the biotite does not only correspond to a simple cation exchange, but rather to a whole recrystallization of the phyllitic structure. Here $Si(OH)_4$ leaching takes place, since the cation/Si ratio is equal to ~1 within the biotite, whereas it is between 1 and 1,5 within the chlorite. The released silica may be consumed by the crystallization of neogenic K-feldspars or quartz, and may probably nourish the albitization of the plagioclases as previously mentioned. If the chloritization occurs without additional cation supply, the volume loss is about 30%, whereas if additional cations (such as the Al released by plagioclases albitization are available to be incorporated in the chlorite crystals, the volume loss may be less substantial than in the previous reaction (Ferry, 1979)

It also has to be noticed that the nature of the chlorite and their chemical composition depend on the original composition of the biotite, the fluid composition and in particular on the oxidizing fugacity of the fluids, since the Fe valence impacts considerably on the composition of the chlorites. While the chloritization of biotite progresses towards the inner part of the blocks, the composition of the fluid changes gradually as well. Consequently the composition of the chlorite evolves too. Thus, the characterization of different chlorite compositions does not necessarily imply successive chloritization phases, but it may be simply the result of changes in the fluid composition during the chloritization process.

**Amphiboles** appear as **less** "sensitive" to chloritization than the biotites, in comparison their chloritization appears delayed. This is probably because their structure does not contain any unstable or mobile cation, such as K in the biotites. The destabilization of the amphiboles occurs most likely as a result of the Mg leaching and perhaps $Fe^{2+}$ oxidation. It can be considered, that amphiboles and in particular hornblendes (which are calcic) are relatively protected against the chloritization because of the Ca liberated by the plagioclase albitization. It is probably for that reason that the chloritization of amphiboles occurs only in the quite alteration-advanced facies, that are albitized, and therefore provide no longer Ca to the fluids.

**Hematitization** is systematically associated to the albitization. Apart from the oxidized pyrite and magnetite (that has been detected by SEM analyses, see Chapter 6), hematite appears almost exclusively scattered within the matrix of the mineral; either as tiny pigments within the neogenic albite, or as better crystallized occurrences (granules, lamina or laths) associated to the ferromagnesian minerals. The very few hematite occurrences within

the micro-fractures result entirely from their proximity with the ferromagnesian minerals, in particular from the chloritized biotites. Hematite within the fractures is also directly linked to chlorite coatings in the shear-zones. These fractures do not crystallize as hematite deposits (colloform) as it appears in the case of direct hematite crystallization from fluids. Thus, hematite occurs always either as directly related to the alteration of the primary ferromagnesian minerals, or as connected to the oxidation of sulphur and/or primary oxides. Such a genetic relationship between hematite and chlorite has also been shown in the albitized and saussuritized granitic rocks in the Paleoproterozoic bedrocks of the Forsmark in central Sweden, where the Fe isotope composition likely reflects the input of partially dissolved chlorite (Dideriksen et al., 2007). The iron never appears as directly related to the fluids within the fractures, which are thus unlikely to be iron-bearing fluids.

**Sericite** development depends on the availability of Al and Si, and particularly of K. Biotite chloritization appears as the quasi-exclusive source of K in the system, since K-feldspar albitization remains marginal and bounded to the fractures walls. Besides, K-release by the chloritization in the early stage of the alteration and in the vicinity of the microfractures is widely evacuated by convective flow. It is present further away from the fractures, where the convective flow decreases and the importance of diffusion increases with respect to the transport of the chemical elements. Hence, the K-content of the interstitial fluids may principally increase in the inner part of the system. Therefore, the sericitization develops dominantly in the light/unstained and moderately altered facies, especially since the “internal” zones are the zone where the Na-content decreases in the interstitial fluids due the increasing distance from the fractures that are the major source of Na. Yet, the albitization of the plagioclases is dependent of the Na availability, and thus more significantly of K/Na ratio. When the K/Na ratio increases, the albitization is limited and K competes with Na to form K-bearing silicates (mainly K-feldspars and illite-mica) in combination with Si and Al (Ben Baccar et al., 1993; Perez and Boles, 2005). This explains why the albitized facies show sericite only in small amount in the core of the primary plagioclases.

If all previous described alteration minerals form mainly by epigenic processes, i.e. direct and by “isovolumic” replacement of the primary minerals, **prehnite** stands out in various aspects: prehnite was observed as euhedral crystals within various minerals, within the veins and microfractures. This variability of prehnite, in particular with respect to its precipitation within the microfractures, witnesses the mobility of its chemical components. Si is mobile, but usual for Ca, and rather unusual for Al, that is known as fairly mobile in a medium close to neutral pH, except in presence of complexing agents (Castet et al., 1993; Farmer and Lumsdon, 1994 ; Oelkers et al., 1994).

In any case, and in the present case, Al appears indeed as fairly mobile. Nevertheless, it seems difficult to assess whether Al was evacuated from the fractures by the fluid circulation. Calcite is relatively uncommon in the studied facies, suggesting that the fluids responsible of the above described alterations were probably $CO_2$-poor fluids (Ferry, 1978).

## 7.3 FLUID / ROCK INTERACTION

The nature and the spatial distribution of the fractures related alteration observed in the granitoïd rocks suggest one single alteration phase, with coupled-reactions that occur successively and form a spatial sequence that results in the mineralogical parageneses zonation with regard to the fracture geometry. The different reaction zones are interconnected by many ion exchanges. Some reactions release ions while others consume them. These coupled reactions make it possible to trace back the geochemical characteristics of the interstitial fluids that trigger the reactions and the evolution of the alteration from the fractures towards the core of the blocks.

The geochemical exchanges between the reactional zones are determined by the transport of the ions in the fluids. The exchanges in the open cracks and in the micro-fractures (that are connected to the major fractures) take place by the circulation of the transport fluids, i.e. by convection. The circulations may be relatively rapid in the major fractures; nevertheless their speed may decrease exponentially with the fracture dimension, their connectivity and tortuosity. The circulation tends to diminish and finally disappear in the "bottom of the bag", like in fractures on the periphery of the connected network. Away from the open cracks, the fluids quantity is reduced and mainly limited to "thin films" at the boundaries of the grains. Within these thin films, the circulation is minimal, and here diffusion prevails over convection. Thus, the displacement of material is extremely reduced and slow and is not controlled by the hydraulic gradient, but rather by the geochemical gradient between the enriched and depleted zones of any chemical element.

Therefore, the alteration reactions are dominantly determined by the presence of voids. Fractures and grain boundaries allow rapid fluid movements through the rock and the development of micro-porosities on the alteration front and in the neogenic mineralogical phases which allows fluids to penetrate further into the successively replaced mineral. However, in this context, with extremely reduced fluid movements, the oversaturation of a fluid with respect to a mineralogical phase is probably limited to the mineral-fluid interface (Putnis et *al*., 2005), and the thin film of fluid at the interface may have a very different composition from that of the flowing fluid, which may remain under-saturated with regard to the mineral precipitating at the interface.

In that context, the coupled-reactions described above are not part of a global geochemical equilibrium related to the fluids in the fractures, but they are rather part of a dynamic geochemical equilibrium which is spatially linked. Differences in the chemical potential exist between the rock matrix and the adjacent fluid. Exchanges tend to equalize the chemical potential between the two media, but the development of the alteration simultaneously maintains the chemical potential difference. The system is only partially open. A geochemical zoning develops and progresses in a chromatographic way, This is characteristic of a metasomatic system (korzhinskii and Oestreich, 1965 ; Brinhall and Dietrich, 1987 ; Guy, 1993). The reactions do not result from a global thermodynamic balance, but from balances that keep occurring spatially, with the formation of sharp fronts. The balances are not determined by the kinetics of the mineralogical reactions, but rather by the kinetics of the ion diffusion in the rock. Thus, thermodynamic reactions which originally seemed incompatible with a global context may occur. Temperature does not appear as a limiting factor, but it allows speeding up the reactions by acceleration of the diffusion. The reaction rate is affected through the diffusion rate. The reactions are extremely slow, but not impossible from a thermodynamical point of view.

Thus, within a system or a rock encircled by fractures, a zoning of the ion transport that determines the geochemical zoning is primary established (Fig. 54). Along the fracture

walls, the convection exchanges prevail and are relatively fast; the mineralogical paragenesis formed is in equilibrium with the fluid thereby reveals the geochemical characteristics of the fluid. Further away from the fractures walls, the exchanges are slow and driven by diffusion and they; the mineralogical parageneses are controlled by local balances that are far from the balance with the fluid. The coupled reactions in the vicinity of the fractures are witnesses of the nature of the fluid circulating.

In the present case, plagioclase albitization and hematite precipitation are symptomatic for the geochemistry of the fluid. These are considered as Na-enriched and relatively K-depleted fluids (Saigal et al., 1988 ; Aagaard et al., 1990 ; Ben Baccar et al., 1993; Perez and Boles, 2005) and thus responsible for the albite formation and the albitization of K-feldspar crosscut by fractures. The fluids are also considered as enriched in oxygen, as witnesses by the formation of hematite. They seem to have a relatively low $CO_2$ fugacity since only little calcite is formed, in spite of the abundance of Ca released during plagioclases albitization. They are also relatively under-saturated in $SiO_2$, Al and Mg since chlorite coating in the fractures is sometimes entirely altered into hematite. At the output of the system, fluids are depleted in Na and $O_2$ that were consumed by the albite formation and the oxidation of the ferromagnesian iron minerals. They are enriched in K, since at the early stage of the alteration, no or just a little sericite is formed within the plagioclases during the chloritization of biotite. The balance is more difficult to establish for $SiO_2$, Al and Ca. $SiO_2$ because the estimation contains uncertainties, but significant amounts of silica are liberated during the biotites chloritization. Thereby it appears likely that it is exported outside of the system, at least in the granodioritic facies that are richer in biotite. Besides, quartz and chalcedony have been locally recognized in some cracks. It may be considered that Al and Ca are balanced between the altered plagioclases and the formation of prehnite and calcite, even if a quantified balance is not available. In any case, such a balance is difficult to establish due to the mineral dispersion and heterogeneity throughout the alteration aureoles. Nevertheless, it is obvious that the Ca is easily exported from the cortical reactional zones in the early stage of the alteration. Al mobility is unlikely to happen here, because the major fractures never show any alumino-silicate deposits.

Correspondinly, the granitic rocks in the Paleoproterozoic bedrock in Forsmark central Sweden, which display a comparable metasomatic paragenesis as those studied here (with sassuritisation, albitisation and chloritisation) show that the red-stained rock adjacent to the fractures underwent only a very limited redistribution of the elements on the whole rock scale, that is mainly manifested by an enrichment of $Na_2O$, a constant Fetot, and a depletion of CaO, FeO, and $SiO_2$ (Drake et al., 2008; Sandström et al., 2010).

In the end, it appears clearly that the responsible fluids of the alterations are oxidized Na-rich fluids, relatively depleted in K in comparison to Na.

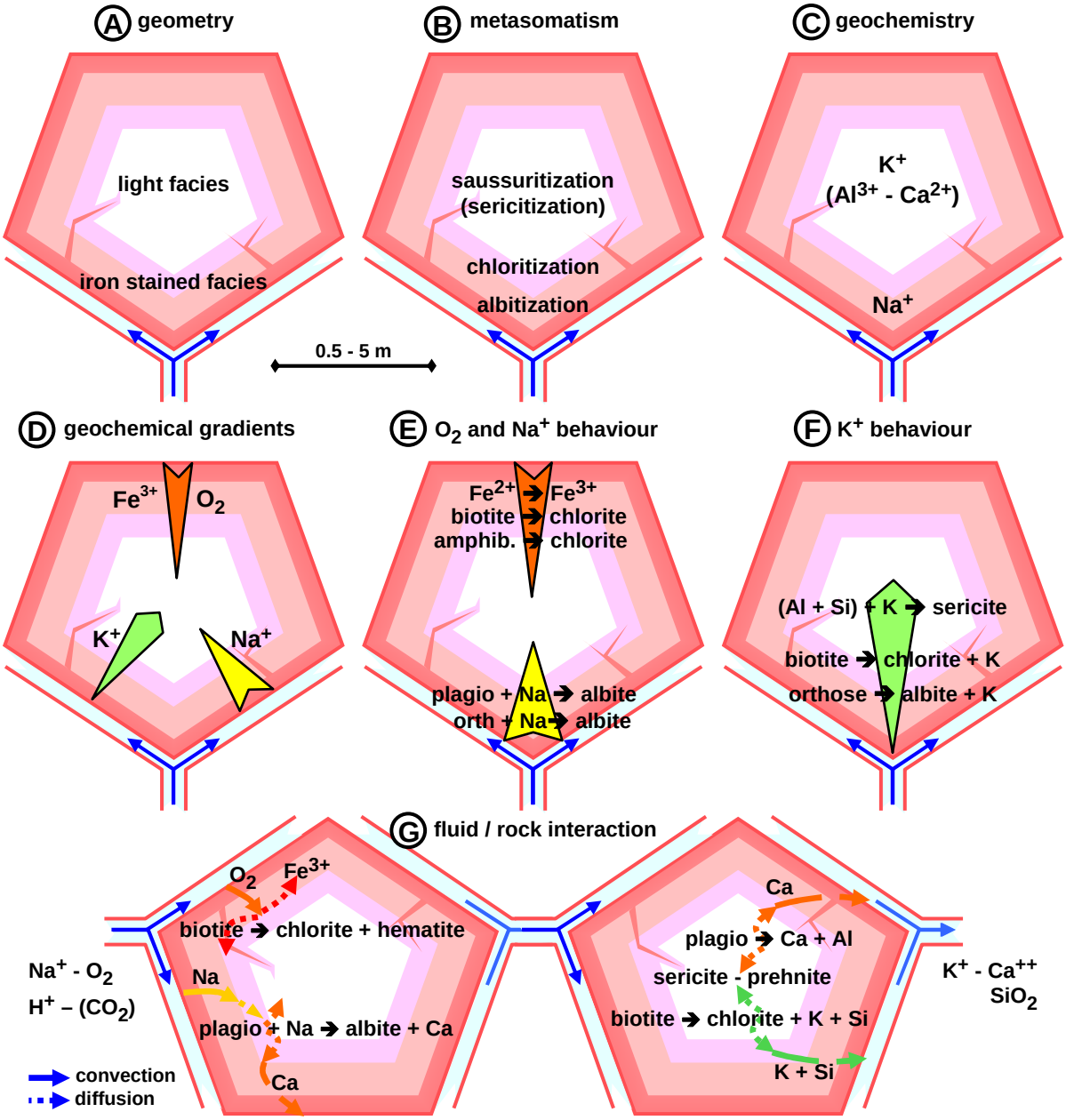


**Figure 54 - Schematic interpretative sketch of the various petrographic parageneses related with the reddening and the albitization of the granitoïd rocks in the Sudetes at the outcrop scale. (A) Geometrical arrangement of the facies: The reddened facies are localized on the fracture walls whereas the light/unstained facies remain only in the core of the blocks. (B) Distribution of the metasomatic alterations: Albitization prevails along the reddened fractures whereas saussuritization and sericitization dominates in the light/unstained core of the blocks. Chloritization occurs in both zones but is more intense near the fracture walls. (C) Geochemistry: $Na^+$ was available along the fractures whereas $K^+$, $Al^{3+}$, and $Ca^{2+}$ were rather present in the core of the blocks. (D) Geochemical gradients: $Na^+$, $Fe^{3+}$ and $O_2$ decrease from the reddened fracture walls towards the unstained core of the blocks whereas $K^+$ content declines in the inversely. (E) $O_2$ and $Na^+$ behaviour: albitization intensity decreases accordingly to the $Na^+$ content towards the core of the blocks, similarly chloritization/hematitization declines towards the unstained core of the blocks in relation to the $O_2$ content. (F) $K^+$ behaviour: Sericitization may decrease towards the fracture walls in agreement with $K^+$ content. (G) Fluid rock interaction: The alterations result probably from the interaction between the rocks and $Na/O_2$-rich fluids within the fractures, and migrating towards the unstained core of the blocks. Fluid/rock exchanges are convective close to the fracture walls, and become progressively diffusive as going towards the core of the blocks.**

***Figure 54 – Schéma d'interprétation à l'échelle de l'affleurement des paragenèses pétrographiques liées au rougiement et à l'albitisation des granitoïdes dans les Sudètes. (A) Géométrie des faciès d'altération : les facies rouges se développent le long des fractures tandis que les facies clairs subsistent uniquement cœur des blocs. (B) Distribution des altérations métasomatiques : l'albitisation prévaut au voisinage des plans de fracture rouge tandis que la saussuritisation et la séricitisation dominent au cœur des blocs. La chloritisation apparaît dans les deux zones mais est plus complète intense à proximité des fractures. (C) Géochimie : $Na^+$ était plus disponible au niveau des fractures rouges, tandis que les activités de $K^+$, $Al^{3+}$, et $Ca^{2+}$ étaient plus fortes au cœur des blocs. (D) Gradient géochimique : la teneur en $Na^+$ et $Fe^{2+}/O_2$ décroît des fractures rouges vers le cœur des blocs alors que la teneur en $K^+$ décroît en sens inverse. (E) Comportement de $O_2$ et $Na^+$ : l'intensité de l'albitisation décroît conformément à la teneur en $Na^+$ vers le cœur des blocs, de même que l'intensité de la chloritisation et de l'hématisation en adéquation avec la teneur en $O_2$. (F) Comportement de $K^+$ : la séricitisation décroît vers le bord des fractures suivant la teneur en $K^+$. (G) Interaction fluide-roche : les altérations résultent des interactions entre la roche et des fluides riches en $Na^+$ et $O_2$ circulant dans les fractures. Les échanges fluides-roches sont convectifs près des fractures et deviennent progressivement diffusifs en allant vers le cœur des blocs.***

## 7.4 IRON OXIDE BEHAVIOUR

. The iron oxides present in the studied facies are an excellent tool to obtain a datingof the alteration event by paleomagnetism, due to the fact that the iron oxides necessarily must have recorded the paleomagnetic field during their (neo)formation. Therefore special attention must be paid to the fact that the iron oxides are closely linked to the metasomatic processes, in particular to the albitization of the plagioclases, and that they do not originate from any other post-albitization process. But this interpretation of hematite related to the albitization depends itself on the interpretation made on the mineralogical sequences:

- Either it is assumed that the mineralogical sequence corresponds to the above described metasomatic sequence, in which the different parageneses that are in geochemical equilibrium and succeed spatially according to the progression of the alteration front. In this case they correspond to one single geodynamical event.
- Or it is considered that each paragenesis of this mineral sequence corresponds to one specific equilibrium (in particular pressure-temperature wise) and in this case the different parageneses succeed (follow) one another temporally and are therefore related to different geodynamical events.

These two points of view have been discussed in literature and different arguments were brought forward during this discussion:

Boone (1969) considered that the assemblage of red albite and chloritized biotite succeed gradually towards grey facies that contain oligoclase and less altered biotite. Jenkins et *al*. (1992) proposed that the sericitization and saussuritization of the chloritized Connemara granites during a single fluid infiltration event and that the recorded $\delta^{18}O$ isotope variations of this fluid (hydrothermal resetting of the oxygen isotopes) result from the low fluid-rock interaction conditions.

In contrary, the studies in the framework of the planned radioactive waste deposit in the proterozoïc basement Forsmark in Sweden have proclaimed a sequential interpretation of the mineralogic paragenesis, based on the structural analyses and radiochronologic datings (Drake et *al*., 2009. Sandström and Tullborg, 2009). According to these authors, the crystalline rocks of this sector would have been altered by successive fluid infiltrations that caused the indenting mineralogical paragenesis during a time period of about 1000 Ma. In this formation Plümper and Putnis (2009) recognize that the albitization and sericitization are cogenetic and results from coupled reactions. But they argue that a sequence of infiltrations is needed to explain the feldspathization of the sericites and the precipitation of the concomitant

hematite. The introduction of oxygen into the system of alteration is generally admitted (Boone, 1969 ; Plümper and Putnis, 2009), but Sandström et *al*. (2010) considered that the red color of the alteration is due to the diffusion of the present hematite instead of a significant oxygen content in the rock.

Thus, all above mentioned aspects and hypotheses might be considered in "playing the devil's advocate" to confirm the emplacement of the iron oxides with regard to the alteration in the studied granitoïd rocks.

### *7.4.1 Origin of the oxidizing fluids*

In general, post-magmatic alterations are explained by a hydrothermal model which uses large convective circuits to bring the superficial fluids in contact with the warm rock complexes, in particular granitic intrusions in which the alterations then take place (Taylor, 1977 ; Fyfe et al., 1978 ; Jenkin et al., 1992 ; Putnis et al., 2007 ; Drake et al., 2008). The magmatic intrusions warm the fluids up and the subsequent loss in density causes the upwelling of these fluids, maintaining the circulation between the surface and the depth. Fluids from deeper origin may be also mixed into this circulation model.

The superficial origin of the fluids, or at least the participation of meteoric water has been evoked by isotope studies on oxygen and hydrogen on the alteration minerals (Simon and Hoefs, 1987 ; Sun and Eadington, 1987 ; Jenkin et al., 1992 ; Boyce et al., 2003). Nevertheless, these models oblige the superficial oxygen-rich fluids to descend very deep (more than 10 km) before they interact with the rock matrix. During their long descent these fluids traverse sedimentary basins and metamorphic terrains, that all have the potential to reduce the fluids and consume the transported dissolved oxygen and therefore these fluids are very likely to be under-saturated in oxygen, when reaching the deep crystalline complexes.

This point is certainly one of the weaknesses of these models and has not yet been sufficiently discussed by the petrologists or geochemists who work on these questions. It was admitted though, because the alterating fluids are proclaimed oxidizing and the alteration is supposed to take place in deep. Nevertheless, this question was addressed recently and the model has shown that the presence of reactive minerals in multiple fracture zones leads to the rapid depletion of the oxygen fugacity of the circulating fluids (MacQuarrie et al. 2010).

### *7.4.2 Distribution of the (iron) oxides*

At the mineral scale in polished sections**,** hematite is never associated with cracks or joints of the grains, as it would be imaginable if the iron was introduced into the rock by solutions. In fact, the hematite is present in fine diffuse pigments, homogenously distributed within the albite crystals that are linked to the albitization process close to the fractures. These secondary albites are relatively nonporous and their sparse vacuoles and defaults seem light (free from any iron oxygen filling) in high resolution optical microscopy. There is no accumulation of iron oxides in the plagioclase at the albitization front, whereas at the dissolution-recrystallization front a slightly higher abundance of vacuoles were observed. The pigmentary hematite is directly included in the albite crystals without any observable associated pore space. In contrary, the most porous albite crystals are those that can be linked to the saussuritization and precipitation to prehnite and sericite, far from the fracture zones towards the core of the blocks. Here, no iron oxides have been identified. Thus, the hematite is cogenetic with the albitization and the iron is likely to originate from an internal redistribution linked to the chloritization of the biotites, and therefore there is no introduction of iron independent from the albitization.

At the outcrop scale the red colorization is related to the fractures and the iron oxides are systematically associated to the albitization. Additionally, the reddened and albitized fractures are never cut by any fractures that do not show this alteration phenomenon. The absence of non-albitized fractures indicates that these alteration is relatively recent at least compared to the major tectonic history of the granite and certainly posterior to its exhumation.

**The distribution of the magnetic carriers** resulting from the thermal demagnetization experiments shows a distinct spatial pattern according to the reddened granitoïd facies and their structural dispositions at the outcrops (Fig. 55). The intense and pervasively reddened facies, such as at the Laski Village outcrop, mainly contain only hematite, whereas the weakly reddened facies, that show only slightly pinkish staining along the fractures planes, such as at Chwalisław quarry, exhibits either a mixed hematite-maghemite or solely maghemite magneto-mineralogy (Szklarska Poręba quarry). The outcrops with reddening dominant along the fracture walls show a more contrasted distribution. The most intensively reddened fracture walls contain hematite or hematite-maghemite mixture, whereas the less intensively reddened fracture walls show predominantly maghemite. Residual magnetite sometimes occurs in the less altered facies that remained grayish in the core of the blocks surrounded by fractures that don't show any reddening. This residual magnetite appears clearly restricted to the unaltered facies and therefore appears as the primary magnetic carrier, whereas hematite characterizes the most altered facies and maghemite appears as developing in the early stages of the reddening alteration.

Maghemite occurs in the less altered granitoïd facies, such as the greenish facies of the microgranite in Szklarska Poręba Quarry and the less altered blocks in the central part of the Laski Quarry section. Maghemite is also more abundant in the basic granitoïd facies enriched in mafic minerals, such as in the Chwalisław area. This paragenesis occurs in the less altered granitoïds, that are not strained with hematite pigments and with remaining unaltered biotite.

Maghemite is metastable with respect to hematite (Wayshunas, 1991; Majzlan et al., 2003). Additionally it is generally admitted that slow and incomplete oxidation of magnetite favours the topotactic maghemite formation, whereas faster magnetite oxidation, under highly oxidating conditions, will result in hematite formation (Steinthorsson and Helgason, 1992; Bowles et al. 2011). The maghemite-hematite transition during oxidation may be attributed to changes in the alteration environment during magnetite oxidizing. In this case the alteration starts with the formation of maghemite under low oxidizing conditions in the unaltered granitoïd rocks, and subsequently continues with the formation of hematite under stronger oxidizing conditions, when ferrous silicates (chlorite and amphibole) are being oxidized. Thus, the occurrence of maghemite and hematite suggests that the oxidizing conditions changed during the granite alteration and the spatial distribution of hematite and maghemite provides a tool to estimate the gradient of these oxidation conditions during the alteration of the granitoïd rocks in the Sudetes. Therefore it may be useful to reconstitute alteration environments and their distribution consolidates the idea that red albitized facies and light saussuritized/sericitized facies reflect gradational changes of a single alteration event.

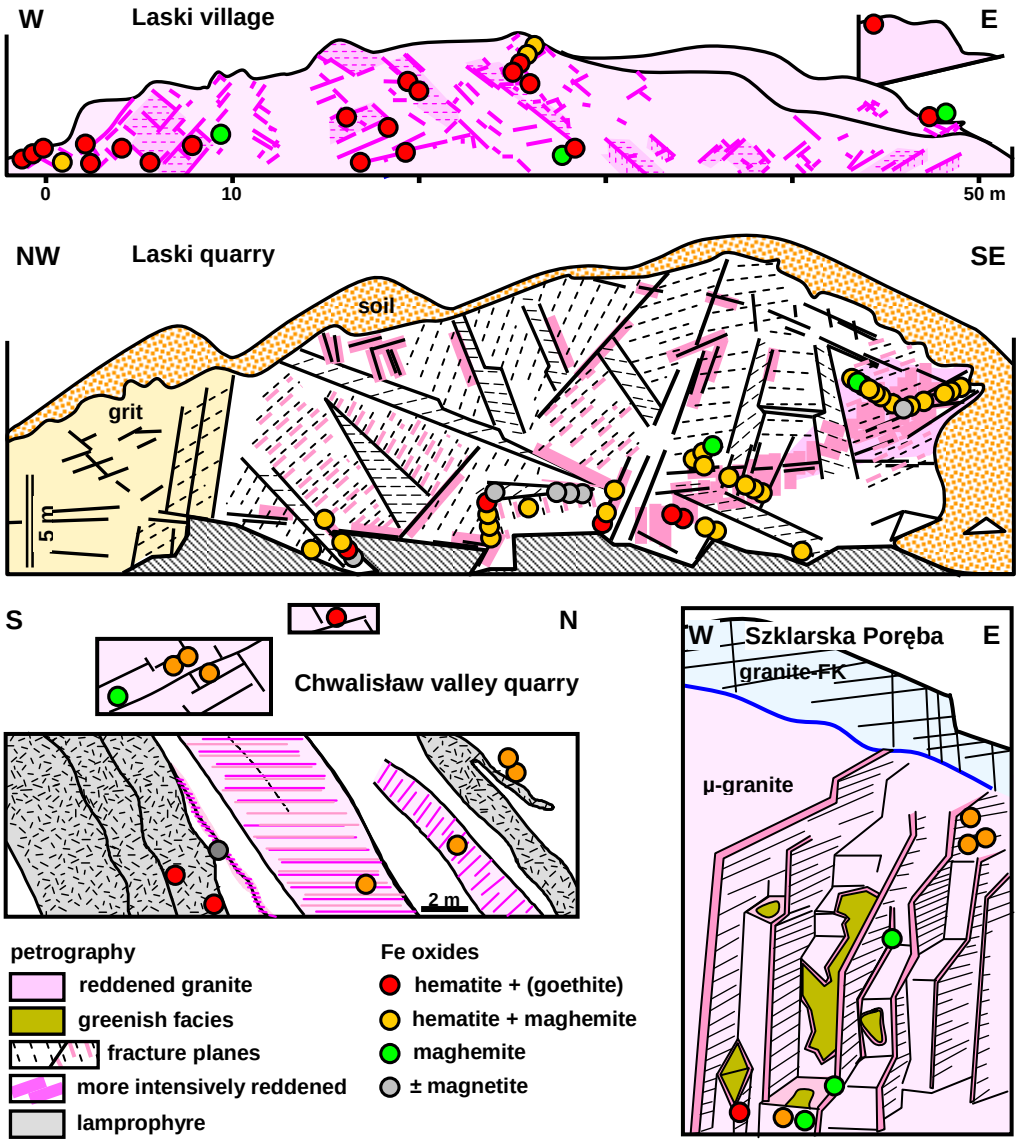


**Figure 55 – Iron oxides distribution throughout the studied sites in the Sudetes.**

***Figure 55- Distribution des oxydes à travers les sites étudiés dans les Sudètes.***

### *7.4.3 Spatial discrepancy between silicate and iron oxide distribution*

From a geochemical point of view there is no contradiction in the presence of a spatial discrepancy between the alteration zones of the silicate minerals and the distribution of the iron oxides. They don't have the same physico-chemical properties that constrain the reactions. The pH is a key-factor in the alteration and crystallisation of the silicates, whereas it is the Eh and the oxygen fugacity which forces the oxidation state of the iron oxides. Theses two parameter may vary in an independent way from each other. Nevertheless, iron oxide minerals precipitation is also facilitated by any pH elevation. Thus, local lowering of the $H^+$ activity at the sites of feldspar alteration will rather favour the localized precipitation of hematite as inclusions within the feldspar crystals (Boone, 1969). This explains even the local distribution of pigmentary hematite inclusions in the albite during the albitization of both, plagioclases and K-feldspar. On the other hand, the intensity of the reddening, or the abundance of the hematite pigments, is related to the oxygen fugacity and therefore is likely to decrease away from the fractures. From the geochemical point of view, the hematite distribution is consistent with the alteration sequence of the silicate minerals and thus hematite appears as part of the paragenesis.

# *RESUME CHAPITRE 8*

# *DATATION ET IMPLICATIONS STRUCTURALES*

## *DATATION PALEOMAGNETIQUE DES SITES ETUDIES*

*Des carottes orientées ont été prélevées à Laski carrière = LSA, Laski village = LSB et LSC, Chwalisław = CHW, Szklarska Poręba Huta (SPH) (Fig. 56). Les directions moyennes obtenues par démagnétisation thermique apparaissent soit typiques de l'hématite, ou de la maghémite, ou des deux à la fois. Il a même été possible d'extraire deux directions moyennes à partir d'un seul échantillon. Les directions obtenues, transformées en paléo-pôles et projetées sur l'APWP, indiquent des âges entre 235-211 Ma (Trias moyen à supérieur) à l'exception de LSA qui montre plutôt des âges du Permien supérieur (260 Ma) (Fig. 57). Dans le détail, les âges les plus jeunes correspondent à des échantillons à hématite seule (LSB et LSC), les âges triasiques plus anciens à des échantillons présentant soit une paragenèse hématite-maghémite ou à maghémite seule (CHW et SPH). Les âges triasiques les plus vieux ont été spécifiquement détectés dans des échantillons de LSA et LSC présentant une paragenèse magnétique mélangée (hématite et maghémite). Les âges Permiens sont donnés par des échantillons de LSA à maghémite avec de la magnétite résiduelle.*

## *AUTRES ESTIMATIONS D'AGE*

*Des datations radiochronologiques avaient donné des âges entre 298-256 Ma pour la mise en place des grabnitoîdes KZS (Depiuch, 1972). Mais ces âges se sont avérés plus jeunes que l'intrusion de KZS comme le suggère de nouvelles datations radiochronologiques (Bachlinski and Halas, 2000 ; Mikulski et al., 2013). De ce fait ces âges jeunes correspondraient à une altération de ces granitoïdes (Mikulski et al., 2013).*

*D'autres datations paléomagnétiques qui n'avaient pas pour but de dater les faciès rouges avaient déjà montré des rajeunissements permo-triasiques (Edel et al., 1997). Ces datations sont d'autant plus évocateurs qu'ils ont été obtenus non seulement sur les granitoïdes de la carrière de Chwalisław, mais aussi sur les amphibolites près de l'intrusion de KZS et dans les dolérites de Izera près de Szklarska Poręba. Les porteurs magnétiques triasiques sont l'hématite et la maghémite comme c'est le cas dans notre étude.*

*La récurrence des âges triasiques avec diverses techniques de datations dans les massifs de KZS et dans la carrière de SP apparaît systématique et montre la cohérence des résultats paléomagnétiques des faciès albitisés/oxydés dans cette étude avec d'autres estimations d'âges.*

## *LIAISON AVEC LA PALEOSURFACE TRIASIQUE*

*Comme il n'est pas connu d'événement géodynamique triasique (tectonique ou magmatique) dans la région des Sudètes, les albitisations rouges des massifs de KZS et de SP sont nécessairement liées à la paléosurface triasique. Ainsi, la géométrie de la paléosurface pourrait être reconstruite en corrélant les sites albitisés. Les faciès les plus rouges seraient proches de la surface tandis que les les plus clairs se situeraient plus en profondeur.*

*La cartographie **des faciès rouges** du massif de Kłodzko Złoty-Stok (KZS) a été menée sur une superficie d'environ 140 km$^2$. Elle a consisté à observer et répertorier les roches en fonction de leurs éventuels pigmentations rouges, et à reporter ces données sur un fond de carte géologique du massif de KZS (Fig. 58).*

*Les affleurements majeurs correspondent aux coupes étudiées et à toutes les autres coupes disponibles, parmis lesquelles celles de Makolno et Laskowna sont les plus importantes. Les coupes ont été cataloguées selon leur degré de rougiement : pervasif, le long des fractures, en taches dispersées, et non affecté (gris). L'extension des faciès a été faite en*

*prenant en compte les affleurements plus restreints et les blocs et débris contenus dans la couverture superficielle. La cartographie a été réalisée selon une grille plus ou moins régulière définie à partir des routes principales*

*Au préalble il faut mentionner que les faciès hématisés/albitisés sont surtout bien exprimés, et donc repérables et cartographiables dans les faciès cristallins grenus. Il est beaucoup plus difficile de reconnaître ces altération dans les faciès schisteux et pellitiques, o^seul une étude minéralogique/pétrographique de chaque échantillon pertmettrait éventuellment d'étendre la carographie ,à ces faciès. Il faut trenir compte de cela dans l'interprétation de la cartographie. Pour les faciès cristallins grenus la cartographie montre que le rougiement est indépendant de la nature des roches. Il est majoritairement présent dans les granitoïdes, cependant certains d'entre eux restent clairs.*

*La* ***distribution spatiale*** *des faciès hématisés/albitisés permet de distinguer deux domaines dans le massif de KZS : (1) des granitoïdes albitisés et rouges dans le nord et (2) dse granitoïdes non albitisés et gris dans le Sud (Fig. 58 et 61).*

*La limite entre granitoïdes albitisés/rouges et granitoïdes non albitisés/gris correspond à une faille proposée par Cymerman (2004) sur une carte structurale récente de KZS (Fig. 58). Cette faille a mis en contact des granitoïdes non albitisés/gris avec des granitoïdes albitisés/rouges. L'âge de la faille pourrait être contraint si l'âge de l'albitisation/rouge est connu.*

***IMPLICATIONS STRUCTURALES***

*La catographie du massif de KZS montre que des granitoïdes non albitisés/gris sont contigus avec des granitoïdes albitisés/rouges. Cette juxtaposition des faciès albitisés et non albitisés souligne l'existence d'une discontinuité dans la géométrie de la paléosurface triasique et qui correspond à une faille proposée par Cymerman (2004) (Fig. 62). Cette discontinuité dans la paléosurface triasique résulte vraisemblablement du mouvement inverse du bloc sud le long de cette faille et de l'érosion subséquente de ce bloc en surrection (Fig. 62). L'albitisation triasique permet d'établir que la faille proposée par Cymerman (2004) est post-triasique de même que l'érosion induite par la surrection du bloc.*

# CHAPTER 8

# 8 DATING AND STRUCTURAL IMPLICATIONS

## 8.1 PALEOMAGNETIC DATING OF THE STUDIED SITES

As already described in the methods Chapter 3.3, a systematic paleomagnetic sampling was performed on the altered (reddened) facies of five principal outcrops, four of them situated in the Kłodzko Złoty-Stok Massif (Laski Quarry = LSA, Laski Village = LSB and LSC, Chwalisław = CHW) and one in Szklarska Poręba Huta (SPH). The paleomagnetic samples were drilled in the vicinity of the principal fractures (Fig. 56).

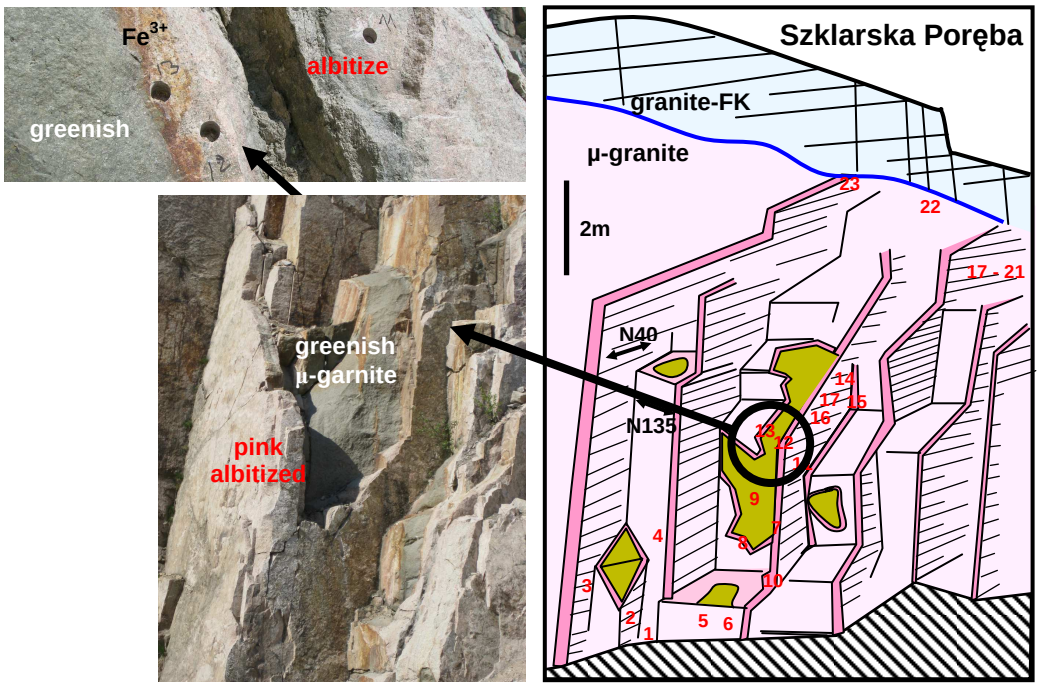


**Figure 56 - Paleomagnetic drill core sampling at the outcrop of Szklarska Poręba Huta. The samples were taken within the different alteration facies that were identified during field work (light, pink and red facies). Their position was marked with respect to the principle fracture zones.**

***Figure 56 – Échantillonnage de carottes paléomagnétiques dans la carrière de Szklarska Poręba. Les échantillons ont été forés dans les différents faciès d'altération identifiés lors de travaux de terrain (faciès clair, rose et rouge). Leurs positions ont été répertoriées selon les zones de fractures principales.***

The thermal demagnetization experiments of the oriented drill core samples permit to separate the different magnetic carriers of the paleomagnetic signal within each analyzed sample. According to the respective temperature intervals at which a specific decay in the magnetic intensity curves was observed, one or several magnetic carriers were identified. In principle, three different types of magnetic assemblages could be observed within the analyzed samples:

a) hematite dominated
b) hematite and maghemite
c) maghemite dominated

In addition to this, the maghemite bearing samples sometimes show a residual presence of presumably primary magnetite that was only observed in samples rather far from fraction zones and in the less altered (light) facies.

The stepwise thermal demagnetization additionally allows obtaining the vector direction recorded by the magnetic minerals. These directions were considered as characteristic for either the maghemite or hematite component (or both), if their inclination and declination values are stable corresponding to the respective considered temperature intervals. Therefore it is possible to sometimes extract two slightly different directional intervals from one single sample, if the two main carriers diverge in their mean direction.

The samples were analysed per outcrop and the average directional information was calculated for each site (for further détails on the paleomagnetic datings please see Franke et al., 2013). In case of LSA, LSC, and CHW the results were "sub-grouped" according to their directional information. At CHW the three distinct mean directions are anyway relatively close (Fig. 57).

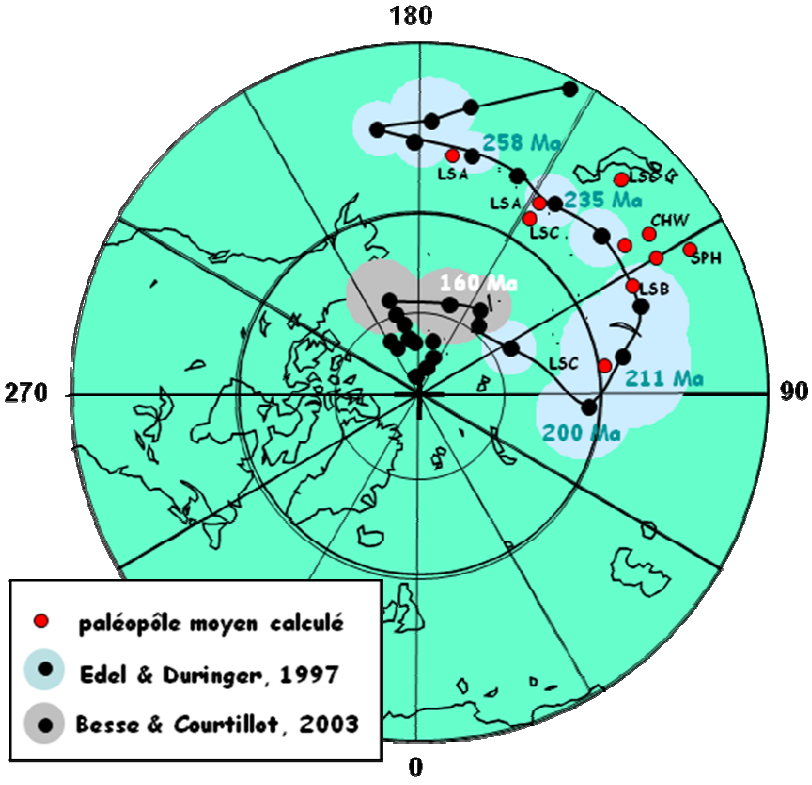


**Figure 57 – Stereographic projection of the paleomagnetic results of the site wise calculated average paleopoles. The obtained paleopoles are projected on the APWP for Eurasia after the combined curve Edel and Duringer, (1997) and Besse and Courtillot (2003); results from Franke et al. (2013).**

***Figure 57 – Projection stéréographique des résultats paléomagnétiques des sites étudiés à partir du calcul moyen des paléopôles. Les paléopôles obtenus sont projetés sur l'APWP de l'Eurasie des courbes combinées de Edel and Duringer, (1997) and Besse and Courtillot (2003) ; résultats d'après Franke et al. (2013).***

The extracted directional information was then transformed into magnetic paleopoles (e.g. Butler, 1998) that were subsequently projected on the apparent polar wander path (APWP) curve for Eurasia (see Fig. 57). It becomes clear that despite one average pole for LSA (that correspond rather to an Upper Permian signal), all other poles plot near the APWP curve for the Middle to Upper Trias and correspond to ages between about ~235 to ~211 Ma.

It seems that, depending on the present iron oxide minerals, the paleomagnetic ages show a dispersion towards rather younger Triassic ages in the samples dominated by a single hematite component (LSB and LSC) and rather older Triassic ages in the mixed hematite-maghemite or dominant maghemite paragenesis (CHW and SPH). The oldest Triassic ages were observed for samples from LSA and LSC that have a mixed magnetic assemblage (hematite and maghemite). The average pole for LSA that corresponds to an

Upper Permian age shows a magnetic mineralogy dominated by maghemite with a residual magnetite component.

## 8.2 OTHER AGE ESTIMATIONS

Radiochronogic datings (K-Ar) were performed by Depciuch (1972) that aimed at estimating the ages of the emplacement of the Kłodzko Złoty-Stok (KZS) granitoïd intrusion. That study resulted in age estimations between 298-256 Ma, and therefore in Permo-Triassic ages. These first datings were formerly interpreted and accepted as the initial age of the KZS granitoïd emplacement, just until the occurrence of new radiochronological dating methods which showed that the data published by Depciuch (1972) was relatively too young than the actual age of the KZS intrusion, which was later stated as Carboniferous, between 330-340 Ma for the KZS Massif (Rb-Sr datings of Bachlinski and Halas, 2000; U-Pb dating of Mikulski et *al*., 2013) and about 311 Ma for the Karkonosze Massif where the Szklarska Poręba (SP) formation is located (Borkowska et *al*., 1980).

However, these rejuvenated ages have not been rejected completely; they are considered by some authors as corresponding to the age of the alteration event of the granitoïds (Mikulski et *al*., 2013). These ages may probably coincide with the age of the albitization described in this study, since they appear as the dominant alteration in the KZS Massif.

The paleomagnetic results mentioned in Chapter 9.1 show that the reddened/albitized granitoïd rocks of KZS and SP exhibit Triassic re-magnetizations, therefore younger than the age emplacement of the granitoïd bodies. These rejuvenated ages seem consistent with other paleomagnetic datings (Edel et *al*., 1997), even if those studies did not aim to determine the age of the albitization, and therefore they have tried to avoid the sampling of the obviously altered (reddened) facies. Edel et *al*. (1997) aimed at determining the primary age of the emplacement of the granitoïd bodies and at the understanding of their tectonic evolution.

In their results, the authors state among others permo-triassic (re)-magnetizations. These re-magnetizations that are obviously younger than the age of the granitoïd intrusion were obtained on granitoïd samples for the Chwalisław quarry outcrop in KZS, in the amphibolites in contact with the KZS intrusion, and in the dolerite of Izera close to the SP quarry (Edel et *al*., 1997). The identified paleomagnetic carriers of these Triassic paleopoles are hematite and maghemite, as also found in this study, while the Carboniferous paleopoles found by Edel et al. (1997) are rather recorded by (primary) magnetite.

The recurrence of the Triassic age in the area of the Kłodzko Złoty-Stok Massif and Szklarska Poręba throughout the different published dating techniques appears as systematic, when looking at the details of the sampled facies. Therefore, a consistency can be established between the results of the paleomagnetic dating of the reddened/albitized facies in this study and other age estimations previously published on facies, which were simply described as “altered”, but which were not clearly characterized as albitized.

## 8.3 LINK TO THE TRIASSIC PALEOSURFACE

As no major orogenic or magmatic event is known during the Trias and thus at the time period of the installation of the reddening alteration of Kłodzko Złoty-Stok and Szklarska Poręba, the albitization must be necessarily linked to the apparent Triassic paleosurface. Thus, the different albitized sites correspond to the overprints on the Triassic paleosurface, which may be reconstructed by matching the different sites according to their albitized/reddened facies. The connection between the albitization and the Triassic paleosurface implies on one hand, in absence of any latter major structural disturbance, that

the most pervasive reddened/albitized facies may correspond to the near-surface while the less reddened/albitized or even non-albitized facies are rather interpreted as deeper facies. On the other hand, all outcropping rocks in the studied massifs must have been impregnated in the same way. Therefore, at the scale of the massifs, the geometry of the Triassic paleosurface should be more or less uniform from a spatial point of view.

### *8.3.1 Mapping of the reddening*

The mapping of the reddened facies within the Kłodzko Złoty-Stok massif represents a approximate surface of 140 $km^2$ from Podzamek in the West to ZłotyStok in the East and from Laskowka in the North towards Droszkow in the South. The dominant rocks encountered during this mapping were primarily granitoïd rocks, metapelites, gneiss and schists, that were albitized in different degrees.

The mapping consisted in observing the rocks and listing them according to the fact that they were or they were not reddened. In case of any present albitization/alteration the reddening intensity was estimated, that reflects the albitization intensity of the facies. The estimation of the extent of the reddened facies was done taking into account the outcropping rocks as well as the debris and sparse blocks composing the superficial cover. The mapping was carried out in two main steps: In a first step, all major outcrops along the main roads/routes were investigated and listed with respect to alteration degree. In a second step, the less accessible facies (superficial cover and minor outcrops) were observed in the same way according to a approximately regular grid. Finally, all this information was summarized/plotted on top of the geological map of the respective zone (Fig. 58). This allows a visual estimation of the extent of the reddening and to characterize the limit between the albitized facies and the non-altered facies.

The major outcrops correspond to the exposed sections of Laski Quarry, Laski Village, Chwalisław Mountain, Chwalisław Quarry, Makolno, and Laskowka, where the reddened albitization is the most spectacular. Besides, these sections allowed the characterization of the different albitization features in particular the pervasive and homogeneous albitization, the intensity of the albitization of fractures walls, and pink spotted albitization. These features will be the base of the mapping. Indeed, the description and the listing of the outcrop and facies encountered off-road will be performed by the search of these different albitization features. Besides, any major outcrops that do not show any red albitization are also be listed and marked on the map.

Off-road outcrops are generally of relatively weathered rock preservation. The superficial cover is composed of rocks debris and sparse blocks found in domestic fields. Rocks debris and sparse blocks surely originate from the nearby outcropping metamorphic or plutonic rocks; therefore they are representative of the eventually present albitization features within the facies composing the massif.

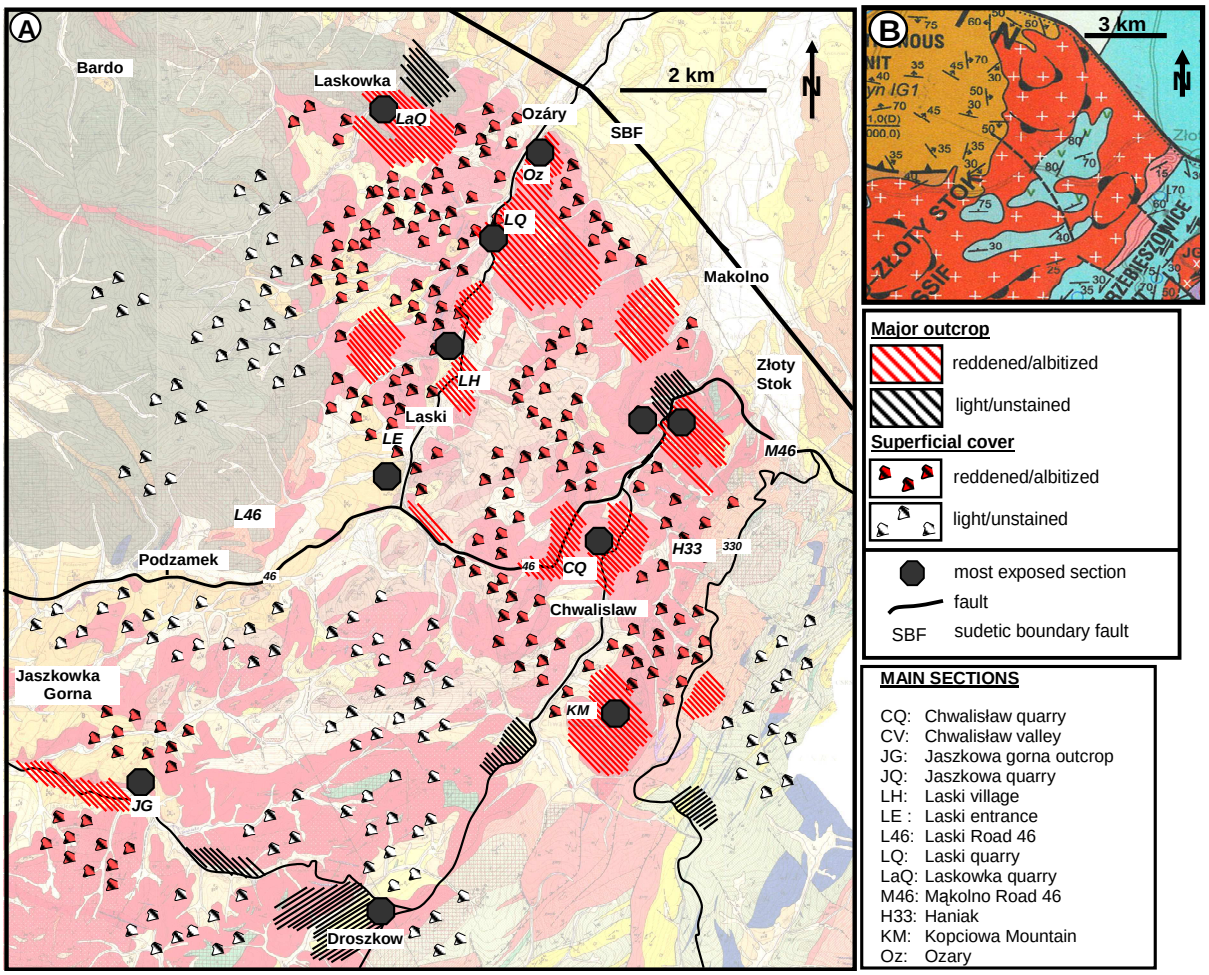


**Figure 58 – (A) Map of the spatial distribution of the reddening in the Kłodzko Złoty-Stok Massif. (Geological background after Cwojdziński, 1974), (B) Structural map of the Kłodzko Złoty-Stok Massif (after Cymerman, 2004).**

***Figure 58 - (A) Carte montrant la distribution spatiale de la pigmentation rouge dans le massif de Kłodzko Złoty-Stok (fond de carte modifiée d'après Cwojdziński, 1974). (B) Carte structurale du massif de Kłodzko Złoty-Stok (d'après Cymerman, 2004).***

The off-road outcrops allow distinguishing the same albitization features as seen in the major outcrops, i.e. they may either be pervasive or restricted to fractures walls. On the other hand, it is not always easy to distinguish for instance the fractures wall albitization features on the debris and sparse blocks, because of their general smaller size and of the fact that they are not in place. Nevertheless, pervasively albitized debris/blocks, spotted debris, grey non-albitized debris/blocks are unambiguous to distinguish.

### *8.3.2 Spatial distribution of the reddening*

The mapping shows that not all the rocks of the Kłodzko Złoty-Stok Massif are affected by the reddening. The metamorphic rocks east and west of the granite intrusion (Fig. 58A) do not show any reddening features except for the Haniak gneiss (H33) that are albitized. They show a strong reddening that is well recorded in their quartzo-feldspathic bands. Anyway, the granitoïd body contains the major part of the reddened facies, even if some unstained granitoïds exist within the Kłodzko Złoty-Stok Massif (Fig. 58A). Therefore it can be concluded that the lack or respectively the presence of the reddening can not consistently be related to the nature of rocks and is therefore facies-independent.

The distribution of the albitized and the non-albitized facies makes it possible to define two major domains from the North to the South of the Kłodzko Złoty-Stok Massif:

(1) In the North, an albitized domain is limited by the Bardo metapelites in the NW, by the Trzebon schist in the SW, and by the Sudetic Boundary Fault in the NE (Fig. 58, Fig. 59, Fig. 60);

(2) In the South of the albitized area, an adjacent continuously non-abitized area exists (Fig. 58).


**Figure 59 - North-west limit between the Laskowka albitized granitoïd rocks and the non-albitized metapelites of Bardo. This limit coincides with the marge of the Kłodzko Złoty-Stok granitoïd intrusion and the lower-carboniferous metapelites of the Bardo Units.**

***Figure 59 – Limite nord-ouest entre les granitoïdes albitisés de Laskowka et les métapélites non albitisés de Bardo. Cette limite coïncide avec la limite entre l'intrusion granitoïde de Kłodzko Złoty-Stok et les unités métapélitiques du Carbonifère inférieur de Bardo.***

The albitized domain may be considered as a NW-SE structure, where the albitization is well recorded in all the facies from the Laskowka granodiorite at the NW, through the most exposed albitized sections of Laski, Chwalisław area and Mąkolno. Besides, the extent of this domain ends towards the South-west at the entrance of the Laski valley and at the Kopciowa Mountain (KM) in the South-east.


**Figure 60 – South-east limit of the albitized domain of Kopciowa-Haniak with the non-albitized Trzebon schist.This limit is obviously discordant putting in contact the non-albitized Proterozoic units of the Trzebon Mountain with the albitized granitoïds units.**

***Figure 60 – Limite sud-est entre le domaine albitisé de Kopciowa-Haniak avec les schistes non albitisés de Trzebon. Cette limite est vraisemblablement discordante mettant en contact des unités protérozoïques non albitisées de la montagne de Trzebon avec les granitoïdes albitisés.***

In the South the non-albitized domain continues adjacent to the albitized area, this presents a NW-SE trend. The non-albitized domain extends further to the South and is interrupted in the SW by a small albitized unit of observed around Jaszkowka Gorna.

The reddening within the granitoïd intrusion of the Kłodzko Złoty-Stok Massif clearly shows two distinct domains:

- a reddened domain in the North and (Fig. 58, Fig. 61)
- a non-altered domain in the South, where the granitoïd facies are almost exclusively light or grey (Fig. 58, Fig. 61).

Nevertheless, extensively reddened facies occur in the south-western part of the domain, around the Jaszkowka Goma area.

The limit between the two main domains corresponds well with to the proposed fault by Cymerman (2004, Fig. 58B, Fig. 61) on the recent structural map of the Kłodzko Złoty-Stok Massif. Besides, it appears likely that this fault contributes to put non-albitized facies in contact to albitized granitoïd facies. The age of this fault would be constrained if the age of the reddening alteration would be known.

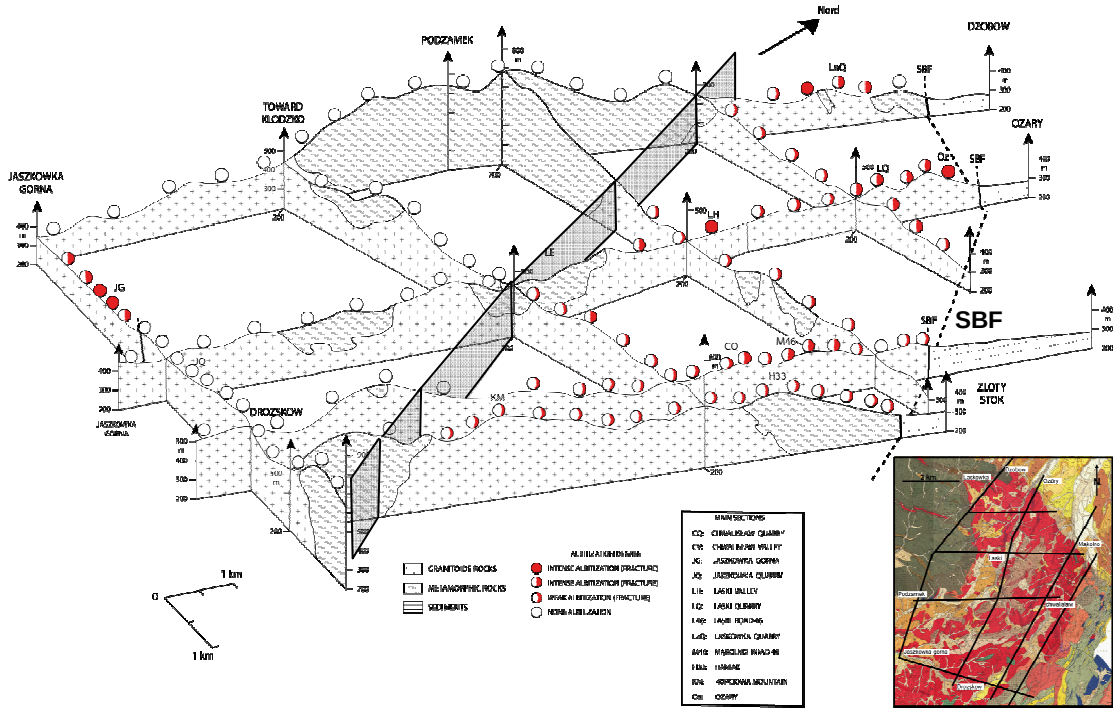


**Figure 61 – 3D block showing the extent of the reddening/albitization alterations in the Kłodzko Złoty-Stok Massif (KZS). The albitized granitoïd domain appears as contiguous to the non-albitized granitoïd domain. The limit between the reddened/albitized and the light/unstained granitoïdes coincides with a fault plane (underlined in grey) parallel to that proposed by Cymerman (2004). The 3D block was obtained by assembling the serial 2D sections along the traces shown on the inset geological map. SBF = Sudetic Boundary Fault.**

***Figure 61 – Bloc-diagramme montrant l'extension de l'albitisation rouge dans le massif de Kłodzko Złoty-Stok (KZS). Un domaine de granitoïdes albitisés est contigu avec un domaine de granitoïdes non albitisés. La limite entre les granitoïdes rouges/albitisés et clairs/non albitisés coïncide avec un plan de faille (souligné en gris) correspondant à celui proposé par Cymerman (2004). Le bloc-diagramme a été obtenu en assemblant les coupes effectuées le long des tracés marqués sur la carte géologique en écart. SBF : faille bordière des Sudètes.***

## 8.4 STRUCTURAL IMPLICATIONS

Yet, the mapping of the reddening/albitization in the KZS highlighted the contact between non-reddened/albitized granitoïd areas with albitized granitoïd rocks, implying discontinuities in the geometry of the Triassic paleosurface (Fig. 62). This can be interpreted that in the KZS Massif some zones show a preservation of the Triassic paleosurface as in other zones it is absent. This discontinuity of the Triassic paleosurface in the mapped KZS area coincides exactly with the fault proposed by Cymerman (2004) (Fig 58 & 61). Therefore, the observed discontinuities in the geometry of the mapped paleosurface are a strong indicator for the presence of this fault.

The spatial arrangement of the albitization with respect to the surface, i.e. probably with decreasing intensity towards the depth, suggests that blocks showing previously deeper non-reddened granitoïds were uplifted in comparison to blocks that are in contact now and which show albitized granitoïd facies that correspond to the strongly altered paleosurface. This uplift therefore occurs inevitably along an existing fault between both granitoïd blocks, and it is necessarily associated to a post-tectonic erosion of the uplifted (and therefore outsticking) block. This erosion probably erased then the Triassic overprints. Thus, the movement of the proposed fault between the two areas seems to result from a reverse slip of the fault associated with an erosion of the uplifted southern block (Fig. 62)

The slip of the fault and the associated erosion are necessarily post-triassic, since the albitization was dated to the Trias. The post-Triassic slip fault may probably be associated to the Variscan Sudetic Boundary Fault, which was rather active during the Tertiary. Anyway, the preservation of parts of the Triassic paleosurface in the northern block is probably less important than the original thickness of the overprint that is defined by the penetration depth of the albitization. But the Triassic albitization allows to establish that the fault proposed by Cymerman (2004) in the KZS must be definitely post-Triassic and may be used as a tool to estimate the post-Triassic erosion and to understand the post–triassic evolution of the block tectonics in the KZS Massif and à fortiori of other massifs.

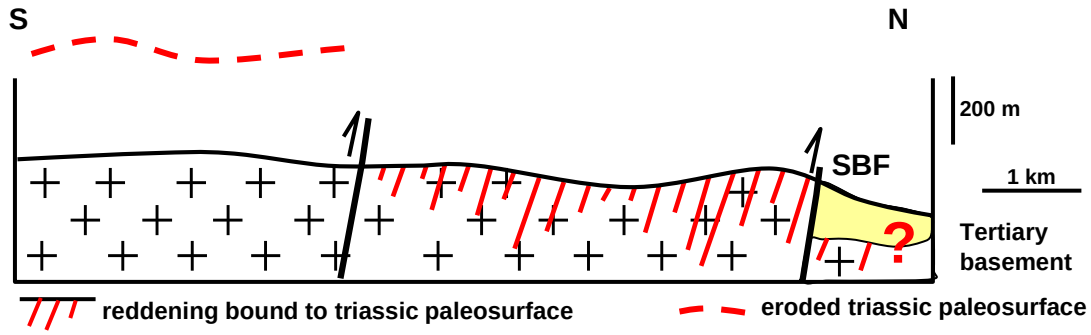


**Figure 62 - Post-Triassic erosion of the Triassic paleosurface within the KSZ Massif. The Triassic paleosurface is discontinuous throughout the massif and these discontinuities may correspond to the fault proposed by Cymerman (2004). The post-Triassic movement of the fault and its subsequent erosion contributed to establish of the actual geometry of the blocks within the KZS.**

***Figure 62 – Érosion post-triasique de la paléosurface triasique au sein du massif de KSZ. La paléosurface triasique est discontinue à travers le massif et la discontinuité coïncide avec à la zone de faille proposée par Cymerman (2004). Le mouvement post-triasique de la faille et son érosion ultérieure explique la géométrie actuelle des blocs.***

## *RESUME CHAPITRE 9*

# *CE QUI EST DERRIERE LA DATATION TRIASIQUE*

### *EXTENSION DES FACIES ALBITISES ET HEMATISES*

*Les albitisations avec hématisation associée sont fréquentes dans les massifs cristallins, mais ont été relativement peu étudiées par les pétrographes des granites qui les considèrent comme des faciès d'altération. Ce sont les métallogénistes qui se sont les premier intéressé à ces facies à partir des années 1970. Une revue rapide montre que ces faciès sont largement répandus dans les massifs paléozoïques d'Europe (Massif central Français, Vosges et Forêt-Noire, en Grande-Bretagne, Irelande, Espagne, Massif de Bohème), mais aussi dans les socles protéroïques (bouclier Scandinave, Canada, Brésil, Maroc, Australie). Certains de ces faciès à paragénèse albite-hématite ont été datés du Trias, d'abord par radiochronologie (Massif Central), puis par paléomagnétisme (Massif Central, Vosges, Catalogne, et les Sudètes polonaises). Des datation paleomagnétiques triassiques ont également été obtenues en Finlande et les rajeunissement triasiques ont été mis en évidence par paléomagnétisme dans de nombreux sites du socle Varisque sans que la présence ou l'absence d'albitisation y soit documentée. Ces roches étaient à l'affleurement au Trias et l'hématite et l'albite cogénétique ont du se développer dans des conditions supergènes, ou au moins à des profondeurs inférieures à quelques centaines de mètres.*

### *POINT D'ANCRAGE POUR L'EVOLUTION TECTONIQUE POST TRIAS*

*Si les faciès albitisés/hématisés s'avèrent être liés à la paléosurface triasique, ils constitueront alors des jalons spatio-temporels précieux pour reconstruire l'évolution post-triasique des massifs paléozoïques, mais également des vieux socles précambriens (Fig. 63). La préservation de ces faciès albitisés/oxydés au sein des massifs indiquerait une érosion faible (<200-300 m), tandis que leur absence impliquerait des érosions plus importantes.*

### *IMPLICATION POUR L'ETUDE DES TRACES DE FISSION DE L'APATITE*

*L'histoire thermique des roches da la croûte supérieure est principalement approchée par l'étude de l'apatite par : (1) le thermochronomètre basé sur la cicatrisation des traces de fission de l'apatite et (2) la datation (U-Th)/He des cristaux d'apatite. L'étude des traces de fission de l'apatite a souvent été appliquée aux socles paléozoïques et protérozoîques et il en est fréquemment résulté un scénario géodynamique admettant une épaisse couverture sédimentaire au Mésozoïque et une dénudation rapide au Tertiaire inférieur. Ces résultats ont souvent été en contradiction avec les études géologiques "classiques" basées sur des arguments sédimentologiques et qui montraient que ces massifs avaient eu une couverture réduite pendant le mésozoïque. En particulier de nouvelles datations des paléoaltérations reposant sur le socle du Massif Central se sont avérées être d'âge jurassique supérieur, ce qui exclu qu'une couverture épaisse ai pu exister sur le Massif Central durant le mésozoîque le préconisaient des études thermochronologiques (Fig. 64).*

*Si les estimations thermochronologiques apparaissent biaisées dans nombre de massifs paléozoîque d'Europe de l'Ouest, il faut identifier la cause de cette dérive. Une explication est peut-être à rechercher dans la recristallisation/néoformation des apatites au cours de la chloritisation des biotites au Trias. Si les apatites secondaires liées aux albitisations s'avèrent différer cristallochimiquement des apatites magmatiques, alors leur comportement vis-à-vis des traces de fission doit être testé.*

### *RESISTANCE A L'EROSION DE LA PALEOSURFACE ALBITISEE*

*Les géomorphologues ont depuis longtemps souligné la remarquable persistance de la paléosurface triasique dans les massifs paléozoïques. La dureté et donc la préservation de la paléosurface triassique est essentiellment liée à son albitisation. Les granites albitisés sont exempt de plagioclases anorthitiques, qui sont beaucoup plus sensible à l'altération chimique que l'albite. En particulier, contrairement aux granites "ordinaires", non albitisés, les granites albitisés ne forment jamais d'arêne. L'albitisation et et la chloritisation concomitante des biotites rendent les roches beaucoup plus résistantes à l'altération et à l'érosion.*

### *ENVIRONNEMENTS DE L'ALTERATION ALBITISANTE*

*Il est généralement avancé dans la littérature, même quand des hypothèses hydrothermales sont avancées pour l'albitisation, que le sodium nécessaire aux albitisation est alimenté par des saumures superficielles provenant de dépôts évaporitiques ou directement de bassins évaporitiques. Dans le cas des albitisations triasiques le sodium est disponible dans les gigantesques accumulations de clhorure de sodium dans les bassins permo-triasiques.*

*Par ailleurs, des essais de modélisation géochimique ont montré qu'il est nécessaire de disposer de solutions avec un fort rapport $Na^+/K^+$ pour albitiser les feldspaths-K. Des saumures avec un rapport initial $Na^+/K^+$ identique à l'eau de mer ne permettent pas l'anbitisation des feldspaths-K. l'enrichissement en Na des solutions est probablement lié carctères géochimiques des environnements triassiques où les pseudomorphoses de cristaux de halite sont communs dans les dépôts épicontinentaux. Le lessivage de ces sels, l'apport d'aérsols marin, de poussières de sel et l'introduction périodique/épisodique d'eau de mer et de solutions évaporitiques sur les continents sont d'autant de sources de sodium susceptible d'alimenter les nappes profondes.*

*Mais, l'échelle de ces profils d'albitisation de l'ordre de 100 m relie cette altération à des environnements de nappes. La faible mobilité de la plupart des éléments chimiques indique vraisemblablement aussi des écoulements très lents d'ine nappe profonde.*

### *LA QUESTION DE LA TEMPERATURE*

*Cette question a toujours été rejetée par les pétrologistes qui considèrent que ces altérations se produisent entre 200 et 400°C en se basant sur les géothermomètres donnés par les silicates calciques. C'est la signification de ces paragenèses minérales qui doit être questionnée. D'un point de vue thermodynamique il n'y a pas d'impossibilité : c'est la composition et les caractéristiques physico-chimiques des solutions qui règlent les équilibres. Mais le développement d'un minéral par rapport à un autre est aussi réglé par la cinétique des réactions, ou plus précisément par les cinétiques relatives entre les différentes réactions.*

*On pourrait envisager, comme d'autres auteurs, que ces paragenèses correspondent à des évènements successifs et indépendants les uns des autres. Nous avons montré ci-dessus que nous ne pouvions disjoindre les différentes réactions d'altération, ni d'un point de vue pétrographique, ni d'un point de vue réactionnel. Par ailleurs, les faciès sont homogènes et similaires dans tous les massifs cristallins paléozoïques, affectant des roches très diverses dans leur composition, leur mode de mise en place, leur contexte géodynamique … et les datations des oxydes de fer associés donnent tous un âge triasique. La datation nous apparaît comme un argument fort et incontournable … quelque soit la signification qu'on lui donne elle indique un phénomène triasique généralisé, apparemment global.*

# CHAPTER 9

# 9 WHAT IS BEYOND THE TRIASSIC DATING?

Demonstrating that the red albitizations are related to the Triassic paleosurface may profoundly renew a number of established ideas, in particular concerning the conditions of the albite formation in the crystalline context, which up to now have consistently been interpreted as linked to deep processes. Taking into account an alternative superficial albitization, the usually given temperatures for the formation of albite have to be reconsidered as well as their role associated to geothermometers. The red albitisations may therefore also represent an additional benchmark for the reconstruction of the Triassic paleosurface, and consequently a temporal marker that allows to understand the post-Triassic evolution of the albitized massifs.

## 9.1 WIDESPREAD ALBITIZATION AND REDDENING OF GRANITOÏD ROCKS

Albitization and the associated hematitization are frequent in the crystalline massifs, however up to present; relatively few studies were devoted to them. In the past, petrologists studying the crystalline massifs were particularly interested in the mineralogical parageneses in order to trace the respective geochemistry of the magma and its evolution. For this discipline, the emplacement of the crystalline massifs represents the primary interest. Therefore, the secondary alteration facies were almost systematically neglected and generally included in the descriptive terms of saussuritization and sericitization, gerenally without a broader attention. Saussuritization and sericitization are considered as post-magmagtic alterations related to the cooling and the exhumation of the crystalline massifs. Thus, petrologists and paleomagnetists try to avoid collecting these altered rocks for their studies.

A particular attention has been paid on these oxidized/albitized facies during the last decades. In the 1970's, the metallogenists were the first to focus on these facies, which are often associated to substantial metal deposits. A quick review indicates that the extension of the albitized and oxidized granitoïd outcrops is broad. Numerous cases of these facies are described in the Palaeozoic massifs of western Europe, among them in the French Massif Central (Chenevoy, 1962 ; Schmitt, 1986 & 1993; Parcerisa et al., 2009), in the Vosges and Black Forest (Fiebig and Hoef, 2002 ; Franke et al., 2012), in Brittany (Carron et al., 1994), in Ireland (Jenkin et al., 1992), in NW England (Lee and Parsons, 1997), and in SE Spain (Fabrega et al., 2012). The phenomenon is also widespread in the Precambrian Scandinavian shield: in Norway (Engvik et al., 2008), Finland (Putnis et al., 2007; Preeden et al., 2009 ; Botsun et al, 2010) and Sweden. For the latter many recent investigations are dedicated to the detailed spatial distribution of these alteration facies due to the radioactive waste depository project in the Simpevarp and Laxemaar areas (SE Sweden; Eliasson, 1993; Putnis et al., 2007 ; Plümper and Putnis, 2009 ; Morad et al., 2010; Sandström et al., 2010). These albitized facies have also been characterized outside of Europe, for example in Canada (Boone, 1969), the USA (Putnis et al., 2007; Hamilton et al., 2012), in Brazil (Putnis et al., 2007), in Egypt (Abdel-Rahman and Martin, 1990), in Morocco (Essalhi et al., 1993), and in Australia (Milnes, 1990). In contrast to that the literature report on albitization of granitoïd rocks without any red-staining has been described to our knowledge only for the Strzelin granite in SW Poland (Ciesielczuk and Janeczek, 2004; Ciesielczuk, 2007).

Some of these albite/hematite parageneses have been dated. The French Massif Central occurrences have first been dated by radiochronology that revealed Triassic ages for the albitization of the Permo-Carboniferous sedimentary series (Bonhomme et al., 1980) as well as for the granitoïd hosted alterations (Schmitt et al., 1984). Recently more results were

published using paleomagnetic methods that allow to date directly the pigmentary hematite present within the neogenic albite. Through this, the Triassic age has been strengthened for the albitization occurences in the French Massif Central (Ricordel et al., 2007). Triassic ages have also been found for the albitization of the Paleozoïc crystalline massifs of the Vosges (Franke and Vercruysse , 2012), Catalonia (SE Spain) and the Polish Sudetes massifs (Franke et al., 2010; Franke et al., 2013). In the Scandinavian shield Permo-Triassic ages have been revealed by paleomagnetic datings of oxidized shear and fault zone rocks in southern Finland (Preeden et al., 2009) as well as in Devonian dykes hosted in pink granite in northern Finland (Botsun et al, 2010). On the other hand, Permo-Triassic paleomagnetic overprints are the most common remagnetizations found in the crystalline rocks from Variscan basements of the Vosges, the French Massif Central and the Bohemian massif (Edel and Schneider, 1995).

The above mentioned case of the Simpevarp and Laxemaar areas in SE Sweden is more complicated. Fracture mineral parageneses have been dated by combining structural analyses and geochronology. They resulted in distinguishing successive metasomatic events over more than 1 Ga (Drake et al., 2009; Sandström et al., 2009). Nevertheless, the actual hematite that is responsible of the red-staining along the fractures has not been dated and in these studies hematite is postulated to be independent of the silicate paragenesis and thus of more recent origin than the albitization.

This literature review reveals the wideranged prevalence of Permo-Triassic ages obtained for the albitized and hematitized facies. Moreover, the albitized rocks in the Palaeozoic massifs (SE Spain, French Massif Central, Vosges and Sudetes) which have been dated have been linked to the Triassic paleosurface. During the Trias, these rocks were outcropping at the surface, so the dated hematite must have formed nearby the surface, and consequently if albite and hematite are co-genetic, the albitization must have developed under supergene conditions or at least at depths less than a few hundred meters.

Moreover, if in future it would be generally admitted that these altered facies, which affect crystalline rocks of various ages, are all linked to the same particular period, than it cannot be referred anymore to the granite emplacement to explain these alterations. Thus, a post-orogenic global cause must be considered, such as the particular paleosurface environment surface and the paleoatmosphere.

## 9.2 BENCHMARKS FOR THE POST PALEOZOIC TECTONIC EVOLUTION

Under the assumption that it could be prooven that the albitized/hematitized facies are related to the Triassic paleosurface, then this will constitute precious spatio-temporal markers to reconstruct the paleosurface and to constrain the post-Triassic geodynamical evolution of the above described Palaeozoic massifs.

The preservation of the albitized/hematitized facies allows the assessment of the post-Triassic erosion rate; that subsequently would be relatively limited in depth (< 200-300 m). And on the other hand, the lack of the albitized paleosurface will then reveal a more substantial erosion of the respective blocks and additionally allows to highlight their post-Triassic tectonic movements, as it has been mentioned in this study of the Polish Sudetes.

The interest of the dating of the albitization is reinforced for the areas of ancient basements, as in the Precambrian shield that lacks any sedimentary cover. In this case, the Triassic dating of these alterations may be an extremely precious marker to constrain the geodynamical evolution and the erosion history of the basement within its limits (Fig. 63).

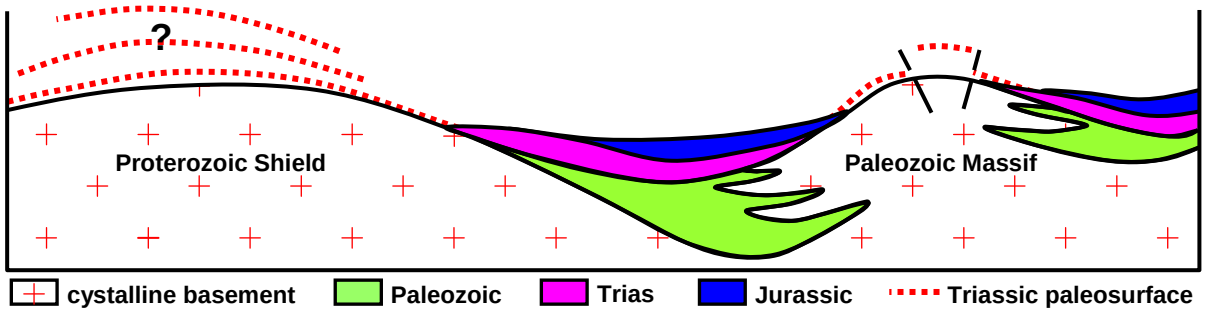


**Figure 63 - Schematic sketch showing the possible position of the Triassic paleosurface in Palaeozoic crystalline areas. The recognition of such paleosurface positions in crystalline basements would allow to set strong constrains for geodynamic modelling.**

***Figure 63 – Schéma montrant la position probable de la paléosurface triasique dans les régions cristallines. La reconnaissance de telles paléosurfaces dans les socles cristallins permettra de fixer des contraintes fortes pour la modélisation géodynamique.***

## 9.3 IMPLICATIONS ON APATITE FISSION TRACKS THERMOCHRONOLOGY

Low-temperature thermochronology allows the determination of the thermal history of upper crustal rocks in the 40-110°C temperature range. This method has been applied with success in various geodynamical contexts including orogen massifs, passive margins and basement complexes and allows the estimation of the amount and timing of erosion and the uplift rate by consideration of the paleo-heat flux and the specific rock properties. Paleotemperatures are determined using two independent techniques: 1) the apatite fission-track thermochronometer which is based on the temperature-controlled progressive annealing of defects formed by natural fissions of U238 atoms, and 2) the (U-Th)/He dating on apatite crystals where He-diffusion is controlled mostly by temperature.

During the last decade, thermochronology by fission tracks has been applied to numerous Hercynian and Variscian basements to estimate their post-Paleozoic geodynamic behaviour. The general trend of almost all these studies was to put forward a (very) thick sedimentary cover during the Mesozoic (2000 to 5000 m), followed by a very rapid denudation during the lower Tertiary. Such scenario have also been suggested for the French Massif Central (Barbarand et al., 2001; Peyaud et al., 2005), for the Catalan Coastal Ranges (NE Spain; Juez-Larré and Andriessen, 2002; Juez-Larré and Ter Voorde, 2009), and the Saxo-Bohemian Massif (Ventura et al., 2009; Danišík et al., 2010; Thomson and Zeh, 2000). Similar results have been forwarded for the Scandinavian Shield suggesting that central Sweden was covered by Paleozoic and Mesozoic sediments until the Tertiary (Larson et al., 1999; Cederbom et al., 2000; Larson et al., 2006; Green and Duddy, 2006).

These results were inconsistent with the “classical” studies of the geologists who considered, with respect to sedimentologic arguments (thickness reduction, coastal facies, etc.), that these massifs have experienced only a limited cover during this period. However, the debate was often restricted to regional meetings of geological societies, these arguments of the “naturalists” are based on spatial and temporal discontinuous observations. The arguments lack physical measurements and modelling results. On the Scandinavian Shield, the existence of a thick Mesozoic sedimentary cover has been refuted for southeast Sweden and instead it has been stated that the area had no significant amount of sedimentation, erosion or uplift since the mid-Permian (Söderlund et al., 2005). Similarly, the hypothesis of a thick sedimentary cover during the Mesozoic in southern Finland has been discarded, arguing that the importance of radiation-enhanced annealing at low-temperature has been overlooked (Hendricks and Redfield, 2005; Hendriks et al., 2007).

Ever since, new arguments have been raised to fuel the debate in the French Massif Central. The paleomagnetism datings of the paleo-alterations and the red azoic continental formations, which were primarily considered as of Tertiary age, rather indicate ages from the upper Jurassic to the lower Cretaceous (Thiry et al., 2006; Ricordel, 2007; Ricordel-Prognon et al., 2010). These datings highlight that the massif was denuded from the upper Jurassic onwards, excluding the possibility of a substantial sedimentary cover during the upper Cretaceous as suggested by the thermochronological studies (Fig. 64), because this would have lead to thicker upper Cretaceous sedimentary deposits on the Palaeozoic massifs than in the adjacent sedimentary basins (Aquitaine basin and Paris basin).

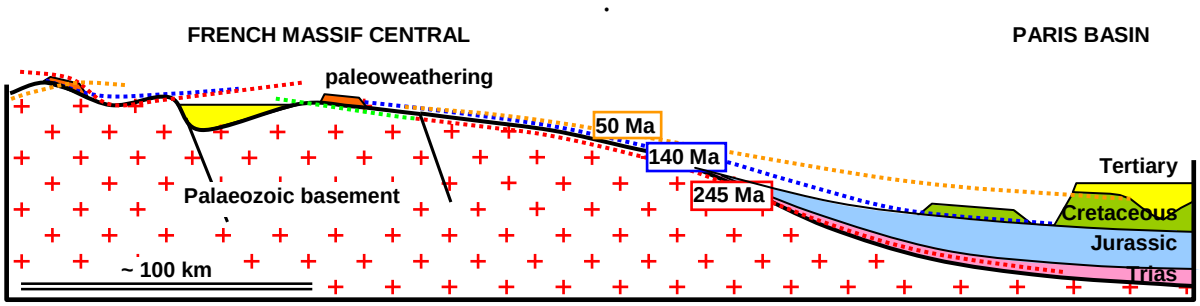


**Figure 64 - Schema of the relation between the Triassic paleosurface, the upper Jurassic/lower Cretaceous paleosurface and the Tertiary paleosurface in the Massif Central and in the Paris basin. The three paleosurfaces collide on the massif proving that there could not be a significant sedimentary cover on top of the massif during the Mesozoic and consequently the post–Triassic erosion rate on the basement is weak.**

***Figure 64 – Schéma des relations entre la paléosurface triasique, la paléosurface du Jurassique supérieur/Crétacé inférieur et la paléosurface tertiaire dans le Massif Central et le Bassin de Paris. Les trois surfaces se télescopent sur le massif, montrant qu'il ne pouvait y avoir de couverture sédimentaire importante sur le massif au cours du Mésozoïque et que l'épaisseur de socle érodée depuis le Trias est faible.***

If the thermochronological estimations show results that are not consistent with the geological observations, the cause of this data inconsistency which seems recurrent in several Palaeozoic massifs of the Western Europe should therefore be reconsidered. A possible explanation may be the nature of the apatite used for the fission track results. In this study we observed that apatite crystals were fed and newly crystallized during the chloritization of the biotites. Similar apatite recrystallizations have also been described as associated to the albitization of the Precambrian series in southern Norway (Engvik et al., 2009). It is generally known that the chemical composition of the apatites influences directly the kinetics of the fission track annealing (Wagner and Van den Haute, 1992; Barbarand and Pagel, 2001; Barbarand et al., 2003; Dempster and Persano, 2006). In fact, secondary apatites related to the albitization effectively exhibit crystallo-chemical features differing from the magmatic ones, so their behaviour should be tested with the regard to the fission track annealing.

## 9.4 RESISTANCE OF THE ALBITIZED PALEOSURFACES WITH RESPECT TO EROSION

Since a long time, the remarkable persistence of the Triassic paleosurface expressed in the Paleozoic massifs has been highlighted by geomorphologists (e.g. Guilcher, 1949; Godard, 1980; Battiau-Queney, 1993; Schmitt and Simon-Coinçon, 1993; Widdowson, 1997). Only recently the link of the paleosurface preservation was drawn to the albitization. The consistency and in particular the resistance to erosion emerges as a major feature of this paleosurface. The paleosurface is preserved in several massifs where it forms the relatively dissected upper morphology. The Triassic paleosurface is also present in the Alpine ranges where it is particularly spectacular in the surfaces caused by glaciers, showing typical features of albitization and hematization along the fractures (Battiau-Queney, 1993; Battiau-Queney, 1997; Thiry, personal comm).

In the Catalan Coastal Ranges (SE Spain) the stratigraphic arrangement of the Mesozoic units indicates that the massif was an outcropping relief during the Mesozoic, remaining exposed probably from the Permian until the Cretaceous. Subsequently the massif has been faulted during the Miocene (Anadón et al., 1979). The albitized and hematitized Triassic paleosurface shows a noticeable preservation beneath the Tertiary deposits and even the present day weathering affected very little these albitized profiles. On the other hand, the non-albitized granitic facies at the fault scarps have been deeply weathered since the Miocene (Parcerisa et al., 2010; Fig. 65).

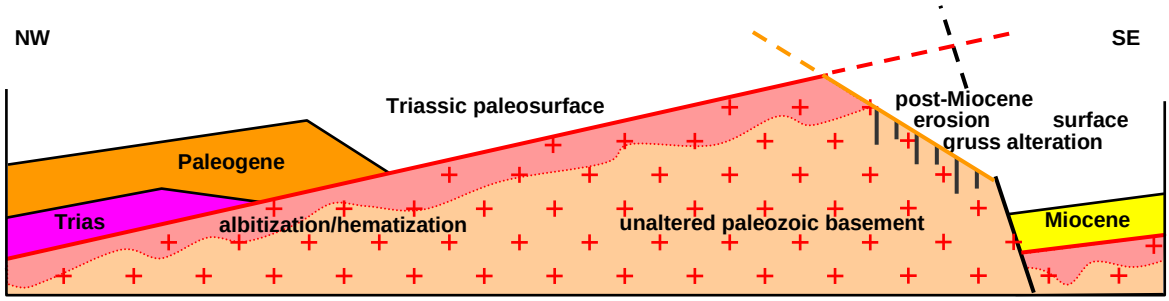


**Figure 65 – Sketch of the structural disposition of the Triassic albitized paleosurface in the Catalan Coastal Ranges. The Triassic albitized paleosurface has been remarquably well preserved most probably from the Mesozoic through the Palaeogene and the Miocene without any major weathering. In opposite the non-albitized granitic facies are deeply weathered into gruss. Figure modified after Parcerisa et al. (2010).**

***Figure 65 – Schéma des caractéristiques structurales de la paléosurface Triasique dans les chaînes côtières Catalanes. La paléosurface Triasique a été remarquablement préservée probablement depuis le Mésozoïque, en passant par le Paléogène et au Miocène sans avoir subi d'altération majeure. A l'opposé, les faciès granitiques non albitisés sont profondément altérés en arène. Figure d'après Parcerisa et al. (2010).***

The hardness and thus the preservation of the Triassic paleosurface seems to be mainly related to the albitization. The albitized granites are entirely lacking anorthitic plagioclases, that are much more sensitive to chemo-mechanical weathering. The development of albite and additional chloritization of the primary biotite crystals render the rocks much more resistant to weathering and erosion.

Similarly, on a regional scale, contrasted geomorphological behaviour may be observed frequently between albitized and non-albitized granites in Brittany (France). The northern coast in Brittany (Côtes d'Armor) is remarkable for its pink granitic rocky coast (Michelin, 2000). The rockiest area can be observed at the Brehat Isles where the granites are fully albitized of show red and pink colour. Sandy bays are very limited and restricted to area

where the granites are actually non-albitized and weathered into gruss. Even on a wider scale, the North coast, where the granites are albitized and hematitized, is entirely rocky, whereas the South coast where granites are mainly of light colour and non-albitized is much sandier.

It appears clearly that albitization has a strong effect on granite weathering and in turn on the regional geomorphology

## 9.5 WEATHERING ENVIRONMENTS

It is generally considered in literature, even in the hypothesis of a hydrothermal albite formation, that the sodium needed for the albitization was feed by superficial brines related to evaporitic deposits or even directly to brines of evaporatic basins (Battles and Barton, 1995; Oliver, 1995, Barton and Johnson, 1996; Frietsch et al., 1997; Davidson, 1998; McLelland et al., 2002). In case of the Triassic albitization the sodium would have been available in the gigantic accumulations of sodium chloride in the Permo-Triassic basins.

Moreover, early attempts of geochemical modelling have indicated that a high $Na^+/K^+$ ratio is required for albitization of K-feldspars (Schmitt, 1994). Brines with an initial $Na^+/K^+$ ration of sea water do not allow such albitization of K-feldspars. The $Na^+$ enrichment is most likely linked with the particular geochemical setting of the Triassic environment where for instance halite moulds are very common in transgressive epicontinental deposits. The leaching of such salts, the role of salty marine aerosols, or a periodic/episodic contribution of seawater and evaporative solutions may be equally invoked.

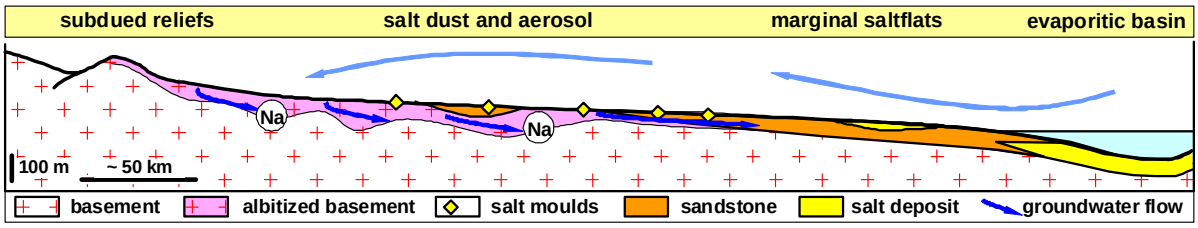


**Figure 66 - Paleogeographic sketch assuming the Triassic evaporitic environmental conditions that are widespread on the continents and that provided salty Na enriched groundwaters. Figure modified after Thiry et al. (2009).**

***Figure 66 – Schéma paléogéographique montrant que les conditions environnementales évaporitiques du Trias étaient répandues sur les continents et fournissaient des eaux souterraines salées et enrichies en Na. Figure d'après Thiry et al. 2009.***

It has also to be highlighted that this alteration may not behave like an "ordinary" weathering profile and occurred under unusual, or at least very specific, geological conditions. The scale of the profiles (> 100 m depth) relates this alteration rather to a groundwater environment. The weak mobility of most chemical elements may point to a groundwater with very low outflows and a deep water table. This may occur in very subdued landscapes and under arid climatic conditions. It has also to be pointed out that this alteration may have lasted for several 10's of Myr.

## 9.6 THE QUESTION OF THE TEMPERATURE

The question of the albitization formation temperature is a vital topic that has been systematically rejected by the igneous rock petrologists, who consider these alterations as late-magmatic occurring at about 200 and 400°C (see Chapter 1). Even if some lower temperature albitizations were recognized as related to the diagenesis in the sedimentary rock series, the presence of Ca-bearing silicates from the prehnite-heulandite series was thoroughly taken as a proof for high-temperature formation conditions. Indeed, these specific minerals are usually considered as geothermometers.

It is the high-temperature interpretation of these mineralogical parageneses that has to be questioned. Thermodynamically, there is no impossibility since the equilibriums are controlled by the mineral composition and the physico-chemical parameters of the solutions. However, the development of one mineral with respect to another one is also governed by the kinetics of the reactions, or more precisely by the kinetics between the different reactions. These are the questions that should be examined in more detail.

In the near futur, the arguments have to be critically examined to be strengthened. We can considered like other authors (Drake et al., 2009; Plümper and Putnis, 2009, Sandström et al., 2010; Morad et al., 2011) that these parageneses do not belong to one unique alteration event, but to successive alterations which are independent on each other. We have demonstrated above (in Chapter 7) that the different alteration reactions could neither be separated from a petrographical view nor from a reactional point of view. Besides, the facies appear as similar and homogeneous in all studied Palaeozoic massifs affecting a wide range of rocks differing in their composition, their emplacement mode, and their geodynamical context. Moreover, all datings of the oxidized iron-bearing minerals show Triassic ages. Therefore, the datings emerges as a strong argument for our hypothesis. Whatever meaning is given to the datings, it shows that a widespread Triassic phenomenon exists that appears to be global.

## 9.7 SUMMARY

If the albitizations and the hematitizations within the crystalline basements are of Triassic age, it follows that:

- The albitized and hematitized facies must be supergenes since the rocks that are affected by the albitization are more or less directly related to the Triassic paleosurface and in any case they could not have been formed at great depth.
- The albitized and hematitized facies appears as benchmarks for the Triassic Paleosurface.
- The geochemistry of these alterations is specific for the Triassic environmental conditions.
- The stability ranges of the accessory minerals such as the Ca-bearing silicates should be reconsidered.
- The nature and the physico-chemical features of the neogenic apatites crystallized during these alterations must taken into account for the thermochronolgial studies.

## *RESUME CONCLUSION*

*Les faciès albitisés et oxydés des socles cristallins sont communs à travers le monde, mais n'ont suscité que relativement peu d'intérêt de la part des pétrographes. Du fait de leur liaison évidente avec des fractures, ils ont toujours été considérés comme tardifs, post-magmatiques et donc sans intérêt immédiat pour la compréhension du magmatisme qui était la préoccupation scientifique majeure des pétrographes. Très tôt ces altérations ont été cataloguées par leurs paragenèses minérales sous les noms génériques d'albitisation, saussuritisation et séricitisation, et cela suffisait pour les écarter du sujet d'études. Les métallogénistes ont souvent marqué plus d'attention à ces faciès oxydés de par leur caractère géochimique vis-à-vis des concentrations métalliques.*

*L'étude pétrographique des faciès albitisés et oxydés du massif des Sudètes montre effectivement des paragenèses considérées comme "classiques". Deux pôles de paragenèses pétrographiques peuvent y être distingués : un pôle à saussuritisation et séricitisation et un pôle à albitisation et hématisation. La chloritisation des biotites et des amphiboles qui accompagne ces altérations apparaît intermédiaire entre les deux pôles précédents, débutant avec la saussuritisation et la séricitisation et se poursuivant dans les faciès albitisés et hématisés jusqu'à la chloritisation complète des minéraux ferro-magnésiens. Ces altérations sont toujours intimement associées, sans qu'apparaisse une rupture ou une discordance spatiale entre elles. Elles sont commandées par la présence de fractures et se disposent spatialement par rapport à ces fractures. L'albitisation et l'hématisation se développent sur les épontes des fractures, la saussuritisation et la séricitisation des plagioclases se développent de manière distale par rapport aux fractures, vers l'intérieur des blocs. Ces altérations peuvent être considérées comme globalement topochimiques : la saussuritisation des plagioclases pourvoyant le Ca pour le développement de la prehnite et la chloritisation des biotites étant la source de K pour la séricitisation. Mais l'albitisation complète des plagioclases et surtout l'albitisation des feldspath-K au voisinage des fractures atteste l'apport de Na et l'hématite associée à l'albite atteste l'oxydation du milieu et donc l'apport en oxygène.*

*Au terme de cette étude pétrographique est proposée une hypothèse superficielle pour ces altérations. Cette hypothèse superficielle s'appuie sur 2 points majeurs :*

1) *la datation par paléomagnétisme indique un âge triasique pour l'hématite et des datations radiochronologiques (K-Ar, Depciuch, 1972) des minéraux silicatés qui ont aussi mis en évidence des rajeunissements du même âge ;*
2) *l'extension géographique de ces altérations que l'on retrouve dans l'ensemble des massifs hercyniens et varisques d'Europe, avec des caractères pétrographiques similaires et surtout des datations identiques dans des massifs cristallins d'âge variés et dans des contextes géodynamiques très différents.*

*En considérant l'âge triasique de ces altérations, celles-ci doivent être regardées comme liées à la paléosurface triasique, puisque ces roches cristallines étaient à l'affleurement au Trias. Le moteur de ces altérations serait les solutions salines, très enrichies en Na, nourries par les gigantesques accumulations de chlorure de sodium dans les bassins permo-triasiques et sur les continents périphériques. L'altération se ferait dans un contexte de nappes phréatiques profondes (100 à 300 m de profondeur ?), et très abaissées par l'aridité du climat. Dans un tel contexte, les écoulements sont extrêmement ralentis ; ce qui explique les très faibles échanges chimiques et le caractère globalement topochimique de ces altérations, à l'exclusion du sodium. La grande stabilité géodynamique de cette période*

*permettant à ces altérations de se poursuivre pendant plusieurs dizaines de millions d'années et aux réactions à cinétiques même très lentes de s'exprimer.*

*Il faut reconsidérer ces faciès sans "a priori" en remettant toutes les données à plat, puis reconsidérer les différents aspects tenus comme des évidences. En particulier se pose la question de la température de formation des paragenèses à prehnite et séricite considérée comme des géothermomètres de "températures élevées". Il convient aussi de prêter une attention particulière aux datations radiochronologiques et paléomagnétiques qui ont été considérées comme évidemment trop jeunes par rapport à la mise en place des massifs cristallins. Par le passé, ces datations ont été systématiquement rejetées et la plupart du temps elles ne sont même pas mentionnées dans les publications. Une prise en compte de ces datations ferait éventuellement apparaître leur cohérence comme cela a été le cas pour les rajeunissements d'âge triasique des formations permiennes mis en évidence par paléomagnétisme (Edel et Schneider, 1995).*

*Même si les paragenèses à séricite et à prehnite s'avéraient ne pas faire intégrante d'une altération unique, conduisant à l'albitisation et à l'oxydation de ces roches cristallines, il reste que l'hématite indique bien la proximité de la paléosurface triasique. Cette oxydation des roches cristallines constitue un repère précieux pour contraindre les géodynamiques post-triasiques et les érosions et évolutions géomorphologiques des massifs paléozoïques.*

# CONCLUSIONS

Albitized and oxidized facies of the crystalline basement are wide spread throughout the world, but until now this subject attracts relatively little interest with respect to petrographers. Due to the obvious connection between the albitization and the fractures of the crystalline rocks, they have generally been considered as a late-magmatic phenomenon and therefore it explains why this is considered without any direct interest for the understanding of the magmatism, which is the major scientific concern of the petrographers. These alterations have been very soon categorized by their typical mineral paragenesis under the generic name of albitization, saussuritization and sericitization and that cause the effect that these phenomenon were often disregarded. Nevertheless, the metalogenists often paid more attention to these oxidized facies, because of their geochemical characteristics with respect to the metal concentrations.

The present study of the oxidized and albitized facies of the Polish Sudetes shows in fact a mineral paragenesis considered as “classical”. Two types of petrographical parageneses may be distinguished there: a saussuritization-sericitization type and an albitization-hematitization type. The chloritization of amphiboles and biotites that is associated to these alterations emerges as intermediate between the previous two poles, beginning with saussuritization and the sericitization and continuing in the albitized and hematitized facies reaching the complete chloritization of the ferromagnesian minerals. These alterations are always closely associated, without showing any break or spatial discordance between them. They are controlled by the presence of fractures and they are spatially arranged with respect to these fractures. Albitization and hematitization occur at the fractures walls, the saussuritization and the sericitization of the plagioclases develop in a distal way with respect to the fracture, towards the center of the blocks. These alterations may be roughly considered as topochemical: the saussuritization of plagioclases provides Ca for prehnite development and the chloritization of biotites emerges as the source of K for the sericitization. However, the complete albitization of the plagioclases and in particular the albitization of the K-feldspars in the vicinity of the fractures testify for the supply of Na, and the hematite associated to albite demonstrates the oxidation of the transport medium (fluids) and therefore the supply of oxygen.

In addition to the petrographical study of the albitized facies, a hypothesis on the superficial origin of the albitization is proposed for these alterations. This assumption is based on two major points:

1) The paleomagnetic datings show Triassic ages for the hematite and the radiochronological datings (K-Ar, Depciuch, 1972) of the silicate minerals highlighted identical rejuvenations ages.

2) The geographical extent of these alterations observed in many European Hercynian and Variscan massifs manifest similar petrographical features and comparable datings of the alteration/albitization regardless the various primary ages of the crystalline massifs and the different geodynamical settings.

Considering the Triassic age of these alterations, they are necessarily related to the Triassic paleosurface, since these crystalline rocks were already outcropping during the Trias. The driving force behind these alterations are the salt-rich solutions, thus highly enriched in Na, which are probably fed by the massive sodium chloride deposits of the Permo-Triassic basins and on the peripheral continents. The alteration may occur in a deep groundwater

context (about 100 to 300 m), which may be strongly lowered by the arid climate of this epoch. In this context, fluid flows are extremely slow, which explain also the very low chemical exchanges and the overall topochemical nature of these alterations, except for the sodium. The exceptional long geodynamic stability of this period allowed the alterations to carry on for tens of millions years and the occurrence of slow kinetic reactions.

These albitized facies should be therefore reconsidered without any “a priori”; the re-examination of all the existing data could subsequently reconsider the various aspects raised by this study. In particular, the question of the prehnite and sericite paragenesis formation temperature should be reconsidered when using them as geothermometer for “high temperatures”.

A particular attention should be paid on the radiochronological and paleomagnetic datings that have been considered as obviously as “too young” with respect to the primary age of the crystalline massifs emplacement. These datings have been systematically rejected as false in the past, and therefore they were often not even mentioned in publications and thus this information got lost. A consideration of these datings may emphasize their consistency as for example shown by Edel and Schneider (1995) for the Permian formations that suffered a Triassic rejuvenation, highlighted by paleomagnetism.

Even if the sericite and prehnite paragenesis should be found as not being part of a unique alteration, leading to the albitization and the oxidation of these crystalline rocks, the fact remains that the hematite clearly indicates the proximity to the Triassic paleosurface. This oxidation of the crystalline rocks represents an important marker to constrain the post-Triassic geodynamics, the erosion rates and the geomorphologic evolution of the Palaeozoic massifs.

# REFERENCES


Aagaard P., Egeberg PK., Saigal GC., Morad S., Bjørlykke K (1990). Diagenetic albitization of detrital K-feldspars in Jurassic, Lower Cretaceous, and Tertiary clastic reservoir rocks from offshore Norway, II. Formation water chemistry and kinetic considerations. Journal of Sedimentary Petrology 60:575–581.

Aagaard P., Egeberg PK., Saigal GC., Jahren, JS (1992). North Sea clastic diagenesis and formation water constraints. In Kharaka YK and Maest AS (eds). Proceedings of the 7th international symposium on water-rock interaction: United States Geological Survey, Menlo Park, California, USA: 1147-1152.

Abdel-Rahman AM., Martin RF (1990). Ther Mount Gharib A type granite, Nubian shield: petrogenesis and role of metasomatism at the source. Contribution of Mineralogy and Petrology 104: 173-183.

Aleksandrowski P., Kryza R., Mazur S., Żaba J (1997). Kinematic data on major Variscan strike-slip faults and shear zones in the Polish Sudetes, northeast Bohemian massif. Geological Magazine 133: 727-739.

Aleksandrowski P., Mazur S (2002). Collage tectonics in the northeasternmost part of the Variscan Belt: the Sudetes, Bohemian Massif). *In*: Winchester, J., Pharaoh T. & Verniers J. (eds), Palaeozoic Amalgamation of Central Europe, Geological Society, London, Special Publications 201: 237-277.

Allaby A., Allaby M (1999). Saussuritization. A dictionnary of Earth Sciences. Encyclopedia.com. http://www.encyclopedia.com/doc/1O13-saussuritization.html.

Anadón P., Colombo F., Esteban M., Marzo M., Robles S., Santanach P., Solé-Sugrañes L (1979). Evolución tectonostratigráfica de los Catalánides, Acta Geologica. Hisp 14: 242-270.

Aslund T., Oliver NHS., Cartwright I., (1995). Metasomatism of the revenue granite and aureole rocks, Mt Isa Inlier, Queensland syndeformational fluid flow and fluid rock interaction. Australian Journal of Earth Sciences 42: 291-299.

Awdankiewicz M (1999). Volcanism in a late Variscan intra-montane trough: Carboniferous and Permian volcanic centres of the Intra-Sudetic Basin, SW Poland. Geologia Sudetica 32: 13-47.

Awdankiewicz M., Awdankiewicz H (2010). Spessartites of the Kłozdko Złoty-Stok dyke swarm. Mineralogia Special Papers 37: 135-139.

Bachliński R., Hałas S (2002). K-Ar dating of biotite from the Kudowa Zdrój granitoids (Central Sudetes, SW Poland). Bulletin of. Polish Academy of sciences, Earth Sciences, 50 (2): 113-116.

Bachliński R., Bagiński B (2007): Kłodzko-Złoty-Stok granitoids massif. In Kozłowski A., Wiszniewska J (eds) In Granitoids in Poland. Archiw. Mineral. Monograph 1: 261-273.

Bastin ES (1935). Aplites of hydrothermal origin associated with Canadian Cobalt-Silver ores. Economic Geology 30: 715-734.

Battiau-Queney Y (1993). Le relief de la France. Coupes et croquis. Masson, géographie: p 252.

Battiau-Queney Y (1997). Preservation of old paleosurfaces in glaciaited areas: examples from the French western Alps. Paleosurfaces: Recognition, Reconstruction and Paleoenvironmental Interpretation, Geological Society 120: 125-132.

Barbarand J., Lucazeau F., Pagel M., Séranne M (2001). Burial and exhumation history of the south-eastern Massif Central (France) constrained by apatite fission track thermochronology. Tectonophysics 335 (3-4): 275-290.

Barbarand J., Pagel M (2001). Contrôle de la cicatrisation des traces de fission dans les cristaux d'apatite : le rôle de la composition chimique. Académie de Sciences de Paris, Sciences de la Terre et des planètes 332 : 259-265.

Barbarand J., Hurford AJ., Carter A (2003). Variation in apatite fission-track length measurement: implications for thermal history modelling. Chemical Geology 198 (1-2): 77-106.

Barton MK., Johnson DA (1996). Evaporitic-source model for igneous-related Fe oxide (REE–Cu–Au–U) mineralization. Geology 24: 259-262.

Battles DA., Barton MD (1995). Arc-related sodic hydrothermal alteration in the western United States. Geology 23: 913-916.

Ben Baccar M., Fritz B., Made´ B (1993). Diagenetic albitization of K-feldspar and plagioclase in sandstone reservoirs: thermodynamic and kinetic modeling. Journal of Sedimentary Petrology 63:1100–1109.

Bernard PC., Van Gricken RE., Brügmann L (1989). Geochemistry of suspended matter from the Baltic Sea. 1.Results of individual particle characterization by automated electron microprobe. Marine Chemistry 26: 155-177.

Besse J., Courtillot V (2003). Apparent true polar wander and the geometry of the geomagnetic field over the last 200 Myr: Correction: Journal of Geophysical Research 108: p 2300.

Bird DK., Hegelson HC (1981). Chemical interaction of aqueous solutions with Epidote-feldspar mineral assemblages in geologic systems: II Equilibrium constraints in metamorphic/geothermal progress. American Journal of Science 281:576–614.

Bird DK., Spieler AR (2004). Epidote in geothermal systems. Reviews in Mineralogy and Geochemistry 56:235–300.

Blanc P, Roger C., Couto H (1994). Recherche de signatures magmatiques et hydrothermales dans des apatites du nord de Portugal : étude par cathodoluminescence, microscopie électronique à balayage et microsonde électronique. Bulletin de la Société Geologique Française 165:329–339.

Boles JR (1982). Active albitization of plagioclase, Gulf Coast Tertiary. American Journal of Science 282:165–180.

Boles JR., Coombs DS (1977). Zeolite facies alteration of sandstones in the southland syncline, New Zealand. American Journal of Science 277:982-1012.

Borg Y., Smith DK (1969). Calculated powder patterns. Part II Six potassium feldspars and barium feldspars. American Mineralogist 54:163-181.

Bonhomme MG., Yerle JJ., Thiry M (1980). DatingK-Ar de fractions fines associées aux minéralisations. Le cas du bassin uranifère permo-houiller de Brousse-Broquiès (Aveyron). Compte Rendus de l'Académie des Sciences de Paris 291(2) :121-124.

Boone GM (1969). Origin of clouded red feldspars, petrology contrasts in a granitic porphyry intrusion. American Journal of Science 267: 633-668.

Borkowska M., Hameurt J., Vidal P (1980). Origin and age of Izera gneisses and Rumburk granites in the Western Sudetes. Acta Geology of Poland, 30: 121-46.

Botsun S., Veselovskiy R., Arzamastsev A., Fetisova A., Koptev A (2010). Results of paleomagnetic studies of Devonian dykes of the NE part of the Baltic Shield. Geophysical Research Abstracts, Vienna EGU2010 12: 611.

Boulvais P., Ruffet G., Cornichet J., Mermet M (2007). Cretaceous albitization and dequartzification of Hercynian peraluminous granite in the Salvezines Massif (French Pyrénées). Lithos 30: 89-106.

Bowles JFW., Howie RA., Vaughan DJ., Zussman J (2011). Non-Silicates: Oxides, Hydroxides and Sulphides. Rock-Forming Minerals, Second Edition, Geological Society of London 5A: p 920.

Boyce AJ., Fulignati P., Sbrana A (2003). Deep hydrothermal circulation in a granite intrusion beneath Larderello geothermal area (Italy): constraints from mineralogy, fluid inclusions and stable isotopes. Journal of Volcanology and Geothermal Research 126(3): 243-262.

Brinhall G., Dietrich W (1987). Constitutive mass balance relations between chemical composition, volume, density, porosity, and strain in metasomatic hydrochemical systems: Results on weathering and pedogenesis. Geochimica and Cosmochimica 51: 567-587.

Brueger MJ (1945). The genesis of twin crystals. American Mineralogist 30: 469-482.

Butler RF (1998). Paleomagnetism: Magnetic domains to geologic terranes. Electronic edition: p 237.

Carron J.P., de Kerneizon M.L.G., Nachit H (1994). Variscan granites from Brittany. In Pre-Mesozoic geology in France and related areas. Springer Berlin Heidelberg: 231-239.

Castet S., Dandurand JL., Schott J., Gout R (1955). Boehmite solubility and aqueous aluminium speciation in hydrothermal solutions (90-350°C) : Experimental study and modeling. Geochimica et Cosmochimica Acta 57: 4869-4884.

Chayes F (1955). Potash feldspar as a by-product of the biotite-chlorite transformation. Journal of Geology 63: 75-82.

Cederbom C., Larsson SA., Tullborg EL., Stigberg JB (2000). Fission track thermochronology applied to Phanerozoic thermotectonic events in central and southern Sweden. Tectonophysics 316: 153-167.

Ciesielclzuk J., Janeczek, J (2004). Hydrothermal alteration of the Strzelin granite, SW Poland. Neues Jahrbuch für Mineralogie Abh 179: 239-264.

Ciesielclzuk J (2007). Hydrothermal activity in the Strzelin granite, SW Poland. Granitoids in Poland, AM Monograph (1): 231-242.

Clément JY (1986). Minéralogie, pétrologie et géochimie du Permien de Lodève (Hérault, France). Diagenèse précoce, altération feldspathisante et mise en place des minéralisations uranifères. Mémoire de Science de la Terre, 2. Paris. Ecole des Mines de Paris (CGGM) : p 137.

Chenevoy M (1962). Sur les phénomènes de recristallisation dans la série métamorphique du Mont Pilat (Massif Central): albitisation et retromorphose. Bulletin Société Française 7 (3) : 409-416.

Clark C., Schmidt Mumm A., Faure K (2005). Timing and nature of fluid flow and alteration during Mesoproterozoic shear zone formation, Olary domain, South Australia. Journal of Metamorphic Geology 23: 147-164.

Cole DR., Larson PB., Riciputi LR., Mora CI (2004). Oxygen isotope zoning profiles in hydrothermally altered feldspars: Estimating the duration of water-rock interaction. Geology 32: 29-32.

Cogné JP (2003). PaleoMac.: a Macintosh$^{TM}$ application for treating paleomagnetic data and making plate reconstructions. Geochemistry Geophysics Geosystems 4 (1): 1007.

Coombs DS (1954). The nature and alteration of some Triassic sediments from Southland, New Zealand. Transactions of the Royal Society (New Zealand) 82:65–109.

Coombs DS., Fyfe WS., Taylor AM (1959). The zeolite facies with comments on the interpretation of hydrothermal syntheses. Geochimica et Cosmochimica Acta 17: 53–107.

Cwojdziński S (1974). Szczegółowa Mapa Geologiczna Sudetów, Złoty-Stok 1/25000. Instytut Geologiczny.

Cwojdziński S., Kozdrój W (2007). Along the road Nysa–Złoty-Stok–Kłodzko- Wałbrzych–Jelenia Góra. In the Sudetes geotourist guide:.199-226.

Cymerman Z (2004). Tectonic map of the Sudetes and the fore-Sudetic block. 1/200000. Państowowy Instytut Geologiczny .

Danišík M., Migoń P., Kuhlemann J., Evans N.J., Dunkl I., Frisch W (1995). Thermochronological constraints on the long-term erosional history of the Karkonosze Mts., Central Europe. Geomorphology 117 (1–2): 78–89.

Davidson GJ (1998). Alkali alteration styles and mecanisms, and their implications for a "brine factory" source of base metals in the rift-related McArthur Group, Australia. Australian Jounal of Earth Sciences 45: 33-49.

De Jong G., Williams PJ (1995). Giant metasomatic systems formed during exhumation of mid-crustal Proterozoic rocks in the vicinity of the Cloncurry fault, northwest Queensland. Australian Journal of Earth science 42: 281-290.

De La Roche H (1957). Eléments pour l'étude de la saussuritisation. Mémoires de l'Institut Scientifique de Madagascar, Série D, Tome VIII : 217-223.

Deer W.A., Howie R.A., Zussman J (1963). An Introduction to the Rock-Forming Minerals. Sheet silicates. Longmans Green and Co : p 270.

Deer W.A., Howie R.A., Zussman J (1971). An Introduction to the Rock-Forming Minerals. Framework silicates. Longman 4 : p 435

Deer W.A., Howie, R.A., Zussman, J (1992) . An Introduction to the Rock-Forming Minerals. Sheet Silicates. Longman Scientific & Technical/Wiley : p 549.

Dempster TJ., Persano C (2006). Low-temperature thermochronology: Resolving geotherm shapes or denudation histories? Geology 34: 73-76.

Depciuch T (1972). Wiek bezwzględny (K-Ar) granitoidów Kłodzko Złotostockich i strefy Niemczy. Kwartalnik Geologiczny 16 (1); 103-111.

Dideriksen K., Christiansen BC., Baker J.A., Frandsen C., Balic-Zunic T., Tullborg E., Morup S., Stipp SLS. (2007). Fe-oxide fracture fillings as a palæo-redox indicator: Structure, crystal form and Fe isotope composition. Chemical Geology 244: 330-343.

Dideriksen K., Christiansen BC., Frandsen C., Balic-Zunic T., Morup S., Stipp SLS. (2010). Paleo-redox boundaries in fractured granite. Geochimica et Cosmochimica Acta 74: 2866-2880.

Drake H., Tullborg EL (2006). Oskarshamn site investigation, Fracture mineralogy of the Götemar granite. Results from drill cores KKR01, KKR02 and KKR03. Svensk Kärnbränslehantering AB P-06-04: p 61.

Drake H., Tullborg EL., Annersten H (2008). Red-staining of the wall rock and its influence on the reducing capacity around water conducting fractures. Applied Geochemistry 23: 1898-1920.

Drake H., Tullborg EL (2009). Paleohydrogeological events recorded by stable isotopes, fluid inclusions and trace elements in fracture minerals in crystalline rock, Simpevarp area, SE Sweden. 12th International Symposium on Water-Rock Interaction. Applied Geochemistry 24 (4): 715-732.

Drake H., Tullborg EL., Page L (2009). Distinguished multiple events of fracture mineralisation related to far-field orogenic effects in Paleoproterozoic crystalline rocks, Simpevarp area, SE Sweden. Lithos 110: 37-49.

Drake H., Tullborg EL., MacKenzie AB (2009). Detecting the near-surface redox front in crystalline bedrock using fracture mineral distribution, geochemistry and U-series disequilibrium. Applied Geochemistry 24 (5): 1023-1039.

Duthou JL., Couturie JP, Mierzejewski MP., Pin C (1991). Age determination of the Karkonosze granite using isochrone Rb-Sr whole rock method. Przegl. Geol 2 : 75-79.

Edel JB., Schneider JL (1995). The Late Carboniferous to Early Triassic geodynamics evolution of the Variscan Europe in the light of magnetic overprints in Early Permian rhyolites from the northern Vosges (France) and the central Black Forest (Germany). Geophysical Journal International 122 (3): 858-876.

Edel JB., Duringer P (1997). The apparent polar wander path of the European plate in Upper Triassic-Lower Jurassic times and the Liassic intraplate fracturing of the Pangea : New palaeomagnetic constraints from NW France and SW Germany. Geophysical Journal International 128 (2): 331-344.

Edel J.-B., Aifa T., Jelenska M., Kadzialko-Hofmokl M., Zelazniewicz A (1997): Réaimantations des formations paléozoïques des Sudètes polonaises et courbe de dérive des pôles géomagnétiques d'Europe du Carbonifère moyen au Jurassique moyen. Comptes Rendus de l'Académie des Sciences - Séries IIA - Earth and Planetary Science Letters, 325: 479-486.

Eggleton RA., Banfield JF (1985). The alteration of granitic biotite to chlorite. American Mineralogist 70: 902-910.

Ehrenborg J., Stejskal V (2004a). Oskarshamn site Investigation. Boremap mapping of core drilled boreholes KSH03A and KSH03B. Svensk Kärnbrandslehantering AB P04-132 : p 109.

Ehrenborg J., Dahlin P (2005). Oskarshamn site Investigation. Boremap mapping of core drilled boreholes KLX05. Svensk Kärnbrandslehantering AB P05-224 : p 85.

Eliasson T (1993). Mineralogy, geochemistry and petrophysics of red coloured granite adjacent to fractures. Technical report. Svensk Kärnbrandslehantering 93-06: p 64.

Engvik AK., Putnis A., Fitz Gerald JD., Austrheim H (2008). Albitisation of granitic rocks: the mechanism of replacement of oligoclase by albite. The Canadian Mineralogist 46: 1401-1415.

Engvik AK., Golla-Schinder U., Berndt J., Austrheim H., Putnis A (2009). Intragranular replacement of chlorapatite by hydroxy-fluor-apatite during metasomatism. Lithos 112 (3-4): 236-246.

Ernst WG (1960). Diabase-Granophyre relations in the Endion Sill, Duluth, Minnesota. Journal of Petrology 1 (3) : 286-303.

Essalhi A., Piantone P., Touray JC (1993). Arguments texturaux minéralogiques et géochimiques pour une origine métasomatique des albitites du Haut Atlas (Maroc). Compte Rendus de l'Académie des Sciences de Paris 316 (II) : 1083-1993.

Fabrega C., Parcerisa D., Thiry M., Franke C., Gomez-Gras D (1994). Albitization profiles related to the Variscan basement; a case study of the Catalan Coastal Ranges and Eastern Pyrnees (NE Iberia). Geofluids VII, Reuil-Malmaison, Abstract volume: 103-107.

Farmer VC., Lumsdon DG (1994). An assessment of complex formation between aluminium and silicic acid in acidic solutions. Geochimica et. Cosmochimica Acta 58 (16): 3331-3334.

Ferry JM (1978). Fluid interaction between granite and sediment durind metamorphism, south-central Maine. American Journal of Science 278:1025-1056.

Ferry JM (1979). Reaction mechanisms, physical conditions, and mass transfer during hydrothermal alteration of mica and feldspar in granitic rocks from south-central Maine, USA. Contributions to Mineralogy and Petrology 68 (2):125-139.

Fiebig J., Hoefs JJ (2002). Hydrothermal alteration of biotite and plagioclase as inferred from intragranular oxygen isotope- and cation-distribution pattern. European Journal of Mineralogy 14: 49–60.

Finch J., Klein J (1998). The causes and petrological significance of cathodoluminescence emissions from alkali feldspars. Contribution Mineralogical petrology 135: 234–243.

Fischer RA (1953). Dispersion on a sphere. Philisophal Transactions of the Royal Society of London Series A 217: p 295.

Franke C., Thiry M., Gomez-Gras D., Jelenska A M., Kadzialko-Hofmokl M., Lagroix F., Parcerisa D., Spassov S., Szuszkiewicz A., Turniak K (2010). Paleomagnetic age constrains and magneto-mineralogic implications for the Triassic paleosurface in Europe. Geophysical Research Abstracts, vol 12, EGU 2010-7858+ poster.

Franke C., Thiry M., Yao KFE., Gomez-Gras D., Ihlen P., Jelenska M., Kadzialko-Hofmokl M., Fabregas C., Parcerisa D., Lagroix F., Szuszkiewicz A., Turniak K (2012). Paleomagnetic age constrains and magneto-mineralogic implications for the Triassic paleosurface in Europe. In Eurosoil Bari Italy.

Franke C., Yao KFE., Fabregas C., Parcerisa D., Thiry M (2013). Caractérisation de la paléosurface triasique européenne par analyse pétrologique et datation paléomagnétique - comparaison de la catalogne avec les Sudètes polonaises. Association des Sédimentologistes Français, ASF 2013.

Franke C., Vercruysse C (2012). Datation des périodes de mise à l'affleurement du socle cristallin dans les Vosges. Rapport ANDRA C.RP.0ARM.12.0001 ; p 51.

Frey M., De C.C., Liou JG (1991). A new petrogenetic grid for low-grade metabasites. In: Sixth meeting of the European Union of Geosciences 3, vol. 1.106. Blackwell Scientific Publications, Oxford International.

Frietsch R., Tuisku P., Martinsson O., Perdahl JA (1997). Early Proterozoic Cu-(Au) and Fe ore deposits associated with regional Na-Cl metasomatism in northern Fennoscandia; Ore Geology Reviews, 12(1):1-34.

Fyfe WS (1960). Stability of epidote minerals. Nature 187: 497–498.

Fyfe WS., Price N., Thompson AB (1978). Fluids in the Earth's Crust. Amsterdam: Elsevier.

Georges E (1985). Les minéralisations uranifères jurassiques liées spatialement à une discordance hercynienne- Pétrographie, minéralogie et géochimie des gisements du Rouergue (Aveyron, France). Thesis, I.N.P.L. (Institut National Polytechnique Lorraine), Nancy, Cent. Géol.Géochim. Uranium, Nancy, Mémoire 9: p 219.

Giencke J (2007). Introduction to EVA. A Complete Orientation to Features and Functions. https://depts.washington.edu/ntuf/facility/docs/T88-E00031 Introduction to EVA (3).pdf

Godard A (1980). Géographie des ensembles cristallins. Recherches géographiques en France 10 : 67-73.

Gold PB (1987). Textures and geochemistry of authigenic albite from Miocene sandstones, Louisiana Gulf Coast. Journal of Sedimentary Petrology 57 (2): 353-362.

Goldschmidt VM (1916). Geologisch-Petrographische studien im Hochgebirge des sudliche Norwegens, IV. Obersicht die Eruptivegesteine im kaledonischen Gebirge zwischen Stavanger und Trondheim. Skrifter. Videnskapsselskapets. Christ 2: 1-140.

Goldsmith JR., Laves F (1954). The microcline-sanidine stability relations. Geochimica et Cosmochimica Acta 5: 1-19.

González-Acebrón L., Arribas J, Mas R (2010). Role of sandstone provenance in the diagenetic albitization of feldspars. A case study of the Jurassic Tera Group sandstone (Cameros Basin, NE Spain). Sedimentary Geology 229: 53-63.

González-Acebrón L., Götze J., Barca D., Arribas J, Mas R., Perez-Garrido C (2012). Diagenetic albitization in the Tera Group, Cameros Basin (NE Spain) recorded by trace elements and spectral cathodoluminescence. Chemical Geology 312-313: 148-162.

Götze J., Krbetscheck MR., Habermann D., Wolf D (2000). High resolution cathodoluminescence studies of feldspar minerals. In Cathodoluminescence in geosciences. Springer eds: 245-270.

Götze J., Plötze M., Habermann D (2001). Origin, spectral characteristics and pratical apllications of the cathodoluminescence (CL) of quartz. A review. Mineralogical Petrology 71: 225-250.

Götze J., Kempe U (2009). Physical principles of cathodoluminescence and its application to geosciences. In Cathodoluminescence and its application in planetary science. Springer eds: 1-22.

Green PF., Duddy IR (2006). Interpretation of apatite (U–Th)/He ages and fission track ages from cratons. Earth and Planetary Science Letters 244(3): 541-547.

Guilcher A (1949). La surface posthercynienne dans l'Europe occidentale. Annuaire de Géologie, 58 ème Année 310: 97-112.

Gunia T (1984). Microfossils from the quartzitic schists in vicinity of Goszów, Śnieźnik Kłodzki Massif, Central Sudetes. Geologia. Sudetica 18 (2): 47-57.

Guy B (1993). Mathematical revision of Korzhinskii's theory of infiltration metasomatic zoning. European Journal of Mineralogy 5(2): 317-339.

Hamilton M., Elmore RD., Weaver B., Dulin S (2012). Paleomagnetic and petrological investigation of Long Montain Granite, Wichita Montains, Oklahoma. Geofluids VII, Reuil-Malmaison, Abstract volume: 139-142.

Hall MMJ., Veeraraghavan VG., Rubin H., Winchell PG (1977). The approximation of symmetric X-ray peaks by Pearson type VII distributions.. Journal of Applied Crystallography 10: 66-68.

Hayama Y (1959). Some considerations on the color of the biotite and its relation with metamorphism. Geological Society of Japan 65 (760) : 21-30.

Hendriks BWH., Redfield TF (1993). Apatite fission track and (U–Th)/He data from Fennoscandia: An example of underestimation of fission track annealing in apatite. Earth and Planetary Science Letters 236: 443–458.

Hendriks B., Andriessen P., Huigen Y., Leighton C., Redfield T., Murrell G., Nielsen SB (2007). A fission track data compilation for Fennoscandia. Norsk Geologisk Tidsskrift 87(1-2): 143-155.

Hirt WG., Wenk HR., Boles JR (1993). Albitization of plagioclase crystals in the Stevens sandstone (Miocene), San Joaquim Basin, California, and the Frio Formation (Oligocene), Gulf Coast, Texas: a TEM/AEM study. Bulletin of the Geological Society of America 105: 708-714.

Hoefs J., Emmermann R (1983). The oxygen isotope composition of Hercynian granites and pre-Hercynian gneisses from the Schwarzwald, SW Germany. Contributions to Mineralogy and Petrology 83(3-4): 320-329.

Holness MB (2003). Growth and albitization of K-Feldspar in crystalline rocks in the shallow crust: a new kind of porosity? Journal of Geochemical Exploration: 78-79 (173-179).

Hövelmann J., Putnis A., Geisler T., Schmidt BC., Golla-Schindler U (2010). The replacement of plagioclase feldspars by albite: observations from hydrothermal experiments. Contribution to Mineralogy and Petrology 159: 43-59.

Jenkin GRT., Fallick AE., Leake BE (1992). A stable isotope study of retrograde alteration in SW Connemara, Ireland. Contributions to Mineralogy and Petrology 110: 269-288.

Juez-Larré J., Andriessen PAM (2002). Post Late Paleozoic tectonism in the southern Catalan Coastal Ranges (NE Spain), assessed by apatite fission track analysis. Tectonophysics 349: 113-129.

Juez-Larré J., Ter Voorde M (2009). Thermal impact of the break-up of Pangea on the Iberian Peninsula, assessed by thermochronological dating and numerical modelling. Tectonophysics 474 (1-2): 200-213.

Kastner M (1971). Authigenic feldspars in carbonate rocks American Mineralogists 56: 1403-1442.

Kastner M., Siever R (1979). Low temperature feldspars in sedimentary rocks. American Journal of Science 279: 435-479.

Kempe U., Trinkler M., Wolf D (1991). Yttrium und die Seltenerdfotolumineszenz naturlicher scheelite. Chemie der Erde 51: 275-289.

Kempe U., Götze J., Dandar S., Habermann D (1999). Magmatic and metasomatic processes during ¨formation of the Nb-Zr-REE deposits from Khaldzan Buregte (Mongolain Altaï): Indications from a combined CL-SEM study. Mineralogical Magazine 63: 165-177.

Kirschvink JL (1980). The least-squares line and plane and the analysis of paleomagnetic data. Geophysical Journal of the Royal Astronomy Society 62: 699-718.

Koržhinskii DS., Oestreich W (1965). Abriss der metasomatischen Prozesse. Akademie-Verlag Berlin: p 195.

Lee MR., Parsons I. (1997). Dislocation formation and albitization in alkali feldspars from the shap granite. American Mineralogist 82: 557–570.

Larson SA., Tullborg EL., Cederbom CE (1999). Sveconorwegian and Caledonian foreland basins in the Baltic Shield revealed by fission-track thermochronology. Terra Nova 11 (5): 210-215.

Larson SÅ., Cederbom C.E., Tullborg EL., Stiberg JP (2006). Comment on “Apatite fission track and (U–Th)/He data from Fennoscandia: An example of underestimation of fission track annealing in apatite” by Hendriks and Redfield. Earth and Planetary Science Letters 248; 561–568.

Leichmann J., Broska I., Zachovalova K (2003) Low-grade metamorphic alteration of feldspar minerals: a CL study. Terra Nova 15: 104–108.

Liou JG., Kim HS., Maruyama S (1983). Prehnite-epidote equilibria and their petrologic applications. Journal of Petrology 24: 321-342.

Machel HG (1985). Cathodoluminescence in calcite and dolomite and its chemical interpretation. Geoscience Canada 12: 139–147.

Machev P., Klain L., Hetch L (2004). Mineralogy and chemistry of biotites from the Belogradochik pluton-Some petrological implications for granitoid magmatism in north west Bulgaria. Bulgarian Geological Society, Annual Scientific Conference : 16–17.

Machowiak K., Armstrong R (2007). SHRIMP U-Pb zircon age of the Karkonosze granite. Mineralogia Polononica Special Papers.

MacQuarrie KTB., Mayer KU., Jin B., Spiessl SM (2010). The importance of conceptual models in the reactive transport simulation of oxygen ingress in sparsely fractured crystalline rock. Journal of contaminant hydrology 112(1): 64-76.

Majzlan J., Grevel KD., Navrotsky A (2003). Thermodynamics of Fe oxides: Part II. Enthalpies of formation and relative stability of goethite (α-FeOOH), lepidocrocite (γ-FeOOH), and maghemite (γ-Fe2O3). American Mineralogist 88: 855-859.

Marmo V., Hyvarinen L (1958). Molybdenum bearing granite and granodiorite Rautio, Finland. Economic Geology 48: 704-714.

Markl G., von Blanckenburg F., Wagner T (2006). Iron isotope fractionation during hydrothermal ore deposition and alteration. Geochimica et Cosmochimica Acta 70: 3011-3030.

Matthews A., Goldshmith JR (1984). The influence of metastability on reaction kinetics involving zoisite formation from anorthite at elevated pressures and temperatures. American Mineralogist 69: 848-857.

Mazur S., Aleksandrowski P., Kryza R., Oberc-Dziedzic T (2006). The Variscan orogen in Poland. Geological Quarterly 50 (1): 89-118.

Mazur S., Aleksandrowski P., Turniak K., Awdankiewicz M (2007). Geology, tectonic evolution and late Paleozoic magmatism of the Sudetes-an overview. . In Kozłowski A., Wiszniewska J (eds). In Granitoids in Poland. Archiw. Mineral. Monograph 1: 59-87.

McFadden PL., McElhinny LW (1988). The combined analysis of remagnetisation circles and direct observation in paleomagnetism. Earth and Planetary Science Letters 87:161-172.

McLelland J., Morrison J., Selleck B., Cunningham B., Olson C., Schmidt K (2002). Hydrothermal alteration of late to post-tectonic Lyon Mountain Granitic Gneiss, Adirondack Mountains, New York: Origin of quartz-sillimanite segregations, quartz-albite lithologies, and associated Kiruna-type low-Ti Fe-oxide deposits. Journal of metamorphic Geology 20:175-190.

Merino E (1975). Diagenesis in Tertiary sandstones from Kettleman north dome, California I diagenetic mineralogy. Journal of Sedimentary Petrology 45 (1): 320-336.

Merrin S (1960). Synthesis of epidote and its apparent P-T stability curve. Bulletin of the Geological Society of America 71: 1229.

Meunier A., Clément JY., Bouchet A., Beaufort D (1988). Chlorite-calcite and corrensite-dolomite crystallization during two surperimposed events of hydrothermal alteration in the “les crêtes” granites, Vosges, France. Canadian Mineralogist 26: 413-422.

Michelin (2008). Bretagne (Vol. 8). Michelin Editions des Voyages.

Mikulski SZ., Williams IS., Baginski B (2013). Early Carboniferous (Visean) emplacement of the collisional Kłodzko–Złoty-Stok granitoïds (Sudetes, SW Poland): constraints from geochemical data and zircon U–Pb ages. International Journal of Earth Science 71: 1229.

Milnes AR (1990). The Encounter bay granite, Fleurieu Peninsula and Kangaroo Island. J.B. Jago & P.S. Moore (eds) "The Evolution of a Late Precambrian-Early Palaeozoic Rift Complex: The Adelaide Geosyncline". Geological Society Australia Special Publications 16: 421-449.

Moody JB., Jenkins JE., Meyer D (1985). An experimental investigation of the albitization of plagioclase. Canadian Mineralogist 23: 583-596.

Mora IM., Ramseyer K (1992). Cathodoluminescence of coexisting plagioclase, Boehls butte anorthosite. CL activators and fluid flows paths. American Mineralogist 77: 1258-1265.

Morad S (1986). Albitization of K-feldspars grains in Proterozoic arkoses and greywackes from southern Sweden. Neues Jahrbuch für Mineralogie 4: 145-156.

Morad S., Bergan M., Knarud R., Nystuen JP (1990). Albitization of detrital plagioclase in Triassic reservoir sandstones from the Snorre field, Norwegian North Sea. Journal of Sedimentary Petrology 60 (3): 411-425.

Morad S., El-Ghaly MAK., Caja MA., Sirat M., Al-Ramadan K., Mansurbeg H (2010). Hydrothermal alteration of plagioclase in granitic rocks from Proterozoic basement of SE Sweden. Geological Journal 45: 105-116.

Morad S., Sirat M., El-Ghaly MAK., Mansurbeg H (2011). Chloritization in Proterozoic granite from Äspö Laboratory, southeastern Sweden: record of hydrothermal alterations and implications for nuclear waste storage. Clay Minerals 46 (3): 495-513.

Nakamura N., Okuno K., Uehara M., Ozawa T., Tatsumi-Petrocholis L., Fuller M (2010). Coarse-grained magnetites in biotite as a possible stable remanence-carrying phase in Vredefort granites. Geological Society of America Special Papers 465: 165-172.

Němec N (1966). Plagioclase albitization in the lamprophyric and lamproid dykes at the Eastern boader of the Bohemian mass. Contribution to Mineralogy and Petrology 17: 340-353.

Němec W., Porebski SJ., Teisseyre AK (1982). Explanatory notes to the lithotectonic molasse profile of the Intra-Sudetic Basin, Polish part (Sudety Mts, Carboniferous-Permian).Veröffentlichungen Zentralinstituts für Physik der Erde, Akad. Der Wissenschaften der DDR 66: 267–278.

Neumann H., Christie OHJ (1962). Observations on plagioclase aventuries from southern Norway. Norsk Geologisk Tidsskrift 42: 389-393.

Oelkers EH., Schott J., Devidal JL (1994). The effect of aluminum, pH, and chemical affinity on the rates of aluminosilicate dissolution reactions. Geochimica et Cosmochimica Acta 58: 2011-2024.

Ogunyomi O., Martin RF., Hesse R (1981). Albite of secondary origin in the Charny sandstones, Québec: a re-evaluation. Journal of Sedimentary Petrology 51: 597-606.

Oliver NHS (1995). Hydrothermal history of the Mary Kathleen Fold Belt, Mt Isa Block, Queensland.Australian Journal of Earth Sciences 42: 267-279.

Pagel M, Demars C., Deloule E., Blanc P., Barbarand J (1996). Cathodoluminescence and trace element distribution in authigenic quartz in sandstones. Intern. Symposium. Society. Core Analysts, Improving reservoir management, Proceedings, Montpellier, 8-10 sept., 9613, p 2.

Pagel M, Barbin V., Blanc P (2000). Cathodoluminescence in geosciences: An introduction. In Cathodoluminescence in geosciences. Springer eds: 1-21

Parcerisa D., Thiry M., Schmitt JM (2009). Albitisation related to the Triassic inconformity in igneous rocks of the Morvan Massif (France). International Journal of Earth Science 99: 527-544.

Parcerisa D., Franke C., Gómez-Gras D., Thiry M (2010). Markers for geodynamic stability of the Variscan basement: case study for the Montseny-Guilleries High (NE Iberia). Geophysical Research Abstracts, vol 12, EGU 2010-15607+ poster.

Parry W.T., Downey L.M (1982). Geochemistry of hydrothermal chlorite remplacing igneous biotite. Clays and Clay Minerals 30 (2): 81-90.

Parneix JC., Beaufort D., Bouchet A., Dudoignon P., Meunier A (1985). Biotite chloritization process in hydrothermally altered granites. Chemical geology 51: 89-101.

Perez RJ., Boles JR (2005). An empirically derived kinetic model for albitization of detrital plagioclase. American Journal of Science 305: 312-343.

Petersson J., Eliasson T (1997). Mineral evolution and element mobility during episyenitization (dequartzification) and albitization in the postkinematic Bohus granite, southwest Sweden. Lithos 42: 123-146.

Peyaud JB., Barbarand J., Carter A., Pagel M (2005). Mid-Cretaceous uplift and erosion on the northern margin of the Ligurian Tethys deduced from thermal history reconstruction. International Journal of Earth Sciences 94: 462-474.

Porębski SJ (1990). Onset of coarse clastic sedimentation in the Variscan realm of the Sudetes (SW Poland): an example from the Upper Devonian-Lower Carboniferous Oewiebodzice succession. Neues Jahrbuch. Geol. Paläont. ABH., 179: 259–274.

Preeden U., Mertanen S., Elminen T., Plado J (2009). Secondary magnetizations in shear and fault zones in southern Finland. Tectonophysics 479: 203-213.

Putnis A (2002). Mineral replacement reactions: from macroscopic observations to microscopic mechanisms. Mineralogical magazine 66 (5): 689-708.

Putnis CV., Tsukamoto K., Nishimura Y (2005). Direct observations of pseudomorphism: Compositional and textural evolution at a fluid-solid interface. American Mineralogist 90: 1909-1912.

Putnis A., Hinrichs R., Putnis CV., Golla Schindler U., Collins LG (2007). Hematite in porous red-clouded feldspars; evidence of large-scale crustal fluid-rock interaction. Lithos 95: 10-18.

Putnis CV., Ruiz-Aguido E (2013). The mineral-water interface: Where minerals react with the environment. Elements 9 (3): 177-182.

Plümper O., Putnis A (2009). The Complex Hydrothermal History of Granitic Rocks: Multiple Feldspar Replacement Reactions under Subsolidus Conditions. Journal of Petrology 50(5): 967-987.

Que M., Allen AR., (1996). Sericitization of plagioclase in the Rosses Granite Complex, Co. Donegal, Ireland. Mineralogical Magazine 60: 927–936.

Ramseyer K., Boles JR., Lichtner PC (1992). Mechanism of plagioclase albitization. Journal of Sedimentary Petrology 62: 349-356.

Ramseyer K., Mullis J (1990). Factors influencing short-lived blue cathodoluminescence in alpha-quartz. American Mineralogists 75:791-800.

Reed SJB (2005). Electron Microprobe Analysis and Scanning Electron Microscopy in Geology. Second edition. Cambridge University Press: p 212.

Ricordel C (2007). Datations par paléomagnétisme des paléoaltérations du Massif Central et de ses bordures : implications géodynamiques. Thèse Ecole des Mines, Paris : p170.

Ricordel C., Parcerisa D., Thiry M., Moreau M-G., Gómez-Gras D (2007). Triassic magnetic overprints related to albitization in granites from the Morvan massif (France). Palaeogeography Palaeoclimatology Palaeoecology 251: 268-282.

Ricordel-Prognon C., Lagroix F., Moreau M.-G., Thiry M (2010). Lateritic paleoweathering profiles in French Massif Central: Paleomagnetic datings. Journal of Geophysical Research 115: p 19.

Robin E., Rabouille C., Martinez G., Lefevre I., Reyss JL., Van Beek P., Jeandel C (2003). Direct barite determination using SEM/EDS-ACC system: implication for constraining barium carriers and barite preservation in marine sediments. Marine Chemistry 82: 289-306.

Roubault M., Fabriès J., Touret J., Weisbrod A (1963). Détermination des minéraux au microscope polarisant. Lamare-poinat eds : p 365.

Saigal GC., Morad S., Bjørlykke K., Egeberg PK., Aagaard P (1988). Diagenetic albitization of detrital K-feldspars in Jurassic, Lower Cretaceous, and Tertiary clastic reservoir rocks from offshore Norway, I Textures and origin. Journal of Sedimentary Petrology 58:1003-1013.

Sandström B., Tullborg EL., Smelie J., MacKenzie AB., Suksi J (2008). Fracture mineralogy of the Forsmark site. SDM-Site Forsmark. Svensk Kärnbränslehantering AB, R-08-102: p 113.

Sandström B., Tullborg EL (2009). Episodic fluid migration in the Fennoscandian Shield recorded by stable isotopes, rare earth elements and fluid inclusions in fracture minerals at Forsmark, Sweden. Chemical Geology 266 (3-4): 126-142.

Sandström B., Annersten H., Tullborg EL (2010). Fracture-related hydrothermal alteration of metagranitic rock and associated changes in mineralogy, geochemistry and degree of oxidation: a case study at Forsmark, central Sweden. International Journal of Earth Science 99: 1-25.

Savard MM., Veizer J., Hinton R (1995). Cathodoluminescence at low Fe and Mn concentration: a SIMS study of zones in natural calcites. Journal of Sedimentary Research 65: 208–213.

Sawicki L (1980). Mapa geologiczna Polski, arkusz Kłodzko. Skala 1:200 000. Państwowy Instytut Geologiczny. Warszawa.

Schmitt JM., Baubron JC., Bonhomme MG (1984). Pétrographie et datations K-Ar des transformations minérales affectant le gîte uranifère de Bertholène (Aveyron-France). Mineralium Deposita 19:123–131.

Schmitt JM., Simon-Coinçon R (1984). La paléosurface infraliasique en Rouergue ; dépôts sédimentaires et altérations associés. Géologie de la France (2) : 125-135.

Schmitt JM (1986). Albitisation triasique, hydrothermalisme jurassique et altération supergène récente: métallogénie des gisements uranifères du Rouergue. Doct. ès Sciences Thesis, Strasbourg, Louis Pasteur University: p 240.

Schmitt JM., Clement JY (1989). Triassic regolithization: a major stage of pre-enrichment in the formation of unconformity related deposits in Southern France. Metallogenesis of uranium deposits. IAEA Technical Committee Meeting, Vienna 542(8): 93-113.

Schmitt JM (1992). Triassic albitization in southern France: an unusual mineralogical record from a major continental paleosurface. In: Schmitt JM, Gall Q (eds). Mineralogical and geochemical records of paleoweathering. Paris, ENSMP, Memoire de Science de la Terre 18: 115-131.

Schmitt JM., Simon-Coinçon R (1993). EnchaÎnement des paysages et genèse de la "Pénéplaine" post-hercynienne dans le Sud de la France. Third International Geomorphology Conference, Hamilton, Canada, Programme with abstracts: p 239.

Schmitt JM (1994). Geochemical modelling and origin of the Triassic albitized regolith in southern France. 14th International sedimentological congress, Recife, Brazil. Abstracts book S8: 19-21.

Simon K., Hoefs J (1987). Effects of meteoric water interaction on Hercynian granites from the Südschwarzwald, southwest Germany. Chemical Geology, 61 (1-4): 253-261.

Słaby E (1992). Changes in the structural state of secondary albite during progressive albitization. Neues Jahrbuch für Mineralogie 7: 321-335.

Słaby E., Galbarczyk-Gąsiorowska L., Baszkiewicz A (2002). Mantled alkali-feldspar megacrysts from the marginal part of the Karkonosze granitoïd massif (SW Poland). Acta geologica Polonica 52 (4): 501-519.

Słaby E., Martin H (2008). Mafic and felsic magma interaction in granites: the Hercynian Karkonosze pluton (Sudetes, Bohemian massif). Journal of Petrology 49 (2): 353-391.

Söderlund P., Juez-Larré J., Page LM., Dunai TJ (2005). Extending the time range of apatite (U–Th)/He thermochronometry in slowly cooled terranes: Palaeozoic to Cenozoic exhumation history of southeast Sweden. Earth and Planetary Science Letters 239 (3-4): 266-275.

Spear FS (1995).Metamorphic Phase Equilibria and Pressure-Temperature-Time paths. Mineralogical Society of America (1995) 2nd Edition: p 799.

Šťastná A., Přikryl R., Černíková A (2011). Comparison of quantitative petrographic, stable isotope and cathodoluminescence data for fingerprinting Czech marbles. Environmental Earth Sciences 63: 1651-1663.

Steinthorsson S., Helgason O (1992). Maghemite in Icelandic basalts. Mineralogical Magazine 56: 185-199.

Stillings LL., Brantley SL (1995). Feldspar dissolution at 25 C and pH 3: Reaction stoichiometry and the effect of cations. Geochimica et Cosmochimica Acta 59 (8): 1483-1496.

Sun SS., Eadington PJ (1987). Oxygen isotope evidence for the mixing of magmatic and meteoric waters during tin mineralization in the Mole Granite, New South Wales, Australia. Economic Geology 82(1), 43-52.

Taylor HP (1977). Water/rock interactions and the origin of H2O in granitic batholiths. Journal of Geological Society of London 133: 509-558.

Thiry M., Quesnel F., Yans J., Wyns R., Vergari A., Théveniaut H., Simon-Coinçon R., Ricordel C., Moreau M.-G., Giot D., Dupuis C., Bruxelles L., Barbarand J., Baele JM (2006). Continental France and Belgium during the Early Cretaceous: paleoweatherings and paleolandforms. Bulletin de la Societé géologique Française 177(3): 155-175.

Thomson SN., Zeh A (2000). Fission-track thermochronology of the Ruhla crystalline complex: new constraints on the post-Variscan thermal evolution of the NW Saxo–Bohemian Massif. Tectonophysics 324: 17–35.

Turner FJ., Verhoogen J (1960). Igneous and metamorphic petrology. McGraw-Hill, New York.

Turniak K., Mazur S., Wysoczański R (1998). SHRIMP U-Pb zircon ages for orthogneisses from the Międzygórze unit (the Orlica-Śnieżnik dome, Sudetes, Poland). Pol Tow Min Pr Spec 11: 174-177.

Tulloch AJ (1979). Secondary Ca-Al silicates as low-grade alteration products of granitoïd biotite. Contributions to Mineralogy and Petrology, 69 (2): 105-117.

Trønnes RG., Brandon AD (1991). Midly peraluminous high-silica granites in a continental rift: the Drammen and Finnemarka Batholiths, Oslo rift, Norway. Contribution to Mineralogy and Petrology 109: 275-294.

Val'ter AA., Feoktislova NV., Kolesov GM., Sapozhnikov DY (1993). REE behavior in granite albitization. Geochemistry International 30(9). Translated from geokhimiya 2: 290-295.

Vance JA (1957). Coalescent growth of plagioclase in igneous rocks. Geological society of America Bulletin 68: 1849.

Vance JA (1961). Polysynthetic Twinnings in Plagioclase. American Mineralogist 46: 1097-1119.

Veblen DR., Ferry JM (1983). A TEM study of the biotite-chlorite reaction and comparison with petrologic observations. American Mineralogist 68: 1160-1168.

Ventura B., Lisker F., Kopp J (2009). Thermal and denudation history of the Lusatian Block (NE Bohemian Massif, Germany) as indicated by apatite fission-track data. in: Lisker, F.,Ventura, B. & Glasmacher,U.A. (eds): The Geological Society of London, Special Publications 324: 1–12.

Wagner G.A., Van den Haute P (1992). Fission tracks dating. Solid Earth Sciences Library Kluwer Academic Publishers 6: p 285.

Walker TR (1984). 1984 SEPM presidential address: diagenetic albitisation of potassium feldspar in arkosic sandstones. Journal of Sedimentary Petrology 54 (1): 3-16.

Wayshunas GA (1991). Crystal Chemistry of oxides and oxyhydroxides. Oxide minerals: petrologic and magnetic significance. Reviews in mineralogy. Lindsey (eds) 25: 11-68.

Whalen JB., Chappel BW (1988). Opaque mineralogy and mafic mineral chemistry of I- and S-type granite of the Lachan fold belt, southeast Australia. American Mineralogist73: 281-296.

Winchester JA., the PACE TMR Network Team (2002). Palaeozoic amalgamation of Central Europe: new results from recent geological and geophysical investigations. Tectonophysics 360 (1-4): 5-21.

Widdowson M (1997). Tertiary palaeosurfaces of the SW Deccan, Western India: implications for pasive margin uplift. In Widdowson M. (eds). Geological Society. Special Publications 120: 221-248.

Wierzchołowski B (1976). Granitoidy kłodzko-złotostockie i ich kontaktowe oddziaływa-nie na skały osłony (studium petrograficzne). Geologia Sudetica 2 : 3-143.

Wilmowski A (2002). Chloritization and polytypism of biotite in the Łomnica granite, Karkonosze Massif, Sudetes, Poland: stable isotope evidence. Chemical Geology 182: 529-547.

Winter JD (2001). An introduction to igneous and metamorphic petrology. Prentice Hall Upple Saddle River, New-Jersey.

White A (1994). Chloritization and polytypism of biotite in the Łomnica granite, Karkonosze Massif, Sudetes, Poland: stable isotope evidence. Chemical Geology 182: 529-547.

Wojdyr M (2010) Fityk: A general-purpose peak fitting program. Journal of Applied Crystallography 43: 1126-1128.

Yerle JJ, Thiry M (1979). Albitisations et minéralisations uranifères dans le socle et les sédiments permo-houillers du bassin de Brousse-Broquiès (Aveyron, France). Bulletin BRGM 4:275-290.

Yu KM., Boggs S., Seyodolali A., Ko J (1997). Albitization of feldspars in sandstones from the Gohan (Permian) and Donggo (Permo-Triassic) formations, Gohan area, Kangwondo,Korea. Geoscience Journal 1: 26-31.

Zak J., Verner K., Klominsky J., Chlupăćovà M (2009). ‘‘Granite tectonics’’ revisited: insights from comparison of K-feldspar shape-fabric, anisotropy of magnetic susceptibility (AMS), and brittle fractures in the Jizera granite, Bohemian Massif. International Journal of Earth Science 98: 949-967.

Zijderveld JDA (1967b). The natural remanent magnetizations of the Exeter Volcanic Traps. (Permian, Europe). Tectonophysics 4 (2):121-153.

# LIST OF FIGURES

# Albitisation et Oxydation des roches granitoïdes en relation avec la paléosurface triasique des Sudètes (SW Pologne)

**RESUME :** Les faciès albitisés et des socles ont toujours été classés comme tardi-magmatiques par référence aux saussuritisations et séricitisations associées à ces faciès. Cependant, l'éventualité d'une origine superficielle triasique a été récemment établie pour certains de ces faciès. L'étude des faciès granitoïdes oxydés du socle paléozoïque des Sudètes polonaises a été entreprise pour préciser les caractéristiques de ces faciès. L'étude pétrographique montre qu'il y a deux grandes catégories d'altération dans les faciès étudiés et qui se disposent spatialement par rapport aux fractures : (1) la saussuritisation et la séricitisation qu'on retrouve dans les faciès clairs, à l'intérieur des blocs et loin des fractures et (2) l'albitisation et l'hématisation associée aux faciès rouges et qui se développent à partir des fractures. Ces altérations s'accompagnent de la chloritisation des minéraux ferromagnésiens, de la formation de minéraux secondaires tels que quartz, feldspath K, prehnite, titanite, calcite et apatite. Il apparaît surtout que les paragenèses associées à ces altérations s'inscrivent dans une phase d'altération unique avec des réactions qui s'enchainent spatialement, et à l'origine de la zonation observée. La datation paléomagnétique des oxydes de fer associés aux faciès oxydés indique des âges triasiques suggérant que l'oxydation est liée à la paléosurface triasique. Or l'hématite apparaît paragénétique et contemporaine de l'albite, par conséquent l'albitisation est aussi supergène et liée à la paléosurface triasique. Les faciès albitisés/oxydés apparaissent ainsi comme des marqueurs de la paléosurface triasique dans les massifs paléozoïques et de ce fait peuvent permettre de contraindre la géodynamique post-triasique de ces massifs.

**Mots clés :** Altération, Oxydation, Pétrographie, Granitoïde, Datation, Paléosurface, Trias, Pologne.

# Albitization and oxidation of the granitoïd rocks related to the Triassic Paleosurface in the Sudetes (SW Poland)

**ABSTRACT:** Albitized and oxidized facies in crystalline basements were generally classified as late-magmatic alterations due to the occurrence of saussuritization and sericitization parageneses. However, the possibility of a Triassic superficial origin has recently been proposed for some of these facies. The reddened granitoid facies in the basement of the Polish Sudetes have been studied in order to precise the characteristics of these alterations. The petrographical study shows that there are two categories of alteration, which are spatially arranged with respect to the fractures: (1) saussuritization and sericitization within the light facies, towards the center of the blocks and thus further away from the fracture walls, and (2) albitization and hematitization prevailing in the reddened facies along the fracture walls. These alterations are associated to the chloritization of the primary ferromagnesian minerals and to the development of secondary minerals, such as quartz, K feldspars, apatite, prehnite, calcite, and titanite. It appears especially that these parageneses associated to these alterations are part of a unique alteration event, with reactions following spatially on from each other, and responsible of the observed zonation. The paleomagnetic dating of the iron oxides associated to these facies clearly indicates Triassic ages suggesting that the oxidation is linked to the Triassic paleosurface. The hematite emerges as paragenetic and contemporaneous to the albite; hence, the albitization must be also of supergene origin and is thus related to the Triassic paleosurface. Therefore, these albitized/oxidized facies appear as a marker of the Triassic paleosurface in the crystalline Paleozoic basements, allowing to constrain the post-Triassic geodynamics of the ancient massifs that usually lack for benchmarks.

**Keywords** : Alteration, Oxidation, Petrography, Granitoïd, Dating, Paleosurface, Trias, Poland.

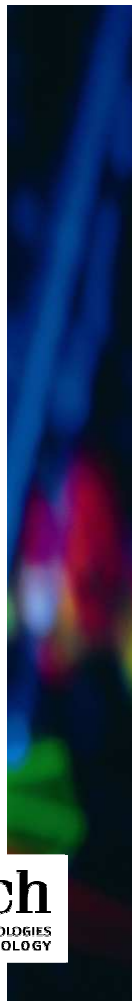

MINES ParisTech

ParisTech
INSTITUT DES SCIENCES ET TECHNOLOGIES
PARIS INSTITUTE OF TECHNOLOGY